Site-selective, orthogonal functionalization of organogermanes, and “batch-forbidden” transformations enabled in cyclic flow mode

Von der Fakultät für Mathematik, Informatik und Naturwissenschaften der
RWTH Aachen University zur Erlangung des akademischen Grades eines
Doktors der Naturwissenschaften genehmigte Dissertation

vorgelegt von

M.Sc. Avetik Gevondian

aus
Kursk, Russland

Berichter: Prof. Dr. Franziska Schoenebeck
Prof. Dr. Meike Niggemann

Tag der mündlichen Prüfung: 08.03.2024

“Was there anything more exciting in life than seeking answers?”

Isaac Asimov

Dedicated to my parents

Acknowledgements

First of all, I would like to thank my supervisor, Prof. Dr. Franziska Schoenebeck, for the unique opportunity of working on complex and interesting topics in a such great and friendly group. At the right moment I always found her support and wise guidance, which played a substantial role not only in my professional, but also in personal development. Moreover, I can barely imagine another place, where I could touch so many fields of organic chemistry and make friendship with so many interesting people. Many thanks to Prof. Dr. Meike Niggemann for her kind agreement to be co-examiner on the thesis defense. Also, I am grateful to other members of the thesis committee for their valuable feedback.

I would like to express my thankfulness to Dr. Wolfgang Bettray, Karin Risse, Lea Flecken and Jasmin Biali for their permanent readiness to help with all kind of administrative issues I encountered during my work. My special thanks are addressed to our technicians Kristina Deckers, Desiree Gilliam and Daniela Dreβler, for constant maintenance of laboratory functioning, without whom experimental work would be practically impossible. Also, thanks to Dr. Christoph Räuber for assistance with NMR analysis and Dr. Wolfgang Bettray for the assistance with MS analysis.

I am grateful to all current and former colleagues I met during my PhD research. This work wouldn't reach the full shape without Grant Sherborne, Amit Dahiya, Ignacio Funes-Ardoiz, Aymane Selmani, William Reid and Christoph Fricke, with whom I had a chance to share scientific projects. Many thanks for your advice and shared knowledge contributed to my background. Special gratitude goes to Theresa Sperger for innumerous discussions, careful corrections of drafts and recommendations regarding the thesis. Also, thanks to Angel, Abdur, Sam, Chris, Tanya, Marvin, Daniel H., Mathilde, Ula, Fritz, Enrico, Nikita, Danijela, Gina, Teresa, Sherif, Italo, Thomas, Indrek, Jegor, Julian R., Julian H., Tatiana, Claudia, Bhaskar, Ajoy, Gourab, Filip O., Sarah, Guillaume, Sinem, Jaime, Daniel M. and many more for scientific or non-scientific talks and great time we spent together. And, the last but not the least, I am grateful to my favorite 4.07, where I spent most of my research time, and particularly to Filip Živković, Eric Ahrweiler and Markus Schötz for nice and in a good way chaotic atmosphere. Memories about time we spent both in and outside the lab always make me smile.

However, a life should not be limited only by the lab work. It is hard for me to overestimate the role of the people outside the laboratory. I would like to express my gratitude to people, who not simply mentally or personally accompanied this way shoulder to shoulder with me, but also kept reminding me that the rest of the world is still around, shared gladness during my ups and empathized my downs. Մեծ շնորհակալություն ծնողներիս՝ Գերասիմ Ղևոնդյանին և Էլմիրա Աղբալյանին, համբերության և անգնահատելի աջակցության համար, որ նրանք ցուցաբերել են, և որը ես միշտ զգացել եմ իմ կողքին՝ չնայած հեռավորությանը: Նաև շնորհակալություն քրոջս՝ Գայանե Ղևոնդյանին և եղբորորդիներիս՝ Հրանտին և Դավիթին: Ձեր սերն ու հոգատարությունը միշտ օրինակ կլինեն ինձ

հաւսաւր: Also, I would like to thank you, Alena, for your patience, true love, infinite aspiration to know more about my work and kind willing to participate in it. You are an example of pure courage and strength to me I wish I had.

Abstract

In many aspects utilization of transition metals in cross-coupling reactions turned out to be huge progress in synthetic chemistry methodology and proved itself as a reliable approach towards synthesis of complex and important organic molecules for agrochemistry, pharmaceuticals and other vital fields. Nowadays, a wide range of nucleophiles were developed and investigated as coupling partners, but none of them is able to show orthogonality in different cross-coupling reactions. This thesis describes reactivity of a relatively novel agent, aryl germanes, in completely different transformations as a robust, highly reactive and orthogonal species prevailing reactivity of other known functionalities, such as halogens, silanes and boronic acid esters.

The first part of the thesis is dedicated to selective Au-catalyzed arylation of aryl germanes with diazonium salts (**Scheme I**). Previous studies of our group showed effective C-H arylation of organogermanes with simple arenes supported by $Au^{(I)}/Au^{(III)}$ catalytic cycle. The reaction requires stoichiometric amounts of an oxidant, which reduces atom economy and produces stoichiometric amounts of waste. Combination of high oxidative potential and an ability to play a role of a cross-coupling agent allows diazonium salts to provide cleaner $Au^{(I)}/Au^{(III)}$-catalyzed arylation of aryl germanes with light assistance. Transformation appeared highly selective towards C-Ge bond ignoring all other potentially reactive sites. We found that while electron-poor salts are highly efficient, electron-rich ones tend to suppress the reaction. To investigate reasons of such reactivity difference between poor and rich salts DFT calculations were done, which shed light on mechanisms for both types of salts. After that we focused on addressing the mentioned challenge and developed another catalytic system enabling less reactive electron-rich salts to participate in the reaction. Also, it was shown that highly substituted aryl germanes are effective cores for complex molecules synthesized in modular fashion.

Scheme I | Gold-catalyzed arylation of aryl germanes with diazonium salts.

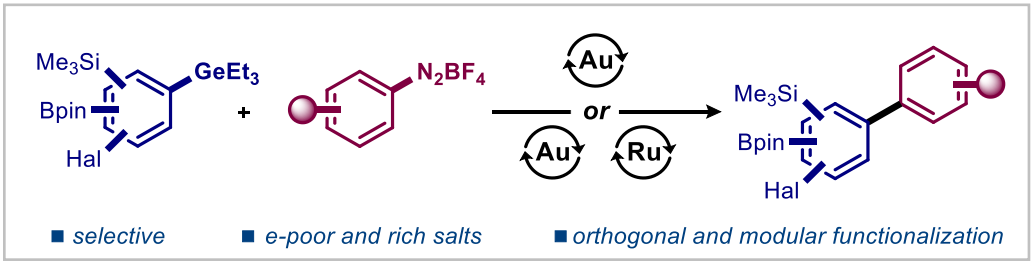

The second chapter describes conversion of C-Ge into C-O and C-N bonds (**Scheme II**). The former consists in development of a mild, ligand-free and fast coupling between aryl germanes and alcohols based on $Pd^{(II)}/Pd^{(IV)}$-catalysis. Using simple Pd-source, $Pd(OAc)_2$, and PIFA as oxidant the transformation provides a coupling with primary, secondary and tertiary alcohols and demonstrates exclusive selectivity

towards germanes tolerating all other types of reactive motifs, such as Bpin, $SiMe_3$ and especially halogens, which are typical reagents in C-O coupling. Moreover, carboxylic acids were introduced as well effectively producing the corresponding aryl esters. Furthermore, we successfully demonstrated orthogonal behavior of aryl germanes in a number of typical C-O bond formation reactions, namely Cu-, Pd- and Ni-reactions. In all mentioned reactions germane fully untouched letting other functionalities to undergo the transformation. Also, though 10 mol% of $Pd(OAc)_2$ was used, we found that the reaction proceeds with the same efficiency with lower catalyst loading affecting mainly reaction time. As for C-N bond formation, we showcased metal-free photocatalyzed nitration of aryl germanes. As it was shown for previously mentioned reactions, the smooth transformation selectively proceeds at C-Ge site. With assistance of DFT analysis we managed to elucidate the observed selectivity towards Bpin and $SiMe_3$ and proposed a mechanism of the reaction.

Scheme II | Conversion of aryl germanes into ethers and esters and nitroarenes.

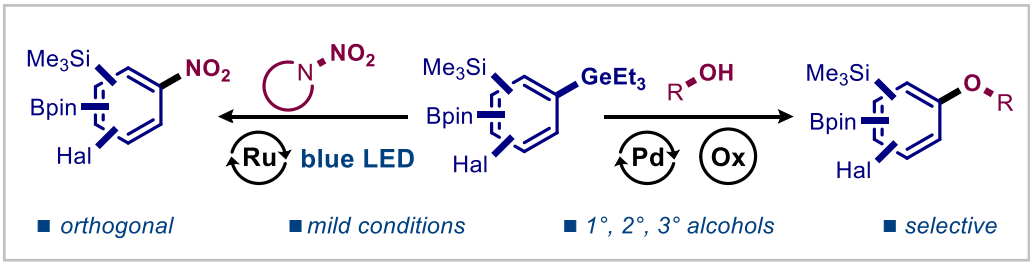

The last chapter discusses a "batch-forbidden" trifluoromethylation of aryl iodides with weakly ligated $(Xantphos)Pd^{(II)}$ (**Scheme III**). To implement this transformation, we designed a cyclic flow setup separating elementary steps, which are impossible to perform in batch due to fast catalyst deactivation. The constructed setup provides successful performance of the coupling using [(Xantphos)Pd(Ph)I] as a catalyst and $TMSCF_3$ as a CF_3-source. Though experiment proceeds in the cyclic manner, the presence of other halogens is not an issue and only C-I bond undergoes trifluoromethylation.

Scheme III | Trifluoromethylation of aryl iodides with weakly ligated Pd-center enabled in cyclic flow.

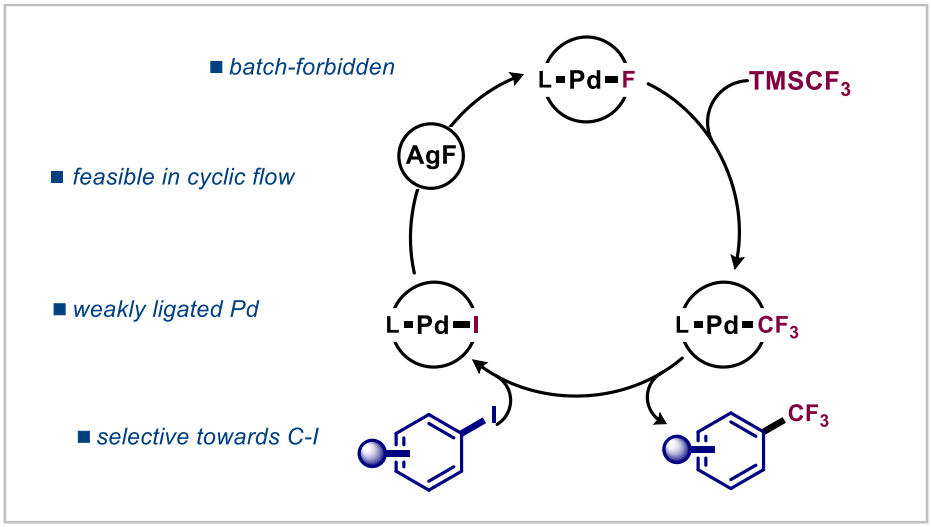

Zusammenfassung

In vielerlei Hinsicht stellte die Verwendung von Übergangsmetallen in Kreuzkupplungsreaktionen einen enormen Fortschritt in der Methodik der synthetischen Chemie dar und erwies sich als zuverlässiger Ansatz zur Synthese komplexer und wichtiger organischer Moleküle für die Agrochemie, Pharmazeutik und andere wichtige Bereiche. Heutzutage wurde eine Vielzahl von Nukleophilen als Kupplungspartner entwickelt und untersucht, aber keines von ihnen ist in der Lage, in verschiedenen Kreuzkupplungsreaktionen Orthogonalität zu zeigen. Diese Arbeit beschreibt die Reaktivität einer relativ neuen Molekülklasse, nämlich Arylgermane, in völlig unterschiedlichen Transformationen als robuste, hochreaktive und orthogonale Spezies, die die Reaktivität anderer bekannter Funktionalitäten wie Halogene, Silane und Boronsäureester übertrifft.

Der erste Teil der Arbeit ist der selektiven Au-katalysierten Arylierung von Arylgermanen mit Diazoniumsalzen gewidmet (**Schema I**). Frühere Studien unserer Gruppe zeigten eine effektive C-H-Arylierung von Organogermanen mit einfachen Arenen, die durch den $Au^{(I)}/Au^{(III)}$-Katalysezyklus unterstützt werden. Die Reaktion erfordert stöchiometrische Mengen eines Oxidationsmittels, was die Atomökonomie verringert und stöchiometrische Mengen an Abfall erzeugt. Die Kombination aus hohem Oxidationspotential und der Fähigkeit, als Kreuzkupplungsmittel zu fungieren, ermöglicht es den Diazoniumsalzen, mit Licht eine sauberere $Au^{(I)}/Au^{(III)}$-katalysierte Arylierung von Arylgermanen bereitzustellen. Die Transformation schien hochselektiv für die C-Ge-Bindung zu sein und ignorierte alle anderen potenziellen reaktiven Stellen. Wir fanden heraus, dass elektronenarme Salze zwar hocheffizient sind, elektronenreiche Salze jedoch dazu neigen, die Reaktion zu unterdrücken. Um die Gründe für diesen Reaktivitätsunterschied zwischen elektronenarmen und -reichen Salzen zu untersuchen, wurden DFT-Rechnungen durchgeführt, die Aufschluss über die Mechanismen beider Salzarten geben. Danach konzentrierten wir uns auf die Bewältigung der genannten Herausforderung und entwickelten ein weiteres katalytisches System, das die Teilnahme weniger reaktiver elektronenreicher Salze an der Reaktion ermöglicht. Außerdem wurde gezeigt, dass hochsubstituierte Arylgermane wirksame Grundgerüste für komplexe, modular synthetisierte Moleküle sind.

Schema I | Goldkatalysierte Arylierung von Arylgermanen mit Diazoniumsalzen.

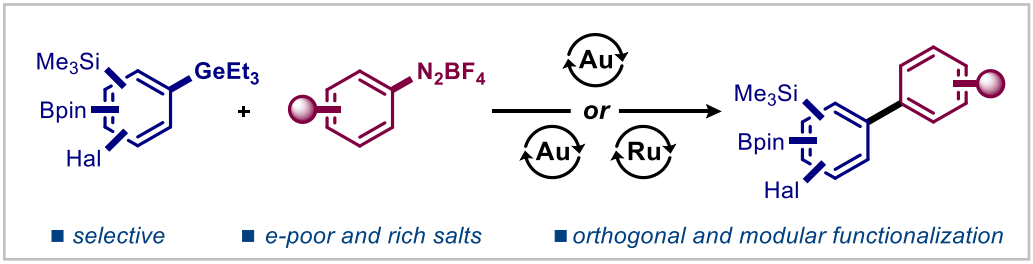

Das zweite Kapitel beschreibt die Umwandlung von C-Ge in C-O und C-N-Bindungen (**Schema II**). Ersteres besteht in der Entwicklung einer milden, ligandenfreien und schnellen Kupplung zwischen Arylgermanen und Alkoholen auf Basis der $Pd^{(II)}/Pd^{(IV)}$-Katalyse. Unter Verwendung einer einfachen Pd-Quelle, $Pd(OAc)_2$ und PIFA als Oxidationsmittel ermöglicht die Transformation eine Kupplung mit primären, sekundären und tertiären Alkoholen und zeigt eine ausschließliche Selektivität gegenüber Germanen, die alle anderen Arten reaktive Gruppen, wie Bpin, $SiMe_3$ und insbesondere Halogene, tolerieren , die typische Reagenzien bei der C-O-Kupplung sind. Darüber hinaus wurden auch Carbonsäuren eingeführt, wodurch die entsprechenden Arylester entstanden. Des Weiteren konnten wir das orthogonale Verhalten von Arylgermanen in einer Reihe typischer C-O-Bindungsbildungsreaktionen, nämlich Cu-, Pd- und Ni-Reaktionen, erfolgreich demonstrieren. Bei allen genannten Reaktionen bleibt die Umwandlung anderer Funktionalitäten völlig unberührt. Auch wenn 10 mol% $Pd(OAc)_2$ verwendet wurden, fanden wir heraus, dass die Reaktion mit der gleichen Effizienz abläuft, wobei eine geringere Katalysatormenge hauptsächlich die Reaktionszeit beeinflusst. Was die Bildung von C-N-Bindungen betrifft, haben wir die metallfreie photokatalysierte Nitrierung von Arylgermanen vorgestellt. Wie für zuvor erwähnte Reaktionen gezeigt wurde, verläuft die Transformation selektiv an der C-Ge-Stelle. Mithilfe der DFT-Analyse gelang es uns, die beobachtete Selektivität gegenüber Bpin und $SiMe_3$ aufzuklären und einen Reaktionsmechanismus vorzuschlagen.

Scheme II | Umwandlung von Arylgermanen in Ether und Ester und Nitroarene.

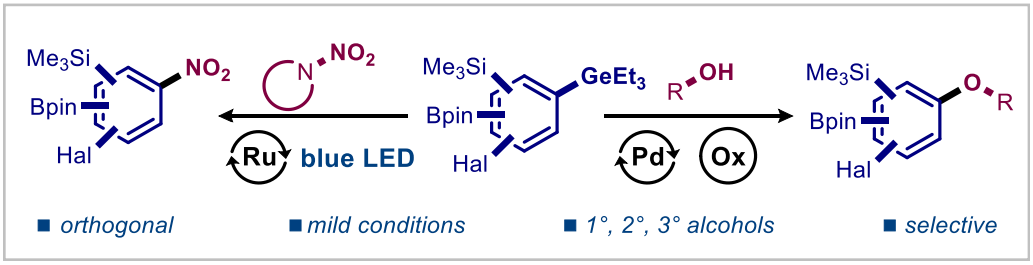

Das letzte Kapitel handelt von einer „batch-verbotenen“ Trifluormethylierung von Aryliodiden mit schwach ligiertem (Xantphos)$Pd^{(II)}$ (**Schema III**). Um diese Transformation umzusetzen, haben wir ein zyklisches „flow“ System entworfen, der Elementarschritte trennt, die aufgrund der schnellen Katalysatordesaktivierung nicht in „batch“ Systemen durchgeführt werden können. Der konstruierte Aufbau ermöglicht eine erfolgreiche Durchführung der Kupplung unter Verwendung von [(Xantphos)Pd(Ph)I] als Katalysator und $TMSCF_3$ als CF_3-Quelle. Obwohl das Experiment zyklisch abläuft, stellt die Anwesenheit anderer Halogene kein Problem dar und nur die C-I-Bindung wird trifluormethyliert.

Scheme III | Trifluormethylierung von Aryliodiden mit schwach ligiertem Pd-Zentrum im zyklischen flow aktiviert.

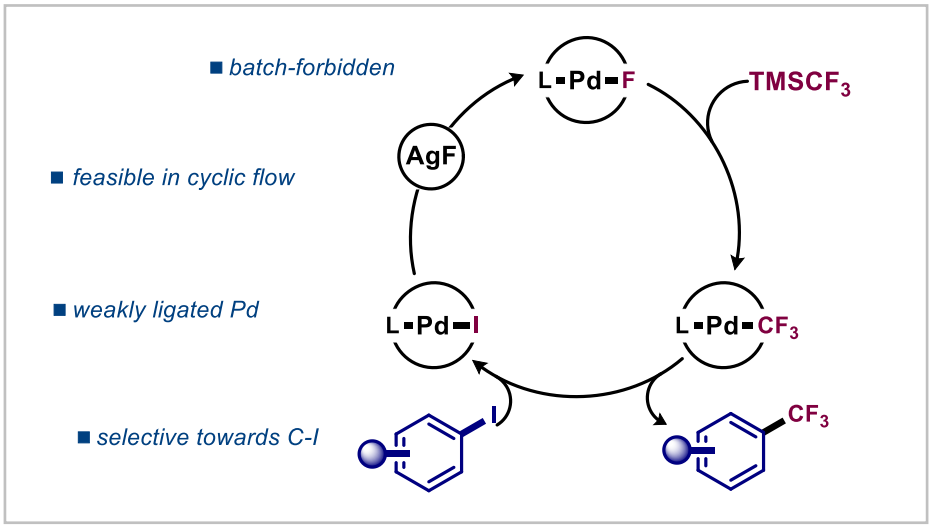

Publications and Copyright Permissions

Parts of the work described in this thesis have already been published in the following publications:

- G. J. Sherborne, A. G. Gevondian, I. Funes-Ardoiz, A. Dahiya, C. Fricke, F. Schoenebeck*. Modular and Selective Arylation of Aryl Germanes (C–$GeEt_3$) over C–Bpin, C–SiR_3 and Halogens Enabled by Light-Activated Gold Catalysis. *Angew. Chem. Int. Ed.* **2020**, 59, 15543–15548.
- A. Dahiya, A. G. Gevondian, F. Schoenebeck*. Orthogonal C–O Bond Construction with Organogermanes. *J. Am. Chem. Soc.* **2023**, 145, 14, 7729–7735.
- A. Dahiya‡, A. G. Gevondian‡, A. Selmani, F. Schoenebeck*. Site-selective Nitration of Aryl Germanes at Room Temperature. *Org. Lett.* **2023**, 25, 39, 7209–7213.

Further publications that have not been featured in this thesis:

- A. Selmani, A. G. Gevondian, F. Schoenebeck*. Germylation of Arenes via Pd(I) Dimer Enabled Sulfonium Salt Functionalization. *Org. Lett.* **2020**, 22, 12, 4802–4805.

Abbreviations

1-Ad	1-adamantyl
6-311++G(d,p)	Pople basis set; split-valence triple-zeta with added diffuse and polarization functions (on heavy atoms and hydrogens)
6-31G(d)	Pople basis set; split-valence double-zeta with added polarization functions on heavy atoms
Å	Ångström (1 Å = 0.1 nm)
AI	alkyne insertion
AIBN	azobisisobutyronitrile (2,2′-Azobis(2-methylpropionitrile))
AIM	atoms-in-molecules theory
Ar	aryl
b:l	branched to linear ratio
B3LYP	DFT method (hybrid metaGGA using Becke's 3-parameter exchange functional and Lee-Yang-Parr correlation functional)
B3LYP-D3(BJ)	dispersion-corrected B3LYP (employing Grimme's D3 correction with Becke-Johnson damping function)
BDE	bond dissociation enthalpy
Bn	benzyl
bpy	2,2′-bipyridyl
BrettPhos	2-(dicyclohexylphosphino)3,6-dimethoxy-2′,4′,6′-tri-*iso*-propyl-1,1′-biphenyl
CC	coupled cluster
CCSD(T)	coupled cluster singles doubles perturbative triples
CMD	concerted metalation deprotonation
cod	1,5-cyclooctadiene
Cp	cyclopentadienyl ligand
CP	chloropalladation
CPCM	conductor polarizable continuum model (solvation model)
CPhos	2-dicyclohexylphosphino-2′,6′-bis(*N*,*N*-dimethylamino)biphenyl
*c*Pr	cyclopropyl
Cy	cyclohexyl
DABCO	1,4-diazabicyclo[2.2.2]octane
DavePhos	2-dicyclohexylphosphino-2′-(*N*,*N*-dimethylamino)biphenyl
dba	dibenzylideneacetone (*trans*,*trans*-1,5-diphenyl-1,4-pentadien-3-one)
def2-TZVP	Ahlrichs basis set; split-valence triple-zeta
DFT	density functional theory
DIPEA	di-*iso*-propylethylamine
DMF	*N*,*N*-dimethylformamide
DMSO	dimethylsulfoxide
DPEPhos	bis[(2-diphenylphosphino)phenyl] ether
dppe	1,2-bis(diphenylphosphino)ethane
dppf	1,1′-ferrocenediyl-bis(diphenylphosphine)
DPPH	1,1-diphenyl-2-picrylhydrazyl radical
ECP	effective core potential
GGA	DFT method using generalized gradient approximation
HAT	hydrogen atom transfer
HF	Hartree-Fock
hppH	1,3,4,6,7,8-hexahydro-2*H*-pyrimido[1,2-α]pyrimidine
iCA	*ipso*-C attack
IHept	1,3-bis(2,6-di-4-heptylphenyl)imidazol-2-ylidene
IPent	1,3-bis(2,6-di-3-pentylphenyl)imidazol-2-ylidene
*i*Pr	*iso*-propyl (2-propyl)
IPr	1,3-bis(2,6-di-*iso*-propylphenyl)imidazol-2-ylidene
Isom	isomerization

JohnPhos	2-(di-*tert*-butylphosphino)biphenyl
L	ligand
LANL2DZ	Los Alamos ECP
LDA	DFT method using local density approximation
LiHMDS	lithium hexamethyldisilazane (lithium bis(trimethylsilyl)amide)
LiTMP	lithium 2,2,6,6-tetramethylpiperidide
LUMO	lowest unoccupied molecular orbital
M06	DFT method (hybrid metaGGA, Minnesota suite)
M06L	DFT method (metaGGA, Minnesota suite)
MD	molecular dynamics
Me	methyl
MeCN	acetonitrile
Mes	mesityl (2,4,6-trimethylphenyl)
metaGGA	DFT method using generalized gradient approximation including the Laplacian of electron density
MM	molecular mechanics
NBO	natural bond order
*n*Bu	*n*-butyl (1-butyl)
NHC	*N*-heterocyclic carbene
NMR	nuclear magnetic resonance spectroscopy
*n*Oct	*n*-octyl (1-octyl)
*n*Pr	*n*-propyl (1-propyl)
OA	oxidative addition
OAc	acetate
OBz	benzoyl
OTf	triflate (trifluoromethanesulfonate)
*o*Tol	*ortho*-tolyl (2-methylphenyl)
PA-Ph	1,3,5,7-tetramethyl-6-phenyl-2,4,8-trioxa-6-phosphaadamantane
PBE0-D3(BJ)	dispersion-corrected DFT method (hybrid GGA by Perdew, Burke and Ernzerhof, employing Grimme's D3 correction with Becke-Johnson damping function)
PC	pre-complex
Pd-PEPPSI	[NHC](3-chloropyridyl)palladium(II) dichloride
Ph	phenyl
phen	phenanthroline
PMP	1,2,2,6,6-pentamethylpiperidine
*p*Ts	*para*-tosyl (4-tolylsulfonyl)
QM	quantum mechanics
QPhos	1,2,3,4,5-Pentaphenyl-1′-(di-*tert*-butylphosphino)ferrocene
RE	reductive elimination
RuPhos	2-dicyclohexylphosphino-2′,6′-di-*iso*-propoxybiphenyl
SDD	Stuttgart/Dresden ECP
SIPr	1,3-bis(2,6-di-*iso*-propylphenyl)imidazolidene
SMD	continuum solvation model by Cramer and Truhlar (based on charge density employing full solute electron density)
*t*Bu	*tert*-butyl
*t*BuBrettPhos	2-(di-*tert*-butylphosphino)-2′,4′,6′- tri-*iso*-propyl-3,6-dimethoxy-1,1′-biphenyl
*t*Bu-Xantphos	9,9-dimethyl-4,5-bis(di-*tert*-butylphosphino)xanthene
*t*BuXPhos	2-di-*tert*-butylphosphino-2′,4′,6′-tri-*iso*-propylbiphenyl
TDAE	tetrakis(dimethylamino)ethylene
TEMPO	2,2,6,6-tetramethylpiperidine-1-oxyl radical
THF	tetrahydrofuran
TIPS	tri-*iso*-propylsilyl
TS	transition state
Ts	tosyl (4-tolylsulfonyl)
Xantphos	4,5-bis(diphenylphosphino)-9,9-dimethylxanthene
Xphos	2-dicyclohexylphosphino-2′,4′,6′-tri-*iso*-propylbiphenyl
xs	excess
β-HE	β-hydride elimination
ωB97XD	hybrid DFT method (long-range and dispersion-corrected)

Table of Contents

1

Gold-catalyzed Arylation of Aryl Germanes

The results described in this chapter were published in Angewandte Chemie International Edition.[1]

1 Gold-catalyzed Arylation of Aryl Germanes

1.1 Selective and Modular Arylation of Aryl Germanes with Aryl Diazonium Salts

Experimental work described in this subchapter was done in collaborations with other members of Schoenebeck group: Dr. Grant Sherborne, Amit Dahiya and Christoph Fricke. Computational studies were performed by Dr. Ignacio Funes-Ardoiz. The results described in this subchapter were published in Angewandte Chemie International Edition.[1]

Biaryls are known as one the most important scaffolds in the fields of materials, natural products and catalysis.[2-6] For many years only a few transformations served as reliable routes to biaryl synthesis, such as Gomberg-Bachmann[7] and Ullmann[8] reactions (**Figure 1**). However, the poor regioselectivity derived by radical mechanism of the former and harsh conditions of the latter limited their synthetic application.[8-12] Moreover, a competitive homocoupling side reaction decreases a yield of heterobiaryls, which therefore complicates practical utilization of the mentioned reactions. However, the discovery of metal-catalyzed cross-coupling reactions, marked by awarding of Nobel Prize in 2010 to Richard F. Heck, Ei-ichi Negishi and Akira Suzuki, revolutionized the biaryl synthesis.[13] Not only dramatically simplifying it but also opening more efficient pathways to unsymmetrical biaryls this class of reactions typically employs aryl (pseudo)halides or aryl diazonium salts as electrophiles with various organometallic agents as nucleophiles to form new Csp^2-Csp^2 bonds.[14]

Figure 1 | The first synthetic pathways to biaryls.

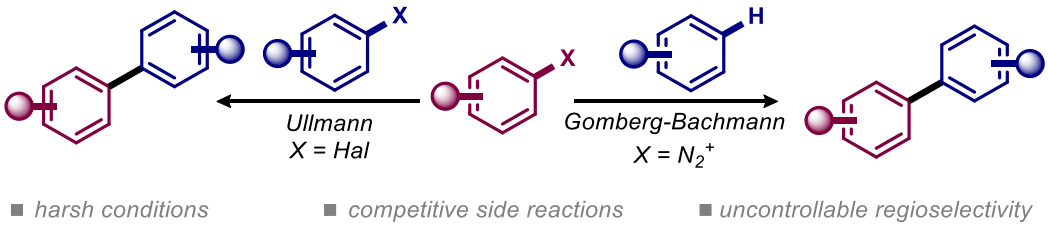

Among nucleophilic arylation agents the most application was found for Grignard reagent (Kumada-Corriu reaction)[15] and organozinc compounds (Negishi reaction),[16] boronic acids (Suzuki-Miyaura reaction)[17] and corresponding esters, silanes and silanols (Hiyama-Denmark reaction)[18, 19] and stannanes (Migita-Kosuge-Stille reaction).[20] Despite each of them is preferable in one or other case, none of them has been demonstrated as an orthogonal cross-coupling agent. In this context, one of 14 group elements, germanium, stayed in the shadow of silicon and tin for a long time and appeared scarcely explored being historically considered as invalid in cross-coupling reactions possessing low reactivity.[21] However, our group has shown that aryl germanes are able to participate in such type reactions with sufficiently electrophilic catalysts. For instance, utilization of Pd-nanoparticles in a reaction between aryl germanes and iodonium salts as well as iodoarenes facilitates the coupling unlike common Pd-complexes.[22] This discovery clearly demonstrates that properly selected catalytic species demonstrating high electrophilicity makes C-Ge bond activation feasible.

While the most common metal catalysis is based on Cu-, Ni- and Pd-complexes,[14] gold was considered as a "catalytically dead" metal for a long time.[23] However, huge aspiration to involve gold into catalysis of the last decades (so called "gold rush") gave rise to numerous investigations, which shed light on its catalytic potential and proved itself as a powerful alternative, particularly in biaryl bond formation.[24-26] Also, it enables C-H functionalization and at the same time provides the advantage of tolerating reactive halogen sites.[27-29] Given the fact that common metals rely on C-X bond (X = Cl, Br, I, OTf) activation, this aspect allows gold-catalysis to implement orthogonality and modularity in cross-coupling reactions making it a powerful synthetic approach.

Later intensive investigations revealed a profitable combination of Au-species and diazonium salts assisted by light.[30] This led to the novel cross-coupling reactions with milder conditions involving various nucleophilic reagents. For instance, Lee and Fouquet have independently developed Au-catalyzed coupling between aryl boronic acids and diazonium salts[31, 32] (**Figure 2, A**). Both protocols allow an effective biaryl formation with a wide range of salts, but the Fouquet's method also involves electron-rich salts. However, both reactions suffer from necessity of a photocatalyst and competitive hydrolysis of boronic acids. Later, Hashmi and coworkers improved the reaction conditions by switching to (p-$CF_3C_6H_4)_3PAuCl$ instead of $(Ph_3P)AuCl$ and removal the photocatalyst[33] (**Figure 2, B**). Then, Patil and coworkers reported light-mediated Au-catalyzed cross-coupling reaction employing aryl silanes with diazonium salts[34] (**Figure 2, C**). The main issue of the method consists in requirement of additionally Cu-catalyst, Ru-photocatalyst and a base. Moreover, only electron-poor diazonium salts showed high yields while the scope of silanes is limited mainly to ones bearing heterocycles. An analogous reaction with aryl stannanes, developed by the same group, proceeds without light and any additives in contrast to silanes[35] (**Figure 2, C**). But toxicity of organostannanes complicate their utilization and compel to find safer alternatives. Moreover, electron-rich diazonium salts showed poor reactivity in the transformation. Later, Hashmi and coworkers improved the method with aryl silanes using solely $(Ph_3P)AuNTf_2$ as a catalyst under blue light irradiation[36] (**Figure 2, D**). The reaction appeared site-selective towards various boron-based handles, such as Bpin, Bnep or BMIDA, and halogens, reacting exceptionally with C-Si site. In addition to it, successfully demonstrated sequential functionalization of the resulting BR_2-containing biaryls enhances synthetic potential of the developed reaction. However, no orthogonality and selectivity towards other relative transmetalation handles and electrophilic centers were demonstrated. Also, unlike the previously mentioned protocols, the more expensive Au-catalyst was utilized. Furthermore, only electron-poor diazonium salts showed the highest yields.

Figure 2 | Gold-catalyzed arylation of aryl boronic acids, silanes and stannanes with diazonium salts.

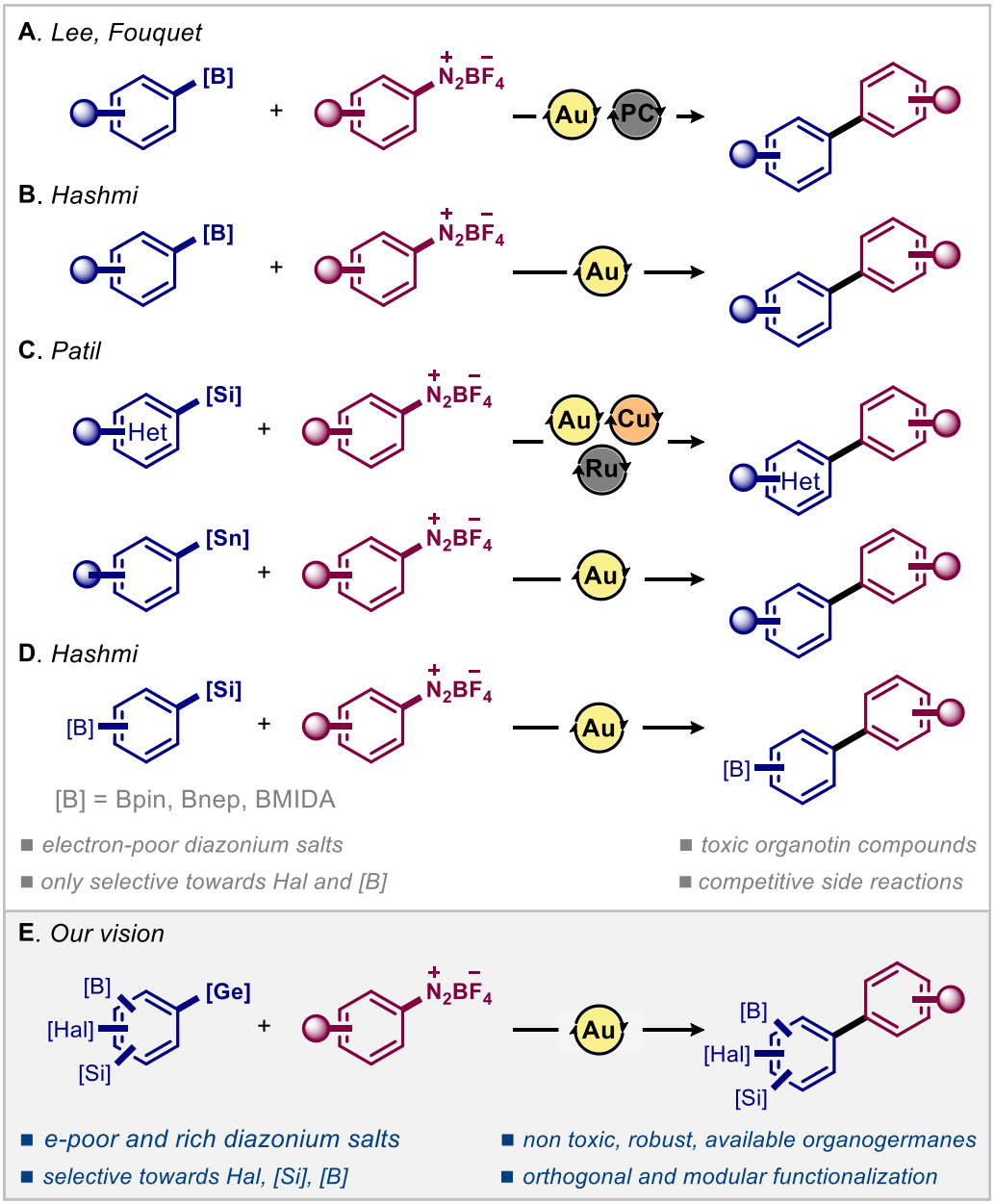

All above-mentioned allows to conclude that a modular and orthogonal approach, tolerating a wider range of transmetalation functionalities and extension to electron-efficient diazonium salts is still an unsolved challenge. Combining these aspects, we set out to develop alternative strategy allowing for truly orthogonal and site-selective coupling with both electron-poor and rich diazonium salts. In the context of orthogonality challenge, aryl germanes can serve as a great platform owing to their robustness and high reactivity. Moreover, their non-toxic and low volatile nature makes them greener alternative in comparison to other functionalities (**Figure 2, E**). Though recently our group has reported an oxidative C-H arylation of simple and polyfluorinated arenes with aryl germanes via activation of C-Ge bond with highly electrophilic $Au^{(III)}$,[37, 38] the reactions require a stoichiometric amount of an external oxidant to support $Au^{(I)}/Au^{(III)}$ catalytic cycle, which can significantly diminish functional group tolerance, and low regioselectivity for arenes resulting in a mixture of the regioisomers. The advantage of aryl diazonium

salts is ability to play a role of both regioselective cross-coupling partner and a strong oxidant for Au-catalyst in assistance with light. Additionally, release of N_2 as a side product makes the reaction ecologically-friendly and enhances its atom economy similar to that, which is achieved in the mentioned reaction with arenes.

We commenced our study using triethyl(4-fluorophenyl)germane and *p*-nitrobenzenediazonium tetrafluoroborate with various the most common $Au^{(I)}$ sources as a potential catalyst and acetonitrile as a solvent (**Table 1**). The screening showed that commercially available, air-stable $(Ph_3P)AuCl$, was the optimal for the cross-coupling reaction. Notably, the presence of a $[Ru(bpy)_3](PF_6)_2$ as a photocatalyst significantly decreased the yield of the desired product. Also, unlike the protocol reported for aryl silanes there is no necessity of using air-, light-, temperature-sensitive and more expensive $(Ph_3P)AuNTf_2$ in our reaction, although it leads to the similar outcome as $(Ph_3P)AuCl$. Moreover, the reaction time appeared significantly shorter than for aryl silanes and aryl stannanes. The use of the optimized conditions resulted in the corresponding product **1** with 96% yield after isolation providing a clean and smooth coupling without undesired side-processes, such as homocoupling of the aryl germane or protodegermylation.

Table 1 | Screening of $Au^{(I)}$-precatalysts.

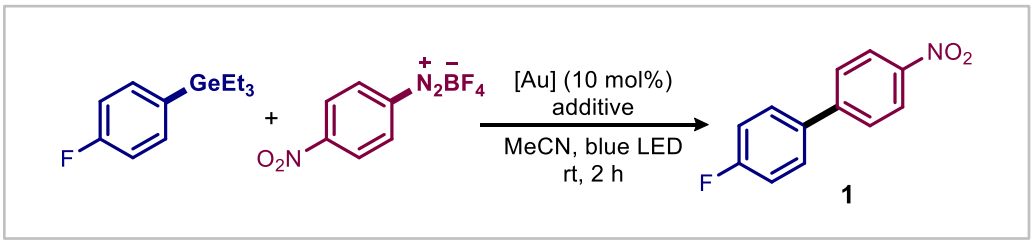

Entry	[Au]	Additive	Yield of 1, %[a]
1	**$[(Ph_3P)AuCl]$**	**–**	**99**
2	$[(Ph_3P)Au]NTf_2$	–	93
3	$[(Me_2S)AuCl]$	–	40
4[b]	$[(Ph_3P)AuCl]$	$[Ru(bpy)_3](PF_6)_2$	67

Reaction conditions: $ArGeEt_3$ (0.05 mmol, 1.0 equiv.), ArN_2BF_4 (0.075 mmol, 1.5 equiv.), $(Ph_3P)AuCl$ (0.005 mmol, 10 mol%), MeCN (0.5 ml), blue LED, rt, 2 h. [a]^{1}H NMR yields are given. [b]$[Ru(bpy)_3](PF_6)_2$ (0.00125 mmol, 2.5 mol%) was used.

With the optimized conditions in hand, next we explored the scope of the reaction testing various aryl germanes and electron-poor diazonium salts (**Table 2**). The complete inertness of $(Ph_3P)AuCl$ towards oxidative addition with aryl halides is an important benefit in the reaction with highly functionalized compounds. Thus, we showed a possibility of achieving excellent yields of the products derived from aryl germanes bearing Cl, Br and I atoms with a number of diazonium salts (**2**-**5**). Highly deactivated containing fluorine was successfully coupled as well (**6**). Electron-rich heteroaromatic germanes, such as sterically bulky isoxazole (**7**), both 2- and 3-thiophenes (**8**, **9**) and 1,3-benzodioxole (**10**) are successfully tolerated, which is challenging for Suzuki-Miyura cross-coupling[39] and previously accessible in the reaction with silanes with the additions of metal catalyst, photocatalyst and base.[34]

Table 2 | Scope for light-mediated Au-catalyzed cross-coupling of aryl germanes and aryl diazonium salts.

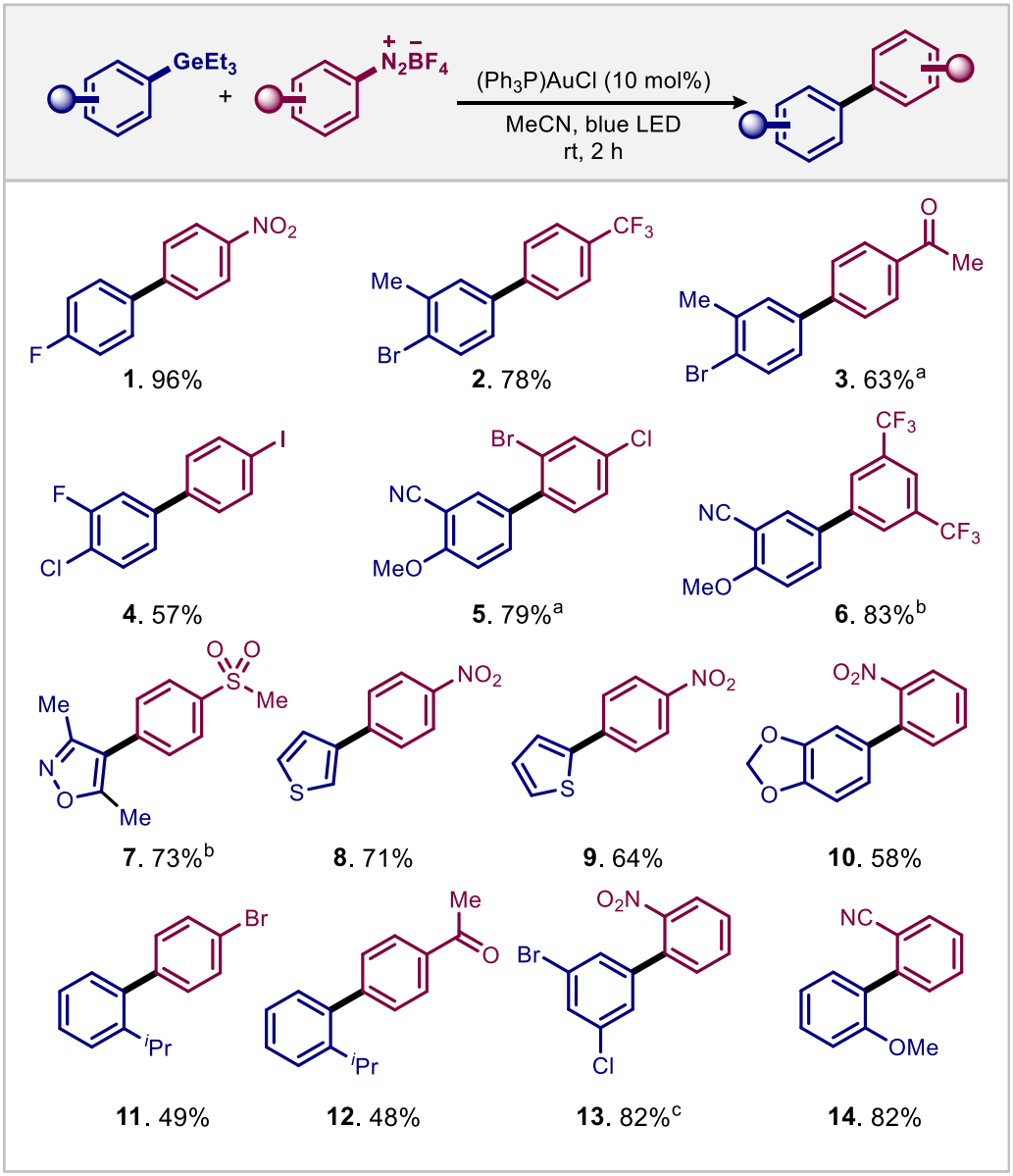

Reaction conditions: $ArGeEt_3$ (0.3 mmol, 1.0 equiv.), ArN_2BF_4 (0.45 mmol, 1.5 equiv.), $(Ph_3P)AuCl$ (0.03 mmol, 10 mol%), MeCN (3.0 ml), blue LED, rt. Isolated yields are given. [a]3 h reaction time. [b]16 h reaction time. [c]5 h reaction time.

Another challenge in silane chemistry is poor conversion of *ortho*-substituted substrates.[40] In this context, *ortho*-substituted aryl germanes show moderate yields with sterically demanding ^{i}Pr-group (**11**, **12**). Tolerance of *ortho*-substituents also extends to diazonium salts. High yields were obtained with salts containing NO_2- (**13**) and CN-groups (**14**) in *ortho*-position. The latter was successfully coupled with *ortho*-substituted germane giving the 3,3'-substituted 2-2'-biphenyl motif.

Selective transformation at a desired site in poly-substituted molecule is utmost of interest when it comes to the synthesis of highly functionalized species. As such, we investigated the selectivity of the cross-coupling reaction in both intra- and intermolecular reactions, versus R_3Si and BR_2 transmetalation handles (experiments with Bpin-containing germanes were done by A. Dahiya). The intramolecular tolerance of these functionalities is demonstrated in **Table 3**, which shows multiple examples of the complete preferential reactivity at C-Ge site in arenes, containing TMS (**15**-**20**). The corresponding

products were isolated in high yields for all mentioned groups and no side products were observed, which demonstrate superior reactivity of germanes and makes their sequential functionalization possible.

Attempts to couple electron-rich diazonium salts showed a significant deviation in their reactivity in comparison with electron-poor substrates. The absence of any observed products indicates no ability of the electron-rich diazonium salts to react with $Au^{(I)}$. We assumed that electron-donating groups can significantly decrease oxidation potentials of diazonium salts, which is the reason of their low reactivity in our reaction. Previously, Fouquet and coworkers showed that addition of a photocatalyst in a similar $Au^{(I)}$-catalyzed cross-coupling of aryl boronic acids with electron-efficient diazonium salts significantly improves yields of products.[32] Stoichiometric experiments (performed by Dr. G. Sherborne and A. Dahiya) confirm that electron-rich diazonium salts react with the photocatalyst under visible light, but stay inert to $Au^{(I)}$. Presumably, the aryl radical, produced after reduction of a diazonium salt by the photocatalyst, undergoes SET with $Au^{(I)}$, forming unstable $Au^{(II)}$, which in its turn is able to undergo disproportionation and followed by a homocoupling of aryl germane. For this reason, we explored the reactivity with a wide range of bidentate stabilizing ligands, pursuing suppression of homocoupling reaction. However, despite the tested ligands were not able to fully inhibit the undesired reaction, we found that dppe was the most efficient ligand, providing the productive coupling in a 4.5:1 ratio for the given substrates (see Supporting Information). With these conditions, we assessed the isolated yields and scope possible with electron-rich diazonium salts (**Table 4**). To our delight, we found consistently great reactivity for highly electron-rich *p*-methoxybenzenediazonium tetrafluoroborate with various aryl germanes (**21**-**23**). The halogen and Me_3Si-selectivity were found to be retained from the photocatalyst-free conditions, with no reaction observed on these sites despite the high reactivity, with reactions completed after 2 hours (**24**-**26**), though some quantity of homocoupled aryl germane was observed. Moreover, diversity in both aryl germane and diazonium salt is well tolerated with alkyl, phenyl diazoniums giving particularly high yields in combination with electron deficient germanes. Also, heterocyclic germane was successfully coupled affording the biaryl in a good yield (**27**). Slightly decreased yield was achieved in case of *ortho*-substituted aryl germane (**28**).

Table 3 | Scope for selectivity of $GeEt_3$ over $SiMe_3$ in the cross-coupling reaction.

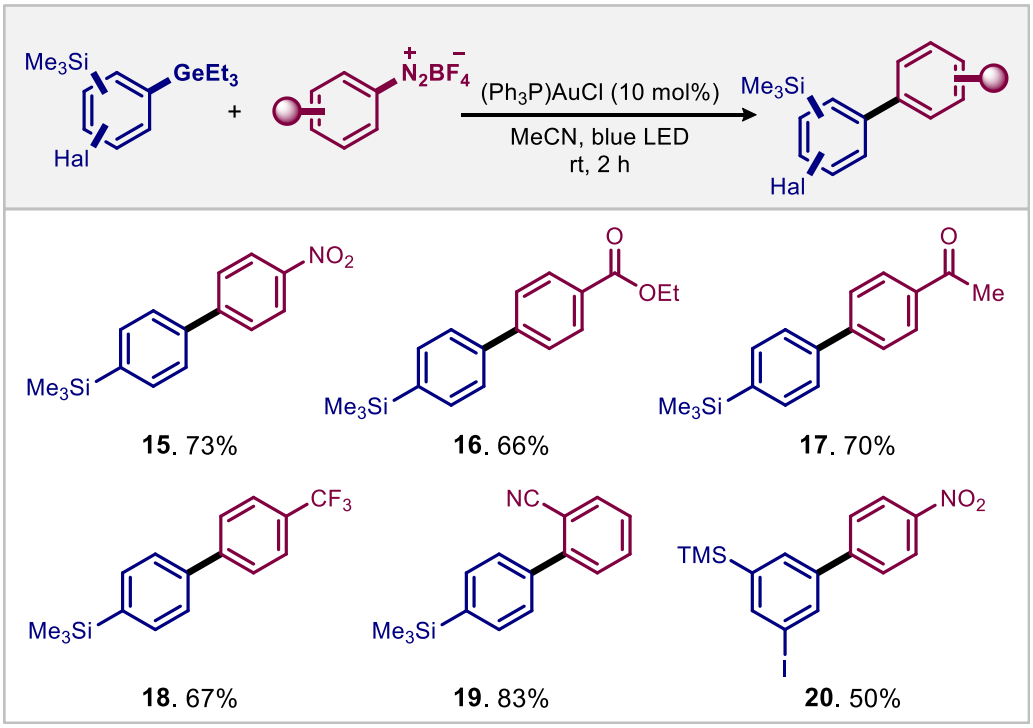

Reaction conditions: $ArGeEt_3$ (0.3 mmol, 1.0 equiv.), ArN_2BF_4 (0.36 mmol, 1.2 equiv.), $(Ph_3P)AuCl$ (0.03 mmol, 10 mol%), MeCN (3.0 ml), blue LED, rt. Isolated yields are given.

Intrigued by such new reactivity we continued mechanistic investigation to reveal the difference between pathways of electron-poor and rich salts. As expected, UV/Vis analysis confirms that neither aryl germane nor $(Ph_3P)AuCl$ absorb in visible light. Also, replacement of NO_2-group with electron-donating OMe-group in *para*-position of aryldiazonium salt causes hypsochromic shift leading to absorption in UV range. Though switching from blue light to UV light does result in full consumption of the salt, only traces of the desired product were detected, indicating another aspect of the divergence (see Supporting Information). For clearer understanding of such different reactivity, our colleague, Dr. I. Funes-Ardoiz, performed DFT investigation of the reaction mechanism (**Figure 3**).

Table 4 | Scope for electron-rich diazonium salts in the cross-coupling reaction.

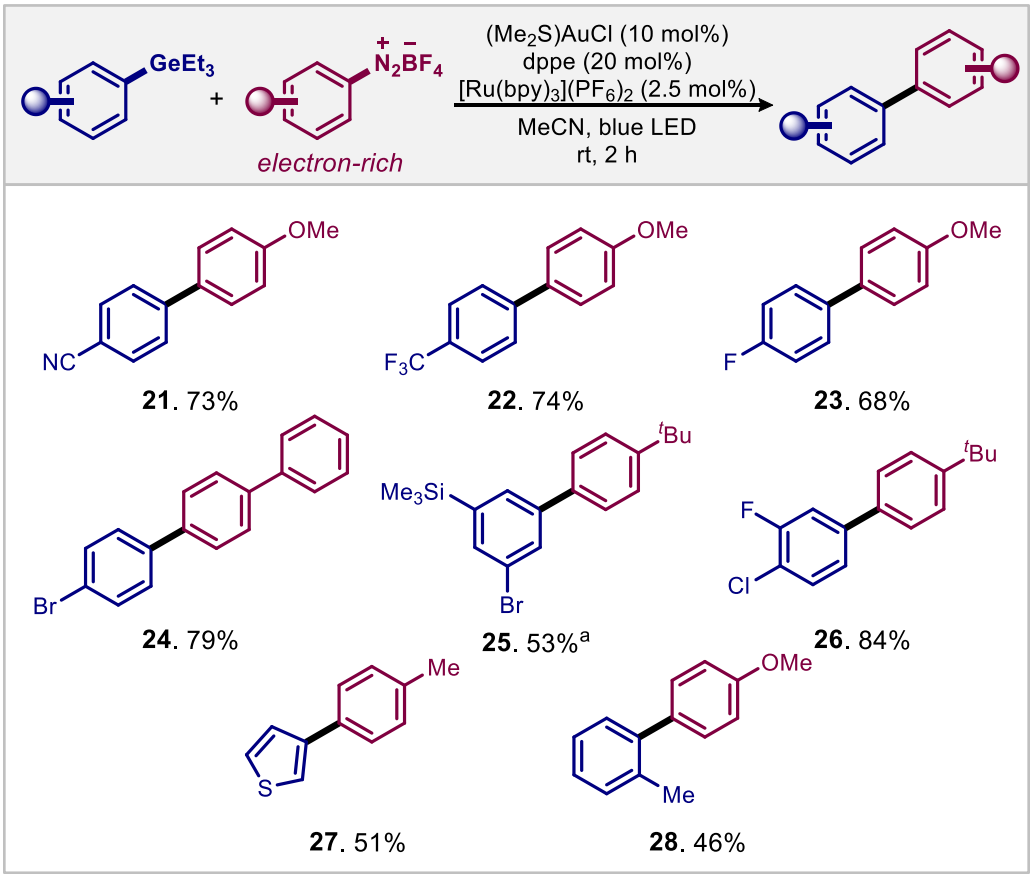

Reaction conditions: $ArGeEt_3$ (0.3 mmol, 1.0 equiv.), ArN_2BF_4 (0.6 mmol, 2.0 equiv.), $(Me_2S)AuCl$ (0.03 mmol, 10 mol%), dppe (0.06 mmol, 20 mol%), [Ru(bpy)3](PF6)2 (0.0075 mmol, 2.5 mol%), MeCN (3.0 ml), rt. Isolated yields are given. [a]1.2 equiv. of ArN_2BF_4 used.

According to the calculations (at the CPCM (MeCN) M06L/6-311++G(d,p)//ωB97XD/6-31G(d) (LANL2DZ for Au and Ru) level of theory), after photoexcitation a complex of $Au^{(I)}$-catalyst with diazonium salt undergoes ISC (Intersystem Crossing) to reach triplet state, which is possible for heavy elements like gold due to spin-orbit coupling.[41] Also, the DFT analysis claims that the fate of the triplet state gold-diazonium species (**^{3}I1** and **^{3}I1'**) depends on electronics of the diazonium salt. The complex with an electron-poor salt **^{3}I1** preferably undergoes arylation of gold with N_2 extrusion (**^{3}I3**). However, for an electron-rich salt ISC of **^{1}I1'** is accompanied by its dissociation to $Au^{(I)}$ and diazonium biradical-cation. For the latter decomposition with N_2 release (**^{3}I2'**) appears more favorable, which therefore leads to no product formation. Thus, computational investigation supports the outcomes observed both in blue and UV light experiments. Combining experimental observations, computational interrogation and our previous reports of $Au^{(III)}$ activation of aryl germanes, we proposed two simplified catalytic cycles, driven by the electronics of the diazonium salt and ligand system (**Figure 3**). In the case of electron-deficient diazonium salts, we envision that the $Au^{(I)}$-catalyst (**I**) undergoes oxidation by the aryl diazonium in the presence of visible light, driven by the irreversible release of N_2 gas and resulting in $Au^{(III)}Ar$ species (**II**).[36, 42, 43] As we have previously reported, this $Au^{(III)}$ cation will activate the aryl germane through S_EAr *ipso*-substitution (**III**) followed by release of the product and regeneration of $Au^{(I)}$. In opposite to electron-poor salts, electron-rich ones require the mediation of a photocatalyst, $[Ru(bpy)_3](PF_6)_2$. Oxidation of the excited photocatalyst $[Ru]^{2+*}$ by a diazonium salt produces an aryl radical with N_2 release. A subsequent reaction

of the aryl radical with the bisligated gold complex forms $Au^{(II)}$ species (**IV**), which reduces $[Ru]^{3+}$ to regenerate the photocatalyst and results in $Au^{(III)}$ formation (**V**), which undergoes transmetalation with aryl germane (**VI**) followed by reductive elimination of the biaryl.

Figure 3 | DFT analysis of the Au-catalyzed photomediated cross-coupling reaction and proposed mechanisms.[i]

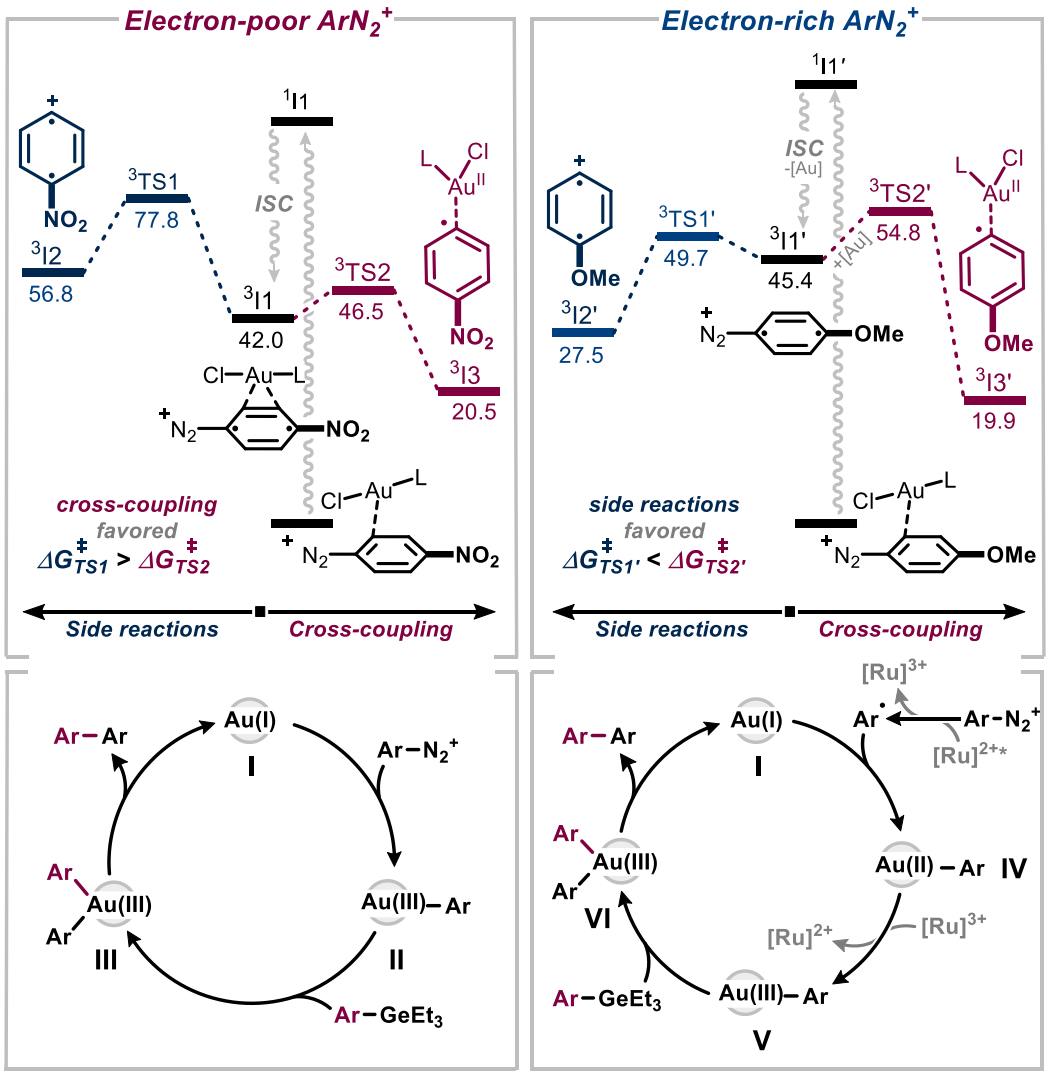

To demonstrate the applicability of the germane functionality to more complex syntheses, we sought to diversify from two simple aryl germane starting materials, harnessing the reactivity, selectivity and orthogonality of the functional group (**Figure 4**). The arylation of di- (**29**) and trisubstituted (**30**) germanes is facile and selective for the germane under our $Au^{(I)}$ conditions, leaving the C-Br and C-Si functionalities untouched. C-Br site is available, for instance, for carbon-carbon cross-coupling reactions such as $Pd^{(I)}$-I dimer catalyzed alkylation established by our group. The remaining TMS site can be excellently converted into phenol ester enabled by Pd-catalysis or electrophilically halogenated. Overall, these synthetic routes show modularity and orthogonality of poly-substituted aryl germanes and great potential in synthesis of highly functionalized molecules (**31**, **32**).

[i]The figure adapted from our publication.[1]

Figure 4 | Modular and orthogonal functionalization of poly-substituted aryl germanes.

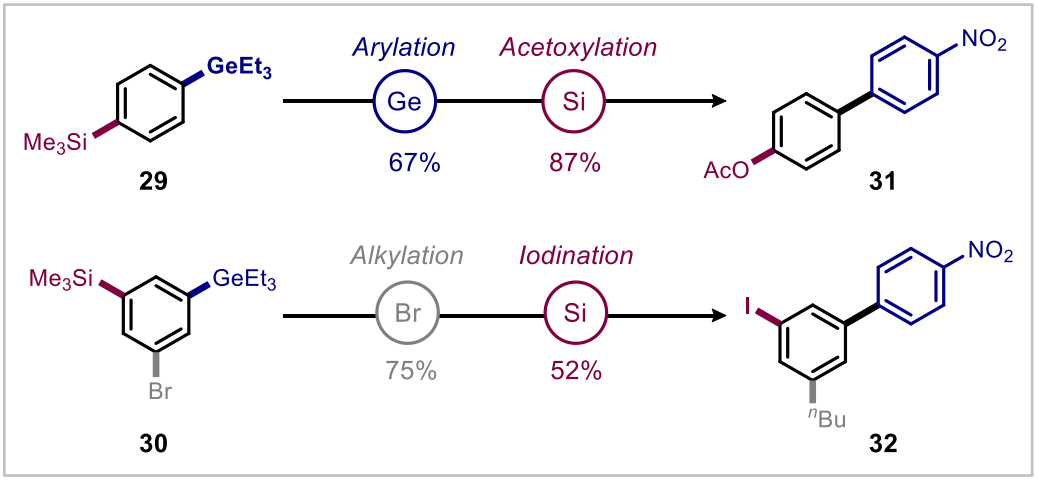

Reaction conditions. *Arylation*: $ArGeEt_3$ (0.3 mmol, 1.0 equiv.), ArN_2BF_4 (0.36–0.45 mmol, 1.2–1.5 equiv.), [$(PPh_3)AuCl$] (0.03 mmol, 10 mol%), MeCN, rt. *Acetoxylation*: $ArSiMe_3$ (0.2 mmol, 1.0 equiv.), $PhI(O_2CCF_3)_2$ (0.3 mmol, 1.5 equiv.), $Pd(OAc)_2$ (0.01 mmol, 5 mol%), AcOH, 80 °C. *Alkylation*: ArBr (0.2 mmol, 1.0 equiv.), ^{n}BuZnCl/LiCl (0.46 mmol, 2.3 equiv.), $Pd^{(I)}$-I-dimer (0.005 mmol, 2.5 mol%), PhMe/THF, rt. *Iodination*: $ArSiMe_3$ (0.3 mmol, 1.0 equiv.), NIS (0.6 mmol, 2.0 equiv.), *p*TsOH (0.6 mmol, 2.0 equiv.), $CHCl_3$, rt. Arylation of **30** was done by Dr. Grant Sherborne.

In conclusion, we have developed the mild and efficient arylation of aryl germanes using diazonium salts, catalyzed by simple $Au^{(I)}$ catalyst systems. Expansion of the scope to electron-rich diazonium salts was enabled through mechanistic interrogation and addresses the inherent difficulty in combining $Au^{(I)}$ catalysis with these substrates. Selectivity and orthogonality of the reaction was shown in multiple intra- and intermolecular competition experiments against commonly employed Bpin and $SiMe_3$ reagents. The demonstration of chemoselectivity in the presence of aryl halides, silanes and boronic esters was further showcased by the diversification of simple precursors to a wide selection of highly functionalized arenes. These developments represent important progress in the area of selective functionalizations, adding an extra dimension of chemoselectivity, while expanding the scope of arylation reactions to access previously challenging substrates.

2

Site-selective Conversion of $C_{(sp^2)}$-Ge to $C_{(sp^2)}$-X Bond

---

The results described in this chapter were published in Journal of American Chemical Society[44] and Organic Letters.[45] Experimental work was carried out in collaboration with other member of Schoenebeck group, whose contributions are stated in the corresponding subchapter.

---

2 Site-selective Conversion of $C_{(sp^2)}$-Ge to $C_{(sp^2)}$-X Bond

2.1 Pd-catalyzed Coupling of Aryl Germanes with Alcohols and Carboxylic Acids

Experimental work was performed in collaboration with other members of Schoenebeck group: Amit Dahiya. The results described in this chapter were published in Journal of American Chemical Society.[44]

The C-O bond is an important structural part widely spread among numerous natural compounds[46] and pharmaceuticals.[47-49] One of the well-known reactions, Williamson reaction from 1850, historically was a main synthetic tool to form various ethers.[50] However, it is limited to primary and secondary alkyl halides and suffers from side-reaction of dehydrohalogenation,[51, 52] especially in case of secondary and tertiary reagents. Another C-O reaction, Ullmann condensation, discovered in 1905, opened a pathway to diaryl ethers, consisting in Cu-catalyzed reaction between aryl halides and phenols.[53] It had been being utilized for 50 years and became a focus of detailed investigation.[10, 54, 55] The drawbacks of the original method are requirement of elevated temperatures (≥ 130 °C), prolonged reaction time and competing side reactions.[56, 57] For this reason, later the protocol was significantly improved, namely by involvement of ligands and bases, which allowed to perform the transformation in milder conditions.[58, 59] However, the necessity of additives and no selectivity for C-X bond (X = Br, I) limits scope of the reaction.

Development of C-O bond couplings of the last decades started from introducing of Pd-catalysis in a reaction between aryl halides and alcohols discovered by Buchwald,[60-63] Hartwig[64-66] and Beller.[67, 68] Despite it opens access to a wide range of aryl alkyl ethers, the reported protocols require high temperatures (≥ 80 °C) and special ligands. Moreover, no tertiary alcohols or carboxylic acids were presented in the scope while the coupling with secondary alcohols appeared less productive due to competing β-hydride elimination.[69-72] Also, the main and common disadvantage of the reported methods is complete absence of chemo- and site-selectivity towards (pseudo)halogens or organometallic moieties. Though the coupling with secondary and even tertiary alcohols (using a Ni-catalyst) became possible in following improved methods, necessity of bulky, expensive, non-commercial ligands and chemoselectivity still remain challenging.[72-74]

Figure 5 | The current state of the art and challenges of metal catalyzed C-O bond formation.

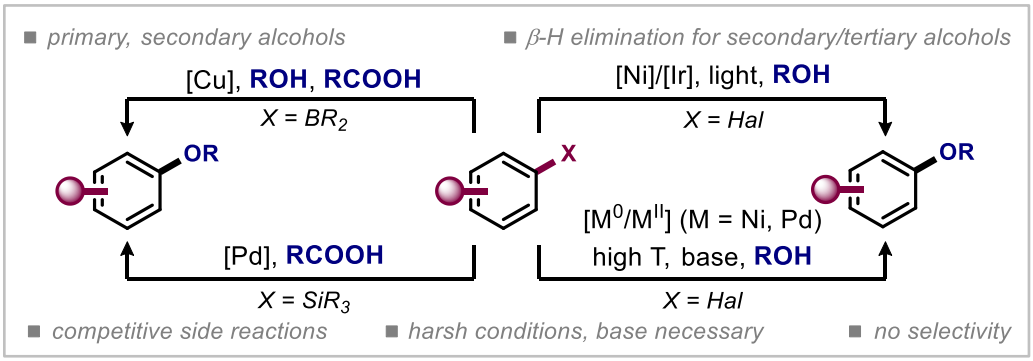

Huge progress in C-O coupling development was achieved by MacMillan and coworkers by introducing visible light. Indeed, Ni-catalyzed etherification supported by photoredox catalysis provides mild conditions and covers a wide range of primary, secondary alcohols and even water.[75] However, utilization of aryl bromides and absence of halogenated examples limit the scope excluding their modular functionalization. The following similar protocol published by the same group broaden the scope with application of carboxylic acids, but solves none of other mentioned challenges.[76]

Along with halogens other reactive motifs, such as boronic acids and their esters or silanes, were demonstrated as possible alternatives for the transformation. For instance, Cu-catalyzed oxygenation of boronic acids and esters almost simultaneously reported by Chan, Lam and Evans[77-80] (known as Chan-Lam-Evans reaction) proceeds in milder conditions (room temperature), in air and needs no ligand unlike the protocols relying on Ni- or Pd-catalysis. Moreover, it was demonstrated that the conditions tolerate halogens. However, owing to their high reactivity boron-based substrates can undergo undesired reactions, like oxidation or protodeboronation, especially known for polyfluorinated boronic acids.[39, 81, 82] Recently, Kitamura and co-workers published oxidative Pd-catalyzed esterification of aryl silanes.[83] The reaction provides smooth conversion of C-Si to C-O bond in the presence of a wide range of substituents, including halogens. But harsh conditions, usage of neat carboxylic acids for most of examples and no report about chemoselectivity towards relative moieties, for instance Bpin, diminish synthetic value of the reaction (**Figure 5**).

To overcome all above-mentioned challenges, we decided to develop a new chemoselective method of C-O bond formation, tolerating a wide range of highly reactive sites. Previously, we have demonstrated organogermanes as robust, non-toxic cross-coupling reagents, providing highly site-selective, modular and orthogonal transformations[84] and seem to be a powerful alternative for a potential C-O coupling. Given the fact that they stay inert in canonical $Pd^{(0)}/Pd^{(II)}$ catalysis and tend to react with highly electrophilic species, we assumed that switching to $Pd^{(II)}/Pd^{(IV)}$ catalytic cycle is more prone to implement activation of C-Ge bond. In this context, hypervalent iodine reagents were employed as strong oxidants in a number of Pd-catalyzed transformations, including C-O bond coupling.[85-89] For this reason, we initiated our experiments using Pd-catalyst in combination with a hypervalent iodine compounds supporting $Pd^{(II)}/Pd^{(IV)}$ redox reaction. After screening of several iodine-based oxidants (performed by Amit Dahiya) bis(trifluoroacetoxy)iodobenzene ($PhI(O_2CCF_3)_2$, PIFA) was the optimal oxidant resulting in selective conversion of C-Ge at room temperature with high rate.

With the C-O bond formation of an aryl germane in a hand, we explored the scope and focused our attention on the challenge of chemo- and site-selective C-O bond formation with aryl germanes containing competing reactive sites, such as C-X (X = Cl, Br, I, OFs), C-$SiMe_3$ and C-Bpin (**Table 5**). Pleasingly, mild conditions resulted in highly selective oxygenation, exclusively reacting at C-Ge site and gave the corresponding products in high yields (**1**-**9**). Considering the fact that most of established protocols involve halogenated substrates in C-O coupling, tolerance of halogens and pseudohalogens opens pathways for further molecule transformations (**1**-**6**). Notably, Bpin-containing aryl germanes require lower catalyst loading (1 mol%) to achieve higher yields (**7**, **8**). Eventually, C-Si bond stays fully untouched despite the excess of alcohol (**9**).

Table 5 | Selectivity of C-Ge site over the other functionalities in Pd-catalyzed etherification.

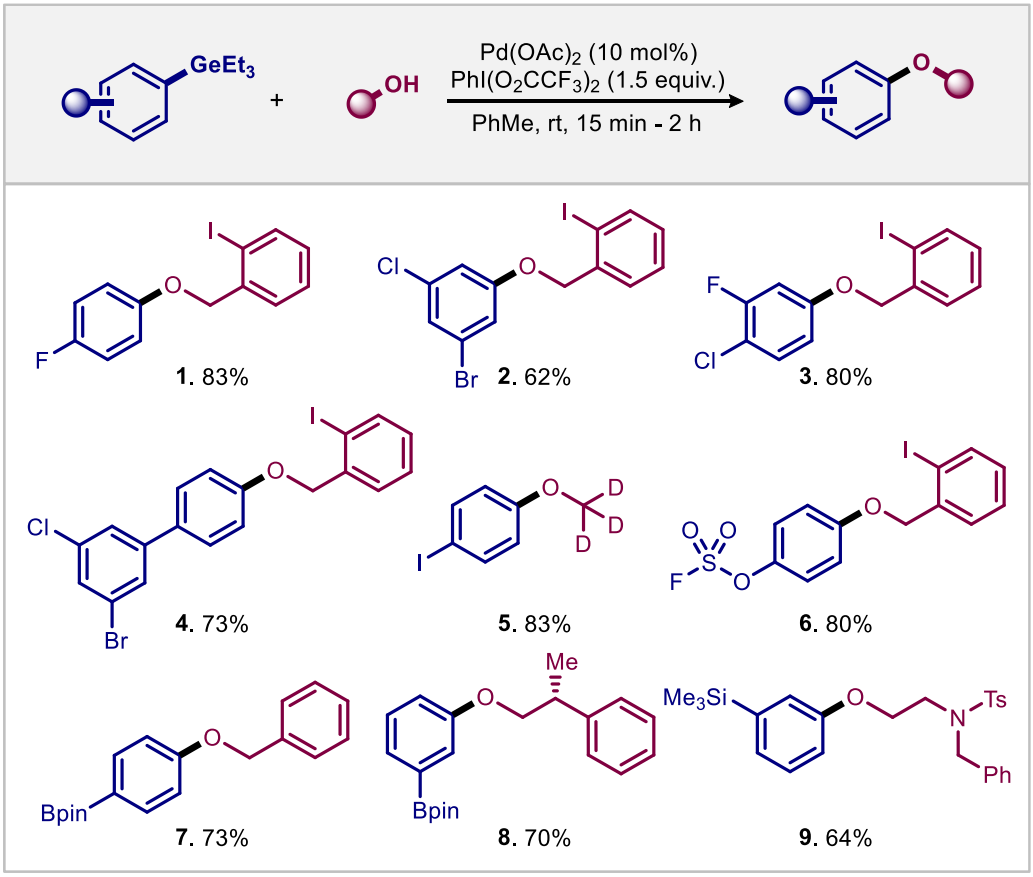

Reaction conditions: $ArGeEt_3$ (0.3 mmol, 1.0 equiv.), ROH (1.5 mmol, 5.0 equiv.), $Pd(OAc)_2$ (0.03 mmol, 10 mol%), $PhI(O_2CCF_3)_2$ (0.45 mmol, 1.5 equiv.), PhMe (1.2 ml), rt, 15 min – 2 h. Isolated yields are given.

Reactions with primary alcohols, possessing chiral centers, such as prolinol or serine, proceeds smoothly and without racemization (**10**-**13**) (**Table 6**). Moderate yields were obtained for the coupling of heterocyclic germane, namely containing thiophene core (**14**, **15**). As for more challenging secondary and tertiary alcohols, experiments demonstrate their full compatibility with the conditions, affording the desired products (**16**-**22**) without detrimental β-hydride elimination. Despite our investigations employed substrates bearing $GeEt_3$ as a key reactive site, which is derived from the most commercially available source, other trialkylgermanium motifs are also effective. For instance, both $GeMe_3$ (**23**) and bulkier Ge^nBu_3 (**24**) display the same reactivity, leading to the desired ethers in high yields.

To highlight orthogonal reactivity of aryl germanes, we applied them in the different typical conditions of C-O coupling, for instance typical $L_nPd^{(0)}/L_nPd^{(II)}$ catalyzed C-O bond formation[68] (**25**), Ni-catalyzed photoredox coupling[75] (**26**) and Cu-catalyzed Ullmann reaction[58] (**27**) (**Figure 6**). All mentioned protocols exclusively functionalize C-X site (X = Br, I) while Chan-Lam reaction proceeds only with C-Bpin oxygenation (**28**). Moreover, C-[Ge] site underwent no transformation even under those conditions, which employ a base and/or high temperature. These results confirm not only high robustness of aryl germanes, but also their orthogonal nature.

Table 6 | General scope of Pd-catalyzed etherification of aryl germanes.

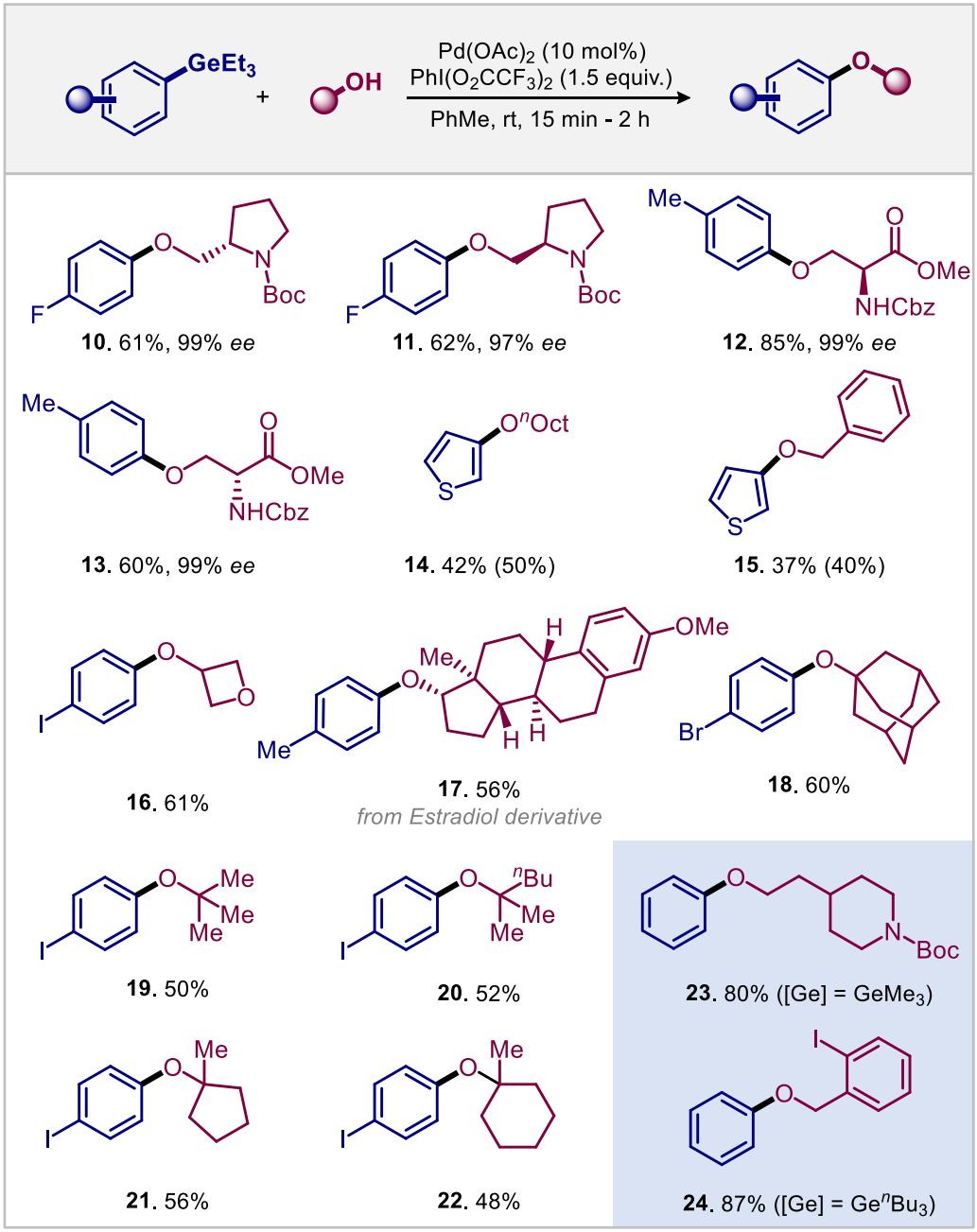

Reaction conditions: $ArGeEt_3$ (0.3 mmol, 1.0 equiv.), ROH (1.5 mmol, 5.0 equiv.), $Pd(OAc)_2$ (0.03 mmol, 10 mol%), $PhI(O_2CCF_3)_2$ (0.45 mmol, 1.5 equiv.), PhMe (1.2 ml), rt. Isolated yields are given. ^1H NMR yield are given in parentheses.

Another type of O-nucleophile, carboxylic acids, were involved in the developed oxygenation. We focused on Me_3Si-substituted germanes to show superior reactivity of [Ge]-site since aryl silanes can be potentially coupled with the same approach (**Table 7**). However, for all examples no side oxygenation of [Si]-site was observed and exclusively products of C-Ge bond oxygenation were obtained (**29**-**34**). Furthermore, aryl germanes containing reactive C-Hal bonds are selectively converted in the corresponding esters as well (**35**, **36**).

Figure 6 | Orthogonality of aryl germanes in various C-O bond formation reactions.[a]

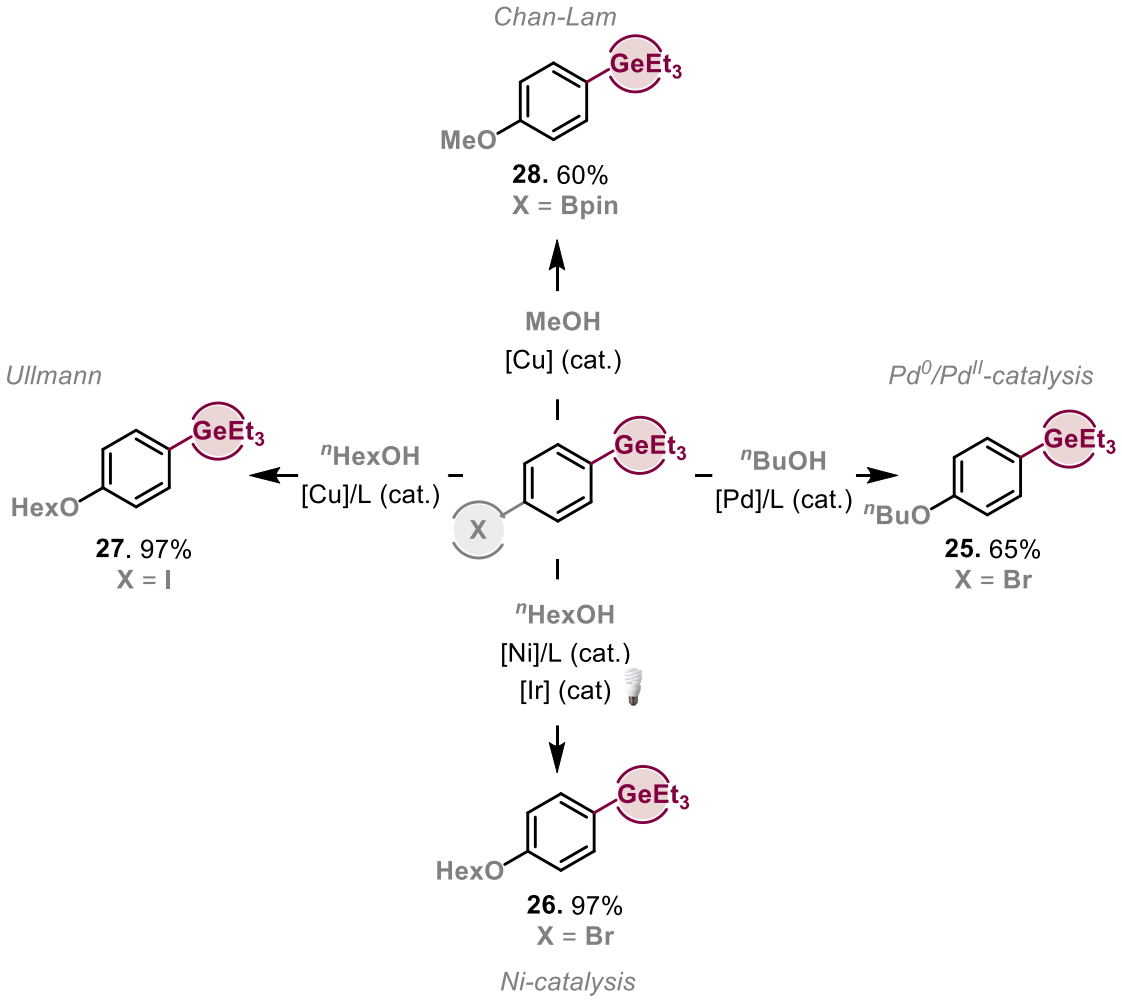

[a]For the experimental details see Supporting Information. Isolated yields are given. Hex represents *n*-hexyl.

Though 10 mol% of $Pd(OAc)_2$ were used for majority of the examples, we investigated dependence of the reaction time and the yield on the catalyst loading (**Table 8**). It was found that the decrease to 5 or even 1 mol% affected only on the reaction time, but still provides full conversion of the aryl germane. However, the lower amount of the catalyst, 0.1 mol%, significantly prolongs the reaction time resulting in 73% of the product in 48 h with unreacted germane observed. As expected, the absence of the Pd-source leads to no reaction. Subsequently, we tested a number of the examples in the reaction with 1 mol% $Pd(OAc)_2$, which were formed in the relatively same yields as with the standard loading.

Previously, our group has reported a cross-coupling reaction of aryl germanes and iodoarenes/diaryl iodonium salts enabled by Pd-nanoparticles.[22] To investigate transmetalation step of aryl germanes with Pd-species DFT calculations were applied, which showed that the transmetalation with $(Ph_3P)Pd(Ph)I$ is energetically quite unfavourable in opposite to nanoparticles. Intrigued by the high reactivity of Ge-site in the developed Pd-catalyzed oxygenation, we turned our attention to quantum chemical analysis to estimate ability of ligandless $Pd(O_2CCF_3)_2$, resulted in ligand exchange between $Pd(OAc)_2$ and PIFA, to activate C-Ge bond. DFT calculations show that *ipso*-substitution of $GeEt_3$ by $Pd(O_2CCF_3)_2$ is thermodynamically favourable, which can be accounted by high electrophilicity of Pd-center in comparison with ligated Pd-species (see Supporting Information).

Table 7 | Pd-catalyzed esterification of aryl germanes with carboxylic acids.

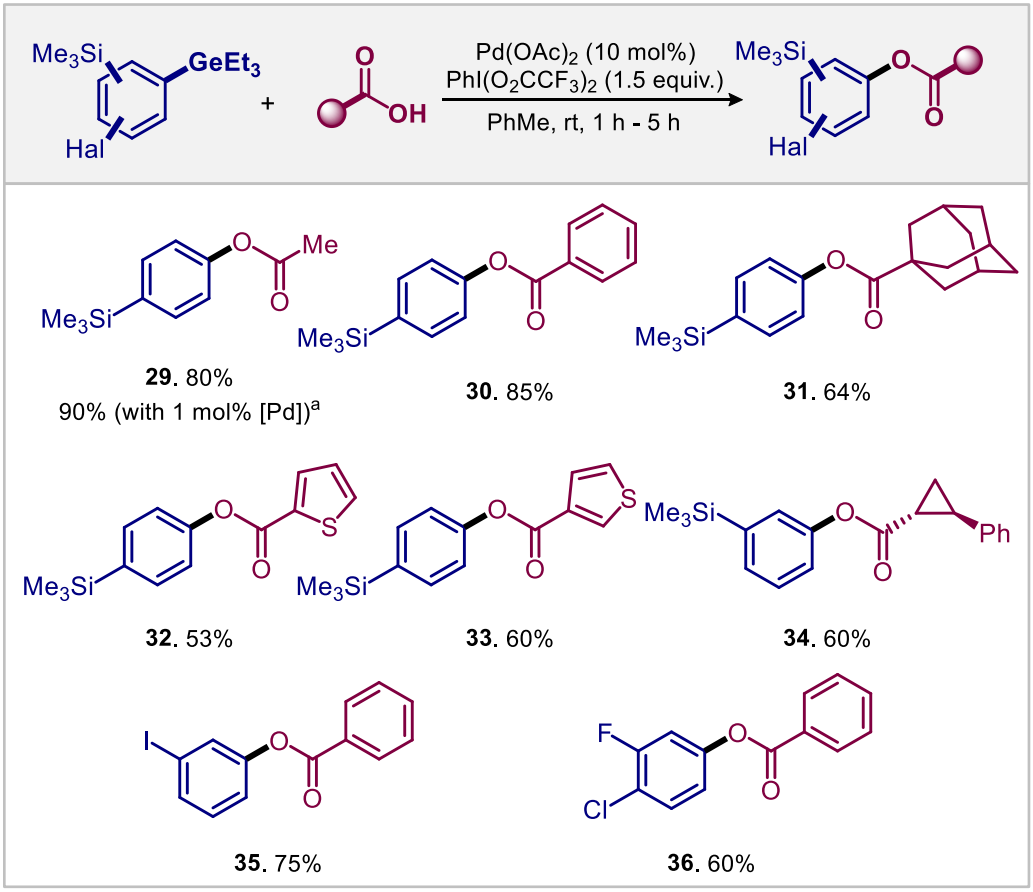

Reaction conditions: $ArGeEt_3$ (0.3 mmol, 1.0 equiv.), RCOOH (1.5 mmol, 5.0 equiv.), $Pd(OAc)_2$ (0.03 mmol, 10 mol%), $PhI(O_2CCF_3)_2$ (0.45 mmol, 1.5 equiv.), PhMe (1.2 ml), rt, 1 - 5 h. Isolated yields are given. [a]Yield determined by ^1H NMR.

To increase atom economy of the method we decided to explore the possibility of germanium recovery for its further reuse. Analysis of a crude mixture shows formation of $Et_3GeO_2CCF_3$ as a side product of transmetalation. Attempts to recover it by vacuum distillation failed or led to significant loss of the material. For this reason, we decided to quench it with excess of aryl Grignard by its direct addition to the crude mixture. This resulted in formation of the corresponding aryl germane isolated with 40% yield (see Supporting Information).

Table 8 | Pd-loading in the C-O bond coupling with aryl germanes.

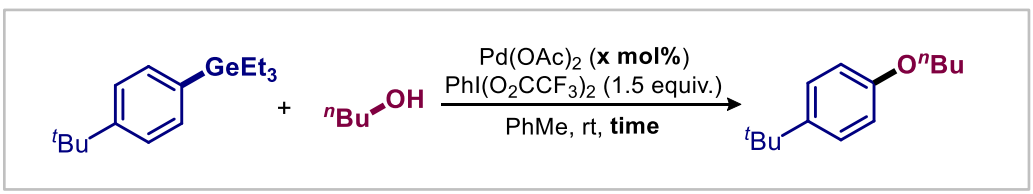

Entry	[Pd] loading, mol%	Time	Yield of the product, %
1	5	30 min	90
2	1	2 h	90
3	0.1	48 h	73
4	0	1 h	0

Yields determined by ^{1}H NMR. Reaction conditions: $ArGeEt_3$ (0.1 mmol, 1.0 equiv.), $^{n}BuOH$ (0.5 mmol, 5.0 equiv.), $Pd(OAc)_2$ (0.005 mmol, 5 mol%; 0.4 ml of stock solutions of $Pd(OAc)_2$ in anhydrous toluene (0.56 mg/mL and 0.056 mg/mL), 1 and 0.1 mol% respectively), $PhI(O_2CCF_3)_2$ (0.15 mmol, 1.5 equiv.), PhMe (0.4 ml), rt.

In conclusion, we have reported the first C-O bond coupling with aryl germanes. This atom-economical transformation is catalyzed by simple and commercially available $Pd^{(II)}$ precatalyst, require no special additives, such as ligand or base, and proceeds in mild conditions in short reaction times. The reaction demonstrates no air- or moisture-sensitivity, can proceed with lower catalyst loading with the relatively same effectiveness. Primary, secondary, tertiary alkyl alcohols and carboxylic acids were selectively coupled with C-GeR_3 site. All types of the reactive handles, such as (pseudo)halides, $SiMe_3$ and Bpin were fully tolerated. Moreover, the $GeEt_3$ moiety demonstrates orthogonality by staying fully untouched in other C-O bond couplings regardless of catalytic system, which also opens pathways for further molecule functionalization in modular and orthogonal fashion.

2.2 Site-selective Light-mediated Nitration of Aryl Germanes

Experimental work was performed in collaboration with other members of Schoenebeck group: Amit Dahiya and Dr. Aymane Selmani. The results described in this chapter were published in Organic Letters.[45]

Historically, nitration of organic compounds, particularly arenes, is one of classical and the most explored reactions in organic chemistry. Nitroarenes occupy a special place in industrial and commercial applications,[90] playing an essential role in agrochemistry, in synthesis of dyes, explosives and polymers.[91-95] Furthermore, they can act as cross-coupling partners[96] or precursors to anilines[97-99] or heterocycles.[96, 100] Also, many of nitroarenes demonstrate great bioactivity and found application in pharmacy (**Figure 7**).[101] One of them, Chloramphenicol, is the first and rare example of nitroarene, which occurs in the nature.[102] Thus, such diverse application together with rare natural abundance expectedly prompted chemists to develop synthetic routes to nitroarenes.

Figure 7 | Examples of nitroarenes possessing bioactivity.

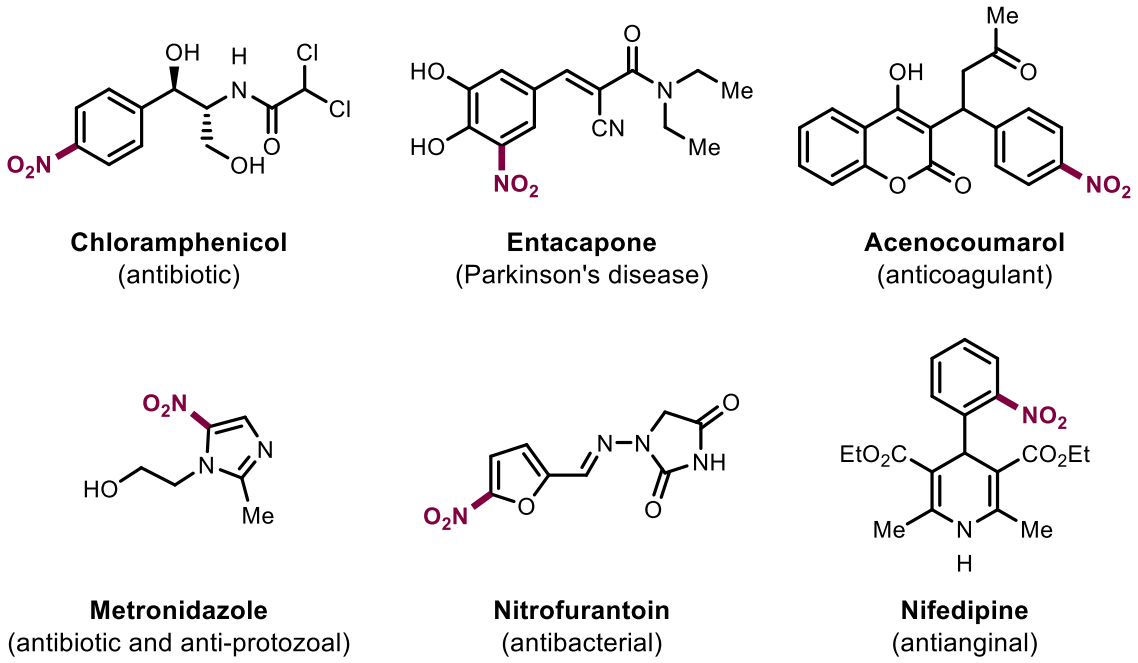

A typical nitration of arenes relies on generation of nitronium ion NO_2^+, which provides electrophilic substitution, in a mixture of concentrated HNO_3 and H_2SO_4. However, while nitroarenes can be synthetically achieved via not only in such harsh and hazardous conditions, but in milder electrophilic aromatic substitution reactions of C-H bond,[103-107] via radical reactions[108-110] or metal catalysis,[111-118] chemo- and site-selectivity are still challenging for such processes. Currently nitration repertoire includes the *ipso*-nitration of aryl (pseudo)halides,[119-121] carboxylates,[122, 123] boronic acids,[124-130] amines,[131-133] aryl stannanes[134] or organometallic species (ArMgX or ArLi).[135] And though a site-selective *ipso*-nitration tolerating alternative reactive moieties, such as halogens, is known,[130, 136, 137] there is no precedent of tolerance towards SiR_3 and $B(OR)_2$, which would be highly valuable for modular synthesis (**Figure 8, A**).

Recently, we have demonstrated organogermanes as a robust, orthogonal and highly reactive coupling partner in various processes, such as C-C, C-Hal (Hal = Br, I) and C-O bond formations (**Figure 8, B**). Achievement of high site-selectivity and demonstration of orthogonality in all mentioned transformations let us envision development of a site-selective *ipso*-nitration of C-Ge site creating C-N bond (**Figure 8, C**). Our investigation of aryl germane electrophilic nitration began with utilization of *N*-nitrosaccharin in HFIP, which is known to form NO_2^+ *in situ*. While we observed highly efficient and mild nitration at room temperature, further investigations revealed that extensions to intramolecular competitions of aryl germanes containing $SiMe_3$ and Bpin encounter incompatibility of these functionalities with the employed reaction conditions. Therefore, we turned our attention to a photocatalyzed approach developed by Katayev for boronic acids, employing *N*-nitrosuccinimide as a NO_2-surrogate and $[Ru(bpy)_3](PF_6)_2$ as a photocatalyst.[106, 130, 138] This protocol proved to be effective and resulted in the desired product derived from *p*-^{t}Bu aryl germane in 84% yield at room temperature using blue LED as a light source. Subsequent optimization of conditions showed that the addition of tetrafluoroborate anion ($AgBF_4$ or $NaBF_4$) was also beneficial and supported the nitration of electron-deficient germanes (these experiments are done by Amit Dahiya).

Figure 8 | The current state of the art and this work.

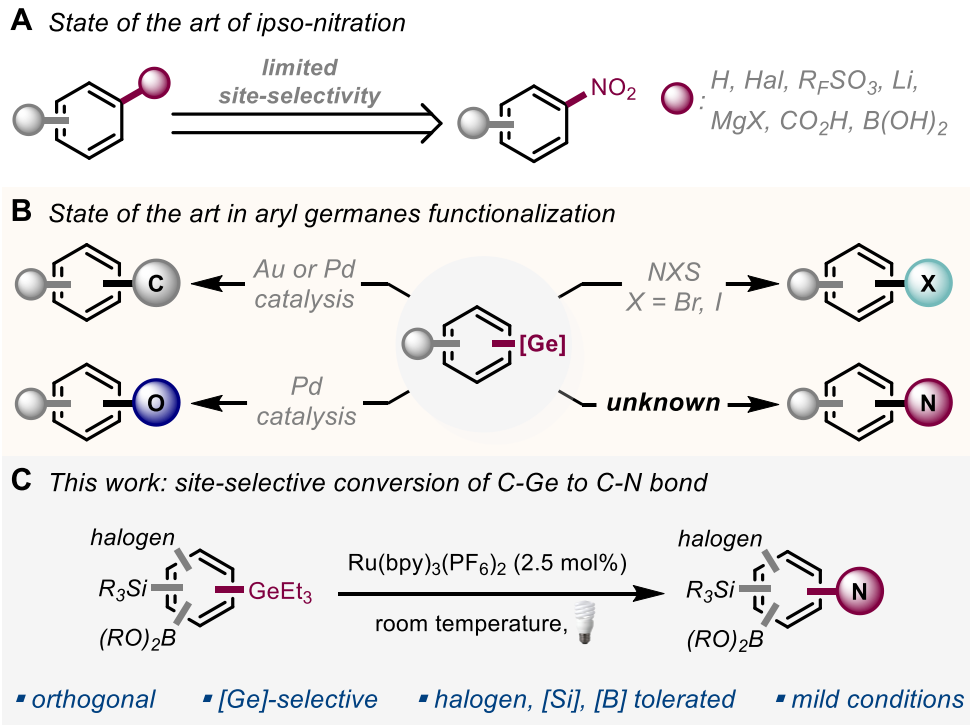

To our delight, site-selective nitration of C-Ge bond in the presence of other functional handles proved to be effective under these conditions as well. We observed the exclusive nitration of the Ge-site over halogens in excellent yields (**1**-**3**) (**Table 9, A**). Moreover, relative $SiMe_3$ moiety is tolerated the corresponding mononitrated products in high yields (**4**, **5**). Reactions with Bpin-containing aryl germanes, which were performed by A. Dahiya, showed full tolerance of the conditions towards the sensitive moiety.

Besides these intramolecular competitions, we also observed Ge-selective nitration in intermolecular competition with $ArSiMe_3$ **6** under these reaction conditions. The reaction proceeded preferably at C-Ge site resulting in 81% of the desired product (**7**). However, 9% of **6** nitration product was also observed (**Table 9, B**).

Despite the high reactivity of organogermanes, in the previous investigations we have successfully showcased their orthogonal nature in various couplings. Subjecting (4-chlorophenyl)triethylgermane in the photocatalyzed reaction the desired product of C-Ge bond nitration was obtained with 60% yield fully tolerating C-Cl site. However, in Pd-catalyzed nitration conditions developed by Buchwald and coworkers[120] the same aryl germane results in exclusively C-Cl bond nitration in 90% yield (**8**) (**Table 9, C**). Notably, C-Ge bond undergoes no transformation regardless of the harsh conditions (130 °C) and excess of nitration agent, which again confirms orthogonal reactivity of aryl germanes.

Table 9 | Selective nitration of aryl germanes containing halogens and $SiMe_3$, intermolecular selectivity and orthogonality experiments.

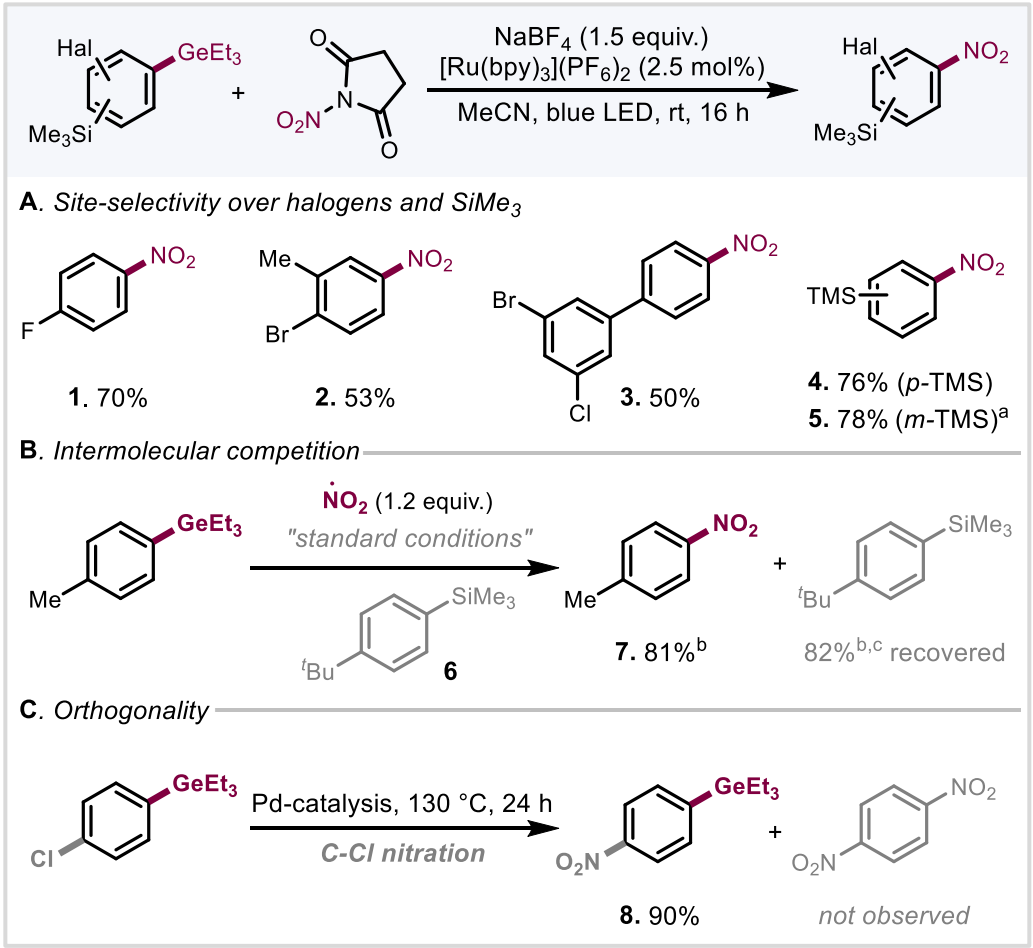

Reaction conditions: **A.** $ArGeEt_3$ (0.3 mmol, 1.0 equiv.), *N*-nitrosuccinimide (0.6 mmol, 2.0 equiv.), $[Ru(bpy)_3](PF_6)_2$ (0.0075 mmol, 2.5 mol%), $NaBF_4$ (0.45 mmol, 1.5 equiv), MeCN (1.2 ml), blue LED, rt. **B.** $ArGeEt_3$ (0.3 mmol, 1.0 equiv.), $ArSiMe_3$ (0.3 mmol, 1.0 equiv.), *N*-nitrosuccinimide (0.36 mmol, 1.2 equiv.), $[Ru(bpy)_3](PF_6)_2$ (0.0075 mmol, 2.5 mol%), $NaBF_4$ (0.45 mmol, 1.5 equiv), MeCN (1.2 ml), blue LED, rt. **C.** $ArGeEt_3$ (0.3 mmol, 1.0 equiv.), $NaNO_2$ (0.6 mmol, 2.0 equiv.), TDA (0.015 mmol, 5 mol%), $Pd_2(dba)_3$ (6.9 mg, 0.0075 mmol, 2.5 mol%) and ^{t}BuBrettPhos (8.7 mg, 0.018 mmol, 6 mol%), ^{t}BuOH (0.6 ml), 130 °C, 24 h. Isolated yields are given. [a]Reaction time 7 h. [b]Yield determined by ^{1}H NMR. [c]9% of nitration of $ArSiMe_3$.

To explain the observed site-selectivity towards $SiMe_3$ and Bpin moieties, we started mechanistic investigation. Previously, Katayev and coworkers showed that the photocatalytic nitration of olefins and

arenes using *N*-nitrosuccinimide proceeds via formation of NO_2 radical via SET.[138] For this reason, we tested the reaction in the presence of several radical quenchers, which completely inhibit the nitration (performed by Amit Dahiya). These results allow to conclude that radical mechanism takes place in the nitration of germanes as well. Moreover, light appears vital for the nitration throughout entire reaction time, which is indicated by a light on/off experiment (see Supporting Information). Then we turned to computational studies assuming that nitration begins with an *ipso*-attack of C-Ge site by the NO_2 radical. To validate the conclusions and accuracy several methods were tested. Our calculations at CPCM (MeCN) M06-2X/def2-TZVP//B3LYP-D3BJ/6-31++G(d,p) (LANL2DZ for Ru) level of theory indicate that the electrophilic substitution at C-Ge site has a barrier of 23.6 kcal/mol and proceeds via formation of σ-complex (**Figure 9, A**). Moreover, the *ipso*-attack attack of $GeMe_3$ was found to be favored over nitration at Bpin and $SiMe_3$ by 3.6 and 0.8 kcal/mol respectively. Selectivity in the presence of Bpin was shown previously in C-H nitration[106] and our higher calculated barrier (27.1 kcal/mol) further supports its unlikely nitration. However, insignificant differences between the barriers for Ge- and Si-sites to form the corresponding σ-complexes suggests nearly the same reactivity for both of them. For this reason, we continued our DFT analysis and found distinction in the further transformation of σ-complexes derived from aryl silane and germane. In contrast to the C-Ge bond, homolytic cleavage of the C-Si bond to rearomatize the ring and thus afford the nitroarene is disfavored leading to a sharp increase of free energy ($\Delta\Delta G$ = 6.4 kcal/mol). Moreover, the barrier of Me_3Si-radical release was found to be higher than the barrier of initial C-Ge site electrophilic attack ($\Delta\Delta G^{‡}$ = 0.8 kcal/mol at M06-2X; 1.8 kcal/mol at PBE0-D3BJ, 3.0 kcal/mol at MN15L, 4.3 kcal/mol at ωB97XD and 7.6 kcal/mol at DLPNO-CCSD(T) level of theory) and also higher or of the same energy as initial electrophilic attack of C-Si site. These data indicate that in case of $ArSiMe_3$ the formation of σ-complex is a reversible process and the release of Me_3Si-radical might be a rate-determining, which are both responsible for the preferential nitration at C-Ge site.

However, it was hypothesized that together with $Me_3X^{\bullet}$ (X = Si, Ge) **II** can also undergo oxidation enabled by $[Ru(bpy)_3]^{3+}$. To evaluate the thermodynamical possibility of these redox reactions we continued our DFT analysis to compare their oxidation potentials $E_{ox}(Me_3Ge^{+}/Me_3Ge^{\bullet})$ and $E_{ox}(\mathbf{II_X}^{+}/\mathbf{II_X}^{\bullet})$. To minimize the error, we decided also to compute values of $E_{ox}(Ru^{3+}/Ru^{2+})$ and $E_{ox}(Ru^{3+}/Ru^{2+*})$ for $[Ru(bpy)_3]^{2+}$, which are +1.29 V vs SCE and -0.81 V vs SCE respectively.[139] For this type of computational investigations previously our group has successfully used ωB97XD and MN15 as functionals, which are recommended for calculations of excited state species and applicable for photochemical reaction.[140] The calculated redox potentials performed at CPCM (MeCN) MN15/def2-TZVPP//ωB97XD/6-31+G(d,p) (SDD for Ru) are summarized in the **Table 10**. While the calculations found $\mathbf{II_X}^{\bullet}$ as a stable intermediate, optimization of its oxidized form $\mathbf{II_X}^{+}$ leads to dissociation of the σ-complex to nitrobenzene and the corresponding Me_3X^{+} (X = Si, Ge). Comparison of the obtained values of $E_{ox}(PhNO_2 + Me_3Ge^{+}/\mathbf{II_{Ge}}^{\bullet})$ and $E_{ox}(Me_3Ge^{+}/Me_3Ge^{\bullet})$ suggests that oxidation of $\mathbf{II_{Ge}}^{\bullet}$ by $[Ru]^{3+}$ (ΔE = 1.87 V) is thermodynamically insignificantly more favorable over oxidation of $Me_3Ge^{\bullet}$ (ΔE = 1.74 V). However, considering that $\mathbf{II}^{\bullet}$ tends to be kinetically ($\Delta\Delta G$ = 2.3 kcal/mol) and thermodynamically ($\Delta\Delta G$ = -4.7 kcal/mol) unstable towards homolytic dissociation and therefore has short lifetime, we assume that the mechanism via formed $Me_3Ge^{\bullet}$ oxidation is more likely. Notably, in case of silicon calculations predict opposite outcome, namely oxidation of $Me_3Si^{\bullet}$ is more facile than oxidation of $\mathbf{II_{Si}}^{\bullet}$ according to the calculated potentials. As for succinimide-anion,

released after nitration agent reduction, its oxidation potential is significantly higher and it can be unlikely oxidized by $[Ru]^{3+}$.

Figure 9 | Energy profile of aryl germane nitration and proposed mechanism.

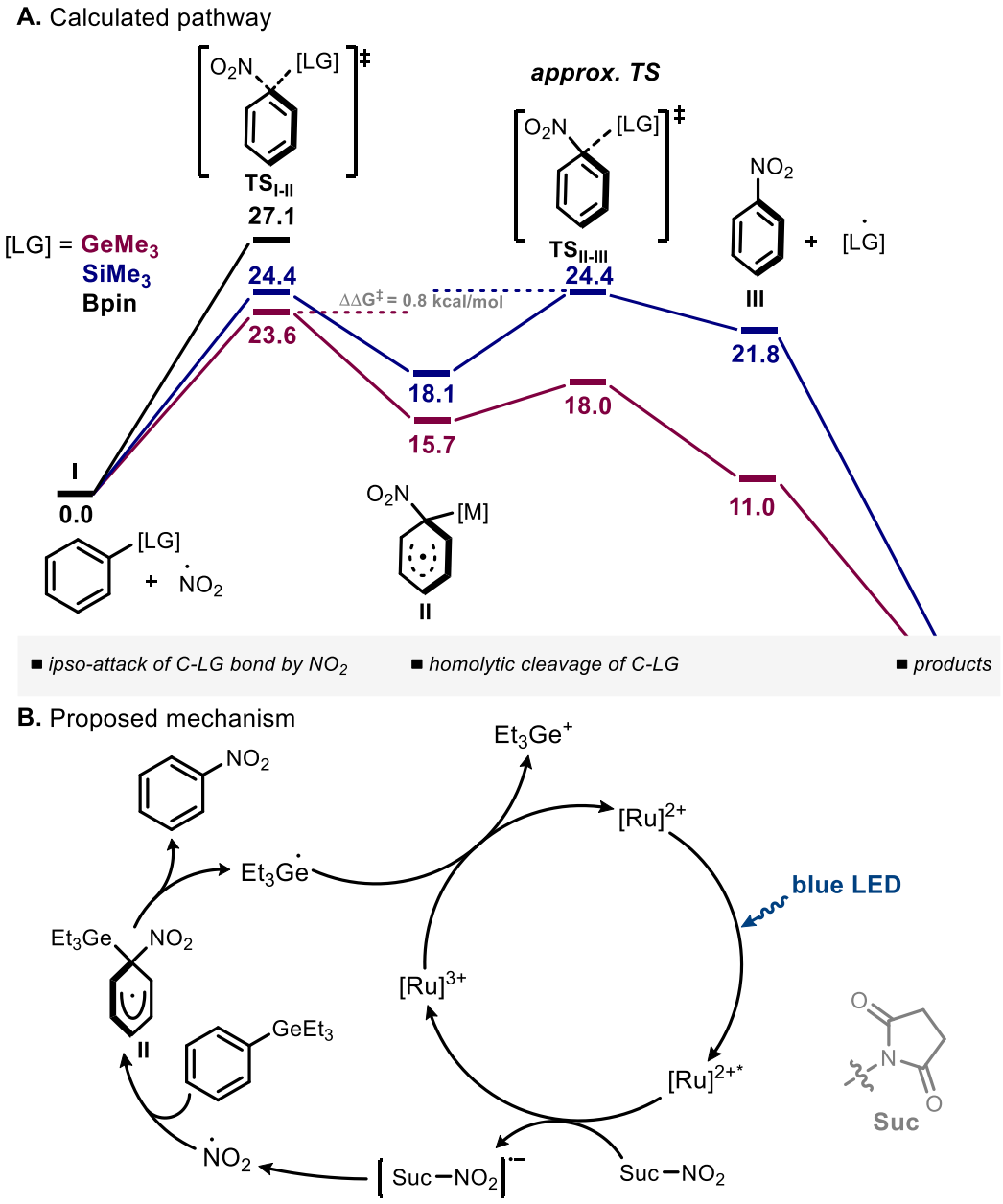

Thus, based on the results obtained from DFT analysis we propose the following mechanism for the aryl germane nitration (**Figure 9, B**). Previously, it was demonstrated that in an excited state the photocatalyst $[Ru]^{2+*}$ is able to reduce *N*-nitrosuccinimide and thereby initiates cleavage of its N-NO_2 bond. The released NO_2 performs *ipso*-attack of C-Ge site to form intermediate **II**, which in turn dissociates into a desired nitroarene and $Et_3Ge^{\bullet}$. Finally, the latter undergoes oxidation by $[Ru]^{3+}$ to regenerate the photocatalyst.

Table 10 | DFT calculated redox potentials.

Redox pair, E_{ox} or E_{red}	**E, V vs SCE**
$Me_3Ge^+/Me_3Ge^\bullet$	-0.68
$PhNO_2 + Me_3Ge^+/\mathbf{II}_{Ge}^\bullet$	-0.81
$Me_3Si^+/Me_3Si^\bullet$	-0.73
$PhNO_2 + Me_3Si^+/\mathbf{II}_{Si}^\bullet$	-0.46
$[Ru]^{3+}/[Ru]^{2+}$	+1.08
$[Ru]^{3+}/[Ru]^{2+*}$	-0.98

In conclusion, we have showed the chemoselective photocatalyzed *ipso*-nitration of aryl germanes using *N*-nitrosuccinimide as a NO_2-surrogate. This transformation demonstrates the first C-N bond formation in radical manner using aryl germanes. Intra- and intermolecular competitions versus silanes and halogens show the superior reactivity of aryl germanes, which was elucidated by DFT analysis.

3

“Batch-Forbidden” Transformations Enabled in a Cyclic Flow Mode

Experimental work was carried out in collaboration with other member of Schoenebeck group, whose contributions are stated in the corresponding subchapter.

3 "Batch-Forbidden" Transformations Enabled in a Cyclic Flow Mode

3.1 Pd-mediated Trifluoromethylation of Aryl Iodides

Experimental work was performed in collaboration with other members of Schoenebeck group: Filip Opincal.

Fluorinated compounds owing to their unique properties have found wide applications in various fields such as agrochemical[141, 142] and pharmaceutical[143-145] industries, positron emission tomography (PET),[146] electronics including solar cells and organic light emitting diodes (OLED),[147] liquid crystals,[148] and batteries.[149] In this context, the trifluoromethyl group is one of the most spread fluorine-containing moieties, which imparts its properties on molecules, thereby significantly modulating their physicochemical characteristics. Due to the enhanced lipophilicity and metabolic stability of molecules containing CF_3-groups,[150, 151] a number of trifluoromethylated compounds are revealed to exhibit an inestimable biological activity acting as important and effective antiretroviral,[150] antidepressant,[150, 152] or anticancer[153] medicaments and also agrochemical activity as pesticides[154] (**Figure 10**).

Figure 10 | Examples of molecules containing CF_3-group used in medicine and agrochemistry.

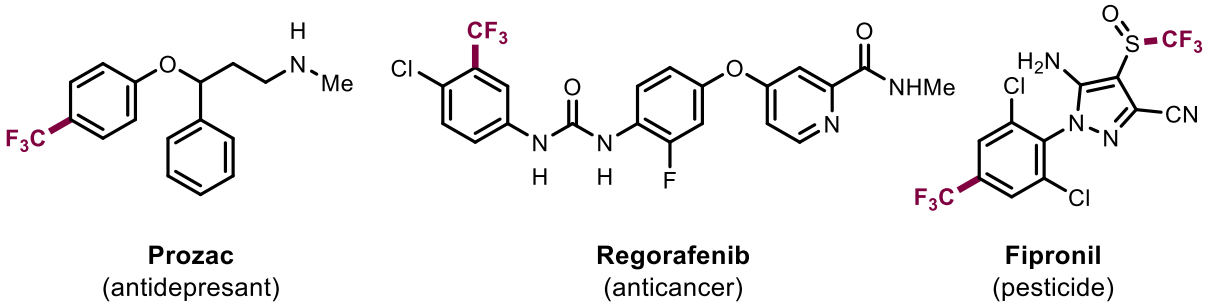

Prozac
(antidepresant)

Regorafenib
(anticancer)

Fipronil
(pesticide)

The first reported arene trifluoromethylation by Swarts employs highly hazardous hydrogen fluoride or reactive antimony(V) fluoride under harsh conditions (125 °C),[155] which stimulated the development of more efficient and eco-friendly synthetic tools for Ar-CF_3 bond construction. Another approach consisted in radical trifluoromethylation of arenes.[156] The method expands the scope of trifluoromethyl arenes, however involves highly reactive, toxic, hazardous or unavailable reagents, for instance $CF_3N(NO)SO_2CF_3$,[157] mixtures of CF_3COOH/XeF_2[158, 159] or CF_3I/Hg.[160] Although low regioselectivity typical for C-H transformations decreases its synthetic value, this aspect gave a rise to development of a huge variety of safer and more available trifluoromethylation agents enabling not only electrophilic, such as CF_3SO_2Na (Langlois' reagent),[161] hypervalent iodine based Togni reagents[162] or *S*-CF_3 sulfonium salts,[163, 164] but also nucleophilic, for instance R_3SiCF_3,[165] manner of the trifluoromethylation.

In this context, metal-catalyzed installation of CF_3-group would serve as an attractive and versatile instrument to form C-CF_3 bond. The first promising report by McLoughlin and Thrower describes Cu-mediated perfluoroalkylation of aryl iodides utilizing the corresponding alkyl iodides.[166] Though the reaction uses stoichiometric amounts of copper, it provides a cleaner transformation affording exclusively a halogen *ipso*-substitution product. Another result of this work is impetuous growth of interest to this

field.[167, 168] Further attempts to develop catalytic trifluoromethylation afforded a Cu-catalyzed reaction between iodoarenes and Si[169] or B-based[170] trifluoromethylation reagents. Apart from aryl halides, C-H trifluoromethylation underwent significant development exploiting a wider number of metals, such as Co,[171] Ag,[172, 173] Cu,[174-176] Ni[177, 178] or Pd.[179] Moreover, addition of directing groups solves the challenge with regioselectivity. But at the same time necessity of such groups limits the scope of compounds accessible by this method as well as their absence either forces to utilize symmetrical arenes or leads to mixtures of regioisomers with unsymmetrical ones.

However, development of a typical cross-coupling reaction, namely trifluoromethylation of haloarenes catalyzed by one of main transition metals, palladium, has been being a focus of thorough investigations as well. The key obstacle to exploit Pd-catalysis in this transformation lies in the notorious stability of the [Pd]-CF_3 bond.[180, 181] Indeed, currently only six phosphine ligands are known to facilitate reductive elimination of Ar-CF_3 from $Pd^{(II)}$-center, namely BrettPhos,[182] RuPhos,[182] dfmpe,[183] tri-*tert*-butylphosphine,[184] D*t*BPF[185] and Xantphos[186] (**Figure 11**).

Figure 11 | Ligands facilitating reductive elimination of Ar-CF_3 from $Pd^{(II)}$.

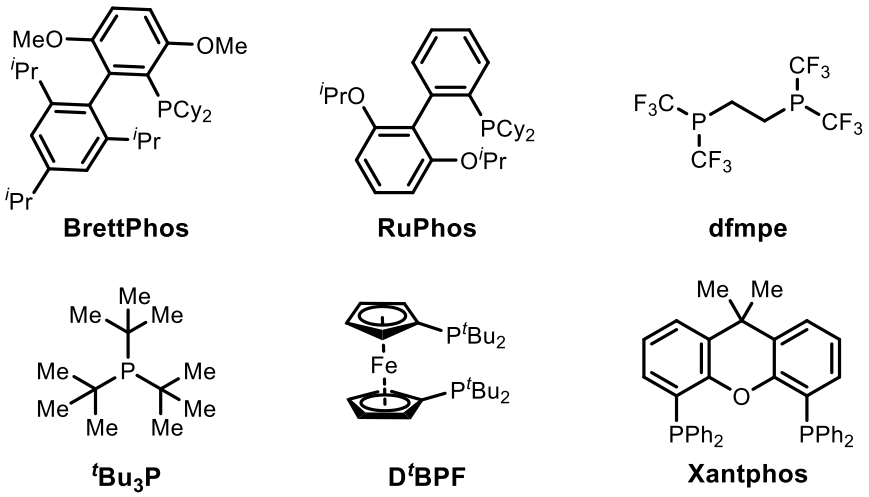

Among the mentioned ligands only the first two were successfully translated to catalysis, but the reaction still requires high temperatures (120-140 °C)[182] (**Figure 12**, **A**). Before that, the latter one, Xantphos, was the first ligand, for which reductive elimination of Ar-CF_3 from the $Pd^{(II)}$-center was found smooth and clean, proceeding under relatively mild conditions (50-80 °C).[186, 187] A wide bite angle of the phosphine could explain such reactivity.[188-191] However, later our group has revealed reasons of such intriguing behavior of [(Xantphos)Pd(Ar)CF_3][192] and shown that several factors should be considered when designing a bidentate phosphine ligand for efficient reductive elimination of Ar-CF_3, proved by successful design of dfmpe.[183] On the one hand, steric and electronic effects of substituents on phosphorus atoms should cause destabilization of the parent complex [LPd(Ar)CF_3] and stabilize a reductive elimination transition state. On the other hand, repulsion between the substituents and to-be-eliminated CF_3-group may result in a decrease of Ar-Pd-CF_3 angle and, hence, the barrier of the reductive elimination.

Figure 12 | The state of the art of stoichiometric and catalytic trifluoromethylation of arenes with Pd and this work.

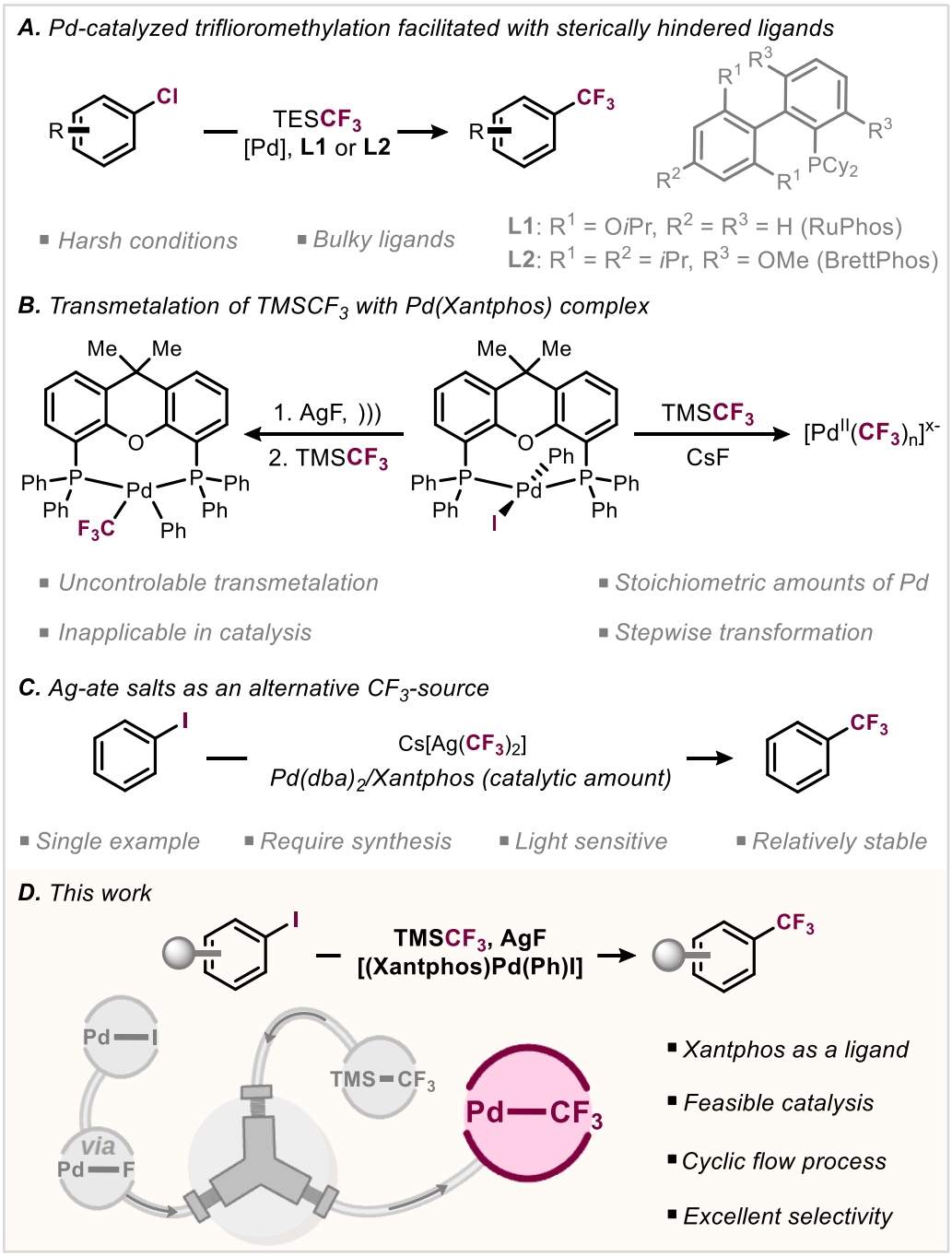

Despite Xantphos meets these requirements and seems to be the best candidate for Pd-catalyzed trifluoromethylation, its crucial drawback is weaker ligation abilities in comparison to CF_3. Grushin reported that direct conversion of [(Xantphos)Pd(Ar)I] into [(Xantphos)Pd(Ar)CF_3] with $TMSCF_3$ in the presence of CsF fails[186] because of uncontrollable transmetalation leading to formation of stable, catalytically inactive complexes[193] (**Figure 12, B**). But in the same publication it was shown that this transformation is still possible in stoichiometric and stepwise manner via intermediate synthesis [(Xantphos)Pd(Ar)F] through I/F-exchange and its further transmetalation with $TMSCF_3$.[186] Thus, it makes catalytic trifluoromethylation with Xantphos ligated palladium in batch mode impossible. Previously, our group has developed a (Xantphos)Pd-catalyzed protocol avoiding the I/F-exchange

achieved by usage of benzoyl fluorides.[194] The catalytic cycle of this approach proceeds directly via [(Xantphos)Pd(Ar)F] formation after oxidative addition of ArCO-F with subsequent extrusion of CO. Thereafter, the complex undergoes transmetalation with $TESCF_3$ followed by reductive elimination of Ar-CF_3. Although this elegant approach allows to implement the reaction in batch using Xantphos as a ligand, it does not solve the mentioned challenge and requires harsh conditions (170 °C).

To overcome the issue, nucleophilic species based on coinage metals (Cu, Ag, Au) were explored as potential CF_3-sources.[195-197] Recently, Perez-Temprano and co-workers have reported the use of synthetically accessible silver ate complexes $M[Ag(CF_3)_2]$ (M = Cs, Bu_4N) as CF_3Ag precursors, which in turn provide smooth and rapid transmetalation with [(Xantphos)Pd(Ph)I][195] (**Figure 12, C**). However, despite trifluoromethylation was demonstrated even with a catalytic amount of palladium, only a single example has been reported. Moreover, relative stability, light sensitivity and necessity for prior preparation of the silver salts make their utilization limited.

In this context, to implement such a batch-forbidden trifluoromethylation with $TMSCF_3$ enabled by weakly ligated palladium we designed a flow system that would be able to provide a catalytic cycle by separation of its incompatible individual reactions into independent compartments (**Figure 12, D**) (the design of the flow setup was done by Filip Opincal). These reactions are I/F-exchange and transmetalation of the resulting fluorinated Pd-species with $TMSCF_3$. To construct the setup, we chose one of the most common tubing made of FEP. This material is chemically inert and provides good resistance towards high temperatures (maximum 200 °C). As for inner diameter, a wide, 1.0 mm, tube was chosen to avoid system clogging in case if precipitation occurs and increase in pressure in the setup, which may complicate functioning of pumps. The starting point of the setup is a round-bottom flask, where a solution of aryl iodide and pre-catalyst [(Xantphos)Pd(Ph)I] is placed. As a model substrate 1-iodonaphthalene was used to provide a non-volatile product. Although the solution is normally homogeneous, the flask is connected to HPLC pump through a filter, which prevents contamination of tubes with any residual solids.

The next step is a compartment for I/F-exchange reaction of the pre-catalyst. Considering that [(Xantphos)Pd(Ph)I] is able to react with AgF affording desired [(Xantphos)Pd(Ph)F][186] and later formed [(Xantphos)Pd(Ph)CF_3] is sensitive to moisture,[198] the compartment should consist of two parts. It is convenient to represent both as columns, filled with the corresponding content. The first one, into which the starting solution of [(Xantphos)Pd(Ph)I] and aryl iodide enters first by means of the HPLC pump, contains activated molecular sieves to support moisture-free conditions. This column is connected to another one, containing AgF in mixture with carrier and in which actual I/F-exchange takes place. Since the halogen exchange reaction is heterogeneous, the carrier is supposed to increase surface area of AgF and thus to accelerate the transformation. Several materials were tested for this purpose, and the best result was achieved with glass dust. In consideration of thermal sensitivity of [(Xantphos)Pd(Ar)F] decomposing at above 20 °C,[186] the columns were placed into a cooled bath at 10 °C. Also, it enhances efficiency of molecular sieves (these preparations were done by Filip Opincal).

After halogen exchange it is turn of transmetalation of formed [(Xantphos)Pd(Ar)F] with $TMSCF_3$. This implies introduction of another flow, which can be achieved by addition of a mixer. For this purpose, output of the column with AgF/glass dust was connected to a syringe pump with $TMSCF_3$ solution via the simplest a Y-mixer, in which transmetalation occurs. As known, this reaction proceeds instantly.[186] This

allows the obtained mixture to travel immediately to a heating reactor (the next compartment). However, two crucial aspects in this part should be considered. The first one is that flow rates of $Pd^{(II)}$-F and $TMSCF_3$ streams must be adjusted the way to provide their mixing in stoichiometric ratio in order to avoid accumulation of $TMSCF_3$ in the system. The second aspect is the flow rate of $Pd^{(II)}$-F stream should be suitable both for efficient mixing with $TMSCF_3$ solution and complete halogen exchange. The flow rate of [(Xantphos)Pd(Ar)F] stream was screened and 2.0 ml/min was found optimal for the reaction (done by Filip Opincal). The advantage of flow chemistry, consisting in separation of these two reaction steps and manipulation with reactive species stoichiometry, over batch reactions is a key point, which enables such kind of processes impossible in batch.

Then it is turn of the reductive elimination of formed [(Xantphos)Pd(Ph)CF_3], which is implemented in the mentioned heating coil reactor. As was mentioned before, the reaction proceeds at 50-80 °C. However, to ensure full conversion of [(Xantphos)$Pd^{(0)}$] back to [(Xantphos)Pd(Ar)I], it was decided to increase the temperature. Indeed, full conversion of aryl iodide depends on heating of the reactor. However, the reaction at 110 °C showed full conversion of the substrate. Since the entire setup functions at atmospheric pressure, helium is needed for degassing of the solution to prevent its boiling inside the reactor upon overheating. The choice of the gas was motivated by its one the lowest solubility characteristics and wide usage for HPLC systems.[199] However, it was observed that heating at T ≥ 115 °C causes intensive boiling of the solution regardless of helium flow intensity. As for the length of the reactor, it is dictated by volumes of the reaction mixture (40 ml) and the rest part of the setup. For this reason, as a starting point, a ~5 ml (t_R = 2.5 min) reactor was installed (done by Filip Opincal) (in this case a volume of the entire setup with loaded columns is ~20 ml). The $Pd^{(II)}$-I complex returns to the initial starting point, and at this stage the elementary cycle is considered done.

In summary, the described flow system consists in four steps: the first step is the formation of [(Xantphos)Pd(Ph)F] via an I/F-exchange between pre-catalyst [(Xantphos)Pd(Ph)I] and AgF. In the second step the fluorinated complex undergoes transmetalation with $TMSCF_3$ to transform it into [(Xantphos)Pd(Ph)CF_3]. To finalize catalytic cycle [(Xantphos)Pd(Ph)CF_3] reductively eliminates the trifluoromethylated arene as the third step followed by oxidative addition of aryl iodide to regenerate the [$Pd^{(II)}$-I] species as the fourth step. Since the latter two reactions are able to occur in the same compartment, the designed flow system consists of a flask, three compartments, a syringe pump for $TMSCF_3$ and an HPLC pump, which cycles the reaction mixture (**Figure 13**) (see Supporting Information for details).

Figure 13 | The design of the cyclic flow setup.

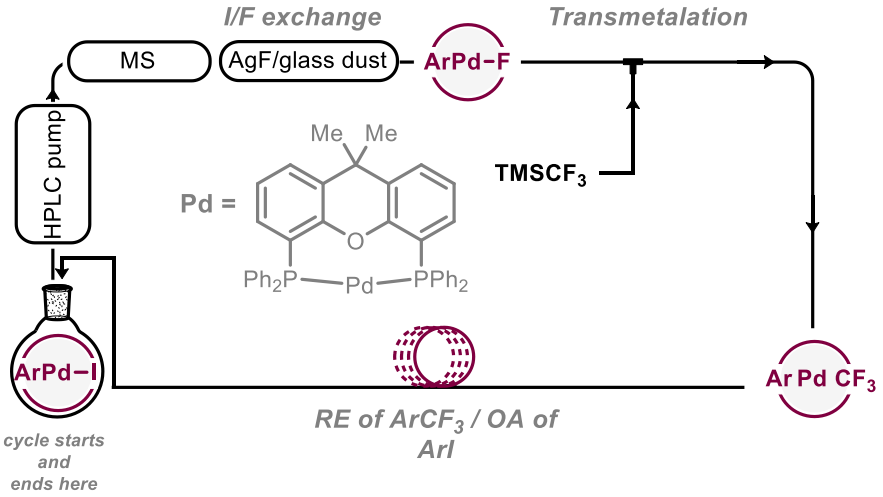

The tested 1-iodonaphthalene successfully underwent the trifluoromethylation affording the desired 1-trifluoromethylnaphthalene **1** in 70% yield (**Table 11**). Thus, the approach has proved the possibility of CF_3-group installation employing Xantphos-ligated $Pd^{(II)}$ with $TMSCF_3$ in cyclic flow regime.

With the reaction conditions in hand, next we decided to expand our protocol with various iodoarenes (**Table 11**). For instance, polyaromatic substrates were successfully converted into the corresponding products (**2**, **3**). However, a lower yield was obtained in case of sterically hindered 9-(trifluoromethyl)anthracene **3**.

Table 11 | The scope of the cyclic flow Pd-mediated trifluoromethylation of iodoarenes.

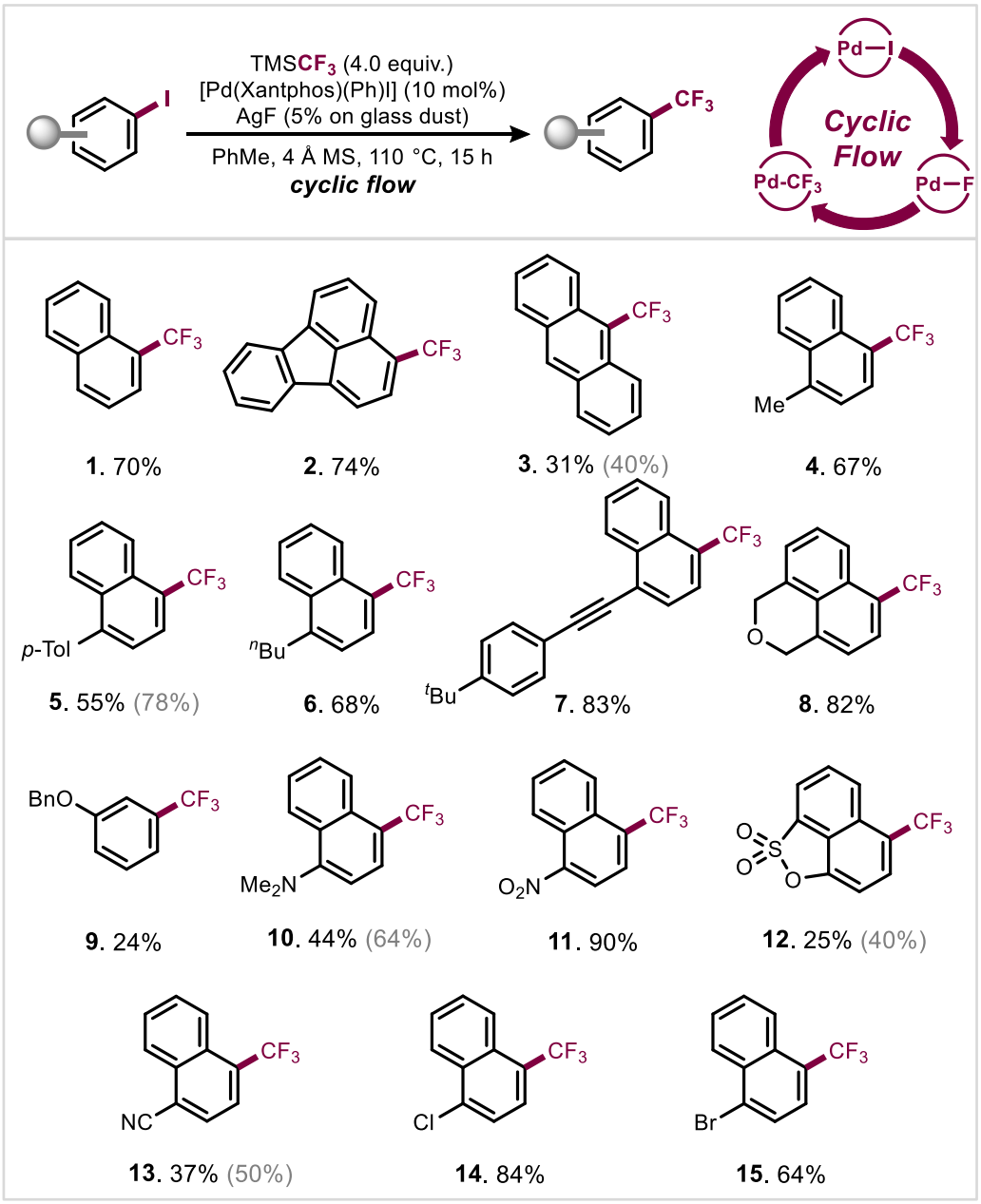

Reaction conditions: ArI (0.4 mmol, 1.0 equiv.), [(Xantphos)Pd(Ph)I] (0.04 mmol, 10 mol%), $TMSCF_3$ (6.0 ml, 0.4 M solution in PhMe), AgF (5 w/w% on glass dust), 4 Å MS, PhMe (40 ml), 110 °C, 15 h. ^{19}F NMR yields are given in parentheses.

Pleasingly, the transformation appeared compatible with a wide range of iodoarenes remaining indifferent to its electronic properties. Indeed, aryl iodides with electron-neutral and rich cores were transformed into the desired $ArCF_3$ with moderate and high yields (**4**-**8**). The reaction demonstrates high tolerance toward various electron-donating functionalities, such as ether **9** and amino **10** groups. The same efficiency was observed with electron-poor substrates tolerating nitro **11**, sultone **12** and nitrile **13**. Next, we examined chemoselectivity of the developed protocol toward relative functionalities such as C-Cl and C-Br bonds, which are potentially able to compete with C-I site. Employed chloro- and bromosubstituted iodonaphthalenes smoothly underwent the trifluoromethylation furnishing the corresponding arenes (**14**, **15**) in high yields. This shows superior reactivity of C-I site in opposite to C-Cl or C-Br handles under continuous cyclic flow conditions. Notably, in some cases starting aryl iodides were

detected in a reaction mixture. Purification by column chromatography or HPLC achieved no full isolation of the desired products owing to similar chromatographical mobility of aryl trifluoromethyls and the corresponding iodides. In these cases, it was decided to get rid of unreacted iodides by its oxidation in the presence of mCPBA and *p*-toluenesulfonic acid leading to highly polar hypervalent iodine species[200] (see Supporting Information). This provided significantly facile isolation of the desired Ar-CF_3 with simple chromatography technique without loss of the yield.

In conclusion, we have designed a continuous flow system implementing the batch-forbidden trifluoromethylation of aryl iodides with $TMSCF_3$ mediated by weakly ligated palladium complex. The concept of a flow reactor with the individual compartments for the incompatible iodine-fluorine exchange of $Pd^{(II)}$-Xantphos complex and following transmetalation with $TMSCF_3$, working in a cyclic mode, supports the catalytic cycle of the reaction in the elegant way and potentially sheds light on other challenging in batch transformations.

4

Supporting Information

4 Supporting Information

4.1 General experimental details

Reagents and solvents

All the reagents and the starting materials were commercially available and used as received unless otherwise stated. Gold complexes were purchased from ChemPur, Sigma-Aldrich and abcr. Anhydrous THF, PhMe, DCM and Et_2O were dried using an Innovative Technology PS-MD-5 solvent purification system. Solvents used in work up, filtration and column chromatography were distilled prior to use.

Purification

Thin layer chromatography (TLC) was performed on Merck Kieselgel 60 F254 aluminium plates with unmodified silica and visualized either under UV light or stained with $KMnO_4$. Flash column chromatography was performed with Merck silica gel 60 (35 – 70 mesh). Preparative HPLC was performed on a Gilson-Abimed HPLC (employing UV detector model 117) using a Merck LiChrosorb Si60 column (porosity 7 µm, 250 x 25 mm).

Characterization of compounds

All the ^{1}H, ^{13}C, ^{19}F and ^{31}P NMR spectra were recorded on Bruker Avance Neo 600, Varian VNMRS 600, Varian VNMRS 400 or Varian VNMRS 300 spectrometers at ambient temperature. Chemical shifts (δ) are reported in parts per million (ppm) and were referenced either to residual solvent peak (for ^{1}H and ^{13}C spectra) or by the instrument internally after locking and shimming to the deuterated solvent (for ^{19}F). Coupling constants (J) are given in Hertz (Hz). Multiplicities of signals in ^{1}H, ^{19}F, and ^{13}C NMR were designated as s (singlet), d (doublet), dd (doublet of doublets), dt (doublet of triplets), ddd (doublet of doublets of doublets), t (triplet), td (triplet of doublets), q (quartet), quint (quintet), sext (sextet), sept (septet), and m (multiplet).

Gas chromatography coupled with mass spectrometry (GC-MS) was performed on an Agilent Technologies 5975 series MSD mass spectrometer under electron ionization (EI) mode combined with an Agilent Technologies 7820A gas chromatograph employing an Agilent 19091s-433 HP-5MS column (30 m × 0.250 µm × 0.250 µm) or Agilent CP-Sil8-CB column (30 m × 0.25 µm × 1.00 µm). High-resolution mass spectrometry (HRMS) was performed using a Thermo Scientific LTQ Orbitrap XL spectrometer, Finnigan MAT95 and Bruker Maxis II LC-MS-System. Low-resolution masses of known compounds were extracted from their GCMS chromatograms. IR spectra were recorded on a Spectrum 100 spectrometer with an UATR Diamond/KRS-5 crystal with attenuated total reflectance (ATR). UV/Vis spectra were recorded on Shimadzu UV-2600 spectrophotometer. Blue LED stripes (1 m, 18.6 W, 465 – 470 nm, λ_{max} = 467 nm) for a photoreactor were purchased from Ledxon® GmbH.

4.1.1 Synthesis procedure and characterization of aryl germanes

Aryl germanes synthesized by other members of the group are not listed here.

General Procedure 1 (GP 1)

The corresponding aryl iodide (1.0 equiv.) and triethylgermane chloride (1.1 equiv.) were dissolved in degassed and anhydrous THF (0.2 M) under an argon atmosphere. Then a solution of ^{i}PrMgCl·LiCl (1.3 M in THF, 1.2 equiv.) was added dropwise and the reaction mixture was left to stir for 3 h at room temperature. The reaction was quenched with water, the organic phase was separated, and the aqueous layer was extracted with DCM (2x). The organic phases were combined and dried with $MgSO_4$. After filtration and evaporation of solvents in vacuo the crude mixture was purified by silica gel chromatography column.

General Procedure 2 (GP 2)

The corresponding aryl bromide (1.0 equiv.) was dissolved in degassed and anhydrous THF (0.5 M) under an argon atmosphere. Solution of ^{i}PrMgCl·LiCl (1.3 M in THF, 1.1 equiv.) was added slowly at -78 °C, and the reaction mixture was left to stir for 1 h at the same temperature. Then triethylgermane chloride (1.1 equiv.) was added dropwise, and the reaction solution was allowed to warm up to room temperature and was stirred overnight. The reaction was quenched with water, the organic phase was separated, and the aqueous layer was extracted with DCM (2x). The organic phases were combined, dried with $MgSO_4$, and filtered. After evaporation of solvents in vacuo the crude mixture was purified by silica gel chromatography column.

General Procedure 3 (GP 3)

The corresponding aryl bromide (1.0 equiv.) was dissolved in degassed and anhydrous THF (0.5 M) under an argon atmosphere. Solution of ^{n}BuLi (2.5 M in hexane, 1.2 equiv.) was added slowly at -78 °C, and the reaction mixture was left to stir for 1 h at the same temperature. Then triethylgermane chloride (1.1 equiv.) was added dropwise, and the reaction solution was stirred overnight at room temperature. The reaction was quenched by addition of water, the organic phase was separated, and the aqueous layer was extracted with DCM (2x). The organic phases were combined, dried with $MgSO_4$, and filtered. After evaporation of solvents in vacuo a crude mixture was purified by silica gel chromatography column.

(4-Bromo-3-methylphenyl)triethylgermane

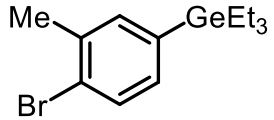

The title product was obtained by using 1-bromo-4-iodomethylbenzene (445.4 mg, 1.50 mmol, 1.0 equiv.) according to GP 1 after purification by column chromatography (*n*-hexane) as a colorless oil (456.8 mg, 1.38 mmol, 92%).

R_f = 0.76 (*n*-hexane). **^{1}H NMR** (400 MHz, $CDCl_3$) δ/ppm = 7.50 (d, *J* = 7.8 Hz, 1H), 7.27 (s, 1H), 7.10 (d, *J* = 7.8 Hz, 1H), 2.41 (s, 3H), 1.10-1.02 (m, 9H), 1.02-0.93 (m, 6H). **^{13}C NMR** (101 MHz, $CDCl_3$) δ/ppm = 139.1, 137.3, 136.4, 133.0, 131.9, 125.5, 23.1, 9.0, 4.3. **IR** (neat): ν/cm^{-1} = 2948, 2873, 2330, 2080, 1898, 1559, 1462, 1365, 1230, 1017, 967, 853, 809, 694. **HRMS** (EI) calculated for $C_{13}H_{21}{}^{79}Br^{74}Ge$: 330.0033 $[M]^+$, found: 330.0000.

(3-Bromo-5-chlorophenyl)triethylgermane

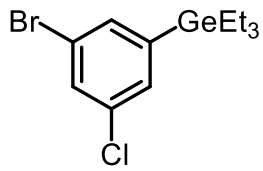

The title product was obtained by using 1-bromo-3-chloro-5-iodobenzene (634.7 mg, 2.00 mmol, 1.0 equiv.) according to GP 1 after purification by column chromatography (*n*-hexane) as a colorless oil (493.8 mg, 1.41 mmol, 70%).

R_f = 0.80 (*n*-hexane). **^{1}H NMR** (300 MHz, $CDCl_3$) δ/ppm = 7.48-7.44 (m, 1H), 7.39 (dd, *J* = 1.9, 0.8 Hz, 1H), 7.29 (dd, *J* = 1.9, 0.8 Hz, 1H), 1.10-0.94 (m, 15H). **^{13}C NMR** (75 MHz, $CDCl_3$) δ/ppm = 145.2, 135.0, 134.6, 132.3, 131.0, 123.1, 8.9, 4.4. **IR** (neat): ν/cm^{-1} = 3854, 2950, 2873, 2659, 2330, 2109, 1906, 1546, 1458, 1422, 1378, 1228, 1114, 1015, 968, 852, 772, 738, 690. **HRMS** (EI) calculated for $C_{12}H_{18}{}^{79}Br^{35}Cl^{74}Ge$: 349.9487 [M]+, found: 349.9501.

Trimethyl(4-(triethylgermyl)phenyl)silane

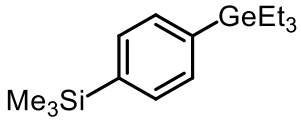

The title product was obtained by using (4-bromophenyl)trimethylsilane (595.9 mg, 2.60 mmol, 1.0 equiv.) according to GP 3 after purification by column chromatography (*n*-hexane) as a colorless oil (723.3 mg, 2.34 mmol, 90%).

R_f = 0.70 (*n*-hexane). **^{1}H NMR** (300 MHz, $CDCl_3$) δ/ppm = 7.51 (d, *J* = 8.0 Hz, 2H), 7.44 (d, *J* = 8.0 Hz, 2H), 1.14-0.93 (m, 15H), 0.28 (s, 9H). **^{13}C NMR** (75 MHz, $CDCl_3$) δ/ppm = 140.8, 140.1, 133.5, 132.8, 9.1, 4.3, -1.0. **HRMS** (EI) calculated for $C_{15}H_{28}{}^{74}GeSi$: 310.1172 $[M]^+$, found: 310.1180. These data are in agreement with those reported previously in the literature.[27]

Trimethyl(3-(triethylgermyl)phenyl)silane

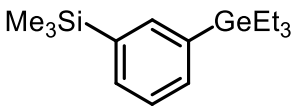

The title product was obtained by using (3-bromophenyl)trimethylsilane (745 µl, 4.00 mmol, 1.0 equiv.) according to GP 3 (using ^{t}BuLi (1.8 M in pentane, 5.0 ml, 6.00 mmol, 1.5 equiv.) after purification by column chromatography (*n*-pentane) as a colorless oil (1.06 g, 3.42 mmol, 86%).

R_f = 0.70 (*n*-pentane). **^{1}H NMR** (600 MHz, $CDCl_3$) δ/ppm = 7.61-7.57 (m, 1H), 7.49 (dt, *J* = 7.3, 1.4 Hz, 1H), 7.43 (dt, *J* = 7.3, 1.4 Hz, 1H), 7.35-7.31 (m, 1H), 1.12-1.04 (m, 9H), 1.03-0.95 (m, 6H), 0.27 (s, 9H). **^{13}C NMR** (151 MHz, $CDCl_3$) δ/ppm = 139.7, 139.1, 139.0, 134.6, 133.3, 127.3, 9.1, 4.4, -1.0. **HRMS** (EI) calculated for $C_{15}H_{28}{}^{74}GeSi$: 310.1167 $[M]^+$, found: 310.1157.

Benzo[*d*][1,3]dioxol-5-yltriethylgermane

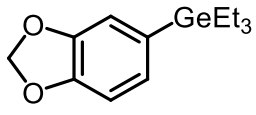

The title product was obtained by using 5-iodo-1,3-benzodioxole (402.0 mg, 2.00 mmol, 1.0 equiv.) according to GP 4 after purification by column chromatography (*n*-hexane) as a colorless oil (475.3 mg, 1.69 mmol, 85%).

R_f = 0.30 (*n*-hexane). **^{1}H NMR** (400 MHz, $CDCl_3$) δ/ppm = 6.93-6.82 (m, 3H), 5.93 (s, 2H), 1.11-1.01 (m, 9H), 1.00-0.91 (m, 6H). **^{13}C NMR** (101 MHz, $CDCl_3$) δ/ppm = 147.8, 147.5, 132.5, 127.4, 113.5, 108.8, 100.5, 9.0, 4.5. **IR** (neat): *ν*/cm^{-1} = 2946, 2318, 2098, 1856, 1600, 1477, 1413, 1320, 1227, 1108, 1038, 937, 876, 803, 697. **HRMS** (EI) calculated for $C_{13}H_{20}{}^{74}GeO_2$: 282.0670 $[M]^+$, found 282.0680.

Triethyl(thiophen-2-yl)germane

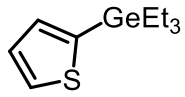

The title product was obtained by using 2-iodothiophene (630.1 mg, 3.00 mmol, 1.0 equiv.) according to GP 1 after purification by column chromatography (5:1 *n*-hexane/EtOAc) as a colorless oil (715.3 mg, 2.94 mmol, 98%).

R_f = 0.91 (5:1 *n*-hexane/EtOAc). **^{1}H NMR** (400 MHz, $CDCl_3$) δ/ppm = 7.59 (dd, *J* = 4.6, 0.9 Hz, 1H), 7.22 (dd, *J* = 4.6, 3.3 Hz, 1H), 7.18 (dd, *J* = 3.3, 0.9 Hz, 1H), 1.14-0.99 (m, 15H). **^{13}C NMR** (101 MHz, $CDCl_3$) δ/ppm = 137.6, 133.4, 129.7, 127.9, 9.0, 5.7. **HRMS** (EI) calculated for $C_{10}H_{18}{}^{74}GeS$: 244.0336 $[M]^+$, found: 244.0342. These data are in agreement with those reported previously in the literature.[27]

Triethyl(thiophen-3-yl)germane

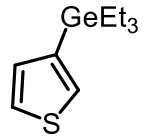

The title product was obtained by using 3-iodothiophene (363.0 mg, 1.72 mmol, 1.0 equiv.) according to GP 1 after purification by column chromatography (*n*-hexane) as a colorless oil (378.0 mg, 1.56 mmol, 90%).

R_f = 0.70 (*n*-hexane). **^{1}H NMR** (600 MHz, $CDCl_3$) δ/ppm = 7.42 (dd, *J* = 4.7, 2.5 Hz, 1H), 7.34 (dd, *J* = 2.5, 1.1 Hz, 1H), 7.14 (dd, *J* = 4.7, 1.1 Hz, 1H), 1.10-1.05 (m, 9H), 1.02-0.95 (m, 6H). **^{13}C NMR** (151 MHz, $CDCl_3$) δ/ppm = 138.4, 131.7, 129.9, 125.2, 9.1, 5.0. **HRMS** (EI) calculated for $C_8H_{13}{}^{74}GeS$: 214.9944 $[M\text{-}Et]^+$, found: 214.9950. These data are in agreement with those reported previously in the literature.[27]

2-Methoxy-5-(triethylgermyl)benzonitrile

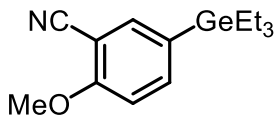

The title product was obtained by using 5-iodo-2-methoxybenzonitrile (362.7 mg, 1.40 mmol, 1.0 equiv.) according to GP 2 after purification by column chromatography (10:1 *n*-pentane/EtOAc) as a colorless oil (320.7 mg, 1.10 mmol, 78%).

R_f = 0.50 (8:1 *n*-pentane/EtOAc). **^{1}H NMR** (600 MHz, $CDCl_3$) δ/ppm = 7.58 (d, *J* = 1.5 Hz, 1H), 7.56 (dd, *J* = 8.3, 1.5 Hz, 1H), 6.96 (d, *J* = 8.3 Hz, 1H), 3.92 (s, 3H), 1.07-1.01 (m, 9H), 1.00-0.94 (m, 6H). **^{13}C NMR** (151 MHz, $CDCl_3$) δ/ppm = 161.4, 139.9, 139.2, 131.7, 117.2, 111.0, 101.9, 56.0, 8.9, 4.3. **IR** (neat): $\tilde{\nu}$/cm^{-1} = 2948, 2226, 2035, 1911, 1584, 1493, 1458, 1375, 1266, 1186, 1139, 1091, 1017, 968, 899, 817, 698. **HRMS** (ESI) calculated for $C_{14}H_{21}{}^{74}GeNNaO$: 316.0727 $[M+Na]^+$, found: 316.0720.

4-(Triethylgermyl)benzonitrile

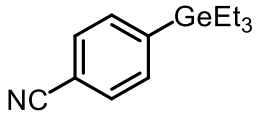

The title product was obtained by using 4-iodobenzonitrile (251.9 mg, 1.10 mmol, 1.0 equiv.) according to GP w after purification by column chromatography (50:1 *n*-pentane/Et_2O) as a yellow oil (199.3 mg, 0.76 mmol, 69%).

R_f = 0.30 (50:1 *n*-pentane/Et_2O). **^{1}H NMR** (400 MHz, $CDCl_3$) δ/ppm = 7.59 (d, *J* = 8.3 Hz, 2H), 7.53 (d, *J* = 8.3 Hz, 2H), 1.09-0.96 (m, 15H). **^{13}C NMR** (101 MHz, $CDCl_3$) δ/ppm = 147.7, 134.6, 131.1, 119.3, 112.0, 8.9, 4.2. **IR** (neat): $\tilde{\nu}$/cm^{-1} = 2949, 2228, 2161, 1922, 1591, 1460, 1383, 1310, 1228, 1081, 1015, 967, 819, 697. **HRMS** (ESI) calculated for $C_{13}H_{19}{}^{74}GeNNa$: 286.0621 $[M+Na]^+$, found: 286.0613.

(4-Chloro-3-fluorophenyl)triethylgermane

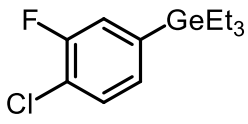

The title product was obtained by using 1-chloro-2-fluoro-4-iodobenzene (615.5 mg, 2.40 mmol, 1.0 equiv.) according to GP 1 after purification by column chromatography (*n*-pentane) as a colorless oil (590.7 mg, 2.04 mmol, 85%).

R_f = 0.80 (*n*-pentane). **^{1}H NMR** (600 MHz, $CDCl_3$) δ/ppm = 7.38-7.33 (m, 1H), 7.18 (dd, *J* = 8.9, 1.3 Hz, 1H), 7.12 (dd, *J* = 7.7, 1.3 Hz, 1H), 1.08-1.02 (m, 9H), 1.01-0.95 (m, 6H). **^{13}C NMR** (151 MHz, $CDCl_3$) δ/ppm = 158.1 (d, *J* = 251.9 Hz), 141.5 (d, *J* = 3.1 Hz), 130.4 (d, *J* = 4.0 Hz), 130.3, 121.6 (d, *J* = 17.8 Hz), 121.0 (d, *J* = 17.6 Hz), 8.9, 4.4. **^{19}F NMR** (565 MHz, $CDCl_3$) δ/ppm = -117.07 – -117.14 (m, 1F). **IR** (neat): ν/cm^{-1} = 2952, 2873, 2332, 2113, 1562, 1479, 1427, 1380, 1274, 1223, 1148, 1049, 1015, 967, 876, 811, 696. **HRMS** (GC-APCI) calculated for $C_{10}H_{13}{}^{35}ClF^{74}Ge$: 260.9896 $[M\text{-}Et]^+$, found: 260.9916.

3,5-Dimethyl-4-(triethylgermyl)isoxazole

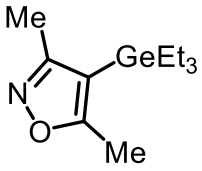

The title product was obtained by using 4-iodo-3,5-dimethylisoxazole (446.0 mg, 2.00 mmol, 1.0 equiv.) according to GP 1 after purification by column chromatography (13:1 *n*-pentane/EtOAc) as a colorless oil (440.0 mg, 1.72 mmol, 86%).

R_f = 0.51 (13:1 *n*-pentane/EtOAc). **^{1}H NMR** (600 MHz, $CDCl_3$) δ/ppm = 2.36 (s, 3H), 2.23 (s, 3H), 1.06-0.95 (m, 15H). **^{13}C NMR** (151 MHz, $CDCl_3$) δ/ppm = 173.0, 163.8, 105.2, 13.2, 12.8, 8.9, 4.7. **IR** (neat): ν/cm^{-1} = 3467, 2953, 2873, 2735, 2184, 1578, 1457, 1397, 1351, 1239, 1093, 1014, 971, 901, 803, 754, 705, 579. **HRMS** (EI) calculated for $C_{11}H_{21}{}^{74}GeNONa$: 280.0727 $[M+Na]^+$, found: 280.0725.

Triethyl(2-methoxyphenyl)germane

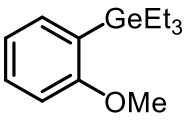

The title product was obtained by using 2-iodoanisole (561.7 mg, 2.40 mmol, 1.0 equiv.) according to GP 1 after purification by column chromatography (*n*-hexane) as a colorless oil (528.1 mg, 1.98 mmol, 82%).

R_f = 0.70 (*n*-pentane). **^{1}H NMR** (600 MHz, $CDCl_3$) δ/ppm = 7.34-7.28 (m, 2H), 6.97-6.93 (m, 1H), 6.85-6.82 (m, 1H), 3.79 (s, 3H), 1.08-0.98 (m, 15H). **^{13}C NMR** (151 MHz, $CDCl_3$) δ/ppm = 163.7, 135.3, 129.9, 127.7, 120.6, 109.5, 55.1, 9.2, 4.8. **IR** (neat): ν/cm^{-1} = 2945, 2871, 2834, 2331, 2159, 1739, 1578, 1458, 1427, 1235, 1169, 1014, 966, 840, 769, 707. **HRMS** (EI) calculated for $C_{13}H_{22}{}^{74}GeO$: 268.0877 $[M]^+$, found: 268.0873.

Triethyl(3-(4,4,5,5-tetramethyl-1,3,2-dioxaborolan-2-yl)phenyl)germane

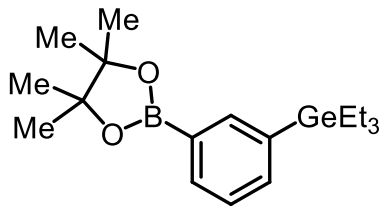

Triethyl(3-iodophenyl)germane (885.3 mg, 2.44 mmol, 1.0 equiv.) was added to a round bottom flask and dissolved in anhydrous and degassed THF (16 ml) under argon. Solution of ^{i}PrMgCl (2.0 M in THF, 1.5 ml, 2.93 mmol, 1.2 equiv.) was added dropwise at 0 °C and the reaction was stirred for 30 min at the same temperature. 2-Isopropoxy-4,4,5,5-tetramethyl-1,3,2-dioxaborolane (600 µl, 2.93 mmol, 1.2 equiv.) was added at 0 °C dropwise, then the reaction mixture was allowed to warm up and was stirred at room temperature for 12 h. Then the mixture was quenched by the addition of water. The organic phase was separated and the aqueous phase was extracted with DCM (3x). The combined organic phases were dried over $MgSO_4$ and the solvent was removed under reduced pressure. The

title product was obtained after purification by column chromatography (50:1 *n*-hexane/EtOAc) as a colorless oil (421.8 mg, 1.34 mmol, 48%).

R_f = 0.38 (50:1 *n*-pentane/EtOAc). **^{1}H NMR** (400 MHz, $CDCl_3$) δ/ppm = 7.87-7.84 (m, 1H), 7.79-7.73 (m, 1H), 7.55-7.51 (m, 1H), 7.36-7.31 (m, 1H), 1.35 (s, 12H), 1.08-0.98 (m, 15H). **^{13}C NMR** (101 MHz, $CDCl_3$) δ/ppm = 140.4, 139.1, 137.1, 134.8, 127.2, 83.8, 25.0, 9.1, 4.3. *Note*: The carbon attached to boron was not observed in ^{13}C NMR.[201] **HRMS** (EI) calculated for $C_{16}H_{26}B^{74}GeO_2$: 335.1232 [M-Et]$^+$, found: 335.1230.

(3'-Bromo-5'-chloro-[1,1'-biphenyl]-4-yl)triethylgermane

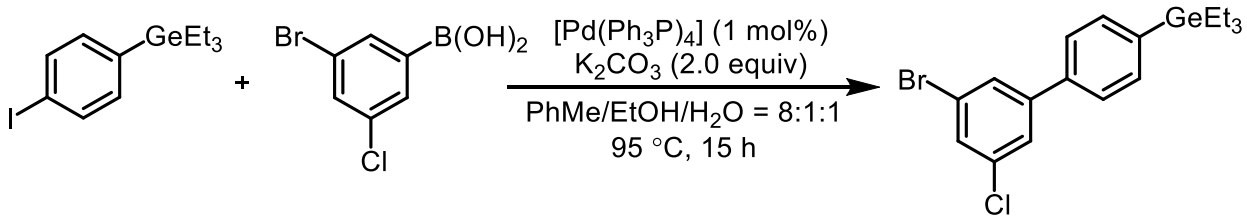

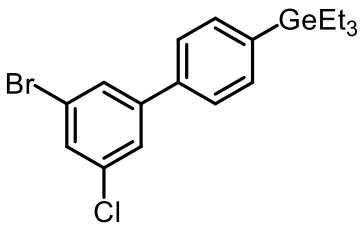

Triethyl(4-iodophenyl)germane (1.09 g, 3.00 mmol, 1.0 equiv.), (3-bromo-5-chlorophenyl)boronic acid (845.0 mg, 3.60 mmol, 1.2 equiv.), and K_2CO_3 (829.3 mg, 6.00 mmol, 2.0 equiv.) were subsequently placed into a round-bottom flask equipped with a stirring bar. Then PhMe (48 ml), EtOH (6 ml), and H_2O (6 ml) were added followed by addition of [$Pd(Ph_3P)_4$] (34.7 mg, 0.09 mmol, 1 mol%) under inert atmosphere. The flask was sealed with a glass stopper, and the obtained mixture was thoroughly stirred at 95 °C for 15 h. After that the reaction mixture was quenched with DCM, and $MgSO_4$ was added under stirring until complete removal of water. The obtained mixture was filtered, washing with DCM, and the solvents were removed *in vacuo*. The title product was obtained after purification of the crude mixture by column chromatography (*n*-pentane) as a colorless oil (788.8 mg, 1.86 mmol, 62%).

R_f = 0.59 (*n*-pentane). **^{1}H NMR** (600 MHz, $CDCl_3$) δ/ppm = 7.63-7.60 (m, 1H), 7.53-7.48 (m, 6H), 1.11-1.06 (m, 9H), 1.05-1.01 (m, 6H). **^{13}C NMR** (151 MHz, $CDCl_3$) δ/ppm = 144.7, 140.8, 138.2, 135.5, 134.8, 130.0, 128.6, 126.5, 126.2, 123.2, 9.1, 4.4. **HRMS** (EI) calculated for $C_{16}H_{17}{}^{79}Br^{35}Cl^{74}Ge$: 396.9408 [M-Et]$^+$, found: 396.9399.

Tributyl(phenyl)germane

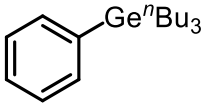

The title product was synthesized according to GP 1 from iodobenzene (612.0 mg, 3.00 mmol, 1.0 equiv.) and tributylchlorogermane (875 µl, 3.30 mmol, 1.1 equiv.) and obtained after purification by column chromatography (*n*-pentane) as a colorless oil (470.6 mg, 1.64 mmol, 82%).

R_f = 0.63 (*n*-pentane). **^{1}H NMR** (600 MHz, $CDCl_3$) δ/ppm = 7.46-7.41 (m, 2H), 7.36-7.28 (m, 3H), 1.43-1.29 (m, 12H), 1.01-0.95 (m, 6H), 0.89 (t, *J* = 6.9 Hz, 9H). **^{13}C NMR** (151 MHz, $CDCl_3$) δ/ppm = 140.9, 134.0, 128.1, 127.9, 27.5, 26.7, 13.9, 12.8. **HRMS** (APCI) calculated for $C_{14}H_{23}{}^{74}Ge$: 265.1006 [M]$^+$, found: 265.1010.

4.2 Supporting information for chapter 1

4.2.1 Supporting information for chapter 1.1

Synthesis Procedure and Characterization of Diazonium Salts

Diazonium salts synthesized by other members of the group are not listed here.

General Procedure 1 (GP 1)

Diazonium salts were synthesised according to literature known procedure.[202] The corresponding aniline (1.0 equiv.) was dissolved in EtOH (0.8 M) followed by addition of an aqueous solution of HBF_4 (48% in water, 2.0 equiv.). Then isoamyl nitrite (2.0 equiv.) was added dropwise at -20 °C. After the reaction mixture was allowed to warm up to room temperature and was stirred for 1 h. Et_2O was added to precipitate the corresponding diazonium salt followed by filtration and washing the solid with Et_2O (30 ml) or recrystallization from Et_2O/acetone mixture. The obtained salt was dried in high vacuum and stored in a freezer.

4-(Trifluoromethyl)benzenediazonium tetrafluoroborate

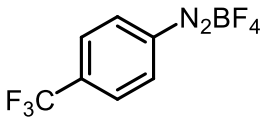

The title product was obtained by using (4-trifluoromethyl)aniline (1.21 g, 7.5 mmol, 1.0 equiv.) according to GP 1 as a white solid (1.50 g, 5.78 mmol, 77%).

^{1}H NMR (300 MHz, DMSO-d_6) δ/ppm = 8.90 (d, *J* = 8.7 Hz, 2H), 8.42 (d, *J* = 8.7 Hz, 2H). **^{13}C NMR** (151 MHz, DMSO-d_6) δ/ppm = 138.1 (q, *J* = 33.7 Hz), 133.8, 128.3 (q, *J* = 3.6 Hz), 122.3 (q, *J* = 274.1 Hz), 121.31. **^{19}F NMR** (282 MHz, DMSO-d_6) δ/ppm = -62.65 (s, 3F), -148.14 and -148.20 (s, BF_4). These data are in agreement with those reported previously in the literature.[203]

2-Bromo-4-chlorobenzenediazonium tetrafluoroborate

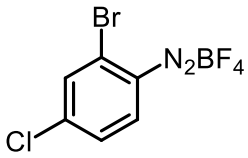

The title product was obtained by using 2-bromo-4-chloroaniline (825.9 mg, 4.00 mmol, 1.0 equiv.) according to GP 1 as a white solid (1.12 g, 3.68 mmol, 92%).

^{1}H NMR (400 MHz, DMSO-d_6) δ/ppm = 8.85 (d, *J* = 8.9 Hz, 1H), 8.62 (d, *J* = 2.0 Hz, 1H), 8.13 (dd, *J* = 8.9, 2.0 Hz, 1H). **^{13}C NMR** (101 MHz, DMSO-d_6) δ/ppm = 147.2, 135.9, 135.2, 130.9, 125.9, 117.6. **^{19}F NMR** (376 MHz, DMSO-d_6) δ/ppm = -148.23 and -148.28 (s, BF_4). These data are in agreement with those reported previously in the literature.[204]

3,5-Bis(trifluoromethyl)benzenediazonium tetrafluoroborate

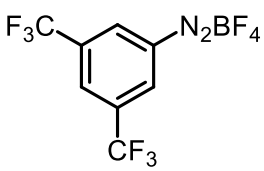

The title product was obtained by using 3,5-bis(trifluoromethyl)aniline (1.40 g, 6.10 mmol, 1.0 equiv.) according to GP 1 as a white solid (1.76 g, 5.38 mmol, 88%).

^{1}H NMR (400 MHz, DMSO-d_6) δ/ppm = 9.51 (s, 2H), 9.18 (s, 1H). **^{13}C NMR** (151 MHz, DMSO-d_6) δ/ppm = 134.8 (m), 134.0 (m), 132.0 (q, *J* = 35.8 Hz), 121.4 (q, *J* = 274.1 Hz), 120.1. **^{19}F NMR** (376 MHz, DMSO-d_6) δ/ppm = -61.84 (s, 6F), -148.27 and -148.32 (s, BF_4). These data are in agreement with those reported previously in the literature.[205]

4-(Ethoxycarbonyl)benzenediazonium tetrafluoroborate

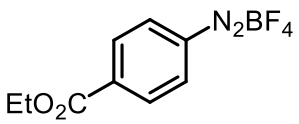

The title product was obtained by using ethyl 4-aminobenzoate (3.30 g, 20.0 mmol, 1.0 equiv.) according to GP 1 as a white solid (4.91 g, 18.6 mmol, 93%).

^{1}H NMR (300 MHz, DMSO-d_6) δ/ppm = 8.80 (d, *J* = 9.0 Hz, 2H), 8.44 (d, *J* = 9.0 Hz, 2H), 4.41 (q, *J* = 7.1 Hz, 2H), 1.36 (t, *J* = 7.1 Hz, 3H). **^{13}C NMR** (75 MHz, DMSO-d_6) δ/ppm = 163.3, 139.4, 133.2, 131.2, 120.2, 62.4, 14.0. **^{19}F NMR** (376 MHz, DMSO-d_6) δ/ppm = -148.23 and -148.28 (s, BF_4). These data are in agreement with those reported previously in the literature.[202]

4-Acetylbenzenediazonium tetrafluoroborate

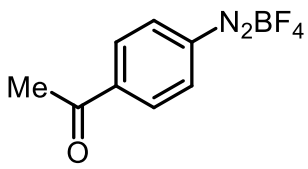

The title product was obtained by using 4-acetylaniline (865.1 mg, 6.46 mmol, 1.0 equiv.) according to GP 1 as a white solid (1.01 g, 4.33 mmol, 67%).

^{1}H NMR (400 MHz, DMSO-d_6) δ/ppm = 8.80 (d, *J* = 8.6 Hz, 2H), 8.41 (d, *J* = 8.6 Hz, 2H), 2.71 (s, 3H). **^{13}C NMR** (101 MHz, DMSO-d_6) δ/ppm = 196.7, 144.6, 133.2, 130.1, 119.5, 27.4. **^{19}F NMR** (376 MHz, DMSO-d_6) δ/ppm = -148.20 and -148.26 (s, BF_4). These data are in agreement with those reported previously in the literature.[205]

4-(Methylsulfonyl)benzenediazonium tetrafluoroborate

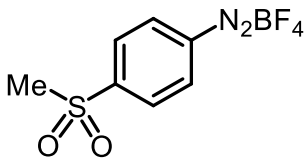

The title product was obtained by using 4-(methylsulfonyl)aniline (702.0 mg, 4.1 mmol, 1.0 equiv.) according to GP 1 as a white solid (1.07 g, 3.97 mmol, 97%).

^{1}H NMR (300 MHz, DMSO-d_6) δ/ppm = 8.92 (d, *J* = 9.1 Hz, 2H), 8.50 (d, *J* = 9.1 Hz, 2H), 3.46 (s, 3H). **^{13}C NMR** (101 MHz, DMSO-d_6) δ/ppm = 149.9, 133.8, 129.4, 121.5, 42.5. **^{19}F NMR** (376 MHz, DMSO-d_6) δ/ppm = -148.21 and -148.27 (s, BF_4).

4-(Phenyl)benzenediazonium tetrafluoroborate

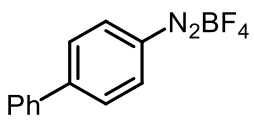

The title product was obtained by using 4-aminobiphenyl (507.7 mg, 3.0 mmol, 1.0 equiv.) according to GP 1 as a white solid (645.9 mg, 2.41 mmol, 80%).

^{1}H NMR (400 MHz, DMSO-d_6) δ/ppm = 8.73 (d, *J* = 8.8 Hz, 2H), 8.32 (d, *J* = 8.8 Hz, 2H), 7.96-7.87 (m, 2H), 7.65-7.56 (m, 3H). **^{13}C NMR** (101 MHz, DMSO-d_6) δ/ppm = 151.5, 136.4, 133.5, 130.8, 129.6, 129.0, 128.0, 113.4. **^{19}F NMR** (376 MHz, DMSO-d_6) δ/ppm = -148.21 and -148.26 (s, BF_4). These data are in agreement with those reported previously in the literature.[202]

4-(*tert*-Butyl)benzenediazonium tetrafluoroborate

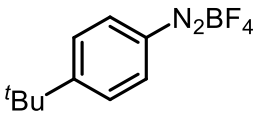

The title product was obtained by using 4-(*tert*-butyl)aniline (597.0 mg, 4.0 mmol, 1.0 equiv.) according to GP 1 as a white solid (578.4 mg, 2.33 mmol, 58%).

^{1}H NMR (600 MHz, DMSO-d_6) δ/ppm = 8.59 (d, *J* = 9.0 Hz, 2H), 8.03 (d, *J* = 9.0 Hz, 2H), 1.35 (s, 9H). **^{13}C NMR** (151 MHz, DMSO-d_6) δ/ppm = 165.5, 132.8, 128.5, 112.2, 36.5, 30.2. **^{19}F NMR** (565 MHz, DMSO-d_6) δ/ppm = -148.20 and -148.26 (s, BF_4). These data are in agreement with those reported previously in the literature.[202]

4-Methylbenzenediazonium tetrafluoroborate

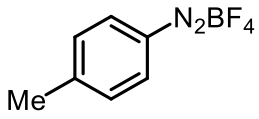

The title product was obtained by using 4-methylaniline (535.8 mg, 5.00 mmol, 1.0 equiv.) according to GP 1 as a white solid (844.9 mg, 4.10 mmol, 82%).

^{1}H NMR (400 MHz, DMSO-d_6) δ/ppm = 8.55 (d, *J* = 8.6 Hz, 2H), 7.79 (d, *J* = 8.6 Hz, 2H), 2.57 (s, 3H). **^{13}C NMR** (101 MHz, DMSO-d_6) δ/ppm = 153.9, 132.7, 131.8, 112.0, 22.4. **^{19}F NMR** (376 MHz, DMSO-d_6) δ/ppm = -148.23 and -148.28 (s, BF_4). These data are in agreement with those reported previously in the literature.[202]

4-Iodobenzenediazonium tetrafluoroborate

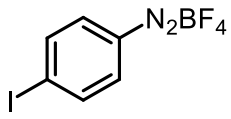

The title product was obtained by using 4-iodoaniline (657.1 mg, 3.00 mmol, 1.0 equiv.) according to GP 1 as a white solid (872.0 mg, 2.74 mmol, 91%).

^{1}H NMR (300 MHz, DMSO-d_6) δ/ppm = 8.43 (d, *J* = 9.1 Hz, 2H), 8.35 (d, *J* = 9.1 Hz, 2H). **^{13}C NMR** (75 MHz, DMSO-d_6) δ/ppm = 140.2, 132.9, 115.2, 113.7. **^{19}F NMR** (282 MHz, DMSO-d_6) δ/ppm = -148.20 and -148.25 (s, BF_4). These data are in agreement with those reported previously in the literature.[205]

Au-catalyzed Arylation of Aryl Germanes and *e*-Poor Diazonium Salts

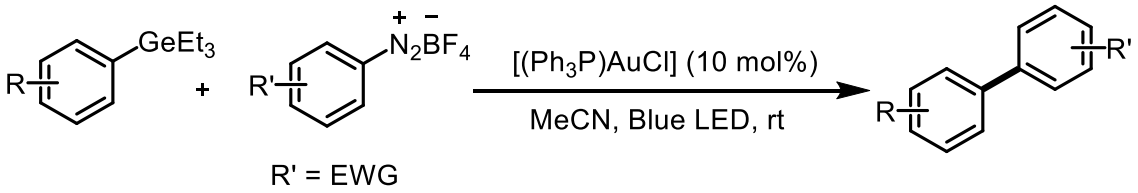

General Procedure 1 (GP 1)

In an argon-filled glovebox, corresponding aryl triethylgermane (0.30 mmol, 1.0 equiv.), diazonium salt (0.45 mmol, 1.5 equiv.), and [(Ph_3P)AuCl] (0.03 mmol, 10 mol%) were mixed in a screw top vial equipped with a magnetic stirring bar and dissolved in anhydrous and degassed MeCN (3 ml). The vial was sealed with a cap, taken out from the glovebox and placed into the blue LED setup. After full consumption of aryl germane (determined by GC-MS) the crude mixture was concentrated *in vacuo*, and residue was purified by silica gel column chromatography. Reaction time is specified for the individual compounds.

4-Fluoro-4'-nitro-1,1'-biphenyl (1)

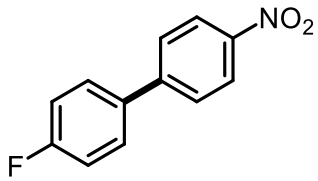

The cross-coupling was performed according to GP 1 by using triethyl(4-fluorophenyl)germane (76.5 mg, 0.30 mmol, 1.0 equiv.) and 4-nitrobenzenediazonium tetrafluoroborate (106.6 mg, 0.45 mmol, 1.5 equiv.). Reaction time: 2 h. The title product was obtained after purification by column chromatography (25:1 *n*-hexane/EtOAc) as a white solid (62.2 mg, 0.286 mmol, 96%).

R_f = 0.50 (20:1 *n*-hexane/EtOAc). **^{1}H NMR** (400 MHz, $CDCl_3$) δ/ppm = 8.28 (d, *J* = 8.7 Hz, 2H), 7.69 (d, *J* = 8.7 Hz, 2H), 7.60 (dd, *J* = 8.7, 5.4 Hz, 2H), 7.23-7.13 (m, 2H). **^{13}C NMR** (101 MHz, $CDCl_3$) δ/ppm = 163.5 (d, *J* = 248.3 Hz), 147.2, 146.7, 135.0 (d, *J* = 3.1 Hz), 129.3 (d, *J* = 8.3 Hz), 127.5, 124.3, 116.3 (d, *J* = 21.6 Hz). **^{19}F NMR** (376 MHz, $CDCl_3$) δ/ppm = -112.67 – -112.82 (m, 1F). **HRMS** (EI) calculated for $C_{12}H_8FNO_2$: 217.0534 $[M]^+$, found: 217.0540. These data are in agreement with those reported previously in the literature.[206]

4-Bromo-3-methyl-4'-(trifluoromethyl)-1,1'-biphenyl (2)

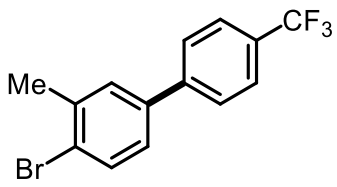

The cross-coupling was performed according to GP 1 by using (4-bromo-3-methylphenyl)triethylgermane (99.0 mg, 0.30 mmol, 1.0 equiv.) and (4-trifluoromethyl)benzenediazonium tetrafluoroborate (117.0 mg, 0.45 mmol, 1.5 equiv.). Reaction time: 7 h. The title product was obtained after purification by column chromatography (*n*-hexane) and preparative HPLC (95:5 *n*-hexane/EtOAc) as a colorless oil (73.7 mg, 0.234 mmol, 78%).

R_f = 0.58 (*n*-hexane). **^{1}H NMR** (600 MHz, $CDCl_3$) δ/ppm = 7.69 (d, *J* = 8.3 Hz, 2H), 7.65 (d, *J* = 8.3 Hz, 2H), 7.62 (d, *J* = 8.2 Hz, 2H), 7.45 (d, *J* = 2.3 Hz, 2H), 7.29-7.25 (m, 1H), 2.48 (s, 3H). **^{13}C NMR** (151 MHz, $CDCl_3$) δ/ppm = 143.9, 139.1, 138.7, 133.1, 129.8 (q, *J* = 32.5 Hz), 129.7, 127.4, 126.3, 125.9 (q, *J* = 3.7 Hz), 125.2, 124.4 (q, *J* = 271.9 Hz), 23.2. **^{19}F NMR** (565 MHz, $CDCl_3$) δ/ppm = -62.47 (s, 3F). **IR** (neat): ν/cm^{-1} = 2952, 2855, 2326, 2102, 1921, 1616, 1562, 1473, 1417, 1381, 1323, 1165, 1119, 1070, 1022, 885, 843, 813, 743, 660. **HRMS** (EI) calculated for $C_{14}H_{10}{}^{79}BrF_3$: 313.9912 $[M]^+$, found: 313.9906.

1-(4'-Bromo-3'-methyl-[1,1'-biphenyl]-4-yl)ethan-1-one (3)

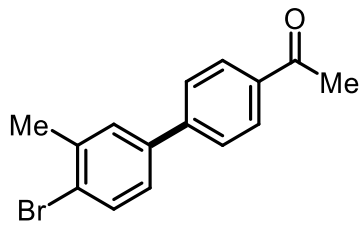

The cross-coupling was performed according to GP 1 by using (4-bromo-3-methylphenyl)triethylgermane (99.0 mg, 0.30 mmol, 1.0 equiv.) and 4-acetylbenzenediazonium tetrafluoroborate (105.3 mg, 0.45 mmol, 1.5 equiv.). Reaction time: 3 h. The title product was obtained after purification by column chromatography (20:1 *n*-pentane/EtOAc) as a white solid (54.7 mg, 0.189 mmol, 63%).

R_f = 0.20 (20:1 *n*-pentane/EtOAc). **^{1}H NMR** (600 MHz, $CDCl_3$) δ/ppm = 8.02 (d, *J* = 8.4 Hz, 2H), 7.65 (d, *J* = 8.4 Hz, 2H), 7.62 (d, *J* = 8.2 Hz, 1H), 7.48 (d, *J* = 2.2 Hz, 1H), 7.30 (dd, *J* = 8.2, 2.2 Hz, 1H), 2.64 (s, 3H), 2.48 (s, 3H). **^{13}C NMR** (151 MHz, $CDCl_3$) δ/ppm = 197.8, 144.9, 139.2, 138.6, 136.2, 133.0, 129.7, 129.1, 127.2, 126.2, 125.3, 26.8, 23.2. **IR** (neat): ν/cm^{-1} = 3055, 2921, 2853, 2324, 2115, 1740, 1675, 1598, 1512, 1469, 1439, 1415, 1351, 1259, 1190, 1151, 1120, 1078, 1021, 955, 899, 845, 809, 746, 705. **LC-MS** (APCI) calculated for $C_{15}H_{14}{}^{79}BrO$: 289.0223 $[M+H]^+$, found: 289.0225.

4-Chloro-3-fluoro-4'-iodo-1,1'-biphenyl (4)

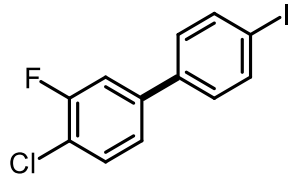

The cross-coupling was performed according to GP 1 by using (4-chloro-3-fluorophenyl)triethylgermane (86.8 mg, 0.30 mmol, 1.0 equiv.) and 4-iodobenzenediazonium tetrafluoroborate (143.0 mg, 0.45 mmol, 1.5 equiv.). Reaction time: 2 h. The title product was obtained after purification by column chromatography (*n*-pentane) and preparative HPLC (97:3 *n*-hexane/EtOAc) as a

white solid (57.1 mg, 0.172 mmol, 57%).

R_f = 0.48 (*n*-pentane). **^{1}H NMR** (600 MHz, $CDCl_3$) δ/ppm = 7.78 (d, *J* = 8.4 Hz, 2H), 7.49-7.41 (m, 1H), 7.33 (dd, *J* = 10.2, 2.1 Hz, 1H), 7.27 (m, 3H). **^{13}C NMR** (151 MHz, $CDCl_3$) δ/ppm = 158.5 (d, *J* = 248.9 Hz), 140.8 (d, *J* = 6.8 Hz), 138.6 (d, *J* = 2.2 Hz), 138.3, 131.2, 128.8, 123.3 (d, *J* = 3.6 Hz), 120.6 (d, *J* = 17.6 Hz), 115.1 (d, *J* = 21.8 Hz), 94.2. **^{19}F NMR** (565 MHz, $CDCl_3$) δ/ppm = -114.73 – -114.86 (m, 1F). **IR** (neat): ν/cm^{-1} = 2922, 2853, 2676, 2322, 2099, 1998, 1911, 1741, 1576, 1551, 1501, 1468, 1418, 1380, 1301, 1248, 1200, 1147, 1106, 1066, 996, 873, 806, 722, 672. **HRMS** (APCI) calculated for $C_{12}H_7{}^{35}ClFI$: 331.9260 $[M]^+$, found: 331.9257.

2'-Bromo-4'-chloro-4-methoxy-[1,1'-biphenyl]-3-carbonitrile (5)

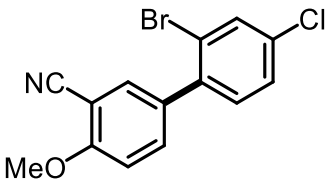

The cross-coupling was performed according to GP 1 by using 2-methoxy-5-(triethylgermyl)benzonitrile (87.6 mg, 0.30 mmol, 1.0 equiv.) and 2-bromo-4-chlorobenzenediazonium tetrafluoroborate (137.4 mg, 0.45 mmol, 1.5 equiv.). Reaction time: 3 h. The title product was obtained after purification by column chromatography (10:1 n-pentane/EtOAc) as a pale brown solid (67.9 mg, 0.210 mmol, 79%).

R_f = 0.30 (10:1 *n*-pentane/EtOAc). **^{1}H NMR** (600 MHz, $CDCl_3$) δ/ppm = 7.69 (d, *J* = 2.1 Hz, 1H), 7.59 (d, *J* = 2.2 Hz, 1H), 7.57 (dd, *J* = 8.7, 2.2 Hz, 1H), 7.36 (dd, *J* = 8.2, 2.1 Hz, 1H), 7.22 (d, *J* = 8.2 Hz, 1H), 7.04 (d, *J* = 8.7 Hz, 1H), 3.99 (s, 3H). **^{13}C NMR** (151 MHz, $CDCl_3$) δ/ppm = 161.0, 138.7, 135.5, 134.6, 134.6, 133.1, 132.9, 131.8, 128.1, 123.2, 116.2, 111.2, 101.9, 56.4. **IR** (neat): ν/cm^{-1} = 3085, 2924, 2850, 2308, 2226, 2116, 1908, 1734, 1608, 1581, 1550, 1502, 1464, 1411, 1367, 1283, 1263, 1191, 1130, 1095, 1065, 1012, 954, 920, 869, 815, 769, 741, 662. **HRMS** (ESI) calculated for $C_{14}H_9{}^{79}Br{}^{35}ClNNaO$: 343.9448 $[M+Na]^+$, found: 343.9443.

4-Methoxy-3',5'-bis(trifluoromethyl)-[1,1'-biphenyl]-3-carbonitrile (6)

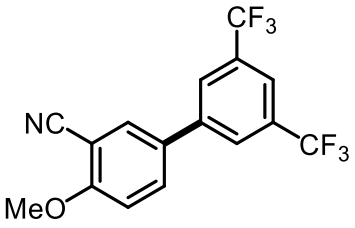

The cross-coupling was performed according to GP 1 by using 2- methoxy-5-(triethylgermyl)benzonitrile (87.6 mg, 0.30 mmol, 1.0 equiv.) and 3,5-bis(trifluoromethyl)benzenediazonium tetrafluoroborate (147.6 mg, 0.45 mmol, 1.5 equiv.). Reaction time: 16 h. The title product was obtained after purification by column chromatography (10:1 *n*-pentane/EtOAc) as an orange solid (85.5 mg, 0.248 mmol, 83%).

R_f = 0.20 (10:1 *n*-pentane/EtOAc). **^{1}H NMR** (600 MHz, $CDCl_3$) δ/ppm = 7.95-7.92 (m, 2H), 7.89-7.86 (m, 1H), 7.82 (d, *J* = 2.4 Hz, 1H), 7.79 (dd, J = 8.7, 2.4 Hz, 1H), 7.12 (d, *J* = 8.7 Hz, 1H), 4.02 (s, 3H). **^{13}C NMR** (151 MHz, $CDCl_3$) δ/ppm = 161.7, 140.9, 133.3, 133.0, 132.7 (q, *J* = 33.4 Hz), 132.50, 131.3, 123.2 (q, *J* = 273.0 Hz), 121.6-121.4 (m), 115.9, 112.3, 103.1, 56.6. **^{19}F NMR** (376 MHz, $CDCl_3$) δ/ppm = -62.92 (s, 6F). **IR** (neat): ν/cm^{-1} = 2925, 2852, 2234, 1610, 1509, 1465, 1374, 1272, 1163, 1113, 1063, 1020, 894, 826, 745, 703, 680. **HRMS** (ESI) calculated for $C_{16}H_9F_6NNaO$: 368.0481 $[M+Na]^+$, found: 368.0477.

3,5-Dimethyl-4-(4-(methylsulfonyl)phenyl)isoxazole (7)

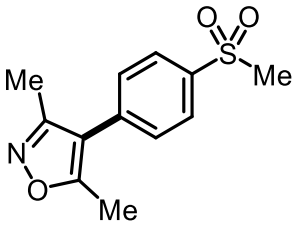

The cross-coupling was performed according to GP 1 by using 3,5- dimethyl-4-(triethylgermyl)isoxazole (76.8 mg, 0.30 mmol, 1.0 equiv.) and 4-(methylsulfonyl)benzenediazonium tetrafluoroborate (121.5 mg, 0.45 mmol, 1.5 equiv.). Reaction time: 16 h. The title product was obtained after purification by column chromatography (1:1 *n*-pentane/EtOAc) as a white solid (55.0 mg, 0.219 mmol, 73%).

R_f = 0.30 (1:1 *n*-pentane/EtOAc). **^{1}H NMR** (600 MHz, $CDCl_3$) δ/ppm = 8.02 (d, *J* = 8.4 Hz, 2H), 7.47 (d, *J* = 8.4 Hz, 2H), 3.11 (s, 3H), 2.45 (s, 3H), 2.30 (s, 3H). **^{13}C NMR** (151 MHz, $CDCl_3$) δ/ppm = 166.4, 158.3, 139.8, 136.6, 130.0, 128.1, 115.5, 44.7, 11.9, 11.0. **IR** (neat): ν/cm^{-1} = 3013, 2923, 2854, 1712, 1621, 1564, 1487, 1419, 1393, 1303, 1235, 1145, 1088, 1024, 997, 953, 893, 840, 772, 722. **HRMS** (ESI) calculated for $C_{12}H_{14}NO_3S$: 252.0689 $[M+H]^+$, found: 252.0686.

3-(4-Nitrophenyl)thiophene (8)

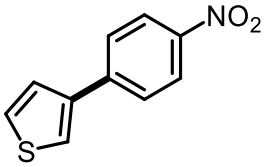

The cross-coupling was performed according to GP 1 by using triethyl(thiophen-3-yl)germane (72.9 mg, 0.30 mmol, 1.0 equiv.) and 4-nitrobenzenediazonium tetrafluoroborate (106.6 mg, 0.45 mmol, 1.5 equiv.). Reaction time: 2 h. The title product was obtained after purification by column chromatography (*n*-pentane to 20:1 *n*-pentane/EtOAc) as a yellow solid (43.5 mg, 0.212 mmol, 71%).

R_f = 0.27 (30:1 *n*-pentane/EtOAc). **^{1}H NMR** (600 MHz, $CDCl_3$) δ/ppm = 8.27 (d, *J* = 8.8 Hz, 2H), 7.74 (d, *J* = 8.8 Hz, 2H), 7.64 (dd, *J* = 2.9, 1.3 Hz, 1H), 7.47 (dd, *J* = 5.0, 2.9 Hz, 1H), 7.44 (dd, *J* = 5.0, 1.3 Hz, 1H). **^{13}C NMR** (151 MHz, $CDCl_3$) δ/ppm = 146.8, 142.1, 140.1, 127.5, 127.0, 126.2, 124.5, 123.3. **HRMS** (ESI) calculated for $C_{10}H_7NNaO_2S$: 228.0090 $[M+Na]^+$, found: 228.0090. These data are in agreement with those reported previously in the literature.[207]

2-(4-Nitrophenyl)thiophene (9)

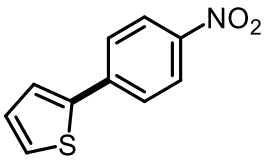

The cross-coupling was performed according to GP 1 by using triethyl(thiophen-2-yl)germane (72.9 mg, 0.30 mmol, 1.0 equiv.) and 4-nitrobenzenediazonium tetrafluoroborate (106.6 mg, 0.45 mmol, 1.5 equiv.). Reaction time: 2 h. The title product was obtained after purification by column chromatography (4:1, 2:1 *n*-hexane/DCM) as a yellow solid (39.7 mg, 0.193 mmol, 64%).

R_f = 0.30 (2:1 *n*-hexane/DCM). **^{1}H NMR** (400 MHz, $CDCl_3$) δ/ppm = 8.24 (d, *J* = 8.9 Hz, 2H), 7.75 (d, *J* = 8.9 Hz, 2H), 7.48 (dd, *J* = 3.6, 1.0 Hz, 1H), 7.44 (dd, *J* = 5.1, 1.0 Hz, 1H), 7.15 (dd, *J* = 5.1, 3.6 Hz, 1H). **^{13}C NMR** (101 MHz, $CDCl_3$) δ/ppm = 146.7, 141.7, 140.7, 128.8, 127.8, 126.1, 125.8, 124.5. **HRMS** (ESI) calculated for $C_{10}H_7NNaO_2S$: 228.0090 $[M+Na]^+$, found: 228.0090. These data are in agreement with those reported previously in the literature.[208]

5-(2-Nitrophenyl)benzo[*d*][1,3]dioxole (10)

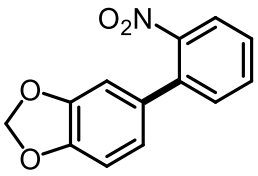

The cross-coupling was performed according to GP 1 by using benzo[*d*][1,3]dioxol-5-yltriethylgermane (84.3 mg, 0.30 mmol, 1.0 equiv.) and 2-nitrobenzenediazonium tetrafluoroborate (106.6 mg, 0.45 mmol, 1.5 equiv.). Reaction time: 2 h. The title product was obtained after purification by column chromatography (12:1 *n*-hexane/EtOAc) as a red oil (40.5 mg, 0.167 mmol, 58%).

R$_f$ = 0.30 (12:1 *n*-hexane/EtOAc). **^{1}H NMR** (600 MHz, $CDCl_3$) δ/ppm = 7.80 (dd, *J* = 8.1, 1.3 Hz, 1H), 7.60-7.56 (m, 1H), 7.47-7.43 (m, 1H), 7.42 (dd, *J* = 7.7, 1.4 Hz, 1H), 6.86 (d, *J* = 7.9 Hz, 1H), 6.80 (d, *J* = 1.8 Hz, 1H), 6.78 (dd, *J* = 7.9, 1.8 Hz, 1H), 6.01 (s, 2H). **^{13}C NMR** (151 MHz, $CDCl_3$) δ/ppm = 149.6, 148.1, 148.0, 136.0, 132.3, 132.0, 131.1, 128.1, 124.2, 121.8, 108.8, 108.6, 101.5. **IR** (neat): ν/cm^{-1} = 2895, 1729, 1608, 1571, 1522, 1471, 1352, 1224, 1145, 1109, 1037, 933, 892, 855, 813, 781, 749, 712, 666. **HRMS** (ESI) calculated for $C_{13}H_9NNaO_4$: 266.0424 $[M+Na]^+$, found: 266.0423.

4'-Bromo-2-isopropyl-1,1'-biphenyl (11)

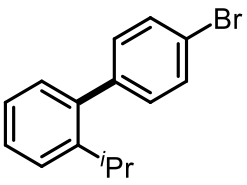

The cross-coupling was performed according to GP 1 by using triethyl(2-isopropylphenyl)germane (83.7 mg, 0.30 mmol, 1.0 equiv.) and 4-bromobenzenediazonium tetrafluoroborate (121.9 mg, 0.45 mmol, 1.5 equiv.). Reaction time: 2 h. The title product was obtained after purification by column chromatography (*n*-hexane) and preparative HPLC (95:5 n-hexane/EtOAc) as a colorless oil (40.5 mg, 0.147 mmol, 49%).

R$_f$ = 0.53 (*n*-hexane). **^{1}H NMR** (400 MHz, $CDCl_3$) δ/ppm = 7.55 (d, *J* = 8.2 Hz, 2H), 7.44-7.34 (m, 2H), 7.25-7.13 (m, 4H), 3.02 (sept, *J* = 6.9 Hz, 1H), 1.18 (d, *J* = 6.9 Hz, 6H). **^{13}C NMR** (101 MHz, $CDCl_3$) δ/ppm = 146.4, 141.1, 139.9, 131.3, 131.1, 129.9, 128.2, 125.8, 125.6, 121.1, 29.5, 24.4. **IR** (neat): ν/cm^{-1} = 3058, 3023, 2961, 2927, 2868, 2324, 2113, 1905, 1588, 1473, 1445, 1386, 1363, 1258, 1094, 1071, 1036, 1004, 946, 826, 756, 722. **HRMS** (APCI) calculated for $C_{15}H_{15}Br$: 274.0352 $[M]^+$, found: 274.0352.

1-(2'-Isopropyl-[1,1'-biphenyl]-4-yl)ethan-1-one (12)

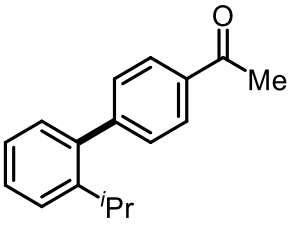

The cross-coupling was performed according to GP 1 by using triethyl(2-isopropylphenyl)germane (83.7 mg, 0.30 mmol, 1.0 equiv.) and 4-acetylbenzenediazonium tetrafluoroborate (105.3 mg, 0.45 mmol, 1.5 equiv.). Reaction time: 2 h. The title product was obtained after purification by column chromatography (20:1 *n*-pentane/EtOAc) as a pale yellow oil (34.1 mg, 0.143 mmol, 48%).

R$_f$ = 0.30 (20:1 *n*-pentane/EtOAc). **^{1}H NMR** (600 MHz, $CDCl_3$) δ/ppm = 8.01 (d, *J* = 8.3 Hz, 2H), 7.43-7.36 (m, 4H), 7.25-7.22 (m, 1H), 7.16 (dd, *J* = 7.6, 1.4 Hz, 1H), 2.99 (sept, *J* = 6.9 Hz, 1H), 2.66 (s, 3H), 1.16 (d, *J* = 6.9 Hz, 6H). **^{13}C NMR** (151 MHz, $CDCl_3$) δ/ppm = 198.0, 147.4, 146.3, 140.1, 135.7, 129.8, 129.7, 128.4, 128.3, 125.9, 125.6, 29.6, 26.8, 24.4. **IR** (neat): ν/cm^{-1} = 3059, 3023, 2962, 2927, 2869, 2324, 2092, 1682, 1603, 1559, 1479, 1443, 1400, 1357, 1262, 1180, 1105, 1035, 1005, 955, 839, 759, 668. **HRMS** (ESI) calculated for $C_{17}H_{18}NaO$: 261.1250 $[M+Na]^+$, found: 261.1250.

3'-Bromo-5'-chloro-2-nitro-1,1'-biphenyl (13)

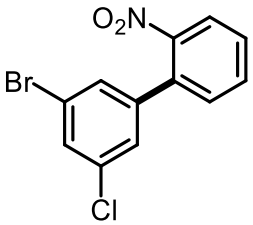

The cross-coupling was performed according to GP 1 by using (3-bromo-5-chlorophenyl)triethylgermane (105.1 mg, 0.30 mmol, 1.0 equiv.) and 2-nitrobenzenediazonium tetrafluoroborate (106.6 mg, 0.45 mmol, 1.5 equiv.). Reaction time: 7 h. The title product was obtained after purification by column chromatography (15:1 n-pentane/EtOAc) as a yellow solid (77.2 mg, 0.247 mmol, 82%).

R_f = 0.27 (15:1 *n*-pentane/EtOAc). **^{1}H NMR** (600 MHz, $CDCl_3$) δ/ppm = 7.96 (dd, *J* = 8.2, 1.3 Hz, 1H), 7.68-7.63 (m, 1H), 7.58-7.54 (m, 2H), 7.39 (dd, *J* = 7.6, 1.4 Hz, 1H), 7.36-7.34 (m, 1H), 7.25-7.23 (m, 1H). **^{13}C NMR** (151 MHz, $CDCl_3$) δ/ppm = 148.7, 140.9, 135.4, 134.0, 133.0, 132.0, 131.3, 129.5, 127.1, 124.7, 123.0. **IR** (neat): ν/cm^{-1} = 3069, 2923, 2858, 2342, 2111, 1738, 1586, 1553, 1518, 1441, 1406, 1346, 1309, 1268, 1145, 1098, 1038, 890, 854, 809, 780, 741, 709, 676. HRMS (ESI) calculated for $C_{12}H_7{}^{79}Br^{35}ClNNaO_2$: 333.9241 $[M+Na]^+$, found 333.9240. The resolution of the ^{13}C NMR does not allow for accurate assignment of all the signals.

2'-Methoxy-[1,1'-biphenyl]-2-carbonitrile (14)

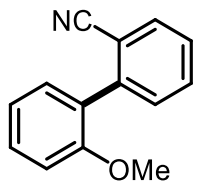

The cross-coupling was performed according to GP 1 by using triethyl(2-methoxyphenyl)germane (80.1 mg, 0.30 mmol, 1.0 equiv.) and 2-cyanobenzenediazonium tetrafluoroborate (97.6 mg, 0.45 mmol, 1.5 equiv.). Reaction time: 5 h. The title product was obtained after purification by column chromatography (20:1 *n*-pentane/EtOAc) as oil (50.8 mg, 0.243 mmol, 82%).

R_f = 0.30 (20:1 *n*-pentane/EtOAc). **^{1}H NMR** (600 MHz, $CDCl_3$) δ/ppm = 7.73 (dd, *J* = 7.8, 1.4 Hz, 1H), 7.64-7.60 (m, 1H), 7.47-7.45 (m, 1H), 7.43-7.40 (m, 2H), 7.26 (dd, *J* = 7.5, 1.7 Hz, 1H), 7.08-7.04 (m, 1H), 7.04-7.02 (m, 1H), 3.85 (s, 3H). **^{13}C NMR** (151 MHz, $CDCl_3$) δ/ppm = 156.6, 142.7, 132.9, 132.5, 131.1, 131.0, 130.5, 127.47, 127.43, 120.9, 118.8, 113.6, 111.5, 55.6. **HRMS** (ESI) calculated for $C_{14}H_{11}NNaO$: 232.0733 $[M+Na]^+$, found: 232.0732. These data are in agreement with those reported previously in the literature.[209]

Trimethyl(4'-nitro-[1,1'-biphenyl]-4-yl)silane (15)

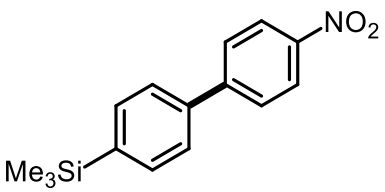

The cross-coupling was performed according to GP 1 by using trimethyl(4-(triethylgermyl)phenyl)silane (92.7 mg, 0.30 mmol, 1.0 equiv.) and 4-nitrobenzenediazonium tetrafluoroborate (85.3 mg, 0.36 mmol, 1.2 equiv.). Reaction time: 2 h. The title product was obtained after purification by column chromatography (6:1 to 2:1 *n*-hexane/DCM) as a pale yellow solid (59.4 mg, 0.219 mmol, 73%).

R_f = 0.12 (8:1 *n*-hexane/DCM). **^{1}H NMR** (400 MHz, $CDCl_3$) δ/ppm = 8.30 (d, *J* = 8.8 Hz, 2H), 7.75 (d, *J* = 8.8 Hz, 2H), 7.67 (d, *J* = 8.1 Hz, 2H), 7.61 (d, *J* = 8.1 Hz, 2H), 0.32 (s, 9H). **^{13}C NMR** (101 MHz, $CDCl_3$) δ/ppm = 147.7, 147.3, 141.8, 139.2, 134.3, 127.9, 126.8, 124.3, - 1.0. **IR** (neat): ν/cm^{-1} = 2956, 2926, 2852, 1595, 1544, 1511, 1411, 1334, 1248, 1179, 1106, 1003, 837, 749, 694. **HRMS** (ESI) calculated for $C_{15}H_{17}NNaO_2Si$: 294.0921 $[M+Na]^+$, found: 294.0921.

Ethyl 4'-(trimethylsilyl)-[1,1'-biphenyl]-4-carboxylate (16)

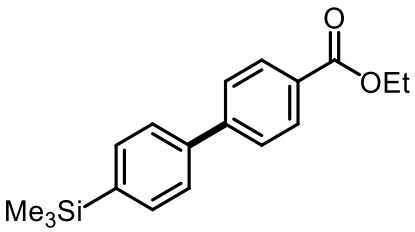

The cross-coupling was performed according to GP 1 by using trimethyl(4-(triethylgermyl)phenyl)silane (92.7 mg, 0.30 mmol, 1.0 equiv.) and 4-(ethoxycarbonyl)benzenediazonium tetrafluoroborate (95.0 mg, 0.36 mmol, 1.2 equiv.). Reaction time: 3 h. The title product was obtained after purification by column chromatography (*n*-hexane to 25:1 *n*-hexane/EtOAc) and preparative HPLC (9:1 *n*-hexane/EtOAc) as a white solid (59.0 mg, 0.198 mmol, 66%).

R_f = 0.30 (25:1 *n*-hexane/EtOAc). **^{1}H NMR** (600 MHz, $CDCl_3$) δ/ppm = 8.12 (d, *J* = 8.4 Hz, 2H), 7.67 (d, *J* = 8.4 Hz, 2H), 7.64-7.60 (m, 4H), 4.41 (q, *J* = 7.1 Hz, 2H), 1.42 (t, *J* = 7.1 Hz, 3H), 0.31 (s, 9H). **^{13}C NMR** (151 MHz, $CDCl_3$) δ/ppm = 166.7, 145.6, 140.6, 140.5, 134.1, 130.2, 129.5, 127.1, 126.7, 61.1, 14.5, -1.0. **IR** (neat): ν/cm^{-1} = 2955, 1712, 1604, 1476, 1446, 1410, 1371, 1311, 1273, 1205, 1178, 1104, 1023, 1003, 838, 756, 700. **HRMS** (ESI) calculated for $C_{18}H_{22}NaO_2Si$: 321.1281 $[M+Na]^+$, found: 321.1274.

1-(4'-(Trimethylsilyl)-[1,1'-biphenyl]-4-yl)ethan-1-one (17)

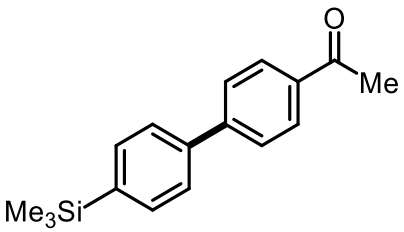

The cross-coupling was performed according to GP 1 by using trimethyl(4-(triethylgermyl)phenyl)silane (92.7 mg, 0.30 mmol, 1.0 equiv.) and 4-acetylbenzenediazonium tetrafluoroborate (84.2 mg, 0.36 mmol, 1.2 equiv.). Reaction time: 2 h. The title product was obtained after purification by column chromatography (15:1 *n*-hexane/EtOAc) as a pale yellow solid (56.6 mg, 0.211 mmol, 70%).

R_f = 0.28 (15:1 *n*-hexane/EtOAc). **^{1}H NMR** (400 MHz, $CDCl_3$) δ/ppm = 8.04 (d, *J* = 8.6 Hz, 2H), 7.70 (d, *J* = 8.6 Hz, 2H), 7.64-7.62 (m, 4H), 2.64 (s, 3H), 0.31 (s, 9H). **^{13}C NMR** (101 MHz, $CDCl_3$) δ/ppm = 197.9, 145.9, 140.8, 140.3, 136.1, 134.1, 129.1, 127.4, 126.7, 26.8, -1.0. **HRMS** (ESI) S9 calculated for $C_{17}H_{20}NaOSi$: 291.1176 $[M+Na]^+$, found: 291.1185. These data are in agreement with those reported previously in the literature.[210]

Trimethyl(4'-(trifluoromethyl)-[1,1'-biphenyl]-4-yl)silane (18)

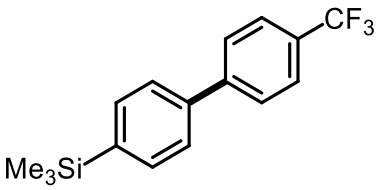

The cross-coupling was performed according to GP 1 by using trimethyl(4-(triethylgermyl)phenyl)silane (92.7 mg, 0.30 mmol, 1.0 equiv.) and (4-trifluoromethyl)benzenediazonium tetrafluoroborate (93.6 mg, 0.36 mmol, 1.2 equiv.). Reaction time: 2 h. The title product was obtained after purification by column chromatography (*n*-hexane) as a white solid (62.9 mg, 0.214 mmol, 67%, purity 96%).

R_f = 0.51 (*n*-hexane). **^{1}H NMR** (600 MHz, $CDCl_3$) δ/ppm = 7.70 (s, 4H), 7.64 (d, *J* = 8.2 Hz, 2H), 7.59 (d, *J* = 8.2 Hz, 2H), 0.32 (s, 9H). **^{13}C NMR** (151 MHz, $CDCl_3$) δ/ppm = 144.8, 140.7, 140.2, 134.2, 129.5 (q, *J* = 32.3 Hz), 127.6, 126.7, 125.9 (q, *J* = 3.8 Hz), 124.4 (q, *J* = 271.8 Hz), -1.0. **^{19}F NMR** (376 MHz, $CDCl_3$) δ/ppm = -62.44 (s, 3F). **IR** (neat): ν/cm^{-1} = 2957, 1696, 1615, 1542, 1413, 1386, 1320, 1252, 1164, 1109, 1067, 1006, 837, 811, 758, 741, 697. **HRMS** (EI) calculated for $C_{16}H_{17}F_3Si$: 294.1046 $[M]^+$, found: 294.1047.

4'-(Trimethylsilyl)-[1,1'-biphenyl]-2-carbonitrile (19)

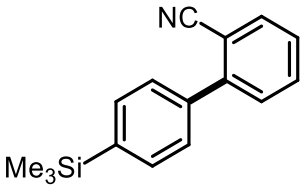

The cross-coupling was performed according to GP 1 by using trimethyl(4-(triethylgermyl)phenyl)silane (92.7 mg, 0.30 mmol, 1.0 equiv.) and 2-cyanobenzenediazonium tetrafluoroborate (78.1 mg, 0.36 mmol, 1.2 equiv.). Reaction time: 2 h. The title product was obtained after purification by column chromatography (15:1 *n*-hexane/EtOAc) as a dark yellow oil (60.3 mg, 0.240 mmol, 80%).

R_f = 0.31 (15:1 *n*-hexane/EtOAc). **^{1}H NMR** (400 MHz, $CDCl_3$) δ/ppm = 7.81-7.75 (m, 1H), 7.70-7.61 (m, 3H), 7.59-7.50 (m, 3H), 7.47-7.41 (m, 1H), 0.32 (s, 9H). **^{13}C NMR** (101 MHz, $CDCl_3$) δ/ppm = 145.6, 141.4, 138.5, 133.9, 133.9, 133.0, 130.2, 128.1, 127.7, 118.9, 111.5, -1.0. **IR** (neat): ν/cm^{-1} = 3065, 2955, 2225, 2092, 1595, 1476, 1442, 1385, 1249, 1115, 1003, 839, 757, 694. **HRMS** (ESI) calculated for $C_{16}H_{17}NNaSi$: 274.1022 $[M+Na]^+$, found: 274.1022.

(5-Iodo-4'-nitro-[1,1'-biphenyl]-3-yl)trimethylsilane (20)

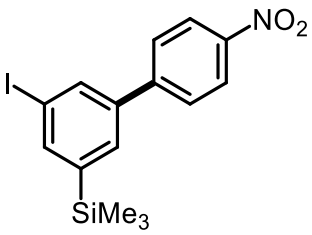

The cross-coupling was performed according to GP 1 by using (3-iodo-5-(triethylgermyl)phenyl)trimethylsilane (130.5 mg, 0.30 mmol, 1.0 equiv.) and 4-nitrobenzenediazonium tetrafluoroborate (85.3 mg, 0.36 mmol, 1.2 equiv.). Reaction time: 2 h. The title product was obtained after purification by column chromatography (30:1 *n*-pentane/EtOAc) and preparative HPLC (95:5 *n*-hexane/EtOAc) as a pale yellow solid (59.4 mg, 0.15 mmol, 50%).

R_f = 0.32 (30:1 *n*-pentane/EtOAc). **^{1}H NMR** (600 MHz, $CDCl_3$) δ/ppm = 8.30 (d, *J* = 8.8 Hz, 2H), 7.94-7.91 (m, 1H), 7.88 (s, 1H), 7.70 (d, *J* = 8.8 Hz, 2H), 7.65-7.64 (m, 1H), 0.32 (s, 9H). **^{13}C NMR** (151 MHz, $CDCl_3$) δ/ppm = 147.6, 146.5, 145.2, 142.4, 140.6, 136.7, 131.3, 128.1, 124.3, 96.1, -1.1. **IR** (neat): ν/cm^{-1} = 2951, 2325, 2085, 1730, 1595, 1543, 1513, 1404, 1383, 1341, 1247, 1193, 1137, 1106, 1044, 992, 834, 790, 745, 682. **HRMS** (ESI) calculated for $C_{15}H_{16}INNaO_2Si$: 419.9887 $[M+Na]^+$, found: 419.9888.

Au-catalyzed Arylation of Aryl Germanes with *e*-Rich Diazonium Salts

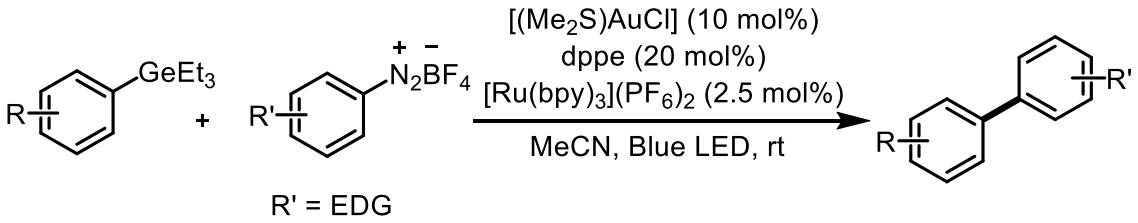

General Procedure (GP)

In an argon-filled glovebox aryl triethylgermane (0.30 mmol, 1.0 equiv.), diazonium salt (0.60 mmol, 2.0 equiv.), [(Me_2S)AuCl] (0.03 mmol, 10 mol%), dppe (0.06 mmol, 20 mol%), and $[Ru(bpy)_3](PF_6)_2$ (0.0075 mmol, 2.5 mol%) were mixed in a screw top vial equipped with magnetic stirring bar and dissolved in anhydrous and degassed MeCN (0.1 M). Then the vial was sealed, taken out from the glovebox and placed into the blue LED

setup. After full consumption of germane (determined by GC-MS) a crude mixture was concentrated *in vacuo* and purified by silica gel column chromatography. The reaction time is specified for the individual compounds.

4'-Methoxy-[1,1'-biphenyl]-4-carbonitrile (21)

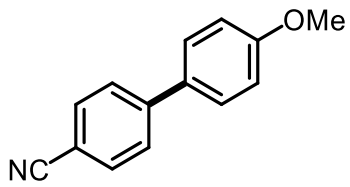

The cross-coupling was performed according to GP 2 by using 4-(triethylgermyl)benzonitrile (52.4 mg, 0.20 mmol, 1.0 equiv.) and 4-methoxybenzenediazonium tetrafluoroborate (88.8 mg, 0.40 mmol, 2.0 equiv.). Reaction time: 2 h. The title product was obtained after purification by column chromatography (15:1 *n*-pentane/EtOAc) as a white solid (30.5 mg, 0.146 mmol, 73%).

R_f = 0.40 (10:1 *n*-pentane/EtOAc). **^{1}H NMR** (400 MHz, $CDCl_3$) δ/ppm = 7.70 (d, *J* = 8.6 Hz, 2H), 7.64 (d, *J* = 8.6 Hz, 2H), 7.54 (d, *J* = 8.8 Hz, 2H), 7.01 (d, *J* = 8.8 Hz, 2H), 3.87 (s, 3H). **^{13}C NMR** (101 MHz, $CDCl_3$) δ/ppm = 160.4, 145.4, 132.7, 131.7, 128.5, 127.3, 119.3, 114.7, 110.3, 55.6. **HRMS** (ESI) calculated for $C_{14}H_{11}NNaO$: 232.0733 $[M+Na]^+$, found: 232.0730. These data are in agreement with those reported previously in the literature.[211]

4-Methoxy-4'-(trifluoromethyl)-1,1'-biphenyl (22)

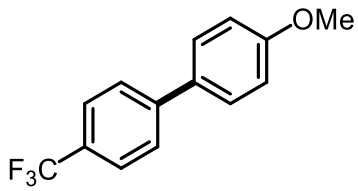

The cross-coupling was performed according to GP 2 by using triethyl(4-(trifluoromethyl)phenyl)germane (91.5 mg, 0.30 mmol, 1.0 equiv.) and 4-methoxybenzenediazonium tetrafluoroborate (133.2 mg, 0.60 mmol, 2.0 equiv.). Reaction time: 2 h. The title product was obtained after purification by column chromatography (20:1 *n*-hexane/EtOAc) as a white solid (56.0 mg, 0.222 mmol, 74%).

R_f = 0.84 (20:1 *n*-hexane/EtOAc). **^{1}H NMR** (600 MHz, $CDCl_3$) δ/ppm = 7.70-7.62 (m, 4H), 7.59-7.52 (m, 2H), 7.05-6.97 (m, 2H), 3.87 (s, 3H). **^{13}C NMR** (151 MHz, $CDCl_3$) δ/ppm = 160.0, 144.4, 132.3, 128.8 (d, *J* = 32.5 Hz), 128.5, 127.0, 125.8 (q, *J* = 3.8 Hz), 124.5 (q, *J* = 271.8 Hz), 114.6, 55.5. **^{19}F NMR** (564 MHz, $CDCl_3$) δ/ppm = -62.32 (s, 3F). **HRMS** (APCI) calculated for $C_{14}H_{11}F_3O$: 252.0757 $[M]^+$, found: 252.0762. These data are in agreement with those reported previously in the literature.[212]

4-Fluoro-4'-methoxy-1,1'-biphenyl (23)

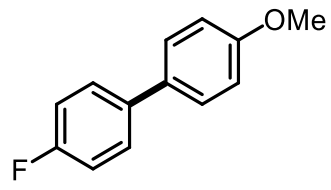

The cross-coupling was performed according to GP 2 by using triethyl(4-fluorophenyl)germane (76.5 mg, 0.30 mmol, 1.0 equiv.) and 4-methoxybenzenediazonium tetrafluoroborate (133.2 mg, 0.60 mmol, 2.0 equiv.). Reaction time: 2 h. The title product was obtained after purification by column chromatography (40:1 n-pentane/EtOAc) as a white solid (41.0 mg, 0.203 mmol, 68%).

R_f = 0.40 (40:1 *n*-pentane/EtOAc). **^{1}H NMR** (600 MHz, $CDCl_3$) δ/ppm = 7.52-7.45 (m, 4H), 7.12-7.08 (m, 2H), 6.97 (d, *J* = 8.7 Hz, 2H), 3.85 (s, 3H). **^{13}C NMR** (151 MHz, $CDCl_3$) δ/ppm = 162.3 (d, *J* = 245.7 Hz), 159.3, 137.1 (d, *J* = 3.1 Hz), 133.0, 128.4 (d, *J* = 8.0 Hz), 128.2, 115.7 (d, *J* = 21.3 Hz), 114.4, 55.5. **^{19}F NMR** (565 MHz, $CDCl_3$) δ/ppm = -116.71 – -116.80 (m, 1F). **HRMS** (APCI) calculated for $C_{13}H_{11}FO$: 202.0788 $[M]^+$, found: 202.0788. These data are in agreement with those reported previously in the literature.[42]

4-Bromo-*p*-terphenyl (24)

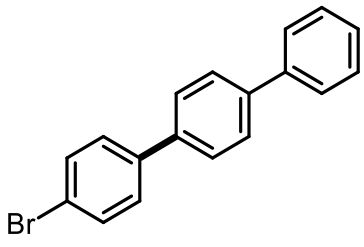

The cross-coupling was performed according to GP 2 by using (4-bromophenyl)triethylgermane (94.7 mg, 0.30 mmol, 1.0 equiv.) and 4-phenylbenzenediazonium tetrafluoroborate (160.8 mg, 0.60 mmol, 2.0 equiv.). Reaction time: 2 h. The title product was obtained after purification by column chromatography (*n*-pentane to 100:1 *n*-pentane/EtOAc) as a pale yellow solid (78.0 mg, 0.252 mmol, 79%).

R_f = 0.29 (*n*-pentane). **^{1}H NMR** (600 MHz, $CDCl_3$) δ/ppm = 7.68 (d, *J* = 8.4 Hz, 2H), 7.66-7.62 (m, 4H), 7.59 (d, *J* = 8.5 Hz, 2H), 7.51 (d, *J* = 8.5 Hz, 2H), 7.49-7.45 (m, 2H), 7.39-7.35 (m, 1H). **^{13}C NMR** (151 MHz, $CDCl_3$) δ/ppm = 140.7, 140.7, 139.8, 139.0, 132.1, 129.0, 128.8, 127.8, 127.6, 127.4, 127.2, 121.8. **HRMS** (APCI) calculated for $C_{18}H_{13}{}^{79}Br$: 308.0195 $[M]^+$, found 308.0195. These data are in agreement with those reported previously in the literature.[213]

(5-Bromo-4'-(*tert*-butyl)-[1,1'-biphenyl]-3-yl)trimethylsilane (25)

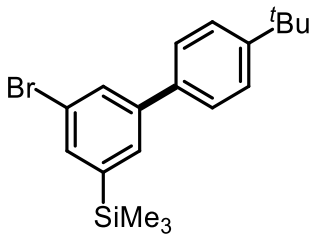

The cross-coupling was performed according to GP 2 by using (3-bromo-5-(triethylgermyl)phenyl)trimethylsilane (116.4 mg, 0.30 mmol, 1.0 equiv.) and 4-(*tert*-butyl)benzenediazonium tetrafluoroborate (89.3 mg, 0.36 mmol, 1.2 equiv.). Reaction time: 2 h. The title compound was obtained after purification by column chromatography (*n*-pentane) as a white solid (57.5 mg, 0.159 mmol, 53%).

R_f = 0.59 (*n*-pentane). **^{1}H NMR** (600 MHz, $CDCl_3$) δ/ppm = 7.71-7.68 (m, 1H), 7.61-7.59 (m, 1H), 7.58-7.55 (m, 1H), 7.52-7.46 (m, 4H), 1.37 (s, 9H), 0.31 (s, 9H). **^{13}C NMR** (151 MHz, $CDCl_3$) δ/ppm = 151.0, 144.1, 142.9, 137.4, 134.5, 130.61, 130.57, 127.1, 126.0, 123.3, 34.7, 31.5, -1.1. **IR** (neat): ν/cm^{-1} = 3034, 2957, 2867, 2324, 2116, 1910, 1739, 1581, 1545, 1513, 1462, 1368, 1249, 1134, 1110, 1054, 1016, 833, 753, 692. **HRMS** (APCI) calculated for $C_{19}H_{25}{}^{79}BrSi$: 360.0903 $[M]^+$, found: 360.0913.

4'-(*tert*-Butyl)-4-chloro-3-fluoro-1,1'-biphenyl (26)

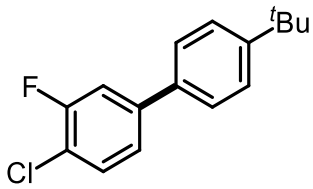

The cross-coupling was performed according to GP 2 by using (4-chloro-3-fluorophenyl)triethylgermane (86.8 mg, 0.30 mmol, 1.0 equiv.) and 4-(*tert*-butyl)benzenediazonium tetrafluoroborate (148.8 mg, 0.60 mmol, 2.0 equiv.). Reaction time: 2 h. The title product was obtained after purification by column chromatography (*n*-pentane) and preparative HPLC (95:5 n-hexane/EtOAc) as a white solid (66.2 mg, 0.252 mmol, 84%).

R_f = 0.46 (*n*-pentane). **^{1}H NMR** (600 MHz, $CDCl_3$) δ/ppm = 7.51-7.46 (m, 4H), 7.43 (m, 1H), 7.37 (dd, *J* = 10.4, 2.1 Hz, 1H), 7.33-7.29 (m, 1H), 1.37 (s, 9H). **^{13}C NMR** (151 MHz, $CDCl_3$) δ/ppm = 158.5 (d, *J* = 248.2 Hz), 151.5, 141.9 (d, *J* = 6.8 Hz), 136.2 (d, *J* = 1.8 Hz), 130.9, 126.7, 126.1, 123.3 (d, *J* = 3.5 Hz), 119.7 (d, *J* = 17.8 Hz), 115.1 (d, *J* = 21.3 Hz), 34.8, 31.5. **^{19}F NMR** (565 MHz, $CDCl_3$) δ/ppm = -115.48 (dd, *J* = 10.0, 8.0 Hz, 1F). **IR** (neat): ν/cm^{-1} = 2964, 2933, 2870, 1606, 1576, 1557, 1476, 1421, 1391, 1366, 1308, 1266, 1248, 1200, 1145, 1110, 1070, 1028, 878, 839, 813, 739, 692. **HRMS** (APCI) calculated for $C_{16}H_{16}{}^{35}ClF$: 262.0919 $[M]^+$, found: 262.0919.

3-(*p*-Tolyl)thiophene (27)

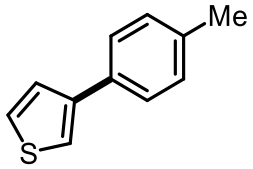

The cross-coupling was performed according to GP 2 by using triethyl(thiophen-3-yl)germane (72.9 mg, 0.30 mmol, 1.0 equiv.) and 4-methylbenzenediazonium tetrafluoroborate (123.6 mg, 0.60 mmol, 2.0 equiv.). Reaction time: 2 h. The title compound was obtained after purification by column chromatography (*n*-pentane) and preparative HPLC (97:3 *n*-hexane/EtOAc) as a white solid (26.7 mg, 0.153 mmol, 51%).

R_f = 0.50 (*n*-pentane). **^{1}H NMR** (400 MHz, $CDCl_3$) δ/ppm = 7.50 (d, *J* = 8.2 Hz, 2H), 7.43-7.40 (m, 1H), 7.39-7.36 (m, 2H), 7.24-7.18 (m, 2H), 2.38 (s, 3H). **^{13}C NMR** (151 MHz, $CDCl_3$) δ/ppm = 142.5, 137.0, 133.3, 129.6, 126.5, 126.2, 119.8, 21.3. **HRMS** (ESI) calculated for $C_{11}H_{11}S$: 175.0576 $[M+H]^+$, found: 175.0573. The resolution of the ^{13}C NMR does not allow for accurate assignment of all the signals.

4'-Methoxy-2-methyl-1,1'-biphenyl (28)

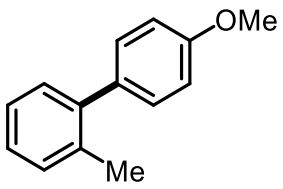

The cross-coupling was performed according to GP 2 by using triethyl(*o*-tolyl)germane (75.3 mg, 0.30 mmol, 1.0 equiv.) and 4-methoxybenzenediazonium tetrafluoroborate (133.2 mg, 0.60 mmol, 2.0 equiv.). Reaction time: 2 h. The title product was obtained after purification by column chromatography (40:1 *n*-pentane/EtOAc) and preparative HPLC (95:5 *n*-hexane/EtOAc) as a colorless oil (27.1 mg, 0.137 mmol, 46%).

R_f = 0.40 (40:1 *n*-pentane/EtOAc). **^{1}H NMR** (600 MHz, $CDCl_3$) δ/ppm = 7.30-7.23 (m, 6H), 6.98 (d, *J* = 8.7 Hz, 2H), 3.88 (s, 3H), 2.30 (s, 3H). **^{13}C NMR** (151 MHz, $CDCl_3$) δ/ppm = 158.7, 141.7, 135.6, 134.5, 130.4, 130.4, 130.1, 127.1, 125.9, 113.6, 55.4, 20.7. **HRMS** (ESI) calculated for $C_{14}H_{14}NaO$: 221.0937 $[M+Na]^+$, found 221.1007. These data are in agreement with those reported previously in the literature.[214]

Derivatization of Biaryal Scaffolds

Pd-catalyzed Desilylative Acetoxylation

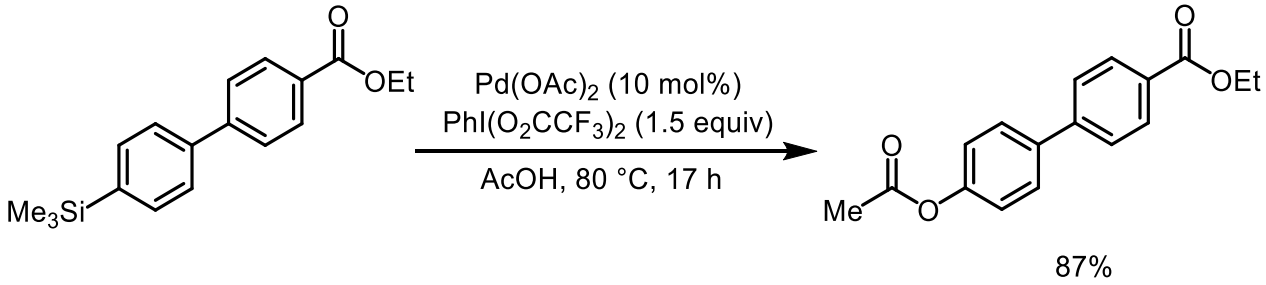

Ethyl 4'-acetoxy-[1,1'-biphenyl]-4-carboxylate

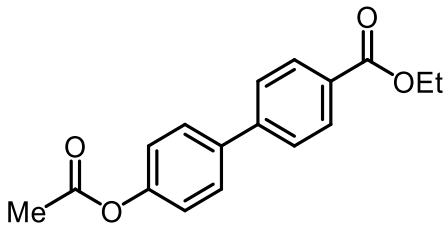

The synthesis was carried out according to the literature.[30] In an argon filled glovebox, 4'-(trimethylsilyl)-[1,1'-biphenyl]-4-carboxylate **16** (59.7 mg, 0.20 mmol, 1.0 equiv.) synthesized according to GP 1, $Pd(OAc)_2$ (2.2 mg, 0.01 mmol, 5 mol. %) and $PhI(O_2CCF_3)_2$ (129.0 mg, 0.30 mmol, 1.5 equiv.) were placed into a screw top vial equipped with magnetic stirring bar and dissolved in AcOH (667 µl). The mixture was stirred at 80 °C for 17 h, after that the reaction mixture was quenched by addition of an aqueous solution of $NaHCO_3$ (sat.). The aqueous phase was extracted with DCM (3 x 20 ml) and the organic phases were combined, dried with $MgSO_4$, filtered, before the solvent was removed *in vacuo*. The title product was obtained after purification by column chromatography (15:1 *n*-pentane/EtOAc) as a white solid (49.6 mg, 0.174 mmol, 87%).
$\mathbf{R_f}$ = 0.30 (10:1 *n*-pentane/EtOAc). **^{1}H NMR** (600 MHz, $CDCl_3$) δ/ppm = 8.11 (d, *J* = 8.4 Hz, 2H), 7.67-7.59 (m, 4H), 7.19 (d, *J* = 8.4 Hz, 2H), 4.40 (q, *J* = 7.1 Hz, 2H), 2.34 (s, 3H), 1.42 (t, *J* = 7.1 Hz, 3H). **^{13}C NMR** (151 MHz, $CDCl_3$) δ/ppm = 169.6, 166.6, 150.9, 144.8, 138.0, 130.3, 129.5, 128.5, 127.1, 122.2, 61.2, 21.3, 14.5. **IR** (neat): ν/cm^{-1} = 2922, 2858, 2334, 1758, 1697, 1600, 1481, 1373, 1278, 1177, 1115, 1003, 904, 844, 769, 704, 662. **HRMS** (ESI) calculated for $C_{17}H_{16}NaO_4$: 307.0941 $[M+Na]^+$, found: 307.0937.

Pd-catalyzed Negishi Cross-coupling with (5-Bromo-4'-nitro-[1,1'-biphenyl]- 3-yl)trimethylsilane

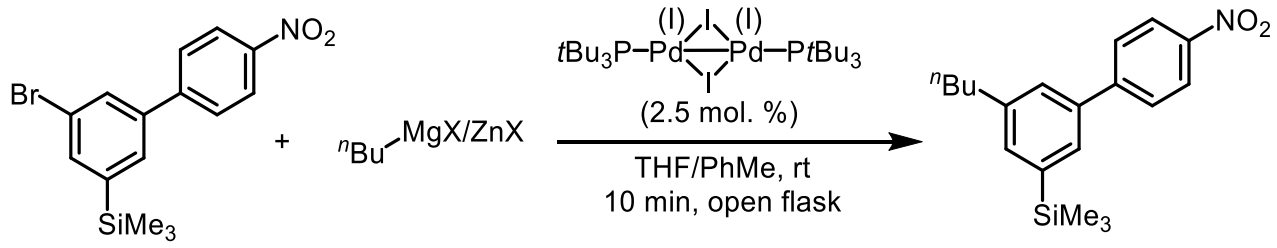

(5-*n*-Butyl-4'-nitro-[1,1'-biphenyl]-3-yl)trimethylsilane

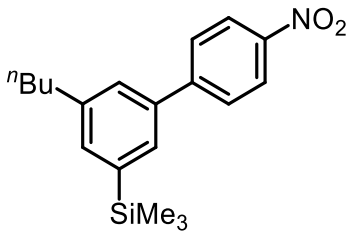

The synthesis was carried out according to the literature.[215] In an oven dried screw top vial equipped with a magnetic stirring bar, to a solution of *n*BuMgCl (2.0 M in THF, 200 µl, 0.4 mmol, 2.0 equiv.) were added $ZnCl_2$ (1.0 M in THF, 420 µl, 0.42 mmol, 2.1 equiv.) followed by addition of LiCl (0.5 M in THF, 920 µl, 0.46 mmol, 2.3 equiv.) under argon atmosphere. The resulting solution was stirred for 20 minutes. Thereafter, it was added slowly to a mixture of (5-bromo-4'-nitro-[1,1'-biphenyl]-3- yl)trimethylsilane (70.1 mg, 0.2 mmol, 1.0 equiv.) and $Pd^{(I)}$-I-dimer (4.4 mg, 0.005 mmol, 2.5 mol. %) in anhydrous toluene (750 µl). The reaction mixture was stirred in an open vial for 10 minutes, diluted with 2 ml of pentane, and filtered through a pad of silica. Solvents were removed under reduced pressure, and the residue was purified by silica gel column chromatography (40:1 *n*-pentane/EtOAc) to afford the final product as a yellow oil (49.4 mg, 0.151 mmol, 75%).

R_f = 0.40 (40:1 *n*-pentane/EtOAc). **^{1}H NMR** (600 MHz, $CDCl_3$) δ/ppm = 8.30 (d, *J* = 8.6 Hz, 2H), 7.74 (d, *J* = 8.6 Hz, 2H), 7.56-7.53 (m, 1H), 7.42-7.39 (m, 2H), 2.72-2.68 (m, 2H), 1.70-1.62 (m, 2H), 1.42 (sext, *J* = 7.4 Hz, 2H), 0.96 (t, *J* = 7.4 Hz, 3H), 0.32 (s, 9H). **^{13}C NMR** (151 MHz, $CDCl_3$) δ/ppm = 148.5, 147.1, 143.2, 141.8, 138.4, 134.2, 129.8, 128.2, 128.1, 124.2, 36.0, 34.0, 22.7, 14.1, -0.9. **IR** (neat): ν/cm^{-1} = 2954, 2861, 2106, 1595, 1517, 1456, 1385, 1343, 1248, 1192, 1142, 1107, 1011, 898, 837, 794, 751, 694. **HRMS** (GC-APCI) calculated for $C_{18}H_{22}NO_2Si$: 312.1414 $[M-Me]^+$, found: 312.1442.

Iodination of (5-*n*-Butyl-4'-nitro-[1,1'-biphenyl]-3-yl)trimethylsilane

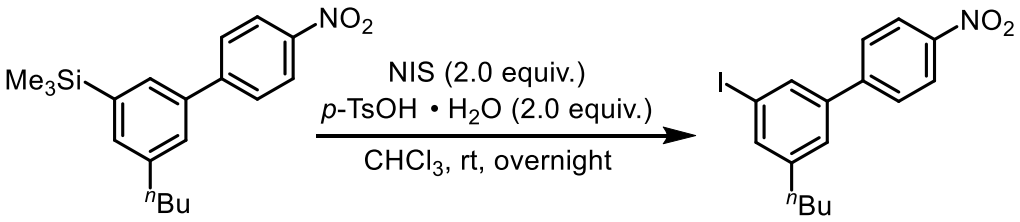

3-*n*-Butyl-5-iodo-4'-nitro-1,1'-biphenyl (32)

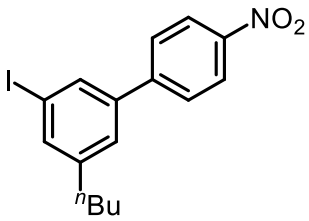

(5-Butyl-4'-nitro-[1,1'-biphenyl]-3-yl)trimethylsilane (49.4 mg, 0.15 mmol, 1.0 equiv.), NIS (67.9 mg, 0.3 mmol, 2.0 equiv.), *p*-toluenesulfonic acid monohydrate (*p*-TsOH·H_2O) (57.4 mg, 0.6 mmol, 2.0 equiv.) were placed into a screw top vial equipped with magnetic stirring bar, dissolved in anhydrous $CHCl_3$ (1.5 ml), and stirred overnight at room temperature. The reaction mixture was quenched by addition of DCM, and washed with water (1x 20 ml). The organic phase was separated, dried with $MgSO_4$, and filtered. After that solvents were removed under reduced pressure and the crude mixture was purified by silica gel column chromatography (40:1 *n*-pentane/EtOAc) to afford the title product as a yellow oil (30.1 mg, 0.079 mmol, 52%).

R_f = 0.33 (40:1 *n*-pentane/EtOAc). **^{1}H NMR** (600 MHz, $CDCl_3$) δ/ppm = 8.29 (d, *J* = 8.5 Hz, 2H), 7.79-7.74 (m, 1H), 7.69 (d, *J* = 8.6 Hz, 2H), 7.62-7.60 (m, 1H), 7.40-7.32 (m, 1H), 2.64 (t, *J* = 7.8 Hz, 2H), 1.63 (quint, *J* = 7.8 Hz, 2H), 1.39 (sext, *J* = 7.4 Hz, 2H), 0.95 (t, *J* = 7.4 Hz, 3H). **^{13}C NMR** (151 MHz, $CDCl_3$) δ/ppm = 147.5, 146.4, 146.2, 140.9, 138.0, 133.8, 128.0, 127.1, 124.3, 95.2, 35.5, 33.6, 22.5, 14.0. **IR** (neat): ν/cm^{-1} = 2927, 2858, 2325, 2087, 1992, 1930, 1594, 1559, 1516, 1438, 1389, 1343, 1290, 1182, 1107, 994, 846, 753, 692. **HRMS** (APCI) calculated for $C_{16}H_{17}INO_2$: 382.0298 $[M+H]^+$, found: 382.0295.

Ligand Screening for *e*-Rich Diazonium Salts

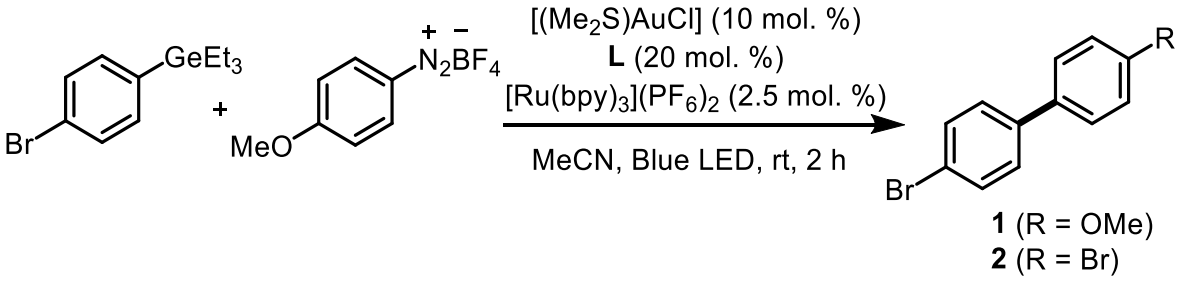

In an argon filled glovebox, (4-bromophenyl)triethylgermane (9.5 mg, 0.03 mmol, 1.0 equiv.), 4-methoxybenzenediazonium tetrafluoroborate (13.3 mg, 0.06 mmol, 2.0 equiv.), [(Me_2S)AuCl] (0.9 mg, 0.003 mmol, 10 mol%), L (0.006 mmol, 20 mol%) and [$Ru(bpy)_3$](PF_6)$_2$ (0.6 mg, 0.00075 mmol, 2.5 mol%) were mixed in a screw top vial equipped with a magnetic stirring bar and dissolved in anhydrous and degassed MeCN (300 µl). The obtained solutions were placed into the blue LED setup and stirred for 2 h. Ratios between hetero- **1** and homocoupling **2** products were determined by GC-MS. Results are shown in

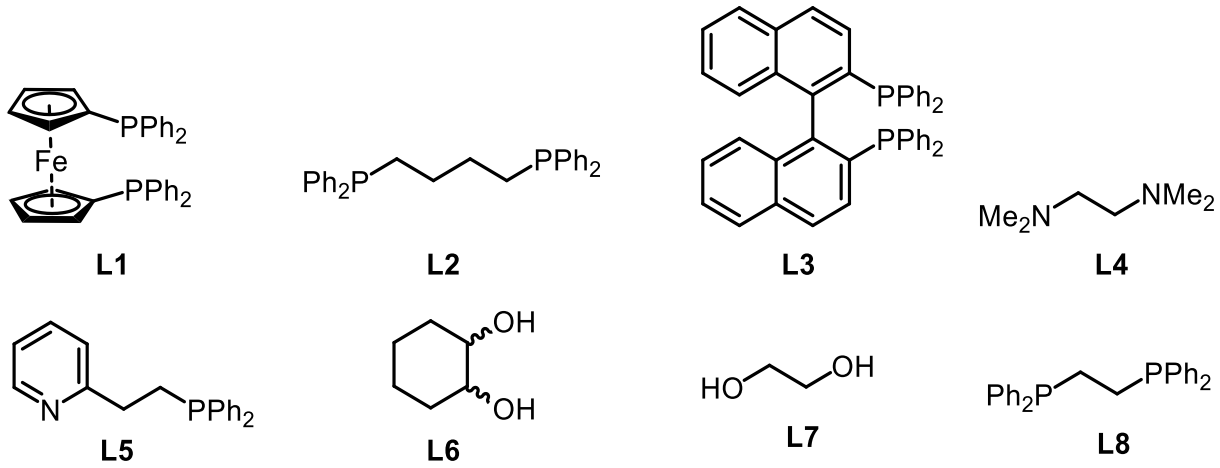

Table S1.

Table S1. Screening of ligands with ratios of desired product **1** to homocoupling **2**

Entry	L	1 : 2
1	Ph_3P	0.8 : 1
2	L1	1.5 : 1
3	L2	2.9 : 1
4	L3	3.6 : 1
5	L4	2.4 : 1
6	L5	2.5 : 1

7	L6	2.0 : 1
8	L7	2.1 : 1
9	**L8**	**4.5 : 1**

UV/Vis Analysis

For the UV/Vis measurements the solutions of 4-nitrobenzenediazonium (**1**) and 4-methoxybenzenediazonium (**2**) salts in anhydrous MeCN (0.5 μM) were prepared and then measured in 1 ml cuvettes. From the obtained spectra it was found that **1** has absorption in visible area (λ_{max} = 402 nm), whereas **2** absorbs in UV field (**Figure S1**).

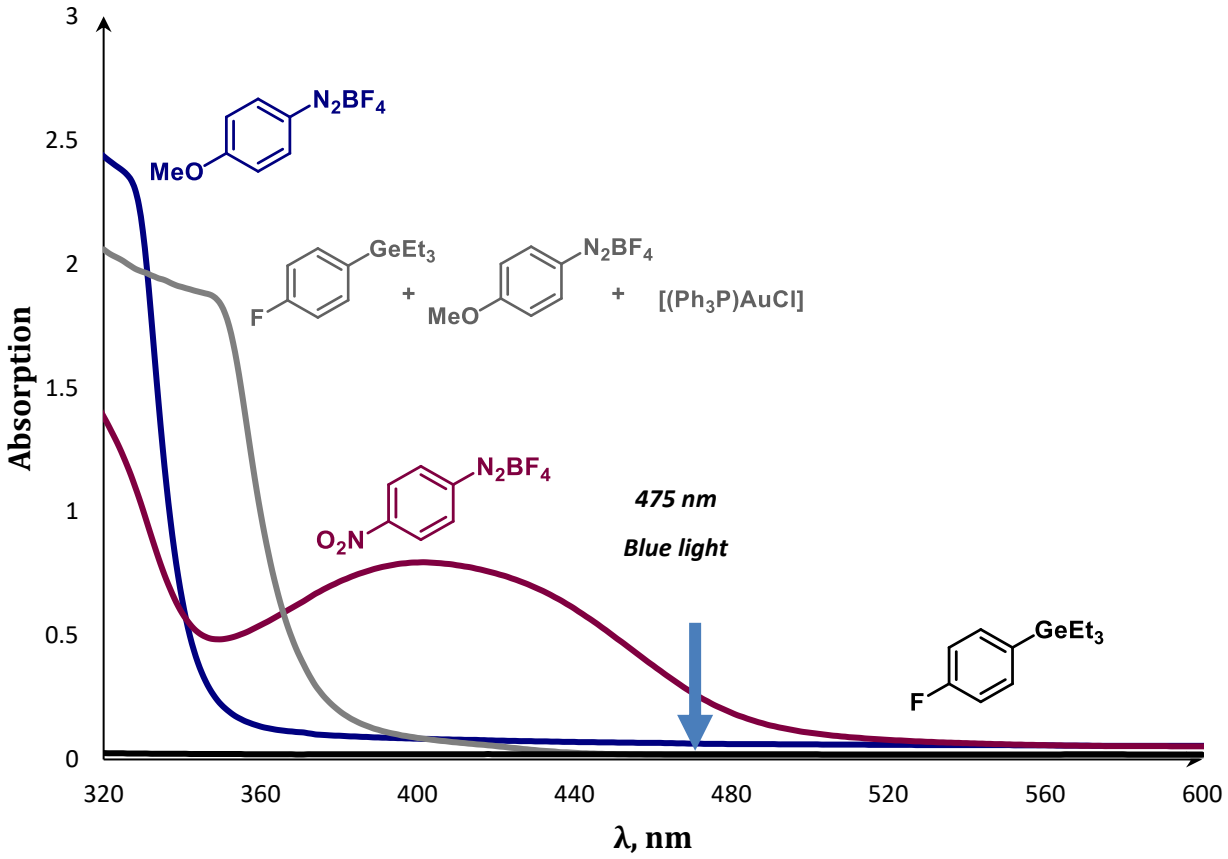

Figure S1. UV-Vis spectrum of electron-rich and -poor diazonium salts (0.5 μM in MeCN).

Reaction under UV Light

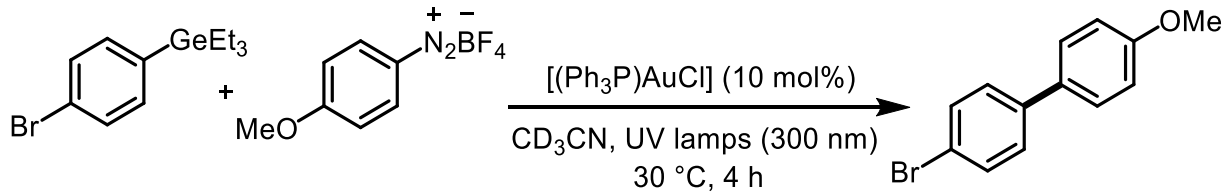

In an argon filled glovebox, (4-bromophenyl)triethylgermane **1** (15.8 mg, 0.05 mmol, 1.0 equiv.), 4-methoxybenzenediazonium salt **2** (22.2 mg, 0.1 mmol, 2.0 equiv.), and [(Ph_3P)AuCl] (2.5 mg, 0.005 mmol, 10 mol%) were mixed in a screw top quartz vial and dissolved in CD_3CN (500 µl). The obtained solution was stirred being irradiated by using of UV reactor (Rayonet Reactor 200 equipped with 6 lamps and air cooling, λ_{max} = 300 nm) for 4 h. The reaction mixture was analyzed by ^1H NMR using mesitylene (13.9 µl, 0.100 mmol, 2.0 equiv.) as internal standard. Results are shown in the **Table S2**.

Table S2. The reaction carried out under UV light.

Consumption of $ArGeEt_3$, %	**Consumption of ArN_2BF_4**, %	**Yield of the product**, %
16	100	traces

4.3 Supporting information for chapter 2

4.3.1 Supporting information for chapter 2.1

Synthesis of Protected Alcohols

_N_-Benzyl-_N_-(2-hydroxyethyl)-4-methylbenzenesulfonamide

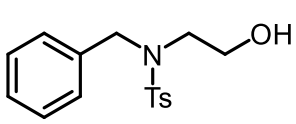

To a solution of 2-(benzylamino)ethan-1-ol (756.1 mg, 5.00 mmol, 1.0 equiv.) and Et_3N (1.4 ml, 10.0 mmol, 2.0 equiv.) in DCM (0.24 M) TsCl (1.05 g, 5.50 mmol, 1.1 equiv.) was added in small portions at room temperature. Then the obtained mixture was stirred overnight at the same temperature. The reaction mixture was quenched with distilled water, after that the organic phase was separated and the aqueous layer was extracted with DCM (3x). The organic phases were combined and dried over $MgSO_4$. The solvents were evaporated *in vacuo* and the crude mixture was purified by silica gel column chromatography (2:1 *n*-pentane/Et_2O) to afford the title product as a colorless solid (1.3 g, 4.26 mmol, 85%).

R_f = 0.29 (2:1 *n*-pentane/Et_2O). **^{1}H NMR** (600 MHz, $CDCl_3$) δ/ppm = 7.75 (d, *J* = 8.3 Hz, 2H), 7.36 – 7.27 (m, 7H), 4.35 (s, 2H), 3.47 (q, *J* = 5.6 Hz, 2H), 3.23 (t, *J* = 5.5 Hz, 2H), 2.45 (s, 3H), 2.00 (t, *J* = 6.0 Hz, 1H). **^{13}C NMR** (151 MHz, $CDCl_3$) δ/ppm = 143.8, 136.4, 136.2, 130.0, 128.9, 128.5, 128.2, 127.4, 61.1, 53.6, 50.8, 21.7. **HRMS** (ESI) calculated for $C_{16}H_{19}NNaO_3S$: 328.0978 $[M+Na]^+$, found: 328.0975.

2-(1-Tosylpiperidin-4-yl)ethan-1-ol

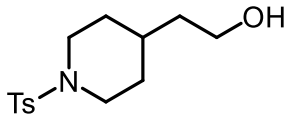

To a solution of 2-(piperidin-4-yl)ethan-1-ol (516.8 mg, 4.00 mmol, 1.0 equiv.) and Et_3N (1.1 ml, 8.00 mmol, 2.0 equiv.) in DCM (0.24 M) TsCl (838.8 mg, 4.40 mmol, 1.1 equiv.) was added in small portions at room temperature. Then the obtained mixture was stirred overnight at the same temperature. The reaction mixture was quenched with distilled water, after that the organic phase was separated and the aqueous layer was extracted with DCM (3x). The organic phases were combined and dried over $MgSO_4$. The solvents were evaporated *in vacuo* and the crude mixture was purified by silica gel column chromatography (EtOAc) to afford the title product as a colorless solid (1.05 g, 3.72 mmol, 93%).

R_f = 0.50 (EtOAc). **^{1}H NMR** (600 MHz, $CDCl_3$) δ/ppm = 7.63 (d, *J* = 8.3 Hz, 2H), 7.31 (d, *J* = 8.0 Hz, 2H), 3.80-3.72 (m, 2H), 3.65 (t, *J* = 6.5 Hz, 2H), 2.43 (s, 3H), 2.24 (td, *J* = 11.7, 2.4 Hz, 2H), 1.78-1.69 (m, 2H), 1.49 (q, *J* = 6.5 Hz, 2H), 1.34 (dqd, *J* = 23.7, 11.1, 5.8 Hz, 3H), 1.21 (s, 1H). **^{13}C NMR** (151 MHz, $CDCl_3$) δ/ppm = 143.5, 133.3, 129.7, 127.9, 60.3, 46.5, 38.8, 31.9, 31.6, 21.7. **HRMS** (ESI) calculated for $C_{14}H_{21}NNaO_3S$: 304.1134 $[M+Na]^+$, found: 304.1130.

(8*R*,9*S*,13*S*,14*S*,17*S*)-3-methoxy-13-methyl-7,8,9,11,12,13,14,15,16,17-decahydro-6*H*-cyclopenta[*a*]phenanthren-17-ol

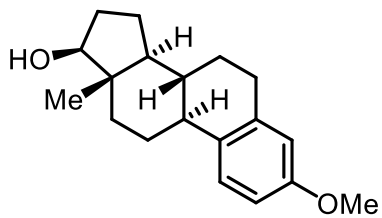

The reaction was performed according to the literature procedure.[216] β-Estradiol (708.2 mg, 2.6 mmol, 1.0 equiv.) was placed into a round bottom flask equipped with a magnetic stirring bar and dissolved in MeCN (0.1 M). Then K_2CO_3 (1.8 g, 13.0 mmol, 5.0 equiv.) and MeI (971 µl, 15.6 mmol, 6.0

equiv.) were subsequently added to the solution. The obtained mixture was refluxed overnight. After that the reaction mixture was allowed to cool to room temperature and was quenched with distilled water. The resulting solution was extracted with DCM (3x). The organic phases were combined and dried over $MgSO_4$. The solvents were evaporated *in vacuo* and the crude mixture was purified by silica gel column chromatography (3:1 *n*-pentane/EtOAc) to afford the title product as a colorless solid (694.7 mg, 2.43 mmol, 93%).

R_f = 0.48 (3:1 *n*-pentane/EtOAc). **^{1}H NMR** (600 MHz, $CDCl_3$) δ/ppm = 7.21 (d, *J* = 8.6 Hz, 1H), 6.71 (dd, *J* = 8.6, 2.8 Hz, 1H), 6.63 (d, *J* = 2.8 Hz, 1H), 3.78 (s, 3H), 3.73 (t, *J* = 8.5 Hz, 1H), 2.92-2.78 (m, 2H), 2.35-2.28 (m, 1H), 2.23-2.08 (m, 2H), 1.98-1.92 (m, 1H), 1.91-1.85 (m, 1H), 1.75-1.66 (m, 1H), 1.57-1.15 (m, 8H), 0.78 (s, 3H). **^{13}C NMR** (151 MHz, $CDCl_3$) δ/ppm = 157.6, 138.1, 132.8, 126.5, 114.0, 111.6, 82.1, 55.4, 50.2, 44.1, 43.4, 39.0, 36.9, 30.8, 30.0, 27.4, 26.5, 23.3, 11.2. **MS** (EI) m/z (%): 287 (21), 286 (100) $[M]^+$, 227 (20), 200 (19), 199 (20), 186 (35), 174 (18), 173 (20), 171 (10), 160 (23), 159 (13), 147 (14). These data are in agreement with those reported previously in the literature.[217]

***tert*-Butyl 4-(2-hydroxyethyl)piperidine-1-carboxylate**

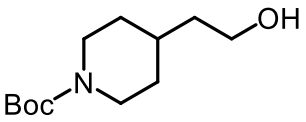

2-(Piperidin-4-yl)ethan-1-ol (646.0 mg, 5.00 mmol, 1.0 equiv.) was placed into a round-bottom flask equipped with a stirring bar and dissolved in DCM (0.33 M). Boc_2O (1.09 g, 5.00 mmol, 1.0 equiv.) was subsequently added, and the obtained mixture was stirred overnight at room temperature. The solvent was evaporated *in vacuo* and the crude mixture was purified by silica gel chromatography column (EtOAc) to afford the title product as a colorless oil (1.10 g, 4.82 mmol, 96%).

R_f = 0.37 (1:1 *n*-pentane/EtOAc). **^{1}H NMR** (600 MHz, $CDCl_3$) δ/ppm = 4.09-4.03 (m, 2H), 3.69 (t, *J* = 6.6 Hz, 2H), 2.72-2.65 (m, 2H), 1.70-1.55 (m, 3H), 1.51 (q, *J* = 6.6 Hz, 2H), 1.44 (s, 9H), 1.20-1.04 (m, 2H). **^{13}C NMR** (151 MHz, $CDCl_3$) δ/ppm = 155.0, 79.4, 60.4, 44.1, 39.4, 32.7, 32.3, 28.6. **HRMS** (ESI) calculated for $C_{12}H_{23}NNaO_3$: 252.1570 $[M+Na]^+$, found: 252.1567. These data are in agreement with those reported previously in the literature.[218]

Pd-catalyzed Coupling of Aryl Germanes with Alcohols and Carboxylic Acids

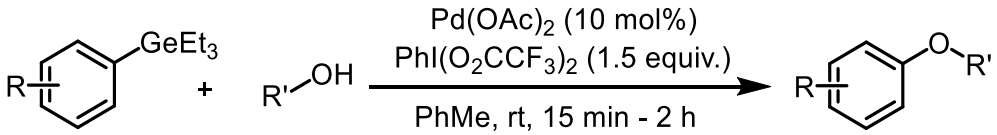

General Procedure

Aryl germane (1.0 equiv.), $Pd(OAc)_2$ (10 mol%), $PhI(O_2CCF_3)_2$ (1.5 equiv.) and alcohol or carboxylic acid (if solid) (5.0 equiv.) were subsequently placed into a screw top vial equipped with a stirring bar. The obtained mixture was dissolved in anhydrous toluene (0.25 M) (liquid alcohols or carboxylic acids were added after addition of toluene). Then the vial was sealed with a cap, and the reaction solution was stirred at room temperature. After consumption of the aryl germane (monitored by GC-MS, the reaction time specified individually for each compound) the solvent was evaporated *in vacuo* and the residue was purified by silica gel column chromatography or preparative TLC affording the desired product.

1-((4-Fluorophenoxy)methyl)-2-iodobenzene (1)

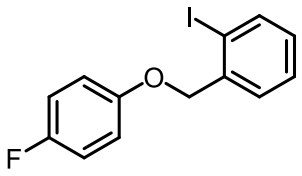

The cross-coupling reaction was performed according to GP using triethyl(4-fluorophenyl)germane (76.5 mg, 0.30 mmol, 1.0 equiv.) and (2-iodophenyl)methanol (210.6 mg, 1.50 mmol, 5.0 equiv.). The title product was obtained after purification by preparative TLC (30:1 *n*-pentane/EtOAc) as a yellow oil (85.3 mg, 0.260 mmol, 87%). Reaction time: 15 min. With 1 mol% $Pd(OAc)_2$ for 15 min 83% of the product was formed, as judged by quantitative ^{19}F NMR analysis (1,4-difluorobenzene as an internal standard).

R_f = 0.30 (30:1 *n*-pentane/EtOAc). **^{1}H NMR** (600 MHz, $CDCl_3$) δ/ppm = 7.91-7.85 (m, 1H), 7.53-7.47 (m, 1H), 7.39-7.36 (m, 1H), 7.07-6.97 (m, 3H), 6.95-6.88 (m, 2H), 5.01 (s, 2H). **^{13}C NMR** (151 MHz, $CDCl_3$) δ/ppm = 157.7 (d, *J* = 239.0 Hz), 154.7 (d, *J* = 2.3 Hz), 139.5, 139.1, 129.7, 128.8, 128.6, 116.2 (d, *J* = 7.8 Hz), 116.1 (d, *J* = 23.0 Hz), 97.3, 74.7. **^{19}F NMR** (565 MHz, $CDCl_3$) δ/ppm = -123.28 – -123.25 (m, 1F). **HRMS** (ESI) calculated for $C_{13}H_{10}FINaO$: 350.9650 $[M+Na]^+$, found: 350.9653. These data are in agreement with those reported previously in the literature.[219]

1-Bromo-3-chloro-5-((2-iodobenzyl)oxy)benzene (2)

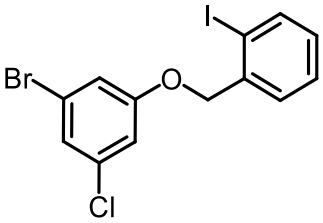

The cross-coupling reaction was performed according to GP using (3-bromo-5-chlorophenyl)triethylgermane (105.1 mg, 0.30 mmol, 1.0 equiv.) and (2-iodophenyl)methanol (351.1 mg, 1.50 mmol, 5.0 equiv.). The title product was obtained after purification by silica gel column chromatography (40:1 *n*-pentane/EtOAc) and preparative TLC (35:1 *n*-pentane/EtOAc) as a colorless oil (78.8 mg, 0.182 mmol, 62%). Reaction time: 3 h. With 1 mol% $Pd(OAc)_2$ for 7 h 62% of the product was formed, as judged by quantitative ^1H NMR analysis (mesitylene as an internal standard).

R_f = 0.53 (20:1 *n*-pentane/EtOAc). **^{1}H NMR** (600 MHz, $CDCl_3$) δ/ppm = 7.88 (d, *J* = 8.0 Hz, 1H), 7.49-7.41 (m, 1H), 7.42-7.36 (m, 1H), 7.17-7.13 (m, 1H), 7.06-7.05 (m, 2H), 6.95-6.92 (m, 1H), 5.01 (s, 2H). **^{13}C NMR** (151 MHz, $CDCl_3$) δ/ppm = 159.7, 139.6, 138.2, 135.8, 130.1, 129.0, 128.7, 124.5, 123.1, 117.1, 114.7, 97.6, 74.5. **MS** (EI) m/z (%): 424 (6), 422 (4) $[M]^+$, 218 (12), 217 (100), 90 (18) (attempts to measure HRMS (APCI, ESI) resulted in no detection of the molecule).

1-Chloro-2-fluoro-4-((2-iodobenzyl)oxy)benzene (3)

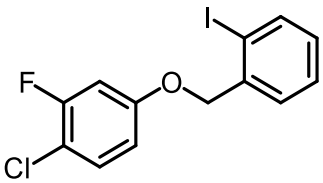

The cross-coupling reaction was performed according to GP using (4-chloro-3-fluorophenyl)triethylgermane (86.8 mg, 0.30 mmol, 1.0 equiv.) and (2-iodophenyl)methanol (351.1 mg, 1.50 mmol, 5.0 equiv.). The title product was obtained after purification by silica gel column chromatography (40:1 *n*-pentane/EtOAc) and preparative HPLC (9:1 *n*-hexane/EtOAc) as a colorless oil (75.9 mg, 0.210 mmol, 80%). Reaction time: 15 min. With 1 mol% $Pd(OAc)_2$ for 30 min 80% of the product was formed, as judged by quantitative ^{19}F NMR analysis (1,4-difluorobenzene as an internal standard).

R_f = 0.54 (20:1 *n*-pentane/EtOAc). **^{1}H NMR** (600 MHz, $CDCl_3$) δ/ppm = 7.89-7.86 (m, 1H), 7.47-7.44 (m, 1H), 7.40-7.35 (m, 1H), 7.31-7.28 (m, 1H), 7.07-7.03 (m, 1H), 6.82-6.78 (m, 1H), 6.75-6.70 (m, 1H), 5.02 (s, 2H). **^{13}C NMR** (151 MHz, $CDCl_3$) δ/ppm = 158.6 (d, *J* = 247.7 Hz), 158.3 (d, *J* = 9.7 Hz), 139.6, 138.4, 130.9-130.7 (m),

130.0, 128.8, 128.6, 113.1 (d, *J* = 17.8 Hz), 111.7 (d, *J* = 3.5 Hz), 104.2 (d, *J* = 24.3 Hz), 97.4, 74.6. **^{19}F NMR** (282 MHz, $CDCl_3$) δ/ppm = -112.78 – -112.87 (m, 1F). **HRMS** (APCI) calculated for $C_{13}H_9{}^{35}ClFIO$: 361.9365 $[M]^+$, found: 361.9371.

3-Bromo-5-chloro-4'-((2-iodobenzyl)oxy)-1,1'-biphenyl (4)

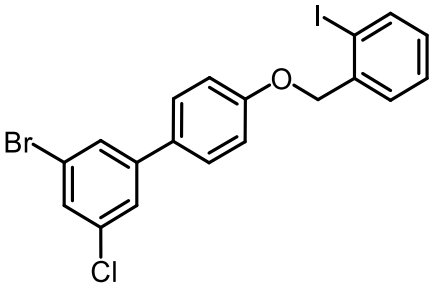

The cross-coupling reaction was performed according to GP using (3'-bromo-5'-chloro-[1,1'-biphenyl]-4-yl)triethylgermane (127.9 mg, 0.30 mmol, 1.0 equiv.) and (2-iodophenyl)methanol (351.1 mg, 1.50 mmol, 5.0 equiv.). The title product was obtained after purification by silica gel column chromatography (35:1 *n*-pentane/EtOAc) and preparative HPLC (95:5 *n*-hexane/EtOAc) as a colorless solid (101.9 mg, 0.204 mmol, 68%). Reaction time: 15 min. With 1 mol% $Pd(OAc)_2$ for 5 h 67% of the product was formed, as judged by quantitative ^{1}H NMR analysis (CH_2Br_2 as an internal standard).

R_f = 0.46 (20:1 *n*-pentane/EtOAc). **^{1}H NMR** (600 MHz, $CDCl_3$) δ/ppm = 7.89 (d, *J* = 7.9 Hz, 1H), 7.59-7.55 (m, 1H), 7.53-7.50 (m, 1H), 7.48 (d, *J* = 8.6 Hz, 2H), 7.47-7.43 (m, 2H), 7.41-7.36 (m, 1H), 7.08-7.02 (m, 3H), 5.10 (s, 2H). **^{13}C NMR** (151 MHz, $CDCl_3$) δ/ppm = 159.0, 144.1, 139.5, 139.0, 135.5, 131.6, 129.8, 129.5, 128.8, 128.6, 128.4, 128.2, 125.8, 123.2, 115.6, 97.4, 74.2. **HRMS** (EI) calculated for $C_{19}H_{13}{}^{79}Br{}^{35}ClIO$: 497.8877 $[M]^+$, found: 497.8876.

1-Iodo-4-(methoxy-d3)benzene (5)

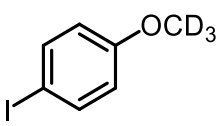

The cross-coupling reaction was performed according to GP using triethyl(4-iodophenyl)germane (108.8 mg, 0.30 mmol, 1.0 equiv.) and methanol-d_4 (61 µl, 1.50 mmol, 5.0 equiv.). The title product was obtained after purification by preparative TLC (*n*-pentane) as a colorless solid (59.0 mg, 0.249 mmol, 83%). Reaction time: 15 min.

R_f = 0.25 (*n*-pentane). **^{1}H NMR** (600 MHz, $CDCl_3$) δ/ppm = 7.56 (d, *J* = 9.0 Hz, 2H), 6.68 (d, *J* = 9.0 Hz, 2H). **^{13}C NMR** (151 MHz, $CDCl_3$) δ/ppm = 159.6, 138.3, 116.5, 82.8, 55.0-54.2 (m). **HRMS** (EI) calculated for $C_7H_4D_3IO$: 236.9730 $[M]^+$, found: 236.9716. These data are in agreement with those reported previously in the literature.[220]

4-((2-Iodobenzyl)oxy)phenyl sulfurofluoridate (6)

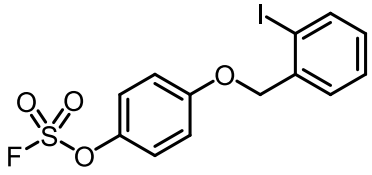

The cross-coupling reaction was performed according to GP using 4-(triethylgermyl)phenyl sulfurofluoridate (33.5 mg, 0.10 mmol, 1.0 equiv.) and (2-iodophenyl)methanol (117.0 mg, 0.50 mmol, 5.0 equiv.). The title product was obtained after purification by preparative TLC (40:1 *n*-pentane/Et_2O) as a yellow oil (32.5 mg, 0.08 mmol, 80%). Reaction time: 15 min.

R_f = 0.27 (30:1 *n*-pentane/Et_2O). **^{1}H NMR** (600 MHz, $CDCl_3$) δ/ppm = 7.95-7.84 (m, 1H), 7.51-7.44 (m, 1H), 7.42-7.35 (m, 1H), 7.28 (d, *J* = 9.2 Hz, 2H), 7.09-7.03 (m, 1H), 7.03 (d, *J* = 9.2 Hz, 2H), 5.06 (s, 2H). **^{13}C NMR** (151 MHz, $CDCl_3$) δ/ppm = 158.3, 144.1, 139.6, 138.4, 130.0, 128.8, 128.7, 122.3, 116.4, 97.4, 74.6. **^{19}F NMR** (565 MHz, $CDCl_3$) δ/ppm = 36.56 (s, 1F). **HRMS** (APCI) calculated for $C_{13}H_{10}FIO_4S$: 407.9323 $[M]^+$, found: 407.9323.

2-(4-(Benzyloxy)phenyl)-4,4,5,5-tetramethyl-1,3,2-dioxaborolane (7)

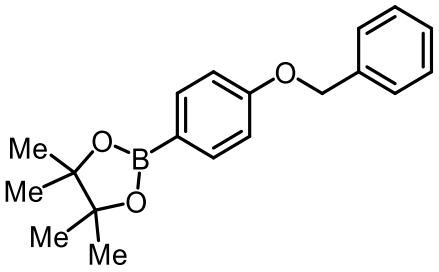

The cross-coupling reaction was performed according to GP using triethyl(4-(4,4,5,5-tetramethyl-1,3,2-dioxaborolan-2-yl)phenyl)germane (72.6 mg, 0.20 mmol, 1.0 equiv.) and benzylic alcohol (104 µl, 1.00 mmol, 5.0 equiv.) using 1 mol% of $Pd(OAc)_2$. The title product was obtained after purification by preparative TLC (20:1 *n*-pentane/EtOAc) as a colorless oil (44.7 mg, 0.144 mmol, 72%). Reaction time: 1 h.

R_f = 0.58 (10:1 *n*-pentane/EtOAc). **^{1}H NMR** (400 MHz, $CDCl_3$) δ/ppm = 7.76 (d, *J* = 8.5 Hz, 2H), 7.46-7.41 (m, 2H), 7.39-7.37 (m, 2H), 7.34-7.30 (m, 1H), 6.97 (d, *J* = 8.5 Hz, 2H), 5.10 (s, 2H), 1.33 (s, 12H). **^{13}C NMR** (151 MHz, $CDCl_3$) δ/ppm = 161.5, 137.0, 136.7, 128.7, 128.1, 127.6, 114.4, 83.7, 69.9, 25.0. *Note*: The carbon attached to boron was not observed in ^{13}C NMR.[201] **HRMS** (ESI) calculated for $C_{19}H_{23}BNaO_3$: 333.1632 $[M+Na]^+$, found: 333.1628. These data are in agreement with those reported previously in the literature.[221]

(*R*)-4,4,5,5-Tetramethyl-2-(3-(2-phenylpropoxy)phenyl)-1,3,2-dioxaborolane (8)

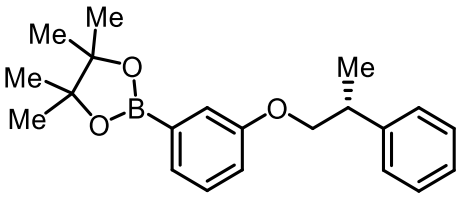

The cross-coupling reaction was performed according to GP using triethyl(3-(4,4,5,5-tetramethyl-1,3,2-dioxaborolan-2-yl)phenyl)germane (72.6 mg, 0.20 mmol, 1.0 equiv.) and (*R*)-2-phenylpropan-1-ol (140 µl, 1.00 mmol, 5.0 equiv.) using 1 mol% of $Pd(OAc)_2$. The title product was obtained after purification by preparative TLC (20:1 *n*-pentane/EtOAc) as a yellow oil (47.4 mg, 0.14 mmol, 70%). Reaction time: 1 h 30 min.

R_f = 0.39 (20:1 *n*-pentane/EtOAc). **^{1}H NMR** (400 MHz, $CDCl_3$) δ/ppm = 7.43-7.20 (m, 8H), 7.02-6.95 (m, 1H), 4.12 (dd, *J* = 9.0, 5.8 Hz, 1H), 4.01-3.95 (m, 1H), 3.30-3.17 (m, 1H), 1.42 (d, *J* = 7.0 Hz, 3H), 1.34 (s, 12H). **^{13}C NMR** (151 MHz, $CDCl_3$) δ/ppm = 158.4, 143.7, 128.9, 128.4, 127.4, 127.1, 126.6, 119.6, 118.2, 83.8, 73.3, 39.7, 24.8, 18.1. *Note*: The carbon attached to boron was not observed in ^{13}C NMR.[201] **HRMS** (ESI) calculated for $C_{21}H_{27}BNaO_3$: 361.1945 $[M+Na]^+$, found: 361.1938.

***N*-benzyl-4-methyl-*N*-(2-(3-(trimethylsilyl)phenoxy)ethyl)benzenesulfonamide (9)**

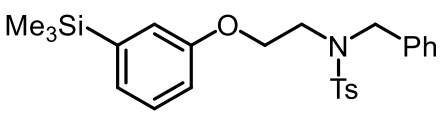

The cross-coupling reaction was performed according to GP using trimethyl(4-(triethylgermyl)phenyl)silane (92.7 mg, 0.30 mmol, 1.0 equiv.) and *N*-benzyl-*N*-(2-hydroxyethyl)-4-methylbenzenesulfonamide (458.1 mg, 1.50 mmol, 5.0 equiv.). The title product was obtained after purification by silica gel column chromatography (7:1 *n*-pentane/Et_2O) as a brown oil (85.3 mg, 0.188 mmol, 63%). Reaction time: 15 min. With 1 mol% $Pd(OAc)_2$ for 5 h 64% of the product was formed, as judged by quantitative ^{1}H NMR analysis (CH_2Br_2 as an internal standard).

R_f = 0.21 (7:1 *n*-pentane/Et_2O). **^{1}H NMR** (600 MHz, $CDCl_3$) δ/ppm = 7.76 (d, *J* = 8.0 Hz, 2H), 7.34-7.27 (m, 7H), 7.21 (dd, *J* = 7.7 Hz, 1H), 7.07 (d, *J* = 7.2 Hz, 1H), 6.83 (d, *J* = 2.7 Hz, 1H), 6.63 (dd, *J* = 8.2, 2.7 Hz, 1H), 4.45 (s, 2H), 3.90 (t, *J* = 6.4 Hz, 2H), 3.49 (t, *J* = 6.4 Hz, 2H), 2.42 (s, 3H), 0.24 (s, 9H). **^{13}C NMR** (151 MHz, $CDCl_3$) δ/ppm = 157.7, 143.6, 142.4, 137.0, 136.4, 129.9, 129.0, 128.8, 128.7, 128.1, 127.4, 126.0, 119.3, 114.5, 66.0, 53.2, 46.7, 21.7, -1.0. **HRMS** (ESI) calculated for $C_{25}H_{31}NNaO_3SSi$: 476.1686 $[M+Na]^+$, found: 476.1673.

tert-Butyl (_S_)-2-((4-fluorophenoxy)methyl)pyrrolidine-1-carboxylate (10)

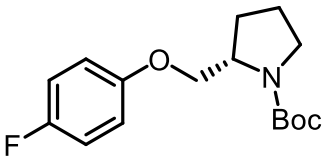

The cross-coupling reaction was performed according to GP from (4-fluorophenyl)triethylgermane (76.5 mg, 0.30 mmol, 1.0 equiv.) and *tert*-butyl (*S*)-2-(hydroxymethyl)pyrrolidine-1-carboxylate (181.1 mg, 1.50 mmol, 5.0 equiv.). The title product was obtained after purification by silica gel column chromatography (5:1 *n*-pentane/Et_2O). Analysis of ^{19}F NMR showed an additional peak (-76.00 ppm) related to an impurity, which is assumed to be trifluoroacetic ester of the alcohol. To remove it the mixture was dissolved in anhydrous THF (1.2 mL) and then *t*-BuOK (67.4 mg, 0.6 mmol, 2.0 equiv.) was added. The obtained solution was stirred overnight at room temperature. After that the solvent was removed *in vacuo*, and the crude mixture was purified by preparative TLC (9:1 *n*-pentane/EtOAc) to afford the desired product as a colorless oil (54.0 mg, 0.183 mmol, 61%, 99% *ee*). Reaction time: 2 h.

R_f = 0.37 (4:1 *n*-pentane/Et_2O). *Note*: Rotamers were observed in ^1H, ^{13}C and ^{19}F NMR. **^{1}H NMR** (600 MHz, $CDCl_3$) δ/ppm = 7.00-6.92 (m, 2H), 6.89-6.83 (m, 2H), 4.19-4.02 (m, 2H), 3.95-3.70 (m, 1H), 3.46-3.30 (m, 2H), 2.11-1.90 (m, 3H), 1.90-1.81 (m, 1H), 1.47 (s, 9H). **^{13}C NMR** (151 MHz, $CDCl_3$) δ/ppm = 157.4 (d, *J* = 237.7 Hz), 155.1, 154.7 (m), 115.9 (d, *J* = 23.1 Hz), 115.7 (d, *J* = 8.0 Hz), 79.9 (m), 69.0 (m), 56.1, 46.9 (m), 28.2 (m), 24.0 (m), 23.0 (m). **^{19}F NMR** (282 MHz, $CDCl_3$) δ/ppm = -123.74 – -124.04 (m, rotamer A), -124.13 – -124.49 (m, rotamer B). **$[\alpha]_D$** +123.2 (0.44 M, $CHCl_3$, 29 °C). **HRMS** (ESI) calculated for $C_{16}H_{22}FNNaO_3$: 318.1476 $[M+Na]^+$, found: 318.1466.

tert-Butyl (_R_)-2-((4-fluorophenoxy)methyl)pyrrolidine-1-carboxylate (11)

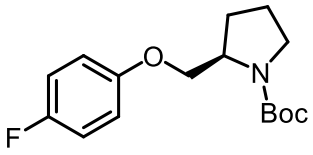

The cross-coupling reaction was performed according to GP using (4-fluorophenyl)triethylgermane (76.5 mg, 0.30 mmol, 1.0 equiv.) and *tert*-butyl (*R*)-2-(hydroxymethyl)pyrrolidine-1-carboxylate (181.1 mg, 1.50 mmol, 5.0 equiv.). The title product was obtained after purification by silica gel column chromatography (5:1 *n*-pentane/Et_2O). Analysis of ^{19}F NMR showed an additional peak (-76.00 ppm) related to an impurity, which is assumed to be trifluoroacetic ester of the alcohol. To remove it the mixture was dissolved in anhydrous THF (1.2 ml) and then *t*-BuOK (67.4 mg, 0.60 mmol, 2.0 equiv.) was added. The obtained solution was stirred overnight at room temperature. After that the solvent was removed *in vacuo*, and the crude mixture was purified by preparative TLC (9:1 *n*-pentane/EtOAc) to afford the desired product as a colorless oil 54.9 mg, 0.186 mmol, 62%). Reaction time: 2 h.

R_f = 0.28 (5:1 *n*-pentane/Et_2O). *Note*: Rotamers were observed in ^1H, ^{13}C and ^{19}F NMR. **^{1}H NMR** (600 MHz, $CDCl_3$) δ/ppm = 6.99-6.92 (m, 2H), 6.89-6.83 (m, 2H), 4.21-4.00 (m, 2H), 3.92-3.69 (m, 1H), 3.47-3.28 (m, 2H), 2.09-1.91 (m, 3H), 1.92-1.79 (m, 1H), 1.47 (s, 9H). **^{13}C NMR** (151 MHz, $CDCl_3$) δ/ppm = 157.4 (d, *J* = 237.0 Hz), 155.1, 154.6 (m), 115.9 (d, *J* = 23.0 Hz), 115.7 (d, *J* = 7.9 Hz), 79.6 (m), 69.2 (m), 56.1, 47.0 (m), 28.2 (m), 23.9 (m), 23.0 (m). **^{19}F NMR** (282 MHz, $CDCl_3$) δ/ppm = -123.73 – -124.00 (m, rotamer A), -124.18 – -124.39 (m, rotamer B). **$[\alpha]_D$** +38.4 (0.39 M, $CHCl_3$, 25°C). **HRMS** (ESI) calculated for $C_{16}H_{22}FNNaO_3$: 318.1476 $[M+Na]^+$, found: 318.1466.

Methyl *N*-((benzyloxy)carbonyl)-*O*-(*p*-tolyl)-*L*-serinate (12)

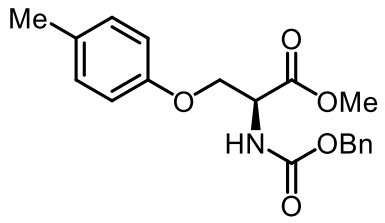

The cross-coupling reaction was performed according to GP using triethyl(*p*-tolyl)germane (75.3 mg, 0.30 mmol, 1.0 equiv.) and methyl ((benzyloxy)carbonyl)-*L*-serinate (379.9 mg, 1.50 mmol, 5.0 equiv.). The title product was obtained after purification by silica gel column chromatography (3:1 *n*-pentane/EtOAc) as a brown oil (87.6 mg, 0.255 mmol, 85%). Reaction time: 1 h.

R_f = 0.54 (3:1 *n*-pentane/EtOAc). **^{1}H NMR** (600 MHz, $CDCl_3$) δ/ppm = 7.39-7.30 (m, 5H), 7.07 (d, *J* = 8.2 Hz, 2H), 6.76 (d, *J* = 8.2 Hz, 2H), 5.75 (d, *J* = 8.6 Hz, 1H), 5.14 (s, 2H), 4.73-4.68 (m, 1H), 4.39 (dd, *J* = 9.3, 3.1 Hz, 1H), 4.20 (dd, *J* = 9.3, 3.1 Hz, 1H), 3.77 (s, 3H), 2.28 (s, 3H). **^{13}C NMR** (151 MHz, $CDCl_3$) δ/ppm = 170.4, 156.2, 156.1, 136.3, 131.0, 130.1, 128.7, 128.4, 128.3, 114.6, 68.3, 67.3, 54.2, 52.9, 20.6. **$[\alpha]_D$** +76.1 (0.29 M, $CHCl_3$, 25 °C). **HRMS** (ESI) calculated for $C_{19}H_{21}NNaO_5$: 366.1312 $[M+Na]^+$, found: 366.1312.

Methyl *N*-((benzyloxy)carbonyl)-*O*-(*p*-tolyl)-*D*-serinate (13)

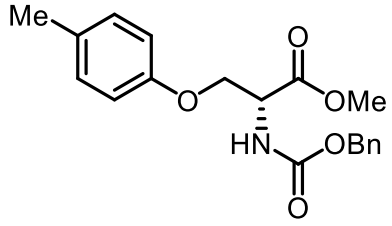

The cross-coupling reaction was performed according to GP using triethyl(*p*-tolyl)germane (75.3 mg, 0.30 mmol, 1.0 equiv.) and methyl ((benzyloxy)carbonyl)-*D*-serinate (379.9 mg, 1.50 mmol, 5.0 equiv.). The title product was obtained after purification by silica gel column chromatography (2:1 *n*-pentane/Et_2O) as a brown solid (61.8 mg, 0.180 mmol, 60%). Reaction time: 1 h.

R_f = 0.28 (2:1 *n*-pentane/Et_2O). **^{1}H NMR** (600 MHz, $CDCl_3$) δ/ppm = 7.42-7.29 (m, 5H), 7.06 (d, *J* = 8.4 Hz, 2H), 6.76 (d, *J* = 8.5 Hz, 2H), 5.74 (d, *J* = 8.6 Hz, 1H), 5.13 (s, 2H), 4.74-4.68 (m, 1H), 4.39 (dd, *J* = 9.4, 3.1 Hz, 1H), 4.20 (dd, *J* = 9.4, 3.1 Hz, 1H), 3.77 (s, 3H), 2.28 (s, 3H). **^{13}C NMR** (151 MHz, $CDCl_3$) δ/ppm = 170.4, 156.2, 156.1, 136.3, 131.0, 130.1, 128.7, 128.4, 128.3, 114.7, 68.4, 67.3, 54.2, 52.9, 20.6. **$[\alpha]_D$** −71.6 (0.5 M, $CHCl_3$, 25 °C). **HRMS** (ESI) calculated for $C_{19}H_{21}NNaO_5$: 366.1312 $[M+Na]^+$, found: 366.1312.

3-(Octyloxy)thiophene (14)

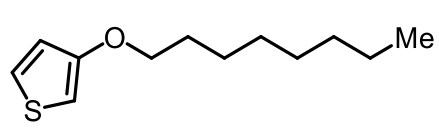

The cross-coupling reaction was performed according to GP using triethyl(thiophen-3-yl)germane (72.9 mg, 0.30 mmol, 1.0 equiv.) and octan-1-ol (237 µl, 1.50 mmol, 5.0 equiv.). The title product was obtained after purification by preparative TLC (*n*-pentane) as a colorless oil (26.8 mg, 0.126 mmol, 42%). ^{1}H NMR yield is 50% (using mesitylene as an internal standard). Reaction time: 15 min.

R_f = 0.25 (*n*-pentane). **^{1}H NMR** (600 MHz, $CDCl_3$) δ/ppm = 7.19-7.14 (m, 1H), 6.77-6.73 (m, 1H), 6.24-6.21 (m, 1H), 3.95-3.92 (m, 2H), 1.81-1.71 (m, 2H), 1.48-1.41 (m, 2H), 1.38-1.23 (m, 8H), 0.92-0.87 (m, 3H). **^{13}C NMR** (151 MHz, $CDCl_3$) δ/ppm = 158.2, 124.6, 119.7, 97.1, 70.4, 32.0, 29.5, 29.4, 29.4, 26.2, 22.8, 14.2. **HRMS** (EI) calculated for $C_{12}H_{20}OS$: 212.1229 $[M]^+$, found: 212.1226.

3-(Benzyloxy)thiophene (15)

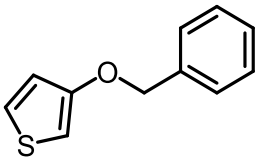

The cross-coupling reaction was performed according to GP using triethyl(thiophen-3-yl)germane (72.9 mg, 0.30 mmol, 1.0 equiv.) and benzylic alcohol (156 µl, 1.50 mmol, 5.0 equiv.). The title product was obtained after purification by preparative TLC (*n*-pentane) as a colorless oil (20.9 mg, 0.11 mmol, 37%). ^{1}H NMR yield is 40% (using mesitylene as an internal standard). Reaction time: 15 min.

R_f = 0.34 (*n*-pentane). **^{1}H NMR** (600 MHz, $CDCl_3$) δ/ppm = 7.46-7.42 (m, 2H), 7.42-7.37 (m, 2H), 7.36-7.31 (m, 1H), 7.23-7.15 (m, 1H), 6.84-6.81 (m, 1H), 6.35-6.32 (m, 1H), 5.03 (s, 2H). **^{13}C NMR** (151 MHz, $CDCl_3$) δ/ppm = 157.8, 136.9, 128.7, 128.3, 127.8, 124.8, 119.8, 98.2, 72.4. **HRMS** (ESI) calculated for $C_{11}H_{11}OS$: 191.0525 $[M+H]^+$, found: 191.0523.

3-(4-Iodophenoxy)oxetane (16)

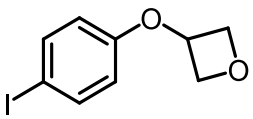

The cross-coupling reaction was performed according to GP using triethyl(4-iodophenyl)germane (108.8 mg, 0.30 mmol, 1.0 equiv.) and oxetan-3-ol (95.2 µl, 1.50 mmol, 5.0 equiv.). The title product was obtained after purification by preparative TLC (5:1 *n*-pentane/EtOAc) as a colorless solid (58.0 mg, 0.21 mmol, 70%). Reaction time: 15 min. With 1 mol% $Pd(OAc)_2$ for 30 min 61% of the product was formed, as judged by quantitative ^{1}H NMR analysis (mesitylene as an internal standard).

R_f = 0.33 (5:1 *n*-pentane/EtOAc). **^{1}H NMR** (400 MHz, $CDCl_3$) δ/ppm = 7.56 (d, *J* = 9.0 Hz, 2H), 6.48 (d, *J* = 9.0 Hz, 2H), 5.16 (p, *J* = 5.6 Hz, 1H), 4.98 – 4.93 (m, 2H), 4.79 – 4.70 (m, 2H). **^{13}C NMR** (101 MHz, $CDCl_3$) δ/ppm = 156.6, 138.7, 117.0, 83.9, 77.9, 70.3. **HRMS** (EI) calculated for $C_9H_9IO_2$: 275.9647 $[M]^+$, found: 275.9642.

(8*R*,9*S*,13*S*,14*S*,17*S*)-3-methoxy-13-methyl-17-(*p*-tolyloxy)-7,8,9,11,12,13,14,15,16,17-decahydro-6*H*-cyclopenta[*a*]phenanthrene (17)

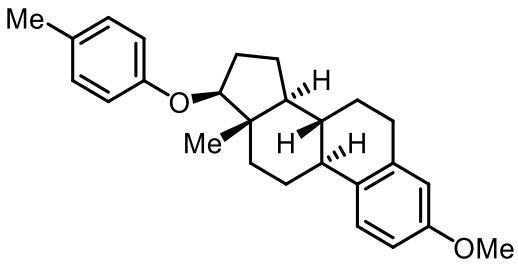

The cross-coupling reaction was performed according to GP using triethyl(*p*-tolyl)germane (25.1 mg, 0.10 mmol, 1.0 equiv.) and (8*R*,9*S*,13*S*,14*S*,17*S*)-3-methoxy-13-methyl-7,8,9,11,12,13,14,15,16,17-decahydro-6*H*-cyclopenta[*a*]phenanthren-17-ol (143.2 mg, 0.50 mmol, 5.0 equiv.). The title product was obtained after purification by preparative TLC (20:1 *n*-pentane/EtOAc) as a colorless oil (21.0 mg, 0.056 mmol, 56%). Reaction time: 15 min.

R_f = 0.30 (20:1 *n*-pentane/EtOAc). **^{1}H NMR** (400 MHz, $CDCl_3$) δ/ppm = 7.20 (d, *J* = 8.6 Hz, 1H), 7.11-7.00 (m, 2H), 6.88-6.78 (m, 2H), 6.74-6.68 (m, 1H), 6.66-6.60 (m, 1H), 4.20 (t, *J* = 8.5 Hz, 1H), 3.78 (s, 3H), 2.91-2.81 (m, 2H), 2.35-2.16 (m, 6H), 2.02-1.94 (m, 1H), 1.94-1.86 (m, 1H), 1.83-1.72 (m, 1H), 1.71-1.59 (m, 1H), 1.57-1.44 (m, 3H), 1.40-1.27 (m, 3H), 0.94 (s, 3H). **^{13}C NMR** (101 MHz, $CDCl_3$) δ/ppm = 157.6, 157.1, 138.1, 132.7, 129.9, 129.7, 126.5, 115.9, 113.9, 111.6, 86.8, 55.4, 50.1, 44.1, 43.9, 38.7, 37.7, 30.0, 28.5, 27.5, 26.5, 23.6, 20.6, 12.2. **HRMS** (EI) calculated for $C_{26}H_{32}O_2$: 376.2397 $[M]^+$, found: 376.2394.

1-(4-Bromophenoxy)adamantane (18)

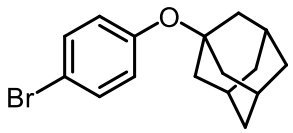

The cross-coupling reaction was performed according to GP using (4-bromophenyl)triethylgermane (94.7 mg, 0.30 mmol, 1.0 equiv.) and adamantan-1-ol (137.0 mg, 1.50 mmol, 5.0 equiv.). The title product was obtained after purification by silica gel column chromatography (pentane to 25:1 *n*-pentane/EtOAc) as a colorless solid (55.1 mg, 0.18 mmol, 60%). Reaction time: 3 h.

R_f = 0.18 (*n*-pentane). **^{1}H NMR** (600 MHz, $CDCl_3$) δ/ppm = 7.36 (d, *J* = 8.8 Hz, 2H), 6.86 (d, *J* = 8.8 Hz, 2H), 2.23-2.14 (m, 3H), 1.88-1.82 (m, 6H), 1.67-1.55 (m, 6H). **^{13}C NMR** (151 MHz, $CDCl_3$) δ/ppm = 153.4, 131.9, 126.9, 116.7, 78.4, 42.9, 36.2, 31.0. **MS** (EI) *m/z* (%) = 136 (11), 135 (100) $[M\text{-}OAr]^+$, 93 (15), 79 (15) (attempts to measure HRMS (ESI, APCI) resulted in no detection of the molecule).

1-(*tert*-Butoxy)-4-iodobenzene (19)

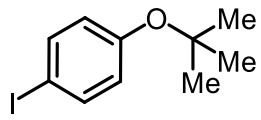

The cross-coupling reaction was performed according to GP using triethyl(4-iodophenyl)germane (108.8 mg, 0.30 mmol, 1.0 equiv.) and 2-methylpropan-2-ol (142 µl, 1.50 mmol, 5.0 equiv.). The title product was obtained after purification by preparative TLC (*n*-pentane) as a light brown oil (41.4 mg, 0.15 mmol, 50%). Reaction time: 1 h.

R_f = 0.35 (*n*-pentane). **^{1}H NMR** (400 MHz, $CDCl_3$) δ/ppm = 7.55 (d, *J* = 8.9 Hz, 2H), 6.75 (d, *J* = 8.9 Hz, 2H), 1.33 (s, 9H). **^{13}C NMR** (100 MHz, $CDCl_3$) δ/ppm = 155.5, 138.0, 126.5, 86.9, 79.1, 28.9. **MS** (EI) m/z (%): 276 (6) $[M]^+$, 221 (12), 220 (100), 93 (11). These data are in agreement with those reported previously in the literature.[222]

1-Iodo-4-((2-methylhexan-2-yl)oxy)benzene (20)

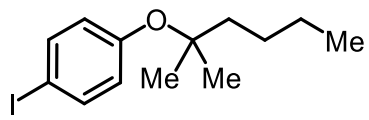

The cross-coupling reaction was performed according to GP using triethyl(4-iodophenyl)germane (108.8 mg, 0.30 mmol, 1.0 equiv.) and 2-methylhexan-2-ol (215 µL, 1.50 mmol, 5.0 equiv.). The title product was obtained after purification by preparative TLC (*n*-pentane) as a colorless oil (49.6 mg, 0.156 mmol, 52%). Reaction time: 1 h.

R_f = 0.34 (*n*-pentane). **^{1}H NMR** (400 MHz, $CDCl_3$) δ/ppm = 7.54 (d, *J* = 8.9 Hz, 2H), 6.73 (d, *J* = 8.9 Hz, 2H), 1.66-1.56 (m, 2H), 1.48-1.29 (m, 4H), 1.26 (s, 6H), 0.92 (t, *J* = 7.2 Hz, 3H). **^{13}C NMR** (100 MHz, $CDCl_3$) δ/ppm = 155.6, 138.0, 126.3, 86.6, 81.4, 41.9, 26.7, 26.6, 23.3, 14.3. **MS** (EI) m/z (%): 318 (1) $[M]^+$, 220 (100) (attempts to measure HRMS (APCI, ESI) resulted in no detection of the molecule).

1-Iodo-4-((1-methylcyclopentyl)oxy)benzene (21)

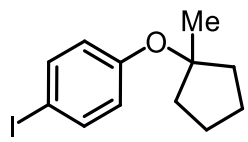

The cross-coupling reaction was performed according to GP using triethyl(4-iodophenyl)germane (108.8 mg, 0.30 mmol, 1.0 equiv.) and 1-methylcyclopentan-1-ol (150.2 mg, 1.50 mmol, 5.0 equiv.). The title product was obtained after purification by preparative TLC (*n*-pentane) as a colorless oil (50.8 mg, 0.168 mmol, 56%). Reaction time: 1 h.

R_f = 0.30 (*n*-pentane). **^{1}H NMR** (400 MHz, $CDCl_3$) δ/ppm = 7.53 (d, *J* = 8.7 Hz, 2H), 6.71 (d, *J* = 8.7 Hz, 2H), 2.11-2.05 (m, 2H), 1.83-1.79 (m, 2H), 1.70-1.59 (m, 4H), 1.45 (s, 3H). **^{13}C NMR** (100 MHz, $CDCl_3$) δ/ppm = 156.2, 138.1, 123.5, 89.3, 84.6, 39.5, 24.9, 24.2. **MS** (EI) m/z (%): 302 (1) $[M]^+$, 220 (100) (attempts to measure HRMS (APCI, ESI) resulted in no detection of the molecule).

1-Iodo-4-((1-methylcyclohexyl)oxy)benzene (22)

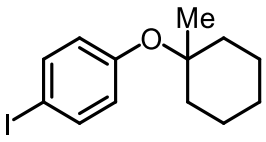

The cross-coupling reaction was performed according to GP using triethyl(4-iodophenyl)germane (108.8 mg, 0.30 mmol, 1.0 equiv.) and 1-methylcyclohexan-1-ol (171.3 mg, 1.50 mmol, 5.0 equiv.). The title product was obtained after purification by preparative TLC (*n*-pentane) as a colorless oil (45.5 mg, 0.144 mmol, 48%). Reaction time: 1 h.

R_f = 0.28 (*n*-pentane). **^{1}H NMR** (600 MHz, $CDCl_3$) δ/ppm = 7.53 (d, *J* = 8.9 Hz, 2H), 6.76 (d, *J* = 8.9 Hz, 2H), 1.89-1.81 (m, 2H), 1.77-1.67 (m, 2H), 1.56-1.42 (m, 5H), 1.40-1.31 (m, 1H), 1.24 (s, 3H). **^{13}C NMR** (151 MHz, $CDCl_3$) δ/ppm = 155.6, 138.0, 126.0, 86.2, 80.4, 37.7, 26.2, 25.7, 22.7. **MS** (EI) m/z (%): 316 (1) $[M]^+$, 220 (100), 81 (11) (attempts to measure HRMS (APCI, ESI) resulted in no detection of the molecule).

***tert*-Butyl 4-(2-phenoxyethyl)piperidine-1-carboxylate (23)**

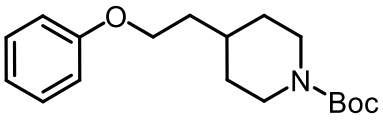

The cross-coupling reaction was performed according to GP from trimethyl(phenyl)germane (59.7 mg, 0.30 mmol, 1.0 equiv.) and *tert*-butyl 4-(2-hydroxyethyl)piperidine-1-carboxylate (344.0 mg, 1.50 mmol, 5.0 equiv.). The title product was obtained after purification by silica gel column chromatography (20:1 *n*-pentane/EtOAc) as a colorless solid (79.7 mg, 0.261 mmol, 87%, from $PhGeEt_3$ and 73.3 mg, 0.240 mmol, 80%, from $PhGeMe_3$, respectively. Reaction time: 15 min.

R_f = 0.31 (20:1 *n*-pentane/EtOAc). **^{1}H NMR** (600 MHz, $CDCl_3$) δ/ppm = 7.28 (dd, *J* = 8.7, 7.3, 2H), 6.96-6.91 (m, 1H), 6.91-6.87 (m, 2H), 4.15-4.05 (m, 2H), 4.01 (t, *J* = 6.1 Hz, 2H), 2.71 (t, *J* = 12.9 Hz, 2H), 1.78-1.67 (m, 5H), 1.46 (s, 9H), 1.22-1.13 (m, 2H). **^{13}C NMR** (151 MHz, $CDCl_3$) δ/ppm = 159.1, 155.0, 129.6, 120.8, 114.6, 79.4, 65.3, 44.0 (br), 35.9, 33.1, 32.2, 28.6. **HRMS** (ESI) calculated for $C_{18}H_{27}NNaO_3$: 328.1883 $[M+Na]^+$, found: 328.1883.

1-Iodo-2-(phenoxymethyl)benzene (24)

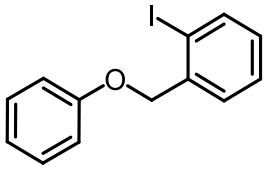

The cross-coupling reaction was performed according to GP using tri-*n*-butyl(phenyl)germane (96.3 mg, 0.30 mmol, 1.0 equiv.) and (2-iodophenyl)methanol (351.1 mg, 1.50 mmol, 5.0 equiv.). The title product was obtained after purification by silica gel column chromatography (30:1 *n*-pentane/EtOAc) and preparative TLC (30:1 *n*-pentane/EtOAc) as a colorless oil (80.9 mg, 0.261 mmol, 87%). Reaction time: 15 min.

R_f = 0.58 (20:1 *n*-pentane/EtOAc). **^{1}H NMR** (600 MHz, $CDCl_3$) δ/ppm = 7.89-7.85 (m, 1H), 7.56-7.50 (m, 1H), 7.41-7.34 (m, 1H), 7.34-7.28 (m, 2H), 7.05-7.01 (m, 1H), 7.01-6.97 (m, 3H), 5.06 (s, 2H). **^{13}C NMR** (151 MHz, $CDCl_3$) δ/ppm = 158.6, 139.40, 139.35, 129.7, 129.6, 128.8, 128.5, 121.4, 115.1, 97.3, 74.0. **HRMS** (EI) calculated for $C_{13}H_{11}IO$: 309.9849 $[M]^+$, found: 309.9848. These data are in agreement with those reported previously in the literature.[223]

4-(Trimethylsilyl)phenyl acetate (29)

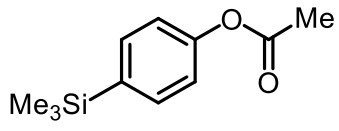

The cross-coupling reaction was performed according to GP using trimethyl(4-(triethylgermyl)phenyl)silane (92.7 mg, 0.30 mmol, 1.0 equiv.) and acetic *acid*

(86.0 µl, 1.50 mmol, 5.0 equiv.). The title product was obtained after purification by silica gel column chromatography (40:1 *n*-pentane/Et_2O) as a yellow solid (50.0 mg, 0.24 mmol, 80%). Reaction time: 1 h. The reaction was also performed with 1 mol% of $Pd(OAc)_2$. ^1H NMR yield is 90% (mesitylene as an internal standard). Reaction time: 2 h.

R_f = 0.29 (30:1 *n*-pentane/EtOAc). **^1H NMR** (600 MHz, $CDCl_3$) δ/ppm = 7.53 (d, *J* = 8.3 Hz, 2H), 7.07 (d, *J* = 8.3 Hz, 2H), 2.30 (s, 3H), 0.26 (s, 9H). **^{13}C NMR** (151 MHz, $CDCl_3$) δ/ppm = 169.6, 151.5, 138.1, 134.7, 121.0, 21.3, -0.9. **MS** (EI) *m/z* (%) = 193 (6) $[M\text{-}Me]^+$, 166 (32), 152 (14), 151 (100). These data are in agreement with those reported previously in the literature.[224]

4-(Trimethylsilyl)phenyl benzoate (30)

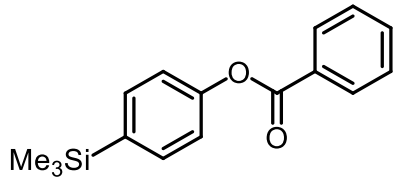

The cross-coupling reaction was performed according to GP using trimethyl(4-(triethylgermyl)phenyl)silane (92.7 mg, 0.30 mmol, 1.0 equiv.) and benzoic acid (183.2 mg, 1.50 mmol, 5.0 equiv.). The title product was obtained after purification by silica gel column chromatography (35:1 *n*-pentane/Et_2O) as a colorless solid (67.6 mg, 0.250 mmol, 85%). Reaction time: 1 h.

R_f = 0.32 (30:1 *n*-pentane/EtOAc). **^1H NMR** (600 MHz, $CDCl_3$) δ/ppm = 8.24-8.19 (m, 2H), 7.66-7.62 (m, 1H), 7.59 (d, *J* = 8.3 Hz, 2H), 7.54-7.49 (m, 2H), 7.21 (d, *J* = 8.3 Hz, 2H), 0.29 (s, 9H). **^{13}C NMR** (151 MHz, $CDCl_3$) δ/ppm = 165.3, 151.8, 138.2, 134.8, 133.7, 130.3, 129.8, 128.7, 121.2, -0.9. **HRMS** (ESI) calculated for $C_{16}H_{18}NaO_2Si$: 293.0968 $[M+Na]^+$, found: 293.0974.

4-(Trimethylsilyl)phenyl adamantane-1-carboxylate (31)

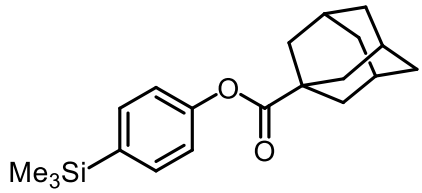

The cross-coupling reaction was performed according to GP using trimethyl(4-(triethylgermyl)phenyl)silane (92.7 mg, 0.30 mmol, 1.0 equiv.) and 1-adamantanecarboxylic *acid* (274.0 mg, 1.50 mmol, 5.0 equiv.). The title product was obtained after purification by silica gel column chromatography (35:1 *n*-pentane/Et_2O) as a colorless solid (63.1 mg, 0.192 mmol, 64%). Reaction time: 5 h.

R_f = 0.36 (30:1 *n*-pentane/EtOAc). **^1H NMR** (600 MHz, $CDCl_3$) δ/ppm = 7.51 (d, *J* = 8.2 Hz, 2H), 7.03 (d, *J* = 8.2 Hz, 2H), 2.11-2.07 (m, 3H), 2.07-2.04 (m, 6H), 1.80-1.74 (m, 6H), 0.26 (s, 9H). **^{13}C NMR** (151 MHz, $CDCl_3$) δ/ppm = 176.3, 151.9, 137.7, 134.6, 121.0, 41.2, 38.9, 36.6, 28.1, -0.9. **HRMS** (ESI) calculated for $C_{20}H_{28}NaO_2Si$: 351.1751 $[M+Na]^+$, found: 351.1750.

4-(Trimethylsilyl)phenyl thiophene-2-carboxylate (32)

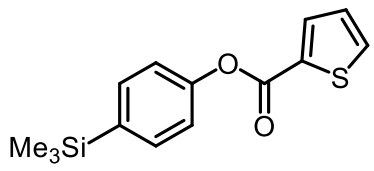

The cross-coupling reaction was performed according to GP using trimethyl(4-(triethylgermyl)phenyl)silane (92.7 mg, 0.30 mmol, 1.0 equiv.) and thiophene-2-carboxylic acid (192.2 mg, 1.50 mmol, 5.0 equiv.). The title product was obtained after purification by silica gel column chromatography (35:1 *n*-pentane/Et_2O) as a colorless solid (44.0 mg, 0.159 mmol, 53%). Reaction time: 1 h.

R_f = 0.29 (30:1 *n*-pentane/Et_2O). **^{1}H NMR** (600 MHz, $CDCl_3$) δ/ppm = 7.98 (d, *J* = 3.6 Hz, 1H), 7.67 (d, *J* = 5.0 Hz, 1H), 7.57 (d, *J* = 8.0 Hz, 2H), 7.21 (d, *J* = 8.0 Hz, 2H), 7.20-7.15 (m, 1H), 0.28 (s, 9H). **^{13}C NMR** (151 MHz, $CDCl_3$) δ/ppm = 160.7, 151.4, 138.3, 134.8, 134.8, 133.6, 133.2, 128.2, 121.1, -0.9. **HRMS** (ESI) calculated for $C_{14}H_{16}NaO_2SSi$: 299.0532 $[M+Na]^+$, found: 299.0535.

4-(Trimethylsilyl)phenyl thiophene-3-carboxylate (33)

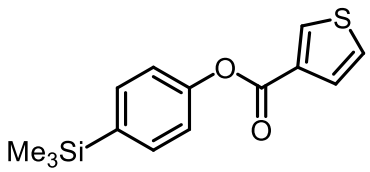

The cross-coupling reaction was performed according to GP using trimethyl(4-(triethylgermyl)phenyl)silane (92.7 mg, 0.30 mmol, 1.0 equiv.) and thiophene-3-carboxylic acid (192.2 mg, 1.50 mmol, 5.0 equiv.). The title product was obtained after purification by silica gel column chromatography (35:1 *n*-pentane/Et_2O) as a colorless solid (48.9 mg, 0.177 mmol, 60%). Reaction time: 2 h.

R_f = 0.26 (30:1 *n*-pentane/Et_2O). **^{1}H NMR** (600 MHz, $CDCl_3$) δ/ppm = 8.33-8.30 (m, 1H), 7.67 (d, *J* = 5.0 Hz, 1H), 7.57 (d, *J* = 7.8 Hz, 2H), 7.39-7.37 (m, 1H), 7.19 (d, *J* = 7.8 Hz, 2H), 0.28 (s, 9H). **^{13}C NMR** (151 MHz, $CDCl_3$) δ/ppm = 161.2, 151.5, 138.2, 134.8, 134.2, 133.1, 128.4, 126.5, 121.1, -0.9. **HRMS** (ESI) calculated for $C_{14}H_{16}NaO_2SSi$: 299.0532 $[M+Na]^+$, found: 299.0535.

3-(Trimethylsilyl)phenyl (1*R*,2*R*)-2-phenylcyclopropane-1-carboxylate (34)

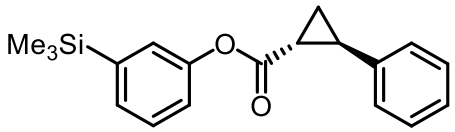

The cross-coupling reaction was performed according to GP using trimethyl(3-(triethylgermyl)phenyl)silane (92.7 mg, 0.30 mmol, 1.0 equiv.) and *trans*-2-phenylcyclopropane-1-carboxylic acid (242.3 mg, 1.50 mmol, 5.0 equiv.). The title product was obtained after purification by silica gel column chromatography (20:1 *n*-pentane/EtOAc) as a colorless solid (55.6 mg, 0.179 mmol, 60%). Reaction time: 1 h.

R_f = 0.25 (30:1 *n*-pentane/EtOAc). **^{1}H NMR** (600 MHz, CD_2Cl_2) δ/ppm = 7.43-7.36 (m, 2H), 7.35-7.30 (m, 2H), 7.26-7.22 (m, 2H), 7.21-7.17 (m, 2H), 7.11-7.08 (m, 1H), 2.68 (ddd, *J* = 9.3, 6.6, 4.1 Hz, 1H), 2.14 (ddd, *J* = 8.4, 5.3, 4.1 Hz, 1H), 1.74 (ddd, *J* = 9.3, 5.3, 4.7 Hz, 1H), 1.49 (ddd, *J* = 8.4, 6.6, 4.7 Hz, 1H), 0.28 (s, 9H). **^{13}C NMR** (151 MHz, CD_2Cl_2) δ/ppm = 172.4, 151.0, 143.2, 140.3, 131.1, 129.2, 128.9, 127.0, 126.6, 126.4, 122.5, 27.3, 24.5, 18.0, -1.2. **HRMS** (ESI) calculated for $C_{19}H_{22}NaO_2Si$: 333.1281 $[M+Na]^+$, found: 333.1274.

3-Iodophenyl benzoate (35)

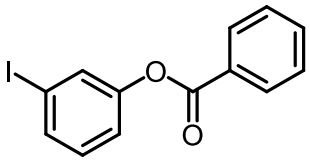

The cross-coupling reaction was performed according to GP using triethyl(3-iodophenyl)germane (72.6 mg, 0.20 mmol, 1.0 equiv.) and benzoic acid (122.1 mg, 1.0 mmol, 5.0 equiv.). The title product was obtained after purification by silica gel column chromatography (30:1 *n*-pentane/EtOAc) as a colorless solid (48.6 mg, 0.15 mmol, 75%). Reaction time: 1 h.

R_f = 0.23 (40:1 *n*-pentane/EtOAc). **^{1}H NMR** (600 MHz, $CDCl_3$) δ/ppm = 8.21-8.15 (m, 2H), 7.68-7.59 (m, 3H), 7.54-7.49 (m, 2H), 7.24-7.20 (m, 1H), 7.19-7.12 (m, 1H). **^{13}C NMR** (151 MHz, $CDCl_3$) δ/ppm = 164.9, 151.4, 135.2, 134.0, 131.1, 130.9, 130.4, 129.3, 128.8, 121.5, 93.7. **HRMS** (EI) calculated for $C_{13}H_9IO_2$: 323.9642 $[M]^+$, found: 323.9642.

4-Chloro-3-fluorophenyl benzoate (36)

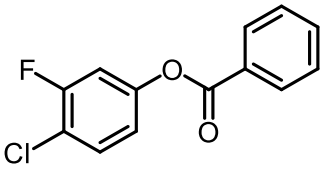

The cross-coupling reaction was performed according to GP using (4-chloro-3-fluorophenyl)triethylgermane (57.9 mg, 0.20 mmol, 1.0 equiv.) and benzoic acid (122.1 mg, 1.0 mmol, 5.0 equiv.). The title product was obtained after purification by silica gel column chromatography (30:1 *n*-pentane/EtOAc) as a colorless solid (35.1 mg, 0.14 mmol, 60%). Reaction time: 4 h.

R_f = 0.38 (20:1 *n*-pentane/EtOAc). **^{1}H NMR** (600 MHz, $CDCl_3$) δ/ppm = 8.21-8.12 (m, 2H), 7.70-7.63 (m, 1H), 7.54-7.51 (m, 2H), 7.47-7.42 (m, 1H), 7.14-7.07 (m, 1H), 7.03-6.99 (m, 1H). **^{13}C NMR** (151 MHz, $CDCl_3$) δ/ppm = 164.7, 158.2 (d, *J* = 250.4 Hz), 150.2 (d, *J* = 9.6 Hz), 134.1, 130.8, 130.4, 129.0, 128.9, 118.6-118.4 (m, 2C), 111.3 (d, *J* = 24.1 Hz). **^{19}F NMR** (565 MHz, $CDCl_3$) δ/ppm = -112.03 (t, *J* = 9.0 Hz, 1F). **MS** (EI) m/z (%): 250 (4) $[M]^+$, 105 (100), 77 (31) (attempts to measure HRMS (APCI, ESI) resulted in no detection of the molecule).

Orthogonal C-O Bond Formation

$Pd^{(0)}/Pd^{(II)}$-catalyzed C-O Bond Formation

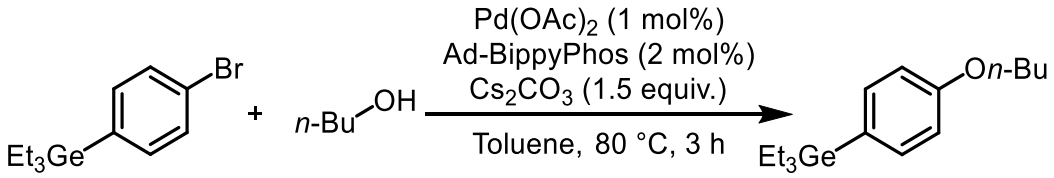

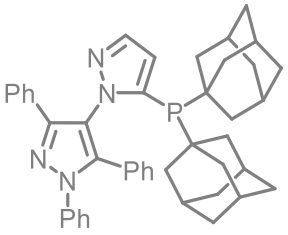

Ad-BippyPhos

(4-Butoxyphenyl)triethylgermane (25)

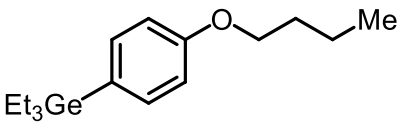

The reaction was performed according to the literature procedure.[68] In an argon-filled glovebox (4-bromophenyl)triethylgermane (157.9 mg, 0.5 mmol, 1.0 equiv.), $Pd(OAc)_2$ (1.1 mg, 0.005 mmol, 1 mol%), Ad-BippyPhos (6.6 mg, 0.01 mmol, 2 mol%), and Cs_2CO_3 (244.4 mg, 0.75 mmol, 1.5 equiv.) were mixed in a vial and dissolved in anhydrous toluene (0.83 mL) followed by addition of *n*-butanol (137 µL, 1.5 mmol, 3.0 equiv.). The vial was sealed with a screw cap and the mixture was stirred at 80 °C for 3 h. The vial was taken out from the glovebox, the reaction mixture was allowed to cool to ambient temperature and was quenched with DCM and filtered through a pad of Celite®. After that the filtrate was concentrated *in vacuo*. The title product was obtained after purification by preparative TLC (*n*-pentane) as a colorless oil (100.4 mg, 0.325 mmol, 65%).

R_f = 0.55 (*n*-pentane). **^{1}H NMR** (400 MHz, $CDCl_3$) δ/ppm = 7.33 (d, *J* = 8.4 Hz, 2H), 6.90 (d, *J* = 8.4 Hz, 2H), 3.96 (t, *J* = 6.5 Hz, 2H), 1.83-1.71 (m, 2H), 1.56-1.44 (m, 2H), 1.12-1.01 (m, 9H), 1.01-0.92 (m, 9H). **^{13}C NMR** (100 MHz, $CDCl_3$) δ/ppm = 159.5, 135.2, 130.2, 114.4, 67.5, 31.5, 19.4, 14.0, 9.1, 4.4. **HRMS** (APCI) calculated for $C_{14}H_{23}{}^{74}GeO$: 281.0955 $[M\text{-}Et]^+$, found: 281.0960.

Ni-catalyzed Photoredox Coupling

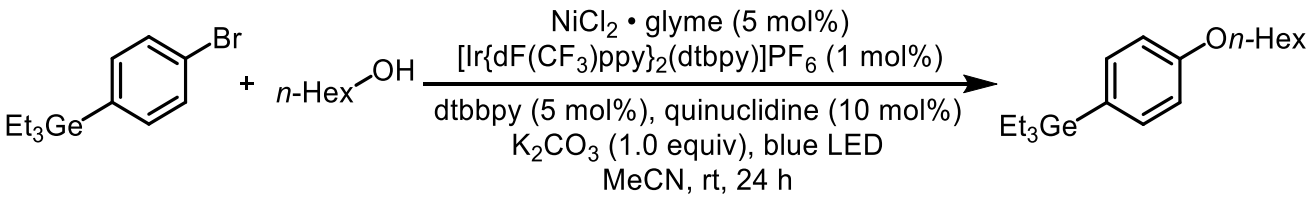

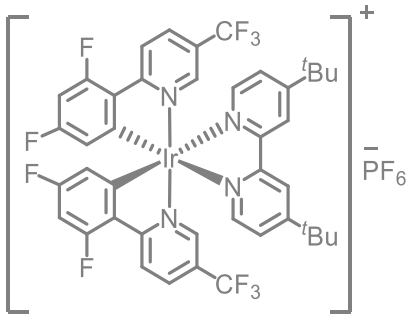

[Ir{dF(CF$_3$)ppy}$_2$(dtbpy)]PF$_6$

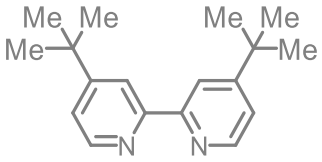

dtbbpy

Triethyl(4-(hexyloxy)phenyl)germane (26)

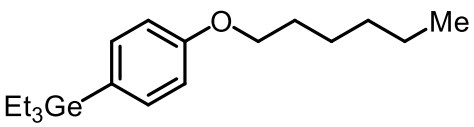

The reaction was performed according to the literature procedure.[75] In an argon-filled glovebox (4-bromophenyl)triethylgermane (31.6 mg, 0.10 mmol, 1.0 equiv.), $NiCl_2 \cdot$ glyme (1.1 mg, 0.005 mmol, 5 mol%), [Ir{dF(CF_3)ppy}$_2$(dtbpy)]PF_6 (1.1 mg, 0.001 mmol, 1 mol%), K_2CO_3 (13.8 mg, 0.10 mmol, 1.0 equiv.), dtbbpy (1.3 mg, 0.005 mmol, 5 mol%) and quinuclidine (1.1 mg, 0.01 mmol, 10 mol%) were mixed in a vial and dissolved in anhydrous MeCN (0.4 ml). Then *n*-hexanol (19 µl, 0.15 mmol, 1.5 equiv.) was subsequently added. The vial was sealed with a screw cap, taken out from the glovebox and the mixture was placed into a blue LED reactor (λ = 467 nm, 18.6 W)[1] with air cooling to maintain ambient temperature for 24 h. The reaction solution was quenched with Et_2O and filtered through a pad of Celite®. After that the filtrate was concentrated *in vacuo*. The title product was obtained after purification by preparative TLC (*n*-pentane) as a colorless oil (68.7 mg, 0.29 mmol, 97%).

R_f = 0.52 (*n*-pentane). **^{1}H NMR** (600 MHz, $CDCl_3$) δ/ppm = 7.33 (d, *J* = 8.6 Hz, 2H), 6.90 (d, *J* = 8.6 Hz, 2H), 3.95 (t, *J* = 6.6 Hz, 2H), 1.82-1.73 (m, 2H), 1.50-1.42 (m, 2H), 1.36-1.33 (m, 4H), 1.08-1.02 (m, 9H), 1.00-0.87 (m, 9H). **^{13}C NMR** (151 MHz, $CDCl_3$) δ/ppm = 159.6, 135.2, 130.2, 114.4, 67.9, 31.8, 29.5, 25.9, 22.8, 14.2, 9.1, 4.5. **HRMS** (EI) calculated for $C_{16}H_{27}{}^{74}GeO$: 309.1268 $[M\text{-}Et]^+$, found: 309.1268.

Cu-catalyzed Ullmann Coupling

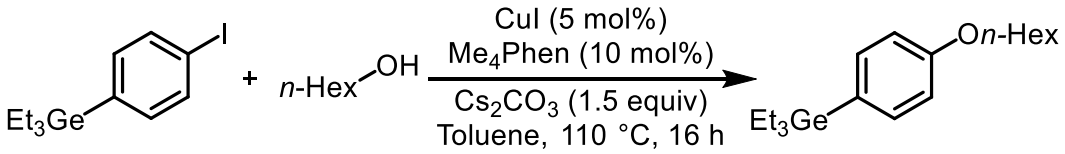

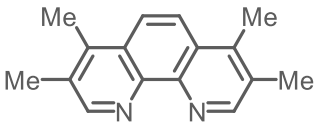

Me_4Phen

Triethyl(4-(hexyloxy)phenyl)germane (27)

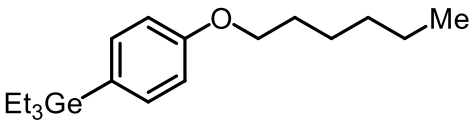

The reaction was performed according to the literature procedure.[58] In an argon-filled glovebox triethyl(4-iodophenyl)germane (108.8 mg, 0.30 mmol, 1.0 equiv.), *n*-hexanol (56 µl, 0.45 mmol, 1.5 equiv.), CuI (2.9 mg, 0.015 mmol, 5 mol%), Me_4Phen (7.1 mg, 0.03 mmol, 10 mol%) and Cs_2CO_3 (158.8 mg, 0.45 mmol, 1.5 equiv.) were mixed in a pressure tube and dissolved in anhydrous toluene (0.25 mL). The tube was sealed with a screw cap, taken out from the glovebox and the mixture was stirred at 110 °C for 16 h. The reaction solution was quenched with Et_2O and filtered through a pad of Celite®. After that the filtrate was concentrated *in vacuo*. The title product was obtained after purification by preparative TLC (*n*-pentane) as a colorless oil (68.7 mg, 0.29 mmol, 97%).

R_f = 0.52 (*n*-pentane). **^{1}H NMR** (600 MHz, $CDCl_3$) δ/ppm = 7.33 (d, *J* = 8.6 Hz, 2H), 6.90 (d, *J* = 8.6 Hz, 2H), 3.95 (t, *J* = 6.6 Hz, 2H), 1.82-1.73 (m, 2H), 1.50-1.42 (m, 2H), 1.36-1.33 (m, 4H), 1.08-1.02 (m, 9H), 1.00-0.87 (m, 9H). **^{13}C NMR** (151 MHz, $CDCl_3$) δ/ppm = 159.6, 135.2, 130.2, 114.4, 67.9, 31.8, 29.5, 25.9, 22.8, 14.2, 9.1, 4.5. **HRMS** (EI) calculated for $C_{16}H_{27}{}^{74}GeO$: 309.1268 $[M\text{-}Et]^+$, found: 309.1268.

Cu-catalyzed Chan-Lam Coupling

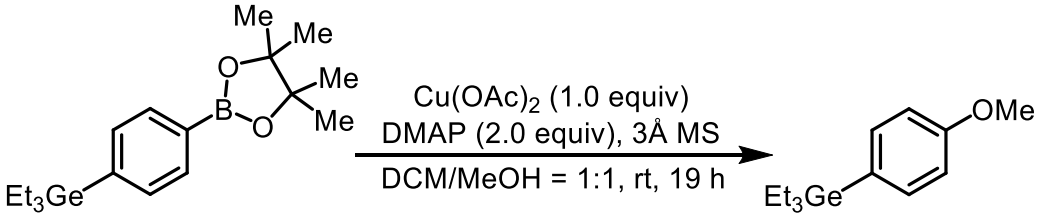

Triethyl(4-methoxyphenyl)germane (28)

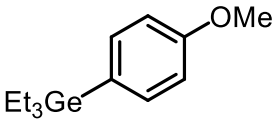

The reaction was performed according to the literature procedure.[225] Triethyl(4-(4,4,5,5-tetramethyl-1,3,2-dioxaborolan-2-yl)phenyl)-germane (72.6 mg, 0.2 mmol, 1.0 equiv.) was placed into a vial equipped with a stirring bar. Then $Cu(OAc)_2$ (36.3 mg, 0.2 mmol, 1.0 equiv.), DMAP (48.9 mg, 0.4 mmol, 2.0 equiv.) and 3Å molecular sieves (14 mg, activated) were added. Thereafter, anhydrous DCM (1 ml) and anhydrous MeOH (1 ml) were added and the vial was sealed with a cap. The obtained mixture was stirred for 19 h at ambient temperature. After that the solvent was evaporated under reduced pressure, Et_2O was added and the mixture was filtered through Celite®. The solvent was evaporated *in vacuo*. The title product was obtained after purification by preparative TLC (*n*-pentane) as a colorless oil (32.0 mg, 0.12 mmol, 60%).

R_f = 0.42 (*n*-pentane). **^{1}H NMR** (600 MHz, $CDCl_3$) δ/ppm = 7.35 (d, *J* = 8.6 Hz, 2H), 6.91 (d, *J* = 8.6 Hz, 2H), 3.81 (s, 3H), 1.09-1.01 (m, 9H), 1.00-0.91 (m, 6H). **^{13}C NMR** (151 MHz, $CDCl_3$) δ/ppm = 159.9, 135.2, 130.5, 113.8, 55.1, 9.1, 4.4. **HRMS** (EI) calculated for $C_{13}H_{22}{}^{74}GeO$: 268.0882 $[M]^+$, found: 268.0890. These data are in agreement with those reported previously in the literature.[22]

Germanium recovery

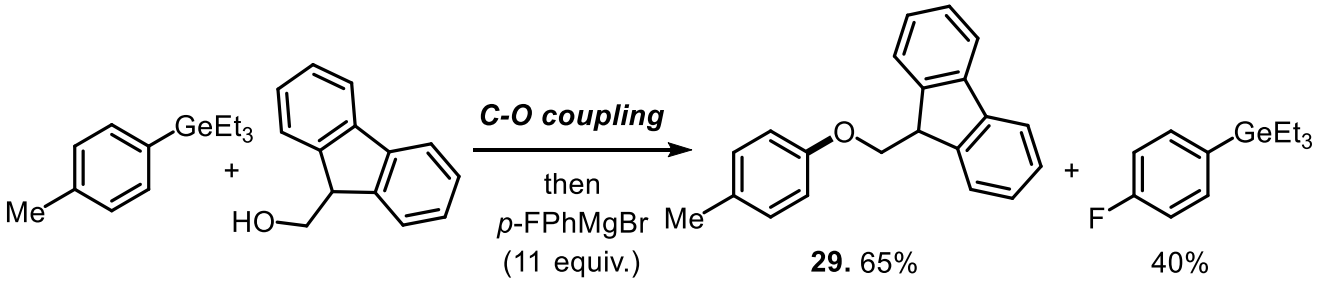

The cross-coupling reaction was performed according to GP from triethyl(*p*-tolyl)germane (251.0 mg, 1.0 mmol, 1.0 equiv.) and (9*H*-fluoren-9-yl)methanol (981.3 mg, 5.0 mmol, 5.0 equiv.). After full consumption of the starting germane (monitored by GC-MS) solution of *p*-FPhMgBr (1.0 M in THF, 11 ml, 11.0 mmol, 11.0 equiv.) was added dropwise at 0 °C. The obtained mixture was stirred at the same temperature for 1 h and then was allowed to warm up to ambient temperature. The obtained solution was stirred overnight. Thereafter, the reaction was quenched with Et_2O and filtered through a pad of Celite®. The filtrate was concentrated *in vacuo* and dissolved in 10 mL of $CHCl_3$. Then 1,4-difluorobenzene (102.8 µl, 1.0 mmol, 1.0 equiv.) was added as an internal standard and an aliquot (200 µl) was transferred into NMR tube. To the aliquot $CDCl_3$ (500 µl) was added to determine the ^{19}F NMR yield (40%) of the aryl germane. After that the aliquot was returned to the crude mixture and the

obtained solution was concentrated *in vacuo*. The residue was purified by silica gel column chromatography (*n*-pentane to 50:1 *n*-pentane/EtOAc) to afford triethyl(4-fluorophenyl)germane (102.0 mg, 0.40 mmol, 40%) and **29** (202.7 mg, 0.65 mmol, 65%, 5% impurity).

Data for 29: $\mathbf{R_f}$ = 0.72 (50:1 *n*-pentane/EtOAc). **^{1}H NMR** (600 MHz, $CDCl_3$) δ/ppm = 7.82-7.76 (m, 2H), 7.74-7.72 (m, 2H), 7.46-7.39 (m, 2H), 7.36-7.30 (m, 2H), 7.13-7.08 (m, 2H), 6.95-6.86 (m, 2H), 4.41 (t, *J* = 7.6 Hz, 1H), 4.20 (d, *J* = 7.6 Hz, 2H), 2.30 (s, 3H). **^{13}C NMR** (151 MHz, $CDCl_3$) δ/ppm = 156.9, 144.6, 141.4, 130.3, 130.1, 127.8, 127.2, 125.6, 120.1, 114.6, 70.9, 47.6, 20.6. **HRMS** (ESI) calculated for $C_{21}H_{18}NaO$: 309.1250 $[M+Na]^+$, found: 309.1250.

Data for the aryl germane: $\mathbf{R_f}$ = 0.86 (*n*-pentane). **^{1}H NMR** (600 MHz, $CDCl_3$) δ/ppm = 7.45-7.35 (m, 2H), 7.09-6.98 (m, 2H), 1.09-1.02 (m, 9H), 1.01-0.93 (m, 6H). **^{13}C NMR** (151 MHz, $CDCl_3$) δ/ppm = 163.2 (d, *J* = 246.4 Hz), 135.5 (d, *J* = 7.3 Hz), 134.9 (d, *J* = 3.6 Hz), 115.0 (d, *J* = 19.4 Hz). **^{19}F NMR** (565 MHz, $CDCl_3$) δ/ppm = -113.72 – -113.90 (m, 1F).

DFT Analysis of C-Ge Bond Activation with $Pd(O_2CCF_3)_2$

DFT calculations were carried out in Gaussian 16 (A.03) program package.[226] Geometry optimizations and frequency analyses were calculated with B3LYP-D3BJ/def2-SVP (and the associated pseudopotential for Pd), including solvation through the CPCM implicit solvent model (solvent = toluene). Frequencies were used to determine the nature of the stationary point as minima (no imaginary frequency). Electronic energies were calculated with B3LYP-D3BJ/def2-TZVPP (and the corresponding pseudopotential for Pd). Energies are calculated at the sum of the high-basis set electronic energies plus the thermochemistry corrections at standard conditions (298.15 K and 1 atm).

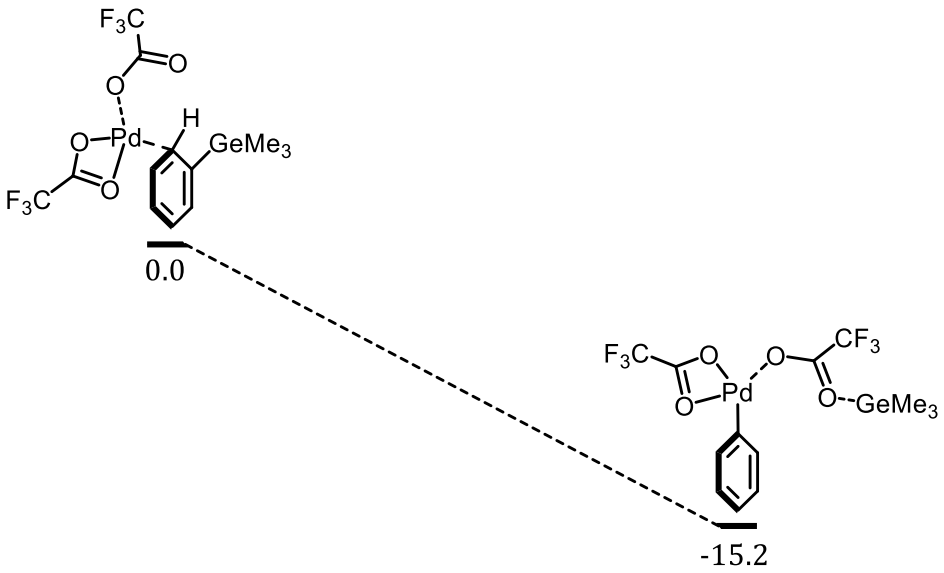

Figure S2. Free energy profile of C-Ge bond activation by $Pd(OCOCF_3)_2$ (energies are in kcal/mol).

XYZ Coordinates and Energies of Optimized Structures

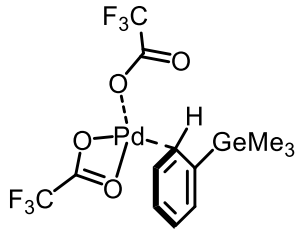

C	-2.40731500	-0.58331300	2.47708500
C	-2.55741100	0.31685200	1.40191500
C	-1.50640500	1.12008100	0.97558700
C	-0.25743800	0.99558100	1.66514400
C	-0.11166500	0.09183300	2.75895300
C	-1.19674900	-0.70465600	3.15107000
H	-3.25658700	-1.20159100	2.77604000
H	-3.52099800	0.35963800	0.88978700
H	0.51011600	1.76001200	1.51436500
H	0.81951900	0.07928200	3.33001100
H	-1.08910500	-1.40639100	3.97971100
Ge	-1.67443400	2.37901300	-0.54282200
C	0.00973400	2.32802200	-1.54860200
H	-0.00485400	3.07890500	-2.35311400
H	0.86996800	2.53583300	-0.89427900
H	0.12570100	1.32616700	-1.98518100
C	-3.20042600	1.80749200	-1.63154400
H	-3.03712600	0.77604600	-1.97474500
H	-4.13802600	1.85828000	-1.05713200
H	-3.29925900	2.46362600	-2.50962800
C	-1.96995800	4.16872200	0.22199200
H	-2.05359200	4.91487000	-0.58326700
H	-2.89660400	4.18674800	0.81544400
H	-1.12938900	4.45214400	0.87372500
Pd	0.87780100	-0.56902500	0.54663800
C	-1.29923700	-1.66673500	-0.84187600
O	-0.65915300	-1.80165900	0.26948800
O	-1.08475600	-0.88397900	-1.74664700
C	3.24918000	-0.32737600	-0.11318100
O	2.66205500	-1.31191000	-0.60528100
O	2.65828600	0.45922500	0.69388300
C	4.70147200	0.00519300	-0.50071100
C	-2.50081700	-2.64656700	-0.92192000
F	-3.10173600	-2.56700700	-2.10825500
F	-3.41346900	-2.34623300	0.02193300
F	-2.11293700	-3.91271100	-0.72749300
F	4.70787200	1.04519400	-1.34475400
F	5.40921500	0.33765100	0.58214600
F	5.28594700	-1.03034200	-1.09600400

Zero-point correction = 0.259108 (Hartree/Particle)
Thermal correction to Energy = 0.288026
Thermal correction to Enthalpy = 0.288970
Thermal correction to Gibbs Free Energy = 0.194136
Sum of electronic and zero-point Energies = -3607.338506
Sum of electronic and thermal Energies = -3607.309588
Sum of electronic and thermal Enthalpies = -3607.308644
Sum of electronic and thermal Free Energies = -3607.403477
E(B3LYP-D3BJ/Def2TZVPP) = -3609.544263

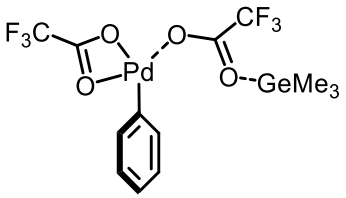

Pd	-0.56607700	0.65209300	-0.72929700
C	-0.01995300	3.63292000	2.20294600
C	-0.51738200	2.56512900	1.44685600
C	0.16585900	2.15437900	0.29516700
C	1.32778300	2.82172600	-0.11179700
C	1.81195900	3.89391500	0.64957600
C	1.14561700	4.29768700	1.80912300
H	-0.55434000	3.94759000	3.10334100
H	-1.43834300	2.06574300	1.75072500
H	1.86383200	2.51881300	-1.01127600
H	2.71913100	4.41205400	0.32753600
H	1.52957600	5.13148400	2.40157100
Ge	0.83722300	-2.09031000	1.26170700
C	2.08587000	-3.19930200	2.25848000
H	2.70205200	-2.57557100	2.92217900
H	1.52189200	-3.91933900	2.87138600
H	2.74033900	-3.75197300	1.56948000
C	-0.11429100	-3.04167200	-0.14184500
H	-0.62611100	-3.89948000	0.32272300
H	-0.86150400	-2.40836300	-0.63836700
H	0.60309800	-3.42555900	-0.88197600
C	-0.16172000	-0.85912900	2.38888500
H	0.46615000	0.00384300	2.65048500
H	-1.06793600	-0.49835800	1.88684500
H	-0.43754600	-1.39346300	3.31136800
C	-3.02369200	-0.09843100	-0.73266100
O	-2.36697700	-0.82940400	-1.48743700
O	-2.53581400	0.88886000	-0.09672700
C	-4.50861100	-0.40790100	-0.45262900
F	-5.03086900	-1.19208100	-1.39600200
F	-4.61008300	-1.04898300	0.72625900
F	-5.23854700	0.70907400	-0.37937900
C	2.23852000	-0.40524600	-0.77137200
O	2.17810000	-1.07089700	0.30716600
O	1.34553300	0.17302400	-1.39720100
C	3.66614800	-0.26083900	-1.35899600
F	3.64112200	-0.41464000	-2.68289100
F	4.12447500	0.96876100	-1.08369100
F	4.50775800	-1.15167100	-0.84094300

Zero-point correction = 0.259178 (Hartree/Particle)
Thermal correction to Energy = 0.288411
Thermal correction to Enthalpy = 0.289355
Thermal correction to Gibbs Free Energy = 0.192202
Sum of electronic and zero-point Energies = -3607.361764
Sum of electronic and thermal Energies = -3607.332531
Sum of electronic and thermal Enthalpies = -3607.331587
Sum of electronic and thermal Free Energies = -3607.428739
E(B3LYP- D3BJ/Def2TZVPP) = -3609.566576

4.3.2 Supporting information for chapter 2.2

Site-selective Light-mediated Nitration of Aryl Germanes

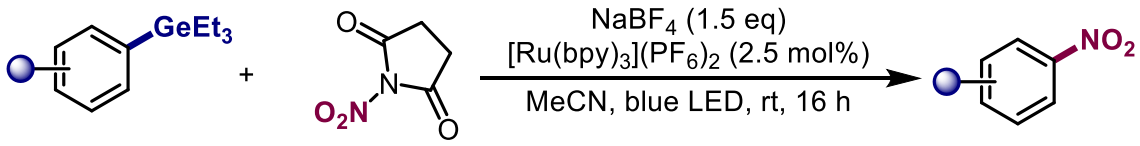

General Procedure

In an argon-filled glovebox, aryl germane (1.0 equiv.), *N*-nitrosuccinimide (2.0 equiv.), $NaBF_4$ (1.5 equiv.) (if required), and $[Ru(bpy)_3](PF_6)_2$ (2.5 mol%) were subsequently placed into a vial equipped with a stirring bar. The obtained mixture was dissolved in anhydrous acetonitrile (0.25 M) and after that the vial was sealed with a cap, taken out from the glovebox, placed into a blue LED reactor[1] and stirred at room temperature under blue light irradiation. After consumption of the aryl germane (monitored by GC-MS) the solvent was evaporated and the residue was purified by silica gel column chromatography affording the desired product.

1-Fluoro-4-nitrobenzene (1)

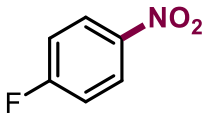

The nitration was performed according to GP from triethyl(4-fluorophenyl)germane (76.5 mg, 0.30 mmol, 1.0 equiv.) and obtained after purification by silica gel column chromatography (20:1 *n*-pentane/EtOAc) as a yellow oil (29.5 mg, 0.21 mmol, 70%).

R_f = 0.49 (20:1 *n*-pentane/EtOAc). **^{1}H NMR** (600 MHz, $CDCl_3$) δ/ppm = 8.30-8.26 (m, 2H), 7.24-7.19 (m, 2H). **^{13}C NMR** (151 MHz, $CDCl_3$) δ/ppm = 166.4 (d, *J* = 257.9 Hz), 144.5, 126.5 (d, *J* = 10.1 Hz), 116.6 (d, *J* = 23.8 Hz). **^{19}F NMR** (565 MHz, $CDCl_3$) δ/ppm = -101.86 – -102.20 (m, 1F). **HRMS** (EI) calculated for $C_6H_4FNO_2$: 141.0226 $[M]^+$, found: 141.0221. These data are in agreement with those previously reported in literature.[227]

1-Bromo-2-methyl-4-nitrobenzene (2)

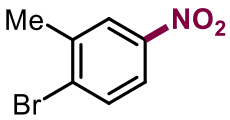

The nitration was performed according to GP from (4-bromo-3-methylphenyl)triethylgermane (99.0 mg, 0.30 mmol, 1.0 equiv.) and obtained after purification by silica gel column chromatography (20:1 *n*-pentane/EtOAc) as a yellow solid (34.3 mg, 0.159 mmol, 53%).

M.p. = 74-77 °C (lit. 76 °C).[228] **R_f** = 0.44 (20:1 *n*-pentane/EtOAc). **^{1}H NMR** (600 MHz, $CDCl_3$) δ/ppm = 8.11 (d, *J* = 2.7 Hz, 1H), 7.91 (dd, *J* = 8.8, 2.7 Hz, 1H), 7.71 (d, *J* = 8.8 Hz, 1H), 2.51 (s, 3H). **^{13}C NMR** (151 MHz, $CDCl_3$) δ/ppm = 147.2, 140.0, 133.4, 132.5, 125.4, 122.3, 23.3. **HRMS** (EI) calculated for $C_7H_6{}^{79}BrNO_2$: 214.9582 $[M]^+$, found: 214.9580.

3-Bromo-5-chloro-4'-nitro-1,1'-biphenyl (3)

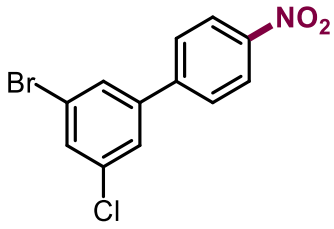

The nitration was performed according to GP from (3'-bromo-5'-chloro-[1,1'-biphenyl]-4-yl)triethylgermane (85.3 mg, 0.20 mmol, 1.0 equiv.) and obtained after purification by silica gel column chromatography (20:1 *n*-pentane/EtOAc) as a yellow solid (31.3 mg, 0.10 mmol, 50%).

M.p. = 148-150 °C (lit. 147-148 °C).[229] **R_f** = 0.40 (20:1 *n*-pentane/EtOAc). **^{1}H NMR** (600 MHz, $CDCl_3$) δ/ppm = 8.32 (d, *J* = 8.8 Hz, 2H), 7.70 (d, *J* = 8.8 Hz, 2H), 7.65 (dd, *J* = 1.8, 1.8 Hz, 1H), 7.59 (dd, *J* = 1.8, 1.8 Hz, 1H), 7.53 (dd, *J* = 1.8, 1.8 Hz, 1H). **^{13}C NMR** (151 MHz, $CDCl_3$) δ/ppm = 148.0, 144.8, 142.1, 136.1, 131.7, 128.9, 128.2, 126.5, 124.5, 123.7. **HRMS** (EI) calculated for $C_{14}H_9NO_2$: 223.0628 $[M]^+$, found: 223.0627.

Trimethyl(4-nitrophenyl)silane (4)

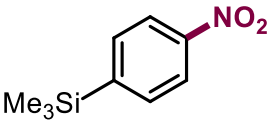

The nitration was performed according to GP from trimethyl(4-(triethylgermyl)phenyl)silane (92.7 mg, 0.30 mmol, 1.0 equiv.) and obtained after purification by silica gel column chromatography (50:1 *n*-pentane/EtOAc) as a viscous liquid (44.5 mg, 0.23 mmol, 76%).

R_f = 0.39 (50:1 *n*-pentane/EtOAc). **^{1}H NMR** (600 MHz, $CDCl_3$) δ/ppm = 8.17 (d, *J* = 8.6 Hz, 2H), 7.68 (d, *J* = 8.6 Hz, 2H), 0.32 (s, 9H). **^{13}C NMR** (151 MHz, $CDCl_3$) δ/ppm = 150.0, 148.6, 134.3, 122.4, -1.3. **HRMS** (EI) calculated for $C_8H_{10}NO_2{}^{28}Si$: 180.0475 $[M\text{-}CH_3]^+$, found: 180.0473. These data are in agreement with those reported previously in the literature.[230]

Trimethyl(3-nitrophenyl)silane (5)

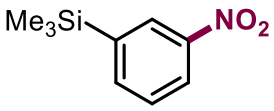

The nitration was performed according to GP (reaction time: 7 h) from trimethyl(3-(triethylgermyl)phenyl)silane (92.7 mg, 0.30 mmol, 1.0 equiv.) and obtained after purification by silica gel column chromatography (30:1 *n*-pentane/EtOAc) as a yellow oil (45.6 mg, 0.233 mmol, 78%).

R_f = 0.56 (20:1 *n*-pentane/EtOAc). **^{1}H NMR** (600 MHz, $CDCl_3$) δ/ppm = 8.37-8.32 (m, 1H), 8.22-8.15 (m, 1H), 7.86-7.76 (m, 1H), 7.56-7.43 (m, 1H), 0.33 (s, 9H). **^{13}C NMR** (151 MHz, $CDCl_3$) δ/ppm = 148.0, 143.5, 139.5, 128.9, 127.9, 123.9, -1.2. **HRMS** (ESI) calculated for $C_9H_{13}NNaO_2Si$: 218.0608 $[M+Na]^+$, found: 218.0614.

Orthogonal Pd-catalyzed Nitration

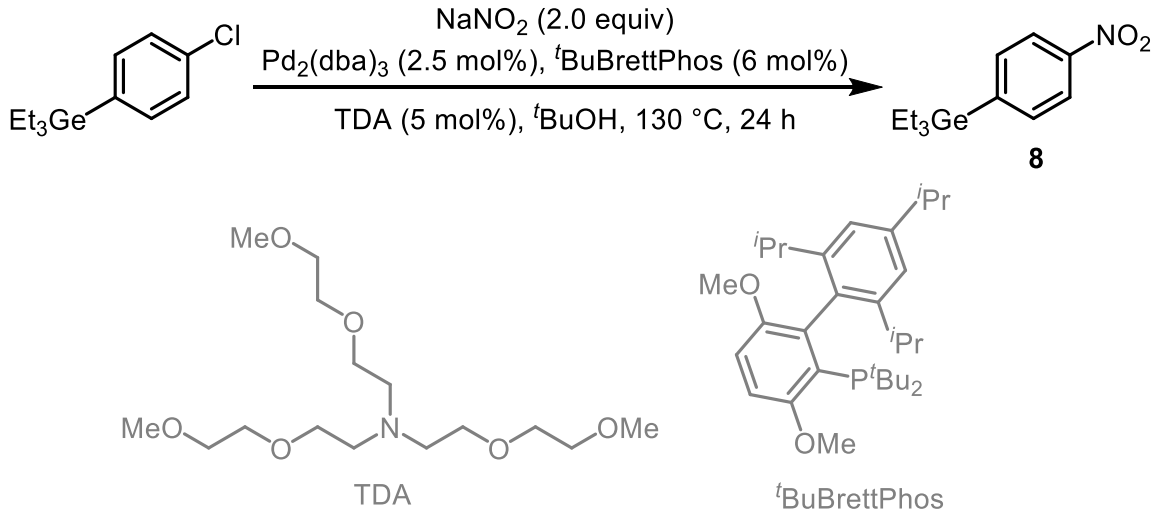

Triethyl(4-nitrophenyl)germane (8)

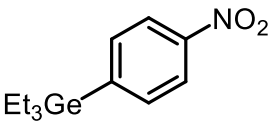

The reaction was performed according to the literature procedure.[120] In an argon filled glovebox (4-chlorophenyl)triethylgermane (81.4 mg, 0.30 mmol, 1.0 equiv.), $NaNO_2$ (41.4 mg, 0.60 mmol, 2.0 equiv.), TDA (6 µl, 0.015 mmol, 5 mol%), $Pd_2(dba)_3$ (6.9 mg, 0.0075 mmol, 2.5 mol%) and ^{t}BuBrettPhos (8.7 mg, 0.018 mmol, 6 mol%) were subsequently placed into an 8 ml vial equipped with a stirring bar followed by addition of ^{t}BuOH (0.6 ml). The vial was tightly sealed with a cap, taken out from the glovebox and stirred at 130 °C for 24 h. After that the reaction mixture was diluted with Et_2O and concentrated *in vacuo*. The title product was obtained after purification of the crude mixture by preparative TLC (30:1 *n*-pentane/Et_2O) as a yellow oil (76.1 mg, 0.27 mmol, 90%).

R_f = 0.53 (20:1 *n*-pentane/Et_2O). **^{1}H NMR** (600 MHz, $CDCl_3$) δ/ppm = 8.16 (d, *J* = 8.6 Hz, 2H), 7.61 (d, *J* = 8.6 Hz, 2H), 1.10-1.00 (m, 15H). **^{13}C NMR** (151 MHz, $CDCl_3$) δ/ppm = 150.4, 148.4, 134.9, 122.4, 8.9, 4.3. **GC-MS** (EI) m/z (%): 256 (26), 255 (14), 254 (100) $[M\text{-}Et]^+$, 253 (34), 252 (79), 250 (62), 228 (17), 226 (74), 225 (23), 224 (57), 222 (44), 200 (18), 198 (79), 197 (23), 196 (67), 194 (51), 152 (19), 150 (21), 148 (16). These data are in agreement with those reported previously in the literature.[231]

Light on/off experiment

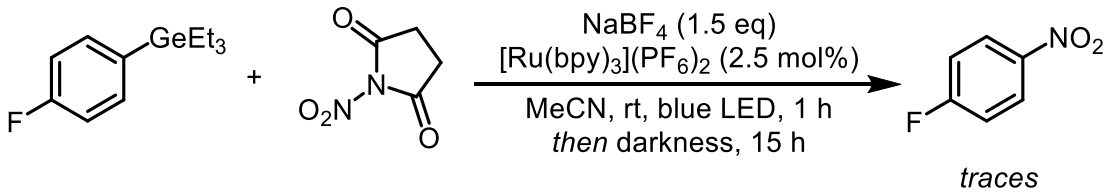

In an argon-filled glovebox, triethyl(4-fluorophenyl)germane (25.6 mg, 0.10 mmol, 1.0 equiv.), *N*-nitrosuccinimide (28.8 mg, 0.20 mmol, 2.0 equiv.), $NaBF_4$ (16.6 mg, 0.15 mmol, 1.5 equiv.) and $[Ru(bpy)_3](PF_6)_2$ (2.1 mg, 2.5 μmol, 2.5 mol%) were subsequently placed into a vial equipped with a stirring bar. The obtained mixture was dissolved in anhydrous acetonitrile (0.4 ml, 0.25 M) and after that the vial was sealed with a cap, taken out from the glovebox, placed into blue LED reactor[1] and stirred at room temperature under blue light irradiation for 1 h. Then the light was turned off and the reaction mixture was stirred for 15 h in darkness. The reaction mixture was analyzed by GC-MS. Only untouched aryl germane starting material and traces of the product were detected.

Intermolecular competition investigation with $ArSiMe_3$

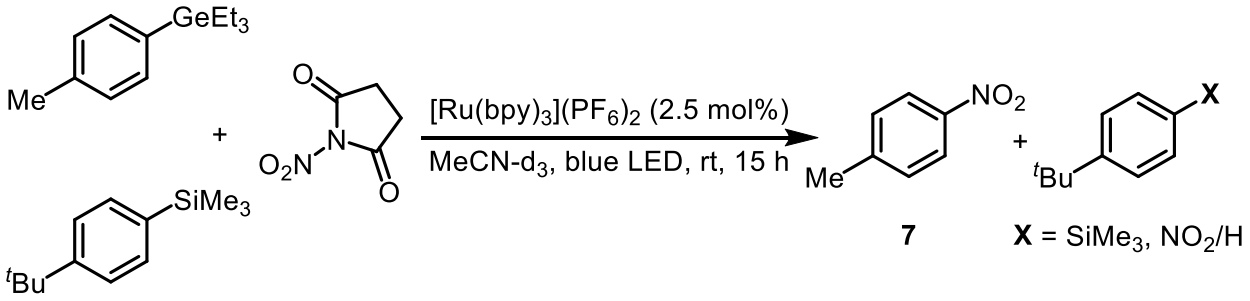

In an argon-filled glovebox, triethyl(*p*-tolyl)germane (12.6 mg, 0.05 mmol, 1.0 equiv.), (4-(*tert*-butyl)phenyl)trimethylsilane (10.6 mg, 0.05 mmol, 1.0 equiv.), *N*-nitrosuccinimide (9.4 mg, 0.065 mmol, 1.3 equiv.), $NaBF_4$ (8.2 mg, 0.075 mmol, 1.5 equiv.) and $[Ru(bpy)_3](PF_6)_2$ (1.1 mg, 1.25 μmol, 2.5 mol%) were subsequently placed into a vial equipped with a stirring bar. The obtained mixture was dissolved in anhydrous CD_3CN (0.2 ml, 0.25 M) and after that the vial was sealed with a cap, taken out from the glovebox, placed into blue LED reactor[1] and stirred at room temperature under blue light irradiation for 15 h. CH_2Br_2 (9.1 mg, 0.05 mmol, 1.0 equiv.) was added as internal standard and the obtained mixture was analyzed by ^1H NMR. The results are presented in **Table S3**.

Table S3. Intermolecular competition between aryl germane and aryl silane

Yield (7), %[a]	Recovery ($ArSiMe_3$), %[a]	Nitration/desilylation of $ArSiMe_3$, %[a]
81	78	13

[a]Yields are determined from quantitative ^1H NMR by using CH_2Br_2 as internal standard.

DFT Analysis of Aryl Germane Nitration Mechanism and Selectivity Towards $SiMe_3$ and Bpin

DFT calculations were carried out in Gaussian 16 (A.03) program package.[226] Geometry optimizations and frequency analyses were calculated with B3LYP-D3BJ/6-31++G(d,p) (LANL2DZ for Ru) including solvation through the CPCM implicit solvation model (solvent = MeCN). Frequencies were used to determine the nature of the stationary points as minima (no imaginary frequency) or transition states (one imaginary frequency). Electronic energies were calculated with different functionals (M06-2X, PBE0-D3BJ, MN15L, ωB97XD) and def2-TZVP basis set including solvation using CPCM (MeCN). Additionally, single point energies were also computed (based on the B3LYP-D3BJ optimized structures) using DLPNOCCSD(T) as implemented in ORCA 5.0.0.[ii][232] Energies are calculated at the sum of the high-basis set electronic energies plus the thermochemistry corrections at standard conditions (298.15 K and 1 atm). All energies were corrected to 1 M standard state (addition of 1.89 kcal/mol to every species).

Method comparison

Table S4. Gibbs free energies (in kcal/mol, relative to Ph-LG + $NO_2^{\bullet}$) at *method*/def2-TZVP//B3LYP-D3BJ/6-31++G(d,p) (LANL2DZ for Ru) level of theory.

	M06-2X	*PBE0-D3BJ*	*MN15L*	*wB97XD*	*DLPNO-CCSD(T)*
$TS1_{Ge}$	**23.6**	**22.3**	**22.1**	**25.6**	**26.8**
I_{Ge}	15.7	15.2	15.3	19.6	20.6
$TS2_{Ge}$	18	19.1	19	24.3	30.4
$PhNO_2 + Me_3Ge^{\bullet} + [Ru]^{3+}$	11	14.6	11.7	18.9	20.3
$PhNO_2 + Me_3Ge^{+} + [Ru]^{2+}$	-30	-25.5	-29.4	-22.7	-7.0
$TS1_{Si}$	**24.4**	23.1	23.1	26.4	27.3
I_{Si}	18.1	17.5	18.1	21.4	21.4
$TS2_{Si}$	**24.4**	**24.1**	**25.1**	**29.9**	**34.4**
$PhNO_2 + Me_3Si^{\bullet} + [Ru]^{3+}$	21.8	23.7	22.6	27.6	27.9
$PhNO_2 + Me_3Si^{+} + [Ru]^{2+}$	-21.1	-17.3	-20.5	-14.8	-2.3
$\Delta\Delta G^{\ddagger}_{Si}$	**0.8**	**1.8**	**3.0**	**4.3**	**7.6**
$TS1_B$	**27.2**	**26.1**	**27.9**	**28.6**	**28.7**
$\Delta\Delta G^{\ddagger}_{B}$	**3.6**	**3.8**	**5.8**	**3.0**	**1.8**

[ii]The calculations in ORCA were done by Dr. Theresa Sperger.

XYZ coordinates and energies for Figure 9

Ar-GeMe$_3$

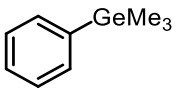

C	1.46791800	1.20898600	-0.00534100
C	2.86697600	1.20649100	0.00097200
C	3.56392300	-0.00569800	0.00545700
C	2.85239000	-1.21039700	0.00099100
C	1.45452500	-1.19542300	-0.00619200
C	0.73349100	0.01136800	-0.00960700
H	0.94603000	2.16261900	-0.01123500
H	3.40984200	2.14776800	0.00298900
H	4.65026500	-0.01228000	0.01039600
H	3.38416400	-2.15798300	0.00300000
H	0.92147300	-2.14387300	-0.01029100
Ge	-1.22997500	0.00408900	-0.00097200
C	-1.88541700	1.82583500	-0.33969300
H	-2.97938800	1.82914900	-0.32103200
H	-1.52497200	2.51953500	0.42563100
H	-1.55131500	2.18000800	-1.31926100
C	-1.85899500	-0.62492500	1.75596300
H	-2.95222400	-0.67213300	1.76976600
H	-1.46243500	-1.62299100	1.96579700
H	-1.52637300	0.05728200	2.54385000
C	-1.86157000	-1.22304600	-1.40372300
H	-2.95435200	-1.27891500	-1.38794600
H	-1.54119900	-0.86986000	-2.38820700
H	-1.45975000	-2.22833200	-1.24533000

Zero-point correction = 0.200325 (Hartree/Particle)
Thermal correction to Energy = 0.213263
Thermal correction to Enthalpy = 0.214208
Thermal correction to Gibbs Free Energy = 0.159778
Sum of electronic and zero-point Energies = -2426.036489
Sum of electronic and thermal Energies = -2426.023550
Sum of electronic and thermal Enthalpies = -2426.022606
Sum of electronic and thermal Free Energies = -2426.077035
E(M06-2X) = -2428.384937
E(PBE0-D3BJ) = -2427.871763
E(MN15L) = -2428.235947
E(wB97XD) = -2428.498603
E(DLPNO-CCSD(T)) = -2426.334412

Ar-SiMe$_3$

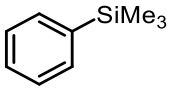

C	1.16272100	1.21684100	0.00000000
C	2.56228700	1.20570900	0.00001900
C	3.25206300	-0.01006700	0.00000400
C	2.53495000	-1.21179100	-0.00002000
C	1.13750200	-1.19032700	-0.00004200
C	0.41948200	0.02219800	-0.00003700
H	0.64790200	2.17382500	0.00000600
H	3.11165200	2.14314100	0.00004300
H	4.33821200	-0.02243300	0.00002300
H	3.06370100	-2.16097000	-0.00002400
H	0.60107900	-2.13685600	-0.00005600
Si	-1.47195400	0.00822500	0.00000900
C	-2.12034600	1.77872300	-0.00063500
H	-3.21638800	1.77542700	-0.00068200
H	-1.78693900	2.32922100	0.88621000
H	-1.78684600	2.32856800	-0.88785300
C	-2.07254000	-0.90370500	1.54091100
H	-3.16737200	-0.95726700	1.55884900
H	-1.68422900	-1.92821200	1.56727700
H	-1.74140400	-0.39352800	2.45245200
C	-2.07259500	-0.90478200	-1.54023100
H	-3.16742700	-0.95820400	-1.55822200
H	-1.74131300	-0.39530200	-2.45211600
H	-1.68442300	-1.92935900	-1.56585300

Zero-point correction = 0.201446 (Hartree/Particle)
Thermal correction to Energy = 0.213724
Thermal correction to Enthalpy = 0.214668
Thermal correction to Gibbs Free Energy = 0.162877
Sum of electronic and zero-point Energies = -640.799800
Sum of electronic and thermal Energies = -640.787523
Sum of electronic and thermal Enthalpies = -640.786579
Sum of electronic and thermal Free Energies = -640.838369
E(M06-2X) = -640.875529
E(PBE0-D3BJ) = -640.529350
E(MN15L) = -640.673648
E(wB97XD) = -640.947402
E(DLPNO-CCSD(T)) = -639.7942747

Ar-Bpin

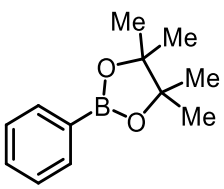

C	2.40127000	-1.19784200	-0.15514800
C	3.79810700	-1.20140200	-0.15664900
C	4.49845500	0.00001600	-0.00016000
C	3.79811500	1.20141600	0.15652500
C	2.40127900	1.19782000	0.15535400
C	1.67811900	-0.00002200	0.00018800
H	1.86156800	-2.13307600	-0.27484800
H	4.34021600	-2.13474400	-0.27800500
H	5.58466400	0.00003900	-0.00030600
H	4.34024100	2.13476200	0.27777200
H	1.86160700	2.13304700	0.27525000
B	0.12469800	-0.00002500	0.00033200
O	-0.63353900	-1.12337800	-0.22939600
O	-0.63356700	1.12335200	0.22981400
C	-2.02395700	-0.78236500	0.07932200
C	-2.02392700	0.78237600	-0.07931000
C	-2.93581500	1.52438300	0.88917900
H	-2.86375300	2.60092200	0.70942500
H	-3.97722200	1.22354300	0.73826600
H	-2.66329300	1.33026700	1.92799200
C	-2.27950700	1.24574800	-1.51613700
H	-3.31909100	1.07370000	-1.80816700
H	-2.07610500	2.31804800	-1.58378100
H	-1.62751400	0.72725000	-2.22479100
C	-2.27996300	-1.24594700	1.51599100
H	-3.31969100	-1.07411900	1.80762400
H	-2.07640300	-2.31821800	1.58362400
H	-1.62833300	-0.72740300	2.22496100
C	-2.93555200	-1.52416500	-0.88959900
H	-2.86312700	-2.60080200	-0.71060100
H	-3.97705500	-1.22377200	-0.73848300
H	-2.66308400	-1.32919700	-1.92827900

Zero-point correction = 0.272331 (Hartree/Particle)
Thermal correction to Energy = 0.286676
Thermal correction to Enthalpy = 0.287620
Thermal correction to Gibbs Free Energy = 0.231501
Sum of electronic and zero-point Energies = -642.771983
Sum of electronic and thermal Energies = -642.757638
Sum of electronic and thermal Enthalpies = -642.756694
Sum of electronic and thermal Free Energies = -642.812813
E(M06-2X) = -642.911277
E(PBE0-D3BJ) = -642.446966
E(MN15L) = -642.601649
E(wB97XD) = -642.977662
E(DLPNO-CCSD(T)) = -641.7840933

NO$_2$ radical

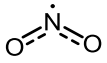

N	0.00000000	0.00000000	0.32688000
O	0.00000000	1.10551500	-0.14301000
O	0.00000000	-1.10551500	-0.14301000

Zero-point correction = 0.008725 (Hartree/Particle)
Thermal correction to Energy = 0.011662
Thermal correction to Enthalpy = 0.012606
Thermal correction to Gibbs Free Energy = -0.014656
Sum of electronic and zero-point Energies = -205.075010
Sum of electronic and thermal Energies = -205.072072
Sum of electronic and thermal Enthalpies = -205.071128
Sum of electronic and thermal Free Energies = -205.098390
E(M06-2X) = -205.077333
E(PBE0-D3BJ) = -204.954498
E(MN15L) = -204.983184
E(wB97XD) = -205.096242
E(DLPNO-CCSD(T)) = -204.8062098

TS1$_{Ge}$

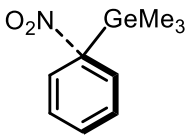

C	3.31300100	-0.94202200	0.01910100
C	2.65689800	-0.69127200	-1.20349500
C	1.36983600	-0.19185600	-1.22146000
C	0.65759700	0.09078300	0.00772600
C	1.35773000	-0.19675100	1.24325300
C	2.64556300	-0.69538800	1.23602600
H	4.32752500	-1.32655500	0.02309700
H	3.16510500	-0.90144200	-2.13993000
H	0.87518900	-0.00354800	-2.16856700
H	0.85445400	-0.00736000	2.18532400
H	3.14543700	-0.90643100	2.17671000
Ge	-1.28536200	-0.49283900	-0.00943900
C	-1.18635900	-2.44182000	-0.20249300
H	-2.19525200	-2.86438700	-0.19707800
H	-0.69575400	-2.70254900	-1.14392600
H	-0.61670200	-2.87028000	0.62653100
C	-2.17517400	0.34366100	-1.54361000
H	-3.18996200	-0.05768500	-1.62099800
H	-2.23231500	1.42714500	-1.41545300
H	-1.64101300	0.12289900	-2.47129100
C	-2.11127400	0.02297000	1.69130600
H	-3.16290900	-0.27839900	1.67512800
H	-1.61749700	-0.47796900	2.52794000
H	-2.05259600	1.10396600	1.83628600
N	0.38812400	1.95351100	0.01213800
O	0.37037500	2.52105700	-1.07133300
O	0.16513700	2.48507300	1.09198000

Zero-point correction = 0.209714 (Hartree/Particle)
Thermal correction to Energy = 0.225898
Thermal correction to Enthalpy = 0.226842
Thermal correction to Gibbs Free Energy = 0.164428
Sum of electronic and zero-point Energies = -2631.095411
Sum of electronic and thermal Energies = -2631.079227
Sum of electronic and thermal Enthalpies = -2631.078283
Sum of electronic and thermal Free Energies = -2631.140696
E(M06-2X) = -2633.440952
E(PBE0-D3BJ) = -2632.807054
E(MN15L) = -2633.200181
E(wB97XD) = -2633.570343
E(DLPNO-CCSD(T)) = -2631.114164

TS1$_{Si}$

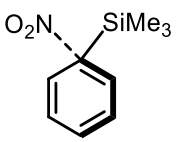

C	3.14273000	-0.71578700	-0.03004300
C	2.44980100	-0.53486800	-1.24494100
C	1.11997500	-0.16820400	-1.24981100
C	0.38758800	0.04900800	-0.00934900
C	1.13861600	-0.16627900	1.21948100
C	2.46719900	-0.53486400	1.19509900
H	4.19040900	-0.99741500	-0.03746000
H	2.96625400	-0.69280200	-2.18708200
H	0.59992800	-0.02922000	-2.19121400
H	0.63234000	-0.03315300	2.16959700
H	2.99695300	-0.69563000	2.12935700
Si	-1.40448200	-0.71422200	0.01619500
C	-1.13399300	-2.55907000	0.26301100
H	-2.09486100	-3.08595200	0.25088600
H	-0.50765000	-2.97308000	-0.53428300
H	-0.64535800	-2.76029300	1.22201800
C	-2.25239200	-0.36740800	-1.62469700
H	-3.27077500	-0.77182300	-1.59466000
H	-2.31664200	0.70581100	-1.82685700
H	-1.72756400	-0.84526800	-2.45822400
C	-2.36685900	0.02594900	1.45204600
H	-3.33828800	-0.47604000	1.52820600
H	-1.84496900	-0.11028600	2.40475100
H	-2.54957600	1.09576200	1.31166200
N	-0.02751200	1.86344700	-0.01172000
O	-0.32611300	2.36726200	-1.08638900
O	-0.04274400	2.43942800	1.06686800

Zero-point correction = 0.211010 (Hartree/Particle)
Thermal correction to Energy = 0.226486
Thermal correction to Enthalpy = 0.227431
Thermal correction to Gibbs Free Energy = 0.167468
Sum of electronic and zero-point Energies = -845.856186
Sum of electronic and thermal Energies = -845.840710
Sum of electronic and thermal Enthalpies = -845.839766
Sum of electronic and thermal Free Energies = -845.899728
E(M06-2X) = -845.930181
E(PBE0-D3BJ) = -845.463263
E(MN15L) = -845.636217
E(wB97XD) = -846.017776
E(DLPNO-CCSD(T)) = -844.5732364

TS1$_{B}$

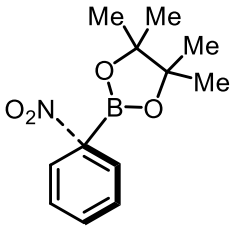

C	2.06725400	-0.35243800	1.28726200
C	3.24210500	-1.06219400	1.31143100
C	3.83912100	-1.52231200	0.11422600
C	3.20670100	-1.27558400	-1.12645100
C	2.04007600	-0.55402900	-1.19519500
C	1.41294900	0.01197000	0.01153100
H	1.59734800	-0.02171400	2.20710800
H	3.70693400	-1.29520400	2.26472500
H	4.76729200	-2.08230300	0.14966200
H	3.64441800	-1.67399000	-2.03690800
H	1.55253800	-0.37823600	-2.14813900
B	-0.17630000	-0.07660500	0.01431500
O	-0.89855100	-0.52627000	1.07805900
O	-0.91979400	0.26032200	-1.07800900
C	-2.31398400	-0.26588900	0.76530900
C	-2.29673400	-0.18281400	-0.80672200
C	-3.25865300	0.83407500	-1.40436000
H	-3.16502400	0.82977300	-2.49393000
H	-4.29074800	0.57353800	-1.15069600
H	-3.05373400	1.84359500	-1.04438100
C	-2.45372800	-1.54168700	-1.49116800
H	-3.47347100	-1.92060200	-1.38296600
H	-2.24042200	-1.42743900	-2.55736400
H	-1.76056300	-2.28054500	-1.07934600
C	-2.66543900	1.06078500	1.44105900
H	-3.72053800	1.30720400	1.29571000
H	-2.47757000	0.97171800	2.51447200
H	-2.05568100	1.88102500	1.05306800
C	-3.15153900	-1.40028900	1.33811000
H	-3.08841300	-1.38634000	2.42978500
H	-4.20162500	-1.27486300	1.05688300
H	-2.80856200	-2.37426200	0.98517600
N	1.62282900	1.73109200	-0.07287500
O	0.90203800	2.39310000	0.66773600
O	2.48890100	2.18240500	-0.80460000

Zero-point correction = 0.281697 (Hartree/Particle)
Thermal correction to Energy = 0.299245
Thermal correction to Enthalpy = 0.300189
Thermal correction to Gibbs Free Energy = 0.235258
Sum of electronic and zero-point Energies = -847.821033
Sum of electronic and thermal Energies = -847.803485
Sum of electronic and thermal Enthalpies = -847.802541
Sum of electronic and thermal Free Energies = -847.867472
E(M06-2X) = -847.960648
E(PBE0-D3BJ) = -847.375325
E(MN15L) = -847.555787
E(wB97XD) = -848.043707

E(DLPNO-CCSD(T)) = -846.5600464

I_{Ge}

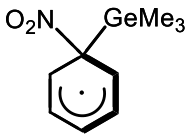

C	3.10156300	-0.60938900	0.00031100
C	2.49850700	-0.22930100	-1.22088100
C	1.31194700	0.46499200	-1.25083200
C	0.58630400	0.73016900	0.00006500
C	1.31186300	0.46530600	1.25109000
C	2.49853000	-0.22874600	1.22141500
H	4.03914000	-1.15379600	0.00042300
H	2.98924900	-0.47174600	-2.15878400
H	0.86074000	0.77788100	-2.18301600
H	0.86064100	0.77864500	2.18310600
H	2.98939600	-0.47063200	2.15939900
Ge	-0.98350500	-0.76627500	-0.00005200
C	-0.02976600	-2.46843200	-0.01267100
H	-0.77671700	-3.26787700	0.00644100
H	0.57359500	-2.56365900	-0.91694300
H	0.61092400	-2.55639200	0.86633500
C	-2.01194100	-0.44635900	-1.63137300
H	-2.86749600	-1.12870400	-1.62759400
H	-2.37407200	0.58303500	-1.66511100
H	-1.39998500	-0.64612000	-2.51356100
C	-1.99704700	-0.46145000	1.64343500
H	-2.86085000	-1.13324600	1.63455400
H	-1.38136900	-0.68286400	2.51783200
H	-2.34636900	0.57158600	1.69631200
N	-0.23024500	1.95647700	-0.00000800
O	-0.58918800	2.43153100	-1.09528700
O	-0.59240000	2.42954500	1.09516000

Zero-point correction = 0.211495 (Hartree/Particle)
Thermal correction to Energy = 0.227572
Thermal correction to Enthalpy = 0.228517
Thermal correction to Gibbs Free Energy = 0.166987
Sum of electronic and zero-point Energies = -2631.104451
Sum of electronic and thermal Energies = -2631.088374
Sum of electronic and thermal Enthalpies = -2631.087429
Sum of electronic and thermal Free Energies = -2631.148959
E(M06-2X) = -2633.456099
E(PBE0-D3BJ) = -2632.820812
E(MN15L) = -2633.213608
E(wB97XD) = -2633.582411
E(DLPNO-CCSD(T)) = -2631.12661

I_{Si}

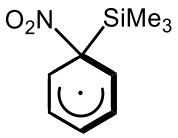

C	-3.02439700	0.25945200	0.00047300
C	-2.35776400	0.00191300	-1.22145800
C	-1.06062200	-0.44525200	-1.25333700
C	-0.27492500	-0.56144400	0.00010000
C	-1.06021100	-0.44501200	1.25377500
C	-2.35736600	0.00212800	1.22224000
H	-4.05033400	0.60981400	0.00060900
H	-2.88807200	0.14149800	-2.15895800
H	-0.56174400	-0.66010800	-2.18919700
H	-0.56102700	-0.65973100	2.18950200
H	-2.88737800	0.14185400	2.15988700
C	-0.09854100	2.54764500	-0.00176400
H	0.54379700	3.43585900	-0.00022400
H	-0.73315900	2.58550000	-0.89119900
H	-0.73651100	2.58487800	0.88530000
C	2.03574500	0.90953100	-1.55606300
H	2.74413600	1.74619000	-1.56621500
H	2.60773100	-0.02204100	-1.59446200
H	1.41967400	0.97638600	-2.45773800
C	2.03417900	0.91145300	1.55671300
H	2.74340100	1.74741700	1.56596200
H	1.41731900	0.98059800	2.45767600
H	2.60517300	-0.02063200	1.59735400
Si	0.99412700	1.02641300	-0.00026400
N	0.65406800	-1.74418700	0.00007800
O	1.05205000	-2.17649100	1.09041600
O	1.05096800	-2.17731300	-1.09032000

Zero-point correction = 0.212735 (Hartree/Particle)
Thermal correction to Energy = 0.228131
Thermal correction to Enthalpy = 0.229075
Thermal correction to Gibbs Free Energy = 0.169559
Sum of electronic and zero-point Energies = -845.861814
Sum of electronic and thermal Energies = -845.846418
Sum of electronic and thermal Enthalpies = -845.845474
Sum of electronic and thermal Free Energies = -845.904990
E(M06-2X) = -845.942342
E(PBE0-D3BJ) = -845.474260
E(MN15L) = -845.64633
E(wB97XD) = -846.027822
E(DLPNO-CCSD(T)) = -844.5847223

$TS2_{Ge}$ (approximate geometry from scan)

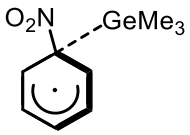

C	-3.05191300	-0.61515800	-0.00027000
C	-2.47430600	-0.20546200	1.21703400
C	-1.33665600	0.58089600	1.24180900
C	-0.69326800	0.93193100	-0.00041200
C	-1.33576000	0.57928100	-1.24265800
C	-2.47334600	-0.20719900	-1.21766900
H	-3.94583100	-1.22909200	-0.00018800
H	-2.93420300	-0.49597600	2.15658000
H	-0.89872300	0.92414000	2.16931900
H	-0.89718100	0.92137700	-2.17029000
H	-2.93248400	-0.49905100	-2.15716800
Ge	1.00168400	-0.86307800	0.00039700
C	-0.08145300	-2.47512900	-0.00337600
H	0.62161900	-3.31558000	0.00520500
H	-0.70982900	-2.52392000	0.88618800
H	-0.69532000	-2.52955100	-0.90267300
C	1.93549600	-0.46547300	1.65931600
H	2.91034900	-0.96186100	1.61608000
H	2.07711900	0.61301200	1.75719000
H	1.36717600	-0.84518900	2.51010700
C	1.94218000	-0.46247300	-1.65396400
H	2.91160500	-0.96959900	-1.61244000
H	1.37167900	-0.83020300	-2.50853900
H	2.09523600	0.61506400	-1.74405200
N	0.27514600	1.98109400	-0.00068300
O	0.69315000	2.43226900	1.11211300
O	0.69347800	2.43147700	-1.11362800

Zero-point correction = 0.210985 (Hartree/Particle)
Thermal correction to Energy = 0.226663
Thermal correction to Enthalpy = 0.227607
Thermal correction to Gibbs Free Energy = 0.166636
Sum of electronic and zero-point Energies = -2631.101852
Sum of electronic and thermal Energies = -2631.086174
Sum of electronic and thermal Enthalpies = -2631.085230
Sum of electronic and thermal Free Energies = -2631.146201
E(M06-2X) = -2633.45208
E(PBE0-D3BJ) = -2632.814336
E(MN15L) = -2633.207294
E(wB97XD) = -2633.5746
E(DLPNO-CCSD(T)) = -2631.110743

$TS2_{Si}$ (approximate geometry from scan)

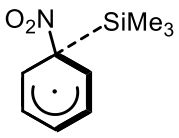

C	-2.98648600	0.15200000	-0.00008600
C	-2.33425000	-0.12595000	-1.21842600
C	-1.05507300	-0.64740600	-1.24442500
C	-0.33958200	-0.83573000	-0.00003700
C	-1.05527300	-0.64784800	1.24428900
C	-2.33444600	-0.12639300	1.21825900
H	-3.99206600	0.55787200	-0.00008900
H	-2.84870700	0.05386000	-2.15749800
H	-0.55549800	-0.88956100	-2.17274600
H	-0.55586000	-0.89032900	2.17261200
H	-2.84906400	0.05309000	2.15730600
C	-0.36498000	2.52782700	0.00010400
H	0.15303200	3.49568100	0.00051800
H	-0.99404400	2.47597800	-0.89099800
H	-0.99442000	2.47544000	0.89091200
C	1.91549400	1.04750300	-1.58031000
H	2.69649300	1.81798600	-1.58184300
H	2.39245000	0.06637400	-1.65599000
H	1.27469800	1.19948100	-2.45292500
C	1.91513900	1.04733900	1.58067200
H	2.69563900	1.81831800	1.58293700
H	1.27390700	1.19844900	2.45312300
H	2.39267500	0.06647300	1.65606800
Si	0.94455100	1.20682300	0.00007300
N	0.80791900	-1.69794800	-0.00009900
O	1.30427100	-2.05363300	1.10853700
O	1.30427300	-2.05349700	-1.10878300

Zero-point correction = 0.211713 (Hartree/Particle)
Thermal correction to Energy = 0.226938
Thermal correction to Enthalpy = 0.227882
Thermal correction to Gibbs Free Energy = 0.168066
Sum of electronic and zero-point Energies = -845.854901
Sum of electronic and thermal Energies = -845.839676
Sum of electronic and thermal Enthalpies = -845.838732
Sum of electronic and thermal Free Energies = -845.898548
E(M06-2X) = -845.930789
E(PBE0-D3BJ) = -845.462267
E(MN15L) = -845.633633
E(wB97XD) = -846.012902
E(DLPNO-CCSD(T)) = -844.5625238

$PhNO_2$

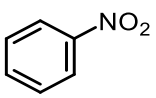

C	-0.42794500	1.22412300	-0.00005500
C	-1.82172100	1.21461300	0.00005200
C	-2.51716900	0.00000100	0.00009200
C	-1.82172000	-1.21461300	0.00002100
C	-0.42794600	-1.22412400	-0.00008400
C	0.24461300	0.00000000	-0.00011700
H	0.13070300	2.15101700	-0.00008800
H	-2.36346400	2.15424600	0.00010500
H	-3.60237100	0.00000000	0.00017800
H	-2.36346600	-2.15424500	0.00004800
H	0.13070400	-2.15101700	-0.00014100
N	1.70880200	0.00000000	-0.00024000
O	2.29610000	1.08720600	0.00011600
O	2.29610100	-1.08720600	0.00015000

Zero-point correction = 0.102947 (Hartree/Particle)
Thermal correction to Energy = 0.109796
Thermal correction to Enthalpy = 0.110740
Thermal correction to Gibbs Free Energy = 0.070870
Sum of electronic and zero-point Energies = -436.700188
Sum of electronic and thermal Energies = -436.693340
Sum of electronic and thermal Enthalpies = -436.692396
Sum of electronic and thermal Free Energies = -436.732265
E(M06-2X) = -436.746121
E(PBE0-D3BJ) = -436.448977
E(MN15L) = -436.551745
E(wB97XD) = -436.775571
E(DLPNO-CCSD(T)) = -436.0365462

$Me_3Ge^{\cdot}$

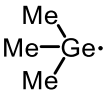

Ge	-0.00000600	-0.00001200	0.32705300
C	1.22994500	-1.40267700	-0.34181000
H	1.21397500	-1.38439500	-1.43867700
H	2.25125600	-1.21613900	0.00046300
H	0.91153300	-2.39085100	0.00043500
C	0.59986900	1.76644600	-0.34178400
H	0.59218400	1.74341100	-1.43864200
H	-0.07231600	2.55774400	0.00031200
H	1.61483600	1.98476600	0.00055700
C	-1.82979500	-0.36374000	-0.34180400
H	-1.80633400	-0.35775900	-1.43867000
H	-2.17844700	-1.34201400	-0.00057500
H	-2.52658900	0.40545000	0.00148500

Zero-point correction = 0.108243 (Hartree/Particle)
Thermal correction to Energy = 0.116181
Thermal correction to Enthalpy = 0.117125
Thermal correction to Gibbs Free Energy = 0.075487
Sum of electronic and zero-point Energies = -2194.385812
Sum of electronic and thermal Energies = -2194.377875
Sum of electronic and thermal Enthalpies = -2194.376930
Sum of electronic and thermal Free Energies = -2194.418569
E(M06-2X) = -2196.699876
E(PBE0-D3BJ) = -2196.355194
E(MN15L) = -2196.649916
E(wB97XD) = -2196.790378
E(DLPNO-CCSD(T)) = -2195.073002

$Me_3Si^{\cdot}$

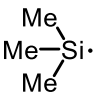

Si	0.00000800	-0.00022400	0.42977700
C	1.56336400	-0.88488600	-0.17808700
H	1.58059400	-0.89371600	-1.27721700
H	2.46930700	-0.37802400	0.17047900
H	1.59525100	-1.92287400	0.16929500
C	-0.01507200	1.79606600	-0.17798500
H	-0.01565800	1.81551100	-1.27709300
H	-0.90684500	2.32763000	0.17034500
H	0.86805100	2.34229600	0.16967800
C	-1.54830400	-0.91097400	-0.17808100
H	-1.56546300	-0.91992700	-1.27721200
H	-1.56259700	-1.94941300	0.16912500
H	-2.46267300	-0.41958300	0.17064200

Zero-point correction = 0.109192 (Hartree/Particle)
Thermal correction to Energy = 0.116648
Thermal correction to Enthalpy = 0.117593
Thermal correction to Gibbs Free Energy = 0.078098
Sum of electronic and zero-point Energies = -409.137087
Sum of electronic and thermal Energies = -409.129631
Sum of electronic and thermal Enthalpies = -409.128687
Sum of electronic and thermal Free Energies = -409.168181
E(M06-2X) = -409.172756
E(PBE0-D3BJ) = -408.997884
E(MN15L) = -409.069796
E(wB97XD) = -409.224904
E(DLPNO-CCSD(T)) = -408.5201471

Me_3Ge^{+}

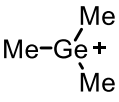

Ge	-0.00030200	-0.00027300	-0.00045000
C	-1.90751700	-0.26938000	0.00036800
H	-2.16969600	-0.85336200	0.88862800
H	-2.43509800	0.68402000	-0.00186200
H	-2.17080300	-0.85888500	-0.88377900
C	0.72044700	1.78591600	0.00090200
H	0.32510000	2.31561900	0.87340500
H	1.80962900	1.76666700	0.02280300
H	0.36295400	2.29826500	-0.89838100

C	1.18799500	-1.51575700	-0.00029300
H	1.79918000	-1.46771300	0.90724400
H	0.62808600	-2.44978000	-0.03508000
H	1.85476700	-1.43076900	-0.86444700

Zero-point correction = 0.109222 (Hartree/Particle)
Thermal correction to Energy = 0.117325
Thermal correction to Enthalpy = 0.118269
Thermal correction to Gibbs Free Energy = 0.075561
Sum of electronic and zero-point Energies = -2194.236138
Sum of electronic and thermal Energies = -2194.228036
Sum of electronic and thermal Enthalpies = -2194.227091
Sum of electronic and thermal Free Energies = -2194.269799
E(M06-2X) = -2196.551656
E(PBE0-D3BJ) = -2196.208444
E(MN15L) = -2196.503422
E(wB97XD) = -2196.647333
E(DLPNO-CCSD(T)) = -2194.926948

Me_3Si^+

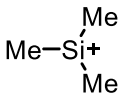

Si	0.00011100	-0.00104200	0.00278300
C	-0.37027400	1.80013300	-0.00164400
H	0.13214500	2.26887900	-0.85704600
H	-1.44249900	2.00040800	-0.04835500
H	0.05081500	2.25400300	0.90440900
C	-1.37546800	-1.21996000	-0.00131600
H	-2.01383300	-1.03774900	-0.87484600
H	-1.01315500	-2.24916100	-0.01627500
H	-1.99773500	-1.05967500	0.88814000
C	1.74549000	-0.57924100	0.00046500
H	1.92789400	-1.14773900	-0.92096000
H	2.45288700	0.24994900	0.06332900
H	1.90343300	-1.26991000	0.83760500

Zero-point correction = 0.109547 (Hartree/Particle)
Thermal correction to Energy = 0.117365
Thermal correction to Enthalpy = 0.118309
Thermal correction to Gibbs Free Energy = 0.077074
Sum of electronic and zero-point Energies = -408.989343
Sum of electronic and thermal Energies = -408.981525
Sum of electronic and thermal Enthalpies = -408.980581
Sum of electronic and thermal Free Energies = -409.021816
E(M06-2X) = -409.026519
E(PBE0-D3BJ) = -408.851458
E(MN15L) = -408.925235
E(wB97XD) = -409.081967
E(DLPNO-CCSD(T)) = -408.3777084

$[Ru(bpy)_3]^{2+}$

N	1.31507600	1.23213300	1.05162400
N	0.41184400	-1.75619400	1.05013800
N	-1.72613400	0.52144800	1.05206000
C	2.04882600	0.84998800	2.11258300
H	1.91533200	-0.17259200	2.44131300
C	2.92696300	1.71223400	2.75937800
H	3.49596100	1.35841300	3.61095000
C	3.05221700	3.01986900	2.28872100
H	3.72788300	3.71978300	2.76754000
C	2.29530000	3.41834100	1.18987500
H	2.38162800	4.42811000	0.81025700
C	1.42899300	2.50566000	0.58223200
C	0.58190300	2.82581400	-0.58098900
C	-0.98001800	1.99551300	-2.11008700
H	-1.55691600	1.14088400	-2.43928600
C	-1.06973700	3.22392600	-2.75507100
C	-0.29855800	4.28718000	-2.28414000
H	-0.34366900	5.25978100	-2.76132500
C	0.53423200	4.08417700	-1.18669600
H	1.13681100	4.89854600	-0.80614600
C	-0.28400200	-2.20225900	2.11169400
H	-1.10382200	-1.57714500	2.44118300
C	0.02665600	-3.39334900	2.75805700
H	-0.56299100	-3.71044200	3.61005100
C	1.09785900	-4.15317500	2.28658600
H	1.36874500	-5.08766300	2.76518800
C	1.81947800	-3.69514700	1.18722600
H	2.65198600	-4.27272100	0.80712800
C	1.45896700	-2.48942000	0.57984500
C	2.15732400	-1.91482400	-0.58424900
C	3.27059500	-2.50121500	-1.19195200
H	3.67616400	-3.43007200	-0.81258500
C	3.85985300	-1.88069700	-2.29053500
H	4.72446400	-2.32678800	-2.76923800
C	3.32175100	-0.68227800	-2.76101400
C	2.21306600	-0.14760000	-2.11440600
H	1.75865000	0.77837300	-2.44289500
C	-1.76294000	1.34752400	2.11336800
H	-0.81101900	1.74489300	2.44129700
C	-2.94889700	1.67459900	2.76112600
H	-2.92743900	2.34413700	3.61283100
C	-4.14326200	1.12678700	2.29151600
H	-5.08734600	1.35957200	2.77133500
C	-4.10900000	0.27260100	1.19229500
H	-5.02590900	-0.15979200	0.81358000
C	-2.88548600	-0.01806000	0.58306900
C	-2.73900000	-0.90964300	-0.58167200
C	-1.23932200	-1.84282200	-2.11359800
H	-0.21077900	-1.91346300	-2.44328500
C	-2.25817700	-2.53401800	-2.75953100
C	-3.56454000	-2.39903000	-2.28803900
H	-4.38442900	-2.92321800	-2.76628000
C	-3.80499300	-1.57872000	-1.18878100
H	-4.81167500	-1.46392300	-0.80861700
H	-2.02395500	-3.16152900	-3.61129800
H	3.74733500	-0.16438900	-3.61236200
H	-1.73189600	3.33567000	-3.60548300
Ru	-0.00058000	-0.00024500	-0.00080000
N	-1.46834400	-1.04836800	-1.05218800
N	1.64062000	-0.74522300	-1.05361100
N	-0.17504900	1.79543300	-1.05081200

Zero-point correction = 0.485283 (Hartree/Particle)
Thermal correction to Energy = 0.513939
Thermal correction to Enthalpy = 0.514884
Thermal correction to Gibbs Free Energy = 0.425532
Sum of electronic and zero-point Energies = -1579.678821
Sum of electronic and thermal Energies = -1579.650164
Sum of electronic and thermal Enthalpies = -1579.649220
Sum of electronic and thermal Free Energies = -1579.738572
E(M06-2X) = -1580.766823
E(PBE0-D3BJ) = -1579.833142
E(MN15L) = -1579.900042
E(wB97XD) = -1581.003794
E(DLPNO-CCSD(T)) = -1577.931278

$[Ru(bpy)_3]^{3+}$

N	0.99637100	-1.53761500	1.00878200
N	-1.81678100	-0.08787700	1.03223400
N	0.86482400	1.61758800	0.99535100
C	0.47052500	-2.22867500	2.03629600
H	-0.52729800	-1.95119500	2.34922600
C	1.17724900	-3.24101800	2.67332500
H	0.72186900	-3.77089200	3.50086900
C	2.46226200	-3.54700300	2.22488800
H	3.03970400	-4.33218700	2.69941800
C	3.00205600	-2.83499200	1.15556100
H	3.99606300	-3.06441000	0.79524100
C	2.24819100	-1.82726300	0.55503200
C	2.70573700	-1.01675700	-0.58329000
C	2.13106300	0.71065300	-2.06649200
H	1.37940800	1.42457000	-2.37613800
C	3.35869100	0.61996500	-2.71095500
C	4.28327800	-0.32399000	-2.26366500
H	5.25110800	-0.41889800	-2.74273400
C	3.95435800	-1.14885500	-1.18990400
H	4.66275100	-1.88354400	-0.83111900
C	-2.13552500	0.71679100	2.06179100
H	-1.38426900	1.43143400	2.37069800
C	-3.36435100	0.62850000	2.70427800
H	-3.58250200	1.28994100	3.53369500
C	-4.28849700	-0.31638700	2.25806000
H	-5.25724000	-0.40953000	2.73563000
C	-3.95800800	-1.14431000	1.18715300
H	-4.66619700	-1.87951100	0.82902900
C	-2.70828500	-1.01436100	0.58231100
C	-2.24962100	-1.82746700	-0.55369700
C	-3.00241500	-2.83748400	-1.15173400
H	-3.99609500	-3.06721100	-0.79073500
C	-2.46195300	-3.55142600	-2.21941400
H	-3.03851300	-4.33849000	-2.69189500
C	-1.17743100	-3.24486300	-2.66887700
C	-0.47166700	-2.23039300	-2.03418500
H	0.52575700	-1.95252900	-2.34798500
C	1.76273500	1.49914800	1.98994000
H	2.02143000	0.49376300	2.29429200
C	2.32304400	2.61171200	2.60492700
H	3.03913700	2.47549600	3.40592100
C	1.94369800	3.88124300	2.16902300
H	2.36261900	4.77018800	2.62668600
C	1.01924000	4.00157300	1.13353000
H	0.71925900	4.98072900	0.78498900
C	0.48869900	2.85005000	0.55240400
C	-0.48242200	2.85136700	-0.55216500
C	-1.76157400	1.50360900	-1.98817800
H	-2.02360100	0.49880600	-2.29164500
C	-2.31860000	2.61755700	-2.60364100
C	-1.93473400	3.88614300	-2.16890600
H	-2.35092400	4.77611900	-2.62705700
C	-1.00945500	4.00422400	-1.13387600
H	-0.70617900	4.98266900	-0.78616500
H	-3.03559300	2.48312500	-3.40412900
H	-0.72165400	-3.77600100	-3.49539500
H	3.57561200	1.27883700	-3.54273400
Ru	-0.00059300	-0.00471600	0.00008800
N	-0.86270600	1.61990200	-0.99422400
N	-0.99798700	-1.53781300	-1.00792800
N	1.81394900	-0.09097300	-1.03408000

Zero-point correction = 0.486514 (Hartree/Particle)
Thermal correction to Energy = 0.515207
Thermal correction to Enthalpy = 0.516151
Thermal correction to Gibbs Free Energy = 0.426410
Sum of electronic and zero-point Energies = -1579.462390
Sum of electronic and thermal Energies = -1579.433697
Sum of electronic and thermal Enthalpies = -1579.432753
Sum of electronic and thermal Free Energies = -1579.522494
E(M06-2X) = -1580.554144
E(PBE0-D3BJ) = -1579.623276
E(MN15L) = -1579.688721
E(wB97XD) = -1580.795302
E(DLPNO-CCSD(T)) = -1577.742562

Redox potentials

Redox potentials were computed from the relative Gibbs free energy differences (at the SMD (MeCN) MN15/def2-TZVPP//SMD (MeCN) ωB97XD/6-31+G(d,p) level of theory) of the reduced and oxidized form of the compounds:[233, 234]

$$E^{\circ}_{1/2} = -\frac{\Delta G^{\circ}_{1/2}}{n_e F} - E^{\circ,SHE}_{1/2} + E^{\circ,SCE}_{1/2}$$

where n_e is the number of transferred electrons (= 1), F is Faraday's constant (23.061 kcal mol^{-1} V^{-1}), $E^{\circ,SHE}_{1/2}$ is the absolute value for the standard hydrogen electrode (SHE, 4.281 V) and $E^{\circ,SCE}_{1/2}$ is the potential of the saturated calomel electrode (SCE) relative to SHE in acetonitrile (−0.141 V). $\Delta G^{\circ}_{1/2}$ is the difference in Gibbs free energies (in kcal mol^{-1}, computed in MeCN) of the reduced form and the oxidized form.

$$E^{\circ}_{1/2} = -\frac{(G[reduced] - G[oxidized])}{23.061} - 4.281 - 0.141$$

Me$_3$Ge$^{\bullet}$

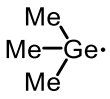

Ge	0.00018700	0.00011200	0.31548900
C	-0.72026000	-1.71063300	-0.32847600
H	-0.71846500	-1.70098000	-1.42611600
H	-0.10579800	-2.54798400	0.01484100
H	-1.74736800	-1.85735200	0.01809800
C	1.84175500	0.23173700	-0.32872800
H	1.83181300	0.23262200	-1.42634000
H	2.26088000	1.18090300	0.01771800
H	2.48165200	-0.58639300	0.01449600
C	-1.12202000	1.47856500	-0.32855000
H	-1.11555500	1.47085500	-1.42616400
H	-2.15402700	1.36455800	0.01584700
H	-0.73596900	2.44215600	0.01649400

Zero-point correction = 0.109057 (Hartree/Particle)
Thermal correction to Energy = 0.116854
Thermal correction to Enthalpy = 0.117799
Thermal correction to Gibbs Free Energy = 0.076584
Sum of electronic and zero-point Energies = -2194.336489
Sum of electronic and thermal Energies = -2194.328692
Sum of electronic and thermal Enthalpies = -2194.327748
Sum of electronic and thermal Free Energies = -2194.368962
E(MN15) = -2196.906324

Me$_3$Ge^{+}

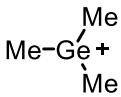

Ge	-0.00042000	-0.00023200	0.00002700
C	0.28222500	1.88874000	-0.00048100
H	0.89522100	2.14473200	-0.87137300
H	-0.66484800	2.42871300	-0.02505900
H	0.84924800	2.14895700	0.90026600
C	-1.77794400	-0.70021000	-0.00027900
H	-2.30086400	-0.31065200	-0.88072900
H	-1.77195800	-1.79083400	-0.00921100
H	-2.29236300	-0.32642900	0.89223700
C	1.49698100	-1.18772300	0.00060100
H	1.44302900	-1.80369500	-0.90409400
H	2.43750900	-0.63620900	0.03066100
H	1.41089300	-1.85201400	0.86737900

Zero-point correction = 0.109560 (Hartree/Particle)
Thermal correction to Energy = 0.117649
Thermal correction to Enthalpy = 0.118594
Thermal correction to Gibbs Free Energy = 0.075959
Sum of electronic and zero-point Energies = -2194.203400
Sum of electronic and thermal Energies = -2194.195310
Sum of electronic and thermal Enthalpies = -2194.194366
Sum of electronic and thermal Free Energies = -2194.237000
E(MN15) = -2196.768073

Suc$^{\bullet}$

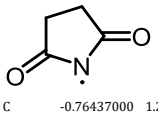

C	-0.76437000	1.23590200	0.00018100
C	0.76436700	1.23590200	-0.00018100
H	-1.19969200	1.71012400	0.88377800
H	-1.20017400	1.71049200	-0.88297400
H	1.20017100	1.71049400	0.88297300
H	1.19968700	1.71012200	-0.88377900
C	1.13201600	-0.23092400	-0.00002500
C	-1.13201400	-0.23092400	0.00002700
O	2.25371900	-0.71183200	0.00008300
O	-2.25371700	-0.71183500	-0.00008800
N	0.00000000	-1.07308900	0.00000400

Zero-point correction = 0.077652 (Hartree/Particle)
Thermal correction to Energy = 0.083783
Thermal correction to Enthalpy = 0.084727
Thermal correction to Gibbs Free Energy = 0.045296
Sum of electronic and zero-point Energies = -359.805475
Sum of electronic and thermal Energies = -359.799344
Sum of electronic and thermal Enthalpies = -359.798400
Sum of electronic and thermal Free Energies = -359.837831
E(MN15) = -359.725484

Suc^{-}

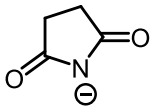

C	-0.76167400	1.22449700	0.00011000
C	0.76172900	1.22448100	-0.00008400
H	-1.20219700	1.69733300	0.88307100
H	-1.20233500	1.69739400	-0.88276400
H	1.20253400	1.69755700	0.88260900
H	1.20213900	1.69714700	-0.88321100
C	1.10951800	-0.26779900	0.00000900
C	-1.10954000	-0.26777900	-0.00000300
O	2.27693200	-0.68005000	0.00006000
O	-2.27693900	-0.68000700	-0.00001900
N	-0.00004100	-1.05562500	-0.00003100

Zero-point correction = 0.079649 (Hartree/Particle)
Thermal correction to Energy = 0.085222
Thermal correction to Enthalpy = 0.086166
Thermal correction to Gibbs Free Energy = 0.049811
Sum of electronic and zero-point Energies = -360.025983
Sum of electronic and thermal Energies = -360.020411
Sum of electronic and thermal Enthalpies = -360.019467
Sum of electronic and thermal Free Energies = -360.055822
E(MN15) = -359.946691

[Ru(bpy)$_3$]$^{2+}$

N	1.27030100	-1.28442600	1.04463200
N	-1.75349400	-0.45872800	1.04843600
N	0.48247000	1.74972300	1.03735300
C	0.91138200	-2.01968700	2.10679300
H	-0.11884700	-1.92416200	2.42979800
C	1.79979100	-2.85587700	2.76675800
H	1.46288800	-3.42975000	3.62229900
C	3.10991500	-2.93223200	2.30653300
H	3.83443600	-3.57339400	2.79722300
C	3.48476100	-2.17324300	1.20449000
H	4.50204300	-2.22117000	0.83678300
C	2.54197700	-1.35487600	0.58603900
C	2.83855300	-0.50367300	-0.58969300
C	1.97183800	1.02282500	-2.11663200
H	1.10225800	1.57890700	-2.44771500
C	3.19280000	1.14007400	-2.76458000
C	4.27022100	0.39589700	-2.29594300
H	5.24014800	0.45951800	-2.77747100
C	4.09074000	-0.43611800	-1.19738500
H	4.92004600	-1.02376100	-0.82343600
C	-2.21747000	0.22925100	2.10158400
H	-1.61942600	1.07397900	2.42377500
C	-3.39377600	-0.11171200	2.75284500
H	-3.72770100	0.47479600	3.60092900
C	-4.11718000	-1.20653700	2.29226600
H	-5.04254800	-1.50305900	2.77453900
C	-3.63963600	-1.92185300	1.20073800
H	-4.19395500	-2.77484400	0.82994200
C	-2.44937800	-1.52704800	0.59358400
C	-1.85228900	-2.22200100	-0.57053700
C	-2.40662000	-3.35666600	-1.15913200
H	-3.31787400	-3.79345200	-0.76976700
C	-1.77663400	-3.93128100	-2.25640700
H	-2.19740100	-4.81480000	-2.72440800
C	-0.60610900	-3.35800600	-2.74159700
C	-0.10530500	-2.23082400	-2.10678100
H	0.80310600	-1.74815600	-2.44818000
C	1.31162200	1.81066600	2.08918100
H	1.73472400	0.86970400	2.42128600
C	1.61678400	3.00394700	2.72729500
H	2.29157200	3.00212900	3.57550500
C	1.04334500	4.17903100	2.25334200
H	1.25997900	5.13180400	2.72468700
C	0.18407800	4.11980300	1.16286500
H	-0.26859100	5.02589400	0.78024200
C	-0.08385900	2.88739600	0.57132100
C	-0.99162100	2.71432100	-0.58620900
C	-1.89784300	1.19809400	-2.09970000
H	-1.94622300	0.16682300	-2.42978200
C	-2.62092000	2.19499800	-2.73803100
C	-2.51690400	3.49949400	-2.26702700
H	-3.06880300	4.30551200	-2.73867200
C	-1.69337300	3.76199300	-1.17888400
H	-1.60484500	4.77244300	-0.79916300
H	-3.25002000	1.94414400	-3.58422100
H	-0.08197100	-3.77092600	-3.59572200
H	3.28649200	1.80207700	-3.61764100
Ru	-0.00398400	0.00047500	-0.00598000
N	-1.10225000	1.44735100	-1.04968200
N	-0.70970900	-1.67446700	-1.04716100
N	1.79513100	0.22204400	-1.05589400

Zero-point correction = 0.490217 (Hartree/Particle)
Thermal correction to Energy = 0.518481
Thermal correction to Enthalpy = 0.519425
Thermal correction to Gibbs Free Energy = 0.431505
Sum of electronic and zero-point Energies = -1580.084996
Sum of electronic and thermal Energies = -1580.056732
Sum of electronic and thermal Enthalpies = -1580.055788
Sum of electronic and thermal Free Energies = -1580.143708
E(MN15) = -1579.583905

[Ru(bpy)$_3$]$^{2+*}$

N	1.03598400	1.55136900	-0.99220600
N	-1.77570300	0.13143200	-1.04114400
N	0.80618600	-1.66217400	-0.98342700
C	0.49533800	2.28094700	-1.97800100
H	-0.52041600	2.03135400	-2.26158300
C	1.19808700	3.29994600	-2.60185100
H	0.72757000	3.86734400	-3.39587000
C	2.49625200	3.56798900	-2.18210300
H	3.07367000	4.36108300	-2.64471100
C	3.05297900	2.81175800	-1.15647900
H	4.06062200	3.01556900	-0.81696600
C	2.29803700	1.80017000	-0.57319600
C	2.77789900	0.94044000	0.52972200
C	2.20358700	-0.77845600	1.99814700
H	1.43845800	-1.47436000	2.32315500
C	3.45468600	-0.74466200	2.59526100
C	4.39289300	0.16733200	2.12434400

H	5.38314400	0.21784600	2.56396200
C	4.05341600	1.01930600	1.07914400
H	4.77688700	1.73131500	0.70197800
C	-2.11729500	-0.66428800	-2.07803700
H	-1.36759400	-1.38140100	-2.39560500
C	-3.33231100	-0.57688300	-2.71245600
H	-3.55627800	-1.22958100	-3.54760700
C	-4.27011700	0.38194500	-2.24079800
H	-5.24232900	0.47192000	-2.71520900
C	-3.94727600	1.18932500	-1.18332400
H	-4.66106200	1.91653100	-0.81281700
C	-2.67287000	1.07522300	-0.55766400
C	-2.22366500	1.84751900	0.53827700
C	-2.95898400	2.88538100	1.17892700
H	-3.95604000	3.12825200	0.82925600
C	-2.40710300	3.57500800	2.22528400
H	-2.97082000	4.36531900	2.71112300
C	-1.09380000	3.25993300	2.66933800
C	-0.41587500	2.25275200	2.02662900
H	0.58948600	1.96957100	2.32175900
C	1.69098100	-1.59054800	-1.98641000
H	1.99460800	-0.59751800	-2.29720000
C	2.19179100	-2.72693000	-2.60318100
H	2.90375800	-2.62794900	-3.41396800
C	1.76048200	-3.97148500	-2.15744000
H	2.13157200	-4.88133700	-2.61665500
C	0.84612500	-4.04373800	-1.11226400
H	0.50318600	-5.00614100	-0.75385000
C	0.38139000	-2.86575700	-0.53736800
C	-0.58417800	-2.81512100	0.58072000
C	-1.77859600	-1.41246100	2.01562700
H	-1.99864400	-0.39227700	2.30717700
C	-2.36026400	-2.49557400	2.65664800
C	-2.03272500	-3.77800300	2.23119500
H	-2.47035300	-4.64751200	2.70950600
C	-1.13529600	-3.94113000	1.18159800
H	-0.87090200	-4.93415100	0.84055000
H	-3.05486700	-2.32618600	3.47063800
H	-0.62755300	3.79032800	3.49087400
H	3.67990900	-1.42387300	3.40877400
Ru	0.00128500	0.02028100	-0.00258500
N	-0.91272900	-1.57246500	1.00521200
N	-0.95170700	1.54834400	1.00671100
N	1.87786900	0.04428300	0.99268000

Zero-point correction = 0.488123 (Hartree/Particle)
Thermal correction to Energy = 0.516787
Thermal correction to Enthalpy = 0.517731
Thermal correction to Gibbs Free Energy = 0.428140
Sum of electronic and zero-point Energies = -1580.011497
Sum of electronic and thermal Energies = -1579.982833
Sum of electronic and thermal Enthalpies = -1579.981889
Sum of electronic and thermal Free Energies = -1580.071480
E(MN15) = -1579.504844

[Ru(bpy)$_3$]$^{3+}$

N	-1.03036300	-1.56108200	-0.98882900
N	1.83753800	-0.09237500	-1.00878900
N	-0.82818300	1.62224900	-0.99858900
C	-0.50506800	-2.27401000	-1.99489300
H	0.50842600	-2.02675200	-2.28836600
C	-1.22260000	-3.27550100	-2.62964000
H	-0.76641100	-3.82920000	-3.44134200
C	-2.51739000	-3.54250500	-2.19905500
H	-3.10653500	-4.32090400	-2.67157500
C	-3.05711300	-2.80449800	-1.15095200
H	-4.06282100	-3.00754300	-0.80525100
C	-2.28853400	-1.81028900	-0.55734700
C	-2.74596100	-0.96405200	0.56318900
C	-2.14915100	0.75789200	2.02540300
H	-1.38543400	1.46174500	2.33455500
C	-3.38230700	0.70512600	2.65580700
C	-4.32234600	-0.21556600	2.20715300
H	-5.29901400	-0.27962100	2.67423100
C	-4.00298400	-1.05865500	1.14834600
H	-4.72846000	-1.77678600	0.78746000
C	2.15926400	0.71543300	-2.02921500
H	1.40781500	1.43120600	-2.34121900
C	3.39165900	0.63910300	-2.65875300
H	3.61358900	1.30648200	-3.48269200
C	4.31494100	-0.29692200	-2.20712400
H	5.29082700	-0.37924300	-2.67300900
C	3.97914500	-1.13323500	-1.14799700
H	4.69091100	-1.86448400	-0.78596500
C	2.72302100	-1.01580200	-0.56506100
C	2.24619300	-1.85567100	0.55206100
C	2.99287500	-2.86564500	1.14694700
H	3.99508100	-3.08870800	0.80357200
C	2.43565300	-3.59306600	2.19329900
H	3.00788000	-4.38309200	2.66727000
C	1.14523400	-3.30040600	2.62040500
C	0.44917200	-2.28526600	1.98351000
H	-0.56025900	-2.01878700	2.27407300
C	-1.68787400	1.51091900	-2.02116400
H	-1.96234200	0.50712000	-2.32210200
C	-2.19865800	2.62572900	-2.66718000
H	-2.88883000	2.49675300	-3.49219000
C	-1.80758800	3.88694000	-2.23207800
H	-2.18933100	4.78006000	-2.71462500
C	-0.91909100	3.99899500	-1.16799100
H	-0.60693300	4.97523200	-0.81934600
C	-0.43924400	2.84375700	-0.56323300
C	0.50706600	2.82990400	0.56969100
C	1.72008000	1.46201400	2.02514800
H	1.96994600	0.45092300	2.32299200
C	2.25903700	2.56190000	2.67388500
C	1.90065900	3.83379100	2.24169300
H	2.30515900	4.71569400	2.72629100
C	1.01586800	3.97114700	1.17751200
H	0.72897600	4.95606200	0.83134900
H	2.94545100	2.41321100	3.49869500
H	0.67604800	-3.84481400	3.43098100
H	-3.59197800	1.37873300	3.47790100
Ru	-0.00194500	-0.01838200	-0.00257700
N	0.86437400	1.59767700	1.00202000
N	0.99160700	-1.58274500	0.97906300
N	-1.84239500	-0.05866300	1.00718300

Zero-point correction = 0.492365 (Hartree/Particle)
Thermal correction to Energy = 0.520319
Thermal correction to Enthalpy = 0.521263
Thermal correction to Gibbs Free Energy = 0.434431
Sum of electronic and zero-point Energies = -1579.890905
Sum of electronic and thermal Energies = -1579.862952
Sum of electronic and thermal Enthalpies = -1579.862007
Sum of electronic and thermal Free Energies = -1579.948840
E(MN15) = -1579.384745

4.4 Supporting information for chapter 3

4.4.1 Supporting information for chapter 3.1

Synthesis and characterization data of starting materials

General Procedure 1 (GP 1)

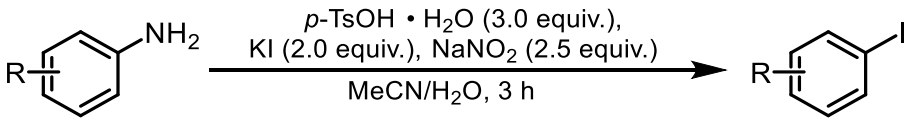

Aryl iodides were synthesized according to the literature procedure.[235] The corresponding aniline (2.0 mmol, 1.0 equiv.) and *p*-toluenesulfonic acid monohydrate (*p*-TsOH•H_2O) (6.0 mmol, 3.0 equiv.) were placed into a flask equipped with a stirring bar and dissolved in MeCN (0.17 M). To the obtained mixture an aqueous solution of mixture of KI (4.0 mmol, 2.0 equiv.) and $NaNO_2$ (5.00 mmol, 2.5 equiv.) in distilled H_2O (0.57 M and 0.71 M respectively) was added dropwise. The resulting solution was stirred for 3 h, then diluted with aqueous solution of $Na_2S_2O_3$ (1.0 M) and extracted with DCM (4x). Organic layers were combined, dried with $MgSO_4$, filtered, and concentrated *in vacuo*. The crude mixture was purified by silica gel column chromatography affording the final product.

General Procedure 2 (GP 2)

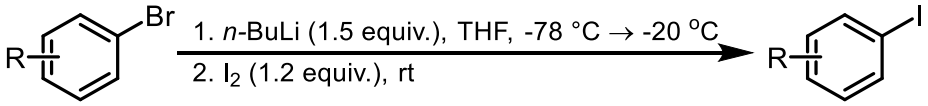

To a solution of the corresponding aryl bromide (1.0 equiv.) in anhydrous THF (0.1 M) a solution of *n*-BuLi (2.5 M in hexane, 1.5 equiv.) was added dropwise at -78 °C. The reaction mixture was stirred for 1.5 h and allowed to reach -20 °C and then iodine (1.2 equiv.) was added. The obtained solution was then stirred for 15 min at room temperature and quenched with an aqueous solution of $Na_2S_2O_3$ (1.0 M) and diluted with DCM. The organic phase was separated and the aqueous phase was extracted with DCM (3x). Organic phases were combined, dried with $MgSO_4$, filtered, and concentrated *in vacuo*. The crude mixture was purified by silica gel column chromatography affording the final product.

General Procedure 3 (GP 3)

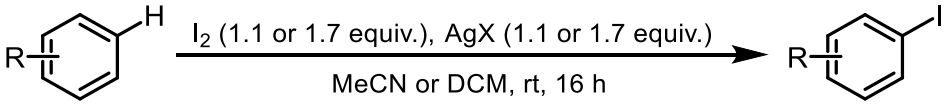

Aryl iodides were synthesized according to the literature procedure.[236] AgOTf or AgOMs (1.1 or 1.7 equiv.) was placed into a vial equipped with a stirring bar and dissolved in DCM or MeCN (0.20 M). Then the corresponding arene (1.0 equiv.) was added followed by addition of iodine (1.1 or 1.7 equiv.). The resulting solution was stirred for 16 h, then diluted with DCM and filtered through pad of Celite®. The filtrate was washed with an aqueous solution of Na_2SO_3 (1.0 M). The aqueous phase was extracted with DCM (2x). Organic layers were combined, dried with $MgSO_4$, filtered, and concentrated *in vacuo*. The crude mixture was purified by silica gel column chromatography affording the desired product.

Characterization Data of Substrates

3-Iodofluoranthene

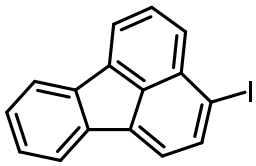

The iodination was performed according to GP 1 by using fluoranthen-3-amine (434.5 mg, 2.0 mmol, 1.0 equiv.). The title product was obtained after purification by silica gel column chromatography (*n*-pentane) as a yellow solid (173.8 mg, 0.520 mmol, 26%).

R_f = 0.31 (*n*-pentane). **^{1}H NMR** (400 MHz, $CDCl_3$) δ/ppm = 8.12 (d, *J* = 7.3 Hz, 1H), 7.92 (d, *J* = 6.9 Hz, 1H), 7.90-7.85 (m, 2H), 7.81 (d, *J* = 8.3 Hz, 1H), 7.72-7.65 (m, 1H), 7.62 (d, *J* = 7.2 Hz, 1H), 7.43-7.35 (m, 2H). **^{13}C NMR** (151 MHz, $CDCl_3$) δ/ppm = 138.95, 138.93, 138.5, 137.9, 137.7, 133.3, 133.0, 130.4, 129.6, 128.3, 128.1, 121.83, 121.77, 121.4, 120.9, 97.5. **HRMS** (APCI) calculated for $C_{16}H_9I$: 327.9743 $[M]^+$, found: 327.9745.

9-Iodoanthracene

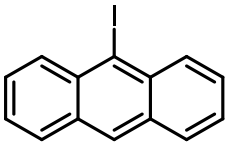

The iodination was performed according to GP 2 (0.08 M instead of 0.1 M) by using 9-bromoanthracene (360.0 mg, 1.40 mmol, 1.0 equiv.). The title product was obtained after purification by silica gel column chromatography (*n*-pentane) as a yellow solid (386.7 mg, 1.27 mmol, 91%).

R_f = 0.32 (*n*-pentane). **^{1}H NMR** (400 MHz, $CDCl_3$) δ/ppm = 8.50-8.44 (m, 3H), 7.99-7.93 (m, 2H), 7.62-7.55 (m, 2H), 7.52-7.46 (m, 2H). **^{13}C NMR** (101 MHz, $CDCl_3$) δ/ppm = 134.1, 133.4, 132.3, 129.0, 128.8, 127.9, 125.8, 104.9. **MS** (EI) *m/z* (%): 305 (15), 304 (100) $[M]^+$, 178 (10), 177 (52), 176 (49), 152 (13), 151 (13), 150 (12). These data are in agreement with those previously reported in literature.[237]

1-Iodo-4-methylnaphthalene

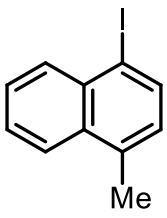

The iodination was performed according to GP 3 by using 1-methylnaphthalene (284.4 mg, 2.0 mmol, 1.0 equiv.), AgOMs (690.0 mg, 3.40 mmol, 1.7 equiv.), I_2 (863.0 mg, 3.40 mmol, 1.7 equiv.) in anhydrous MeCN. The title product was obtained after purification by silica gel column chromatography (*n*-pentane) as a red oil (422.5 mg, 1.58 mmol, 79%).

R_f = 0.53 (*n*-pentane). **^{1}H NMR** (400 MHz, $CDCl_3$) δ/ppm = 8.17-8.09 (m, 1H), 8.03-7.90 (m, 2H), 7.63-7.52 (m, 2H), 7.09-6.99 (m, 1H), 2.67 (s, 3H). **^{13}C NMR** (101 MHz, $CDCl_3$) δ/ppm = 137.3, 135.6, 134.2, 133.7,

133.0, 128.0, 127.5, 126.8, 124.8, 97.2, 19.4. **MS** (EI) *m/z* (%): 269 (15), 268 (100) $[M]^+$, 141 (42), 139 (18), 115 (22). These data are in agreement with those reported previously in the literature.[238]

1-Bromo-4-(*p*-tolyl)naphthalene

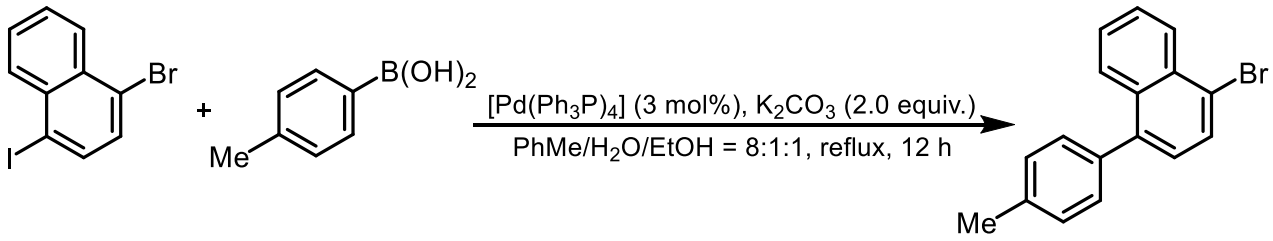

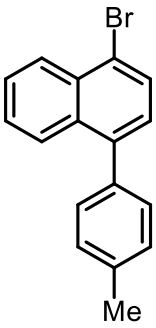

1-Bromo-4-iodonaphthalene (669.3 mg, 2.01 mmol, 1.0 equiv.), *p*-tolylboronic acid (327.7 mg, 2.41 mmol, 1.2 equiv.), $[Pd(Ph_3P)_4]$ (69.3 mg, 0.06 mmol, 3 mol%) and K_2CO_3 (555.6 mg, 4.02 mmol, 2.0 equiv.) were subsequently placed into a flask equipped with a stirring bar followed by addition of toluene (32 ml), water (4 ml) and ethanol (4 ml). Then a condenser was installed, and the obtained mixture was stirred under reflux for 12 h. After that the reaction mixture was transferred into a separatory funnel, diluted with DCM and washed with brine (3x). The organic phase was dried over $MgSO_4$ and concentrated *in vacuo.* The title product was obtained after purification of the residue by silica gel column chromatography (*n*-pentane) as a colorless solid (374.0 mg, 1.26 mmol, 63%).

R_f = 0.51 (*n*-pentane). **^{1}H NMR** (600 MHz, $CDCl_3$) δ/ppm = 8.34-8.31 (m, 1H), 7.92-7.89 (m, 1H), 7.82 (d, *J* = 7.6 Hz, 1H), 7.62-7.57 (m, 1H), 7.50-7.44 (m, 1H), 7.35 (d, *J* = 7.9 Hz, 2H), 7.31 (d, *J* = 7.9 Hz, 2H), 7.26 (d, *J* = 7.6 Hz, 1H), 2.46 (s, 3H). **^{13}C NMR** (151 MHz, $CDCl_3$) δ/ppm = 140.6, 137.5, 137.2, 133.2, 132.3, 130.0, 129.6, 129.2, 127.6, 127.3, 127.3, 126.9, 126.8, 122.2, 21.4. **HRMS** (APCI) calculated for $C_{17}H_{14}Br$: 297.0273 $[M+H]^+$, found: 297.0270. These data are in agreement with those previously reported in literature.[239]

1-Iodo-4-(*p*-tolyl)naphthalene

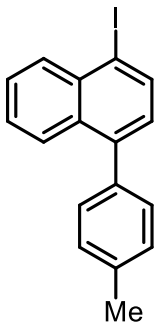

The iodination was performed according to GP 2 by using 1-bromo-4-(*p*-tolyl)naphthalene (168.6 mg, 0.57 mmol, 1.0 equiv.). The title product was obtained after purification by silica gel column chromatography (*n*-pentane) as a colorless solid (113.2 mg, 0.329 mmol, 58%).

R_f = 0.49 (*n*-pentane). **^{1}H NMR** (400 MHz, $CDCl_3$) δ/ppm = 8.17 (d, *J* = 8.5 Hz, 1H), 8.13 (d, *J* = 7.7 Hz, 1H), 7.84 (d, *J* = 8.5 Hz, 1H), 7.61-7.54 (m, 1H), 7.48-7.42 (m, 1H), 7.35 (d, *J* = 7.6 Hz, 2H), 7.30 (d, *J* = 7.7 Hz, 2H), 7.11 (d, *J* = 7.5 Hz, 1H), 2.46 (s, 3H). **^{13}C NMR** (151 MHz, $CDCl_3$) δ/ppm = 141.6, 137.5, 137.2, 137.1, 134.5, 132.8, 132.7, 130.0, 129.2,

128.0, 127.7, 127.0, 126.9, 98.9, 21.4. **MS** (EI) m/z (%): 345 (18), 344 (100) $[M]^+$, 216 (12), 215 (28), 203 (14), 202 (73), 108 (17), 101 (12), 95 (12). These data are in agreement with those previously reported in literature.[238]

1-*n*-Butylnaphthalene

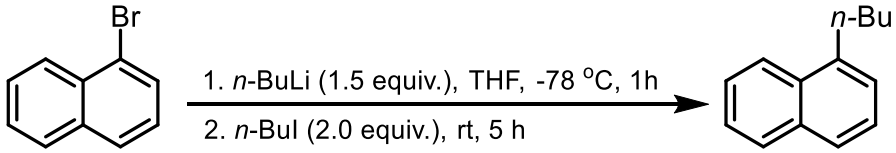

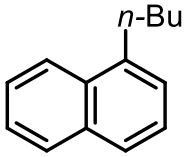

Under inert atmosphere 1-bromonaphthalene (919 µl, 7.0 mmol, 1.0 equiv.) was placed into a flask and dissolved in anhydrous THF (30 ml). The mixture was cooled down to -78 °C and ^{n}BuLi (2.5 M solution in hexane, 4.2 ml, 10.5 mmol, 1.5 equiv.) was added dropwise. The resulting solution was stirred at the same temperature for 1 h, and then *n*-BuI (1.6 ml, 14.0 mmol, 1.5 equiv.) was added dropwise. After that the obtained mixture was allowed to warm up to room temperature and stirred for 5 h. Then the resulting solution was quenched with water. The aqueous layer was separated and extracted with DCM (3x). The organic phases were combined, dried with $MgSO_4$, filtered, and solvents were removed under reduced pressure. The title product was obtained after purification of the residue by silica gel column chromatography (*n*-pentane) as a colorless oil (1237.8 mg, 6.72 mmol, 96%).

$\mathbf{R_f}$ = 0.47 (*n*-pentane). **^{1}H NMR** (600 MHz, $CDCl_3$) δ/ppm = 8.10-8.06 (m, 1H), 7.90-7.85 (m, 1H), 7.74-7.70 (m, 1H), 7.56-7.46 (m, 2H), 7.43-7.39 (m, 1H), 7.36-7.32 (m, 1H), 3.13-3.07 (m, 2H), 1.80-1.73 (m, 2H), 1.49 (sext, *J* = 7.4 Hz, 2H), 1.00 (t, *J* = 7.4 Hz, 3H). **^{13}C NMR** (151 MHz, $CDCl_3$) δ/ppm = 139.1, 134.0, 132.1, 128.9, 126.5, 126.0, 125.74, 125.67 125.5, 124.1, 33.2, 33.0, 23.0, 14.2. **MS** (EI) *m/z* (%): 185 (20), 184 (81) $[M]^+$, 155 (12), 153 (14), 152 (13), 142 (68), 141 (100), 139 (14), 128 (13), 115 (41). These data are in agreement with those reported previously in the literature.[240]

1-*n*-Butyl-4-iodonaphthalene

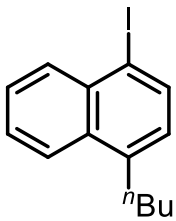

The iodination was performed according to GP 3 by using 1-butylnaphthalene (284.4 mg, 2.0 mmol, 1.0 equiv.), AgOMs (690.0 mg, 3.40 mmol, 1.7 equiv.), I_2 (863.0 mg, 3.40 mmol, 1.7 equiv.) in anhydrous MeCN. The title product was obtained after purification by silica gel column chromatography (*n*-pentane) as a red oil (422.5 mg, 1.58 mmol, 79%).

$\mathbf{R_f}$ = 0.53 (*n*-pentane). **^{1}H NMR** (400 MHz, $CDCl_3$) δ/ppm = 8.17-8.10 (m, 1H), 8.04-7.96 (m, 2H), 7.61-7.50 (m, 2H), 7.04 (d, *J* = 7.5 Hz, 1H), 3.05 (t, *J* = 7.8 Hz, 2H), 1.72 (pent, *J* = 7.8 Hz, 2H), 1.46 (sext, *J* = 7.4 Hz, 2H), 0.98 (t, *J* = 7.4 Hz, 3H). **^{13}C NMR** (101 MHz, $CDCl_3$) δ/ppm = 140.4, 137.3, 134.5, 133.2, 133.0, 127.3, 127.3, 126.6, 124.6, 97.4, 33.0, 32.8, 23.0, 14.1. **MS** (EI) *m/z* (%): 311 (17), 310 (82) $[M]^+$, 268 (20), 267 (100), 141 (17), 140 (26), 139 (26) (attempts to measure HRMS (APCI, ESI) resulted in no detection of the molecule).

1-Bromo-4-((4-(*t*-butyl)phenyl)ethynyl)naphthalene

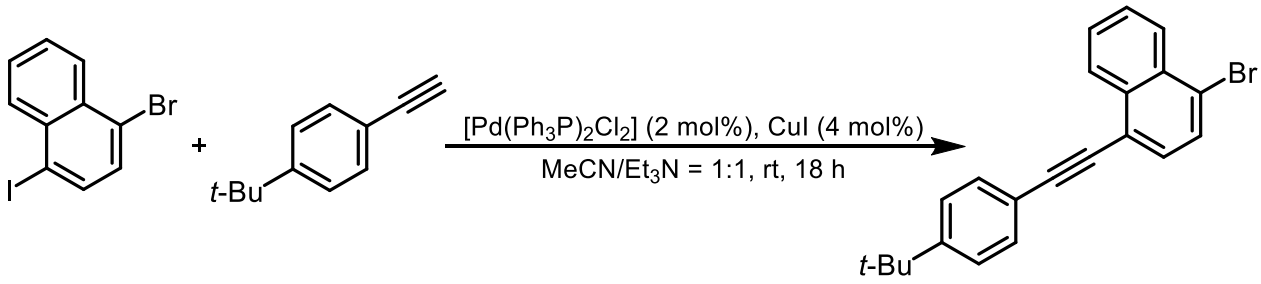

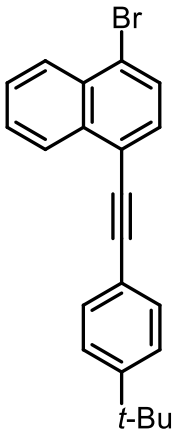

1-Bromo-4-iodonaphthalene (1798.0 mg, 5.40 mmol, 1.0 equiv.), $[Pd(Ph_3P)_2Cl_2]$ (84.0 mg, 0.12 mmol, 2 mol%), CuI (40.0 mg, 0.21 mmol, 4 mol%) were placed into a flask equipped with a stirring bar. Then MeCN (15 ml) and Et_3N (15 ml) were added under inert atmosphere. Argon was bubbled through the stirred solution for 30 min. Thereafter 1-(*t*-butyl)-4-ethynylbenzene (1.1 ml, 6.05 mmol, 1.12 equiv.) was added and the resulting solution was left to stir overnight. After that the mixture was diluted with DCM, transferred into a separatory funnel and washed with aqueous solution of NH_4Cl (sat.) (1x). The aqueous phase was separated and extracted with DCM (3x). The organic layers were combined, dried with $MgSO_4$, filtered, and concentrated under reduced pressure. The residue was purified by silica gel column chromatography (*n*-pentane) affording the title product as a colorless solid (1676.3 mg, 4.59 mmol, 85%).

R_f = 0.38 (*n*-pentane). **^{1}H NMR** (600 MHz, $CDCl_3$) δ/ppm = 8.48-8.44 (m, 1H), 8.29-8.25 (m, 1H), 7.77 (d, *J* = 7.7 Hz, 1H), 7.66-7.63 (m, 2H), 7.60-7.56 (m, 3H), 7.45-7.41 (m, 2H), 1.36 (s, 9H). **^{13}C NMR** (151 MHz, $CDCl_3$) δ/ppm = 152.2, 134.5, 132.0, 131.6, 130.4, 129.6, 127.9, 127.7, 127.6, 127.0, 125.7, 123.5, 121.5, 120.2, 95.7, 86.4, 35.0, 31.3. **HRMS** (APCI) calculated for $C_{22}H_{20}{}^{79}Br$: 363.0743 $[M+H]^+$, found: 363.0741.

1-((4-(*t*-Butyl)phenyl)ethynyl)-4-iodonaphthalene

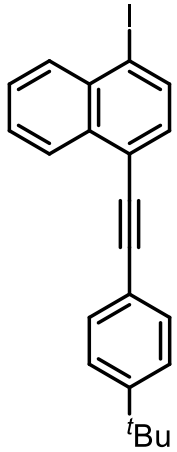

The iodination was performed according to GP 2 by using 1-bromo-4-((4-(*t*-butyl)phenyl)ethynyl)naphthalene (730.8 mg, 2.00 mmol, 1.0 equiv.) and ^{s}BuLi (1.4 M solution in cyclohexane, 2.9 ml, 4.00 mmol, 2.0 equiv.). The title product was obtained after purification by silica gel column chromatography (*n*-pentane) as a pale pink solid (552.0 mg, 1.35 mmol, 67%).

R_f = 0.39 (*n*-pentane). **^{1}H NMR** (600 MHz, $CDCl_3$) δ/ppm = 8.43-8.39 (m, 1H), 8.14-8.10 (m, 1H), 8.07 (d, *J* = 7.6 Hz, 1H), 7.65-7.60 (m, 2H), 7.59 (d, *J* = 8.4 Hz, 2H), 7.45-7.41 (m, 3H), 1.36 (s, 9H). **^{13}C NMR** (151 MHz, $CDCl_3$) δ/ppm = 152.2, 137.1, 134.3, 133.9, 132.8, 131.6, 130.9, 128.4, 127.7, 127.2, 125.7, 122.5, 120.2, 100.3, 96.0, 86.4, 35.0, 31.3. **HRMS** (APCI) calculated for $C_{22}H_{20}I$: 411.0604 $[M+H]^+$, found: 411.0592.

6-Bromo-1*H*,3*H*-benzo[*de*]isochromane

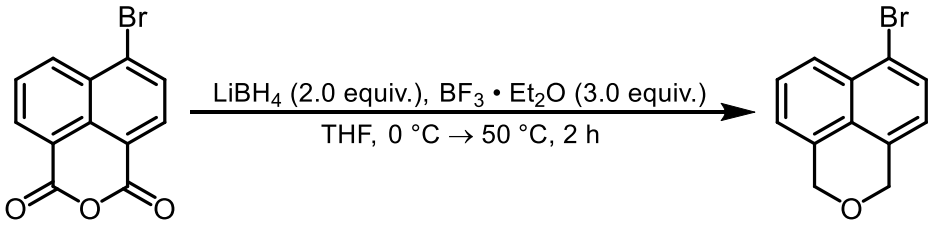

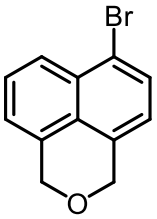

The synthesis was carried out according to the literature procedure.[241] A suspension of 6-bromo-1*H*,3*H*-benzo[*de*]isochromene-1,3-dione (2325.0 mg, 8.40 mmol, 1.0 equiv.) in THF was cooled to 0 °C, then $LiBH_4$ (365.9 mg, 16.8 mmol, 2.0 equiv.) and BF_3•Et_2O (3.1 ml, 25.2 mmol, 3.0 equiv.) were added subsequently at the same temperature. The obtained mixture was stirred at 50 °C for 2 h. After that the reaction mixture was cooled to ambient temperature and water (11 ml) was added. The obtained mixture was extracted with EtOAc (2x). The organic layers were combined, washed with brine (1x), dried with $MgSO_4$ and filtered. After removing the solvents under reduced pressure, a mixture of *n*-pentane and EtOAc (27 ml, 5:1) was added to the crude product and the obtained suspension was stirred at ambient temperature for 2 h. Then the solid was filtered, washed with a minimal volume of *n*-pentane/EtOAc mixture (5:1) and dried affording the title product as a pale brown solid, which was used without further purification (1270.7 mg, 5.12 mmol, 61%).

R_f = 0.40 (20:1 *n*-pentane/EtOAc). **^{1}H NMR** (600 MHz, $(CD_3)_2SO$) δ/ppm = 7.99 (d, *J* = 8.5 Hz, 1H), 7.83 (d, *J* = 7.5 Hz, 1H), 7.67-7.62 (m, 1H), 7.39 (d, *J* = 7.0 Hz, 1H), 7.22 (d, *J* = 7.5 Hz, 1H), 5.03 (s, 2H), 4.99 (s, 2H). **^{13}C NMR** (151 MHz, $(CD_3)_2SO$) δ/ppm = 133.5, 133.1, 130.6, 129.6, 127.6, 127.5, 124.8, 121.4, 121.3, 119.5, 67.99, 67.96. **HRMS** (EI) calculated for $C_{12}H_9{}^{79}BrO$: 247.9831 $[M]^+$, found: 247.9833.

6-Iodo-1*H*,3*H*-benzo[*de*]isochromane

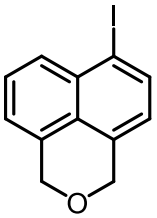

The iodination was performed according to GP 2 by using 6-bromo-1*H*,3*H*-benzo[*de*]isochromane (1184.4 mg, 4.0 mmol, 1.0 equiv.). The title product was obtained after purification by silica gel column chromatography (20:1 *n*-pentane/EtOAc) as a brown solid (208.8 mg, 0.48 mmol, 18%).

R_f = 0.37 (20:1 *n*-pentane/EtOAc). **^{1}H NMR** (400 MHz, $CDCl_3$) δ/ppm = 8.02 (d, *J* = 7.4 Hz, 1H), 7.98-7.94 (m, 1H), 7.55-7.49 (m, 1H), 7.24-7.21 (m, 1H), 6.91 (d, *J* = 7.4 Hz, 1H), 5.08 (s, 2H), 5.03 (s, 2H). **^{13}C NMR** (151 MHz, $CDCl_3$) δ/ppm = 137.1, 134.1, 133.6, 133.2, 130.9, 127.6, 127.5, 121.5, 121.3, 97.1, 69.2 (the resolution of the ^{13}C NMR does not allow for accurate assignment of all signals). **HRMS** (EI) calculated for $C_{12}H_9IO$: 295.9693 $[M]^+$, found: 295.9692.

4-Iodo-*N*,*N*-dimethylnaphthalen-1-amine

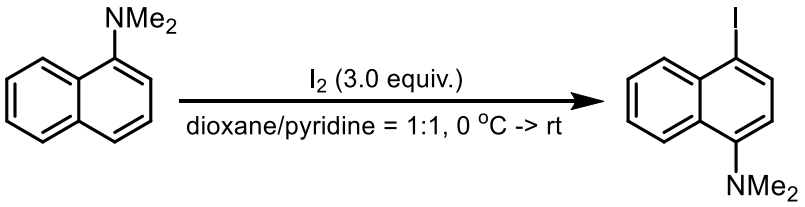

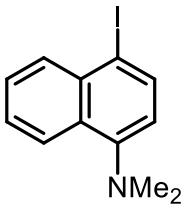

The iodination was performed according to the literature procedure.[242] *N*,*N*-Dimethylnaphthalen-1-amine (256.9 mg, 1.50 mmol, 1.0 equiv.) was placed into the flask equipped with a stirring bar and dissolved in a mixture of dioxane (9 ml) and pyridine (9 ml). Then the resulting mixture was cooled down to 0 °C and I_2 (1142.1 mg, 4.50 mmol, 3.0 equiv.) was added in one portion. The obtained reaction mixture was stirred at the same temperature for 1 h, and thereafter was allowed to warm up to room temperature. After consumption of the starting material (monitored by GC-MS) the aqueous solution of $Na_2S_2O_3$ (10%) was added. The obtained mixture was extracted with DCM (3x), the organic phases were combined, dried with $MgSO_4$, filtered, and the solvents were removed under reduced pressure. The title product was obtained after purification by silica gel column chromatography (20:1 *n*-pentane/EtOAc) as a yellow oil (407.7 mg, 1.37 mmol, 91%).

R_f = 0.57 (20:1 *n*-pentane/EtOAc). **^{1}H NMR** (600 MHz, $CDCl_3$) δ/ppm = 8.21 (d, *J* = 8.3 Hz, 1H), 8.07 (d, *J* = 8.3 Hz, 1H), 7.97 (d, *J* = 7.9 Hz, 1H), 7.58-7.49 (m, 2H), 6.82 (d, *J* = 7.9 Hz, 1H), 2.89 (s, 6H). **^{13}C NMR** (151 MHz, $CDCl_3$) δ/ppm = 152.1, 137.3, 135.2, 132.7, 130.0, 127.6, 126.0, 124.9, 115.7, 92.1, 45.3. **HRMS** (APCI) calculated for $C_{12}H_{13}IN$: 297.0087 $[M+H]^+$, found: 297.0088.

1-Iodo-4-nitronaphthalene

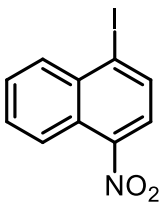

The iodination was performed according to GP 1 by using 4-nitro-1-naphthylamine (376.4 mg, 2.0 mmol, 1.0 equiv.). The title product was obtained after purification by silica gel column chromatography (22:1 *n*-pentane/EtOAc) as a yellow solid (143.4 mg, 0.48 mmol, 24%).

R_f = 0.47 (20:1 *n*-pentane/EtOAc). **^{1}H NMR** (400 MHz, $CDCl_3$) δ/ppm = 8.49-8.46 (m, 1H), 8.30-8.24 (m, 1H), 8.22 (d, *J* = 8.1 Hz, 1H), 7.87 (d, *J* = 8.0 Hz, 1H), 7.79-7.74 (m, 1H), 7.74-7.69 (m, 1H). **^{13}C NMR** (151 MHz, $CDCl_3$) δ/ppm = 136.1, 135.2, 133.4, 130.3, 129.4, 125.4, 123.9, 123.8, 107.7 (the resolution of the ^{13}C NMR does not allow for accurate assignment of all signals). **HRMS** (EI) calculated for $C_{10}H_6INO_2$: 298.9438 $[M]^+$, found: 298.9448.

6-Iodonaphtho[1,8-*cd*][1,2]oxathiole 2,2-dioxide (S_{12})

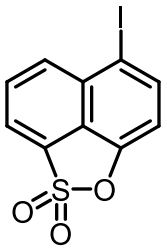

The iodination was performed according to GP 3 by using naphtho[1,8-*cd*][1,2]oxathiole 2,2-dioxide (309.3 mg, 1.50 mmol, 1.0 equiv.), AgOTf (423.9 mg, 1.65 mmol, 1.1 equiv.), I_2 (418.8 mg, 1.65 mmol, 1.1 equiv.) in anhydrous DCM. The title product was obtained after purification by silica gel column chromatography (3:2 *n*-pentane/DCM) as a colorless solid (455.4 mg, 1.37 mmol, 91%).

R_f = 0.31 (3:2 *n*-pentane/DCM). **^{1}H NMR** (600 MHz, $CDCl_3$) δ/ppm = 8.19 (d, *J* = 8.3 Hz, 1H), 8.14 (d, *J* = 7.9 Hz, 1H), 8.05 (d, *J* = 7.2 Hz, 1H), 7.92 (m, 1H), 6.97 (d, *J* = 7.9 Hz, 1H). **^{13}C NMR** (151 MHz, $CDCl_3$) δ/ppm = 147.8, 139.5, 135.4, 133.4, 130.4, 129.2, 122.2, 121.8, 108.3, 88.1. **HRMS** (APCI) calculated for $C_{10}H_5IO_3S$: 331.8999 $[M]^+$, found: 331.8990.

4-Iodo-1-naphthonitrile (S_{13})

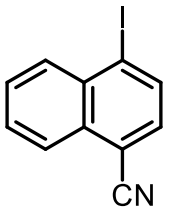

The iodination was performed according to GP 2 by using 4-bromo-1-naphthonitrile (464.2 mg, 2.0 mmol, 1.0 equiv.) and ^{s}BuLi (1.4 M solution in cyclohexane, 2.9 ml, 4.0 mmol, 2.0 equiv.). The title product was obtained after purification by silica gel column chromatography (30:1 *n*-pentane/EtOAc) as a pale pink solid (264.5 mg, 0.94 mmol, 47%).

R_f = 0.25 (30:1 *n*-pentane/EtOAc). **^{1}H NMR** (600 MHz, $CDCl_3$) δ/ppm = 8.22-8.16 (m, 3H), 7.77-7.69 (m, 2H), 7.58 (d, *J* = 7.6 Hz, 1H). **^{13}C NMR** (151 MHz, $CDCl_3$) δ/ppm = 136.9, 134.4, 133.4, 132.7, 132.5, 129.6, 129.5, 126.1, 117.5, 111.3, 107.0. **HRMS** (APCI) calculated for $C_{11}H_7IN$: 279.9618 $[M+H]^+$, found: 279.9611.

1-Chloro-4-iodonaphthalene (S_{14})

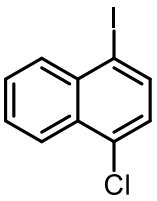

In a two-neck flask equipped with a stirring bar and condenser 1-chloronaphthalene (2439.0 mg, 15.0 mmol, 2.0 equiv) was dissolved in glacial AcOH (30 ml) and CCl_4 (0.6 ml). Then iodine (1903.5 mg, 7.5 mmol, 1.0 equiv.) was added and a dropping funnel containing a mixture of conc. HNO_3 (1.2 ml) and conc. H_2SO_4 (4.2 ml) was installed. The flask was immersed into a preheated oil bath (100 °C) and the mixture of acids was slowly added dropwise with vigorous stirring of the reaction solution. The resulting mixture was stirred for 3 h at the same temperature and then allowed to cool down to room temperature. Distilled H_2O (70 ml) was added and the obtained solution was kept in the freezer overnight. The liquid over the precipitated solid was decanted and the solid was dissolved in DCM. The obtained solution was washed with water (2x) and dried over $MgSO_4$. The crude product was purified by silica gel column chromatography (*n*-pentane) followed by recrystallization (EtOH) affording the title compound as a pale yellow solid (293.1 mg, 1.02 mmol, 7%).

R_f = 0.70 (*n*-pentane). **^{1}H NMR** (400 MHz, $CDCl_3$) δ/ppm = 8.28-8.20 (m, 1H), 8.15-8.09 (m, 1H), 7.99 (d, *J* = 7.9 Hz, 1H), 7.67-7.60 (m, 2H), 7.31 (d, *J* = 7.9 Hz, 1H). **^{13}C NMR** (151 MHz, $CDCl_3$) δ/ppm = 137.1, 135.3, 133.4, 132.9, 131.6, 128.7, 128.1, 127.2, 125.3, 97.9. **HRMS** (EI) calculated for $C_{10}H_6{}^{35}ClI$: 287.9203 $[M]^+$, found: 287.9198.

Pd-mediated Trifluoromethylation of Aryl Iodides

Design of the cyclic flow setup[iii]

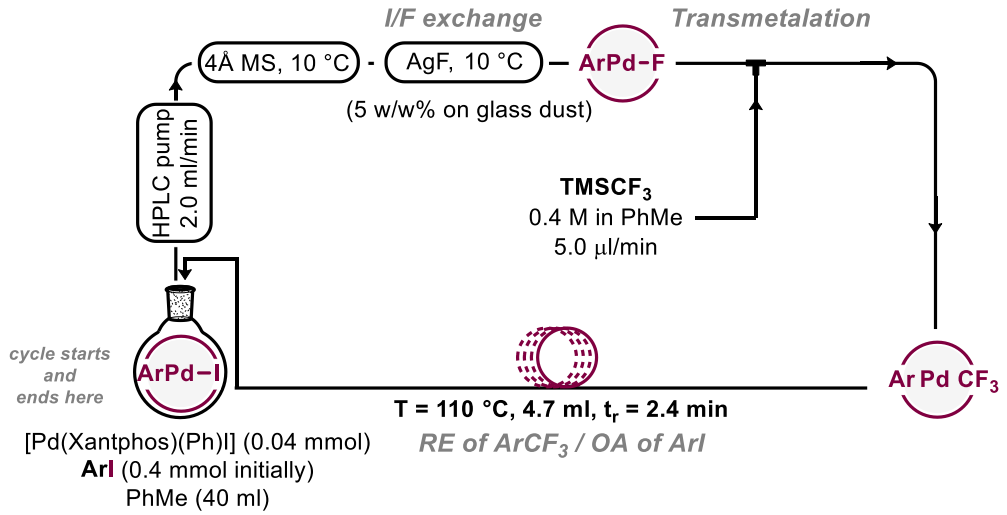

Figure S3. The design of the cyclic flow setup.

The construction of the flow setup is illustrated in the **Figure S3**, and the images of the system and the columns for it are shown in **Figure S4** below. All tubing had an internal diameter of 1.0 mm (FEP), and PTFE connectors were used. During the reaction, the flask with the reaction mixture had three tubes going into it through a septum. One of them was connected to a helium cylinder and was always inserted in the solution to bubble helium through it in order to keep the solution degassed and to maintain an inert atmosphere. The second tube was used to pump the solution by the HPLC pump through a filter. The third tube was always above the solution to return the reaction mixture back in the flask. The flask was equipped with a magnetic stirring bar, so the solution could be stirred throughout the process. Also, the flask was placed into a room temperature water bath to keep the temperature constant. The first part of the system following the flask was the mentioned HPLC pump set at 2 ml/min that was used to cycle the solution through the system. The solution exiting the pump was pushed through two directly connected columns, both of which were placed into a cryostat cooled water bath kept at 10 °C. The columns were prepared from empty polypropylene columns (8 ml, 9.8 cm, 12.4 mm ID; **Figure S4, A**), which were filled as follows: the first column had an upper layer of 4 Å molecular sieve dust (325 mesh), and a bottom layer of glass dust (≤106 µm particles). The layers were separated by a polyethylene frit, and the empty space on the top of the column was filled with frits. The second column was filled with a mixture of AgF and glass dust (5 w/w% AgF on ≤106 µm particles), and was wrapped in aluminium foil (not shown in **Figure S4, A**). All the connections of the columns (between them and between the columns and the tubings) were wrapped with parafilm to prevent any appearance of moisture in the system (**Figure S4, B**). After that, a solution of $TMSCF_3$ in PhMe was added via a syringe pump (~0.4 M, flow rate = 5.0 µl/min) through a tube (1 mm ID, 0.5 m) and mixed with the main solution in a Y-mixer. From the Y-mixer the solution flows through a reactor, which was immersed in an oil bath constantly heated at 110 °C. The temperature of the

[iii]The flow setup was designed by F. Opincal and then slightly modified.

oil bath was controlled with additional thermometer to ensure that the oil bath reached the necessary temperature. The length of the reactor was 6.0 m, and the length from the mixer to the reactor was ~20 cm. The length of the tube from the reactor back to the initial flask was ~30 cm. The length of the tube from the flask to the HPLC pump ~1.5 m (**Figure S4, C**).

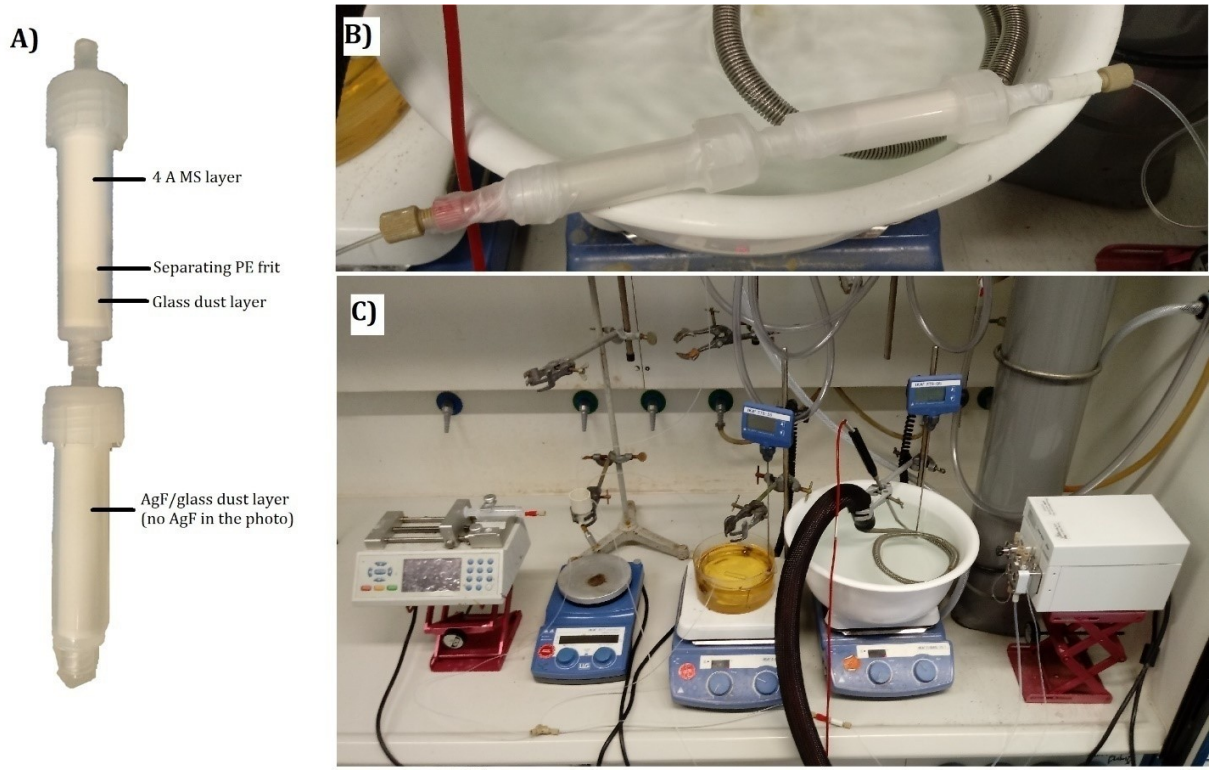

Figure S4. A) The drying (top) and the AgF column (bottom). B) The columns connected to the rest of the system. C) The layout of the entire system without the columns or the flask connected.

Preliminary preparation of the necessary components[iv]

The solid phases for the columns and the $TMSCF_3$ solution were always prepared before the reactions. The 4 Å molecular sieve dust (325 mesh) was purchased in that form and dried at 240 °C under high vacuum for at least 4 hours and were transferred under vacuum to an argon filled glovebox. The glass spheres (≤106 μm, unwashed) were washed and dried as follows. The washing was done by suspending the spheres (250 g) in concentrated H_2SO_4 (150 ml) followed by addition of H_2O_2 (35% in H_2O, 300 ml) when stirring. The suspension was left to stir overnight, after which it was filtered on a glass fritted filter, and the collected solid was thoroughly washed with water until pH indicates neutral media (checked by universal pH paper), methanol (2 x 150 ml), and diethyl ether (2 x 150 ml). The glass beads were then dried under vacuum on the same filter for several hours or left overnight in a fume hood at atmospheric pressure to ensure that all ether was removed. In case agglomerates of the dust were formed, they were grinded with a spatula or a pestle. Then the glass dust was transferred into a round bottom flask and dried in an oven at 180 °C for 48 h. The flask was periodically taken out, shaken for a minute and placed back into the oven. While being hot, the flask was evacuated and under reduced pressure transferred to an

[iv]The procedure of the preparation was developed by Filip Opincal and then was improved.

argon filled glovebox. Then glass dust was placed into a preliminary dried screw top bottle, which after that was constantly kept in the glovebox. The mixture of AgF on glass dust (5 w/w% of AgF) was prepared also in the glovebox by mechanically mixing and grinding the washed and dried glass dust with the appropriate amount of AgF in a dried mortar (AgF must be thoroughly grinded before mixing with glass dust). The mixture was then constantly kept in a freezer (-27 - -30 °C) of the glovebox. The $TMSCF_3$ solution (~0.4 M in PhMe) was prepared in the glovebox as well, and the exact concentration was checked by quantification with ^{19}F NMR using 4-(trifluoromethoxy)anisole (20 µl, 0.13 mmol) as the internal standard (25 s relaxation delay). After that the $TMSCF_3$ solution was kept in the freezer as well.

General flow procedure (GFP)[v]

Before an experiment, the initial reaction solution was prepared in an argon filled glovebox by mixing [Pd(Xantphos)(Ph)I] (35.6 mg, 0.04 mmol) previously prepared according to a literature procedure,[186] with the aryl iodide (0.40 mmol) in a 100 ml round-bottom flask equipped with a stirring bar and dissolved in anhydrous PhMe (40 ml). The flask closed with a septum and then, the columns were loaded and prepared in a glovebox. The columns were purchased with a frit on the bottom, which allows to put the material on them, and then another frit was added on the top and the material was compressed using high-vacuum pump by connecting it to the bottom of the column. For the column with AgF/glass dust mixture (5 w/w% AgF) the entire solid phase was added at once before compression. For the drying column glass spheres were added first, a frit put on top, and the material compressed. Then 4 Å molecular sieve dust was added, another frit added on top, and that part compressed as well. Empty space on top of columns was filled by adding more polyethylene frits. The columns were then connected directly to each other, with the drying column first and the AgF/glass dust column second. The open top and bottom of the connected columns were closed by connecting a needle to the AgF/glass dust column and an empty syringe to molecular sieve column before taking them out of the glovebox. The dead volumes of the columns were determined as ~6 ml for the drying column and ~3 ml for the column with AgF/glass dust. A Hamilton® glass syringe was then filled with the $TMSCF_3$ solution in the glovebox as well and the needle was capped before being taken out. The prepared columns, reaction mixture, and the syringe with the $TMSCF_3$ solution were taken out and instantly connected to the flow system in the way described below.

Before connection of the columns and the syringe to the flow setup, the heating plate of the reactor and the cooler of the cooling bath were turned on and set at their temperatures (110 °C and 10 °C respectively). The flow setup was first filled with anhydrous PhMe (4.0 ml/min, 150-200 ml), which was preliminary degassed with helium, by pumping without the columns and the reaction mixture. Simultaneously, PhMe was also pushed in the system via the syringe pump (0.4 ml/min, 10 ml) to prepare the tube for $TMSCF_3$ solution. Then the columns were connected to the system, placed into the cooling bath, and the system was flushed with more PhMe through the HPLC pump (2 ml/min, 20 ml). The syringe with the $TMSCF_3$ solution in PhMe was then connected and 1 ml of the solution was pumped to fill the tube. After that the flow rate of the syringe pump was set (5.0 µl/min for a 0.4 M solution, the flow rate depends on the exact concentration). When the columns and the entire system were well flushed and

[v]The procedure was developed by Filip Opincal.

cooled down to 10 °C, the HPLC pump was stopped, the helium flow increased, and the septum with the tubes was quickly transferred to the flask containing the reaction mixture. Then a needle was inserted through the septum to allow excess gas to leave, and helium was strongly bubbled through the solution for 1-2 minutes to remove any traces of air. Additionally, helium was used to degas the solution. After that, the helium flow rate was reduced, and the needle removed. The HPLC pump was then turned on again (2 ml/min), and the effluent at the end of the tube leaving the reactor was discarded until the effluent went from colourless to light yellow. The tube was then inserted through the septum in the original flask, mixing the effluent with continuously stirred the starting solution. After cycling for 15 h, the heating of the oil bath and the HPLC pump were stopped, and the tube leading the solution to the pump was moved and immersed into pure PhMe, which was used to flush the entire system while collecting in the reaction flask (40 ml PhMe for flushing, 2 ml/min). After that the reactor was subsequently washed with a concentrated solution of HNO_3 (6-10 ml), distilled water (10 ml), and MeCN (10 ml) by manual injection through the connector for the AgF/glass dust column. For ^{19}F NMR quantification, 4-(trifluoromethoxy)anisole (46 µl, 0.30 mmol) or a capillary with $CFCl_3$ in $CDCl_3$ were used[vi]. In case of the former, the solvent of the entire collected solution was evaporated, then 4-(trifluoromethoxy)anisole was added followed by addition of $CDCl_3$ (0.5 ml). An aliquot (0.5 ml) of the resulting solution was transferred into an NMR tube and diluted with $CDCl_3$ (0.2 ml). In case of the capillary, the crude mixture was diluted with MeCN (25 ml), an aliquot (0.5 ml) was placed into NMR tube with the capillary and diluted with $CDCl_3$ (0.2 ml). Then quantitative ^{19}F NMR was recorded (25 s relaxation delay). The amount of the Ar-CF_3 product was determined by comparing the integral of its signal to the one of 4-(trifluoromethoxy)anisole or $CFCl_3$. For isolation of the product, the solution from the NMR tube was returned to the whole mixture, the volatiles were evaporated under reduced pressure, and the products were purified by silica gel column chromatography or preparative TLC followed by preparative HPLC if necessary.

Characterization Data of Products

1-(Trifluoromethyl)naphthalene (1)

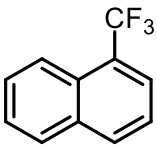

The trifluoromethylation was performed according to GFP by using 1-iodonaphthalene (58.4 µl, 0.40 mmol, 1.0 equiv.). The title product was obtained after purification by preparative TLC (*n*-hexane) as a colorless oil (54.9 mg, 0.28 mmol, 70%).

R_f = 0.60 (*n*-pentane). **^{1}H NMR** (600 MHz, $CDCl_3$) δ/ppm = 8.20 (d, *J* = 8.6 Hz, 1H), 8.03 (d, *J* = 8.3 Hz, 1H), 7.93 (d, *J* = 8.3 Hz, 1H), 7.90-7.86 (m, 1H), 7.67-7.62 (m, 1H), 7.61-7.56 (m, 1H), 7.54-7.49 (m, 1H). **^{13}C NMR** (151 MHz, $CDCl_3$) δ/ppm = 134.1, 132.9, 129.1, 128.9, 127.8, 126.7, 126.3 (q, *J* = 30.4 Hz), 124.88 (q, *J* = 273.5 Hz), 124.85 (q, *J* = 5.9 Hz), 124.4 (q, *J* = 2.4 Hz), 124.3. **^{19}F NMR** (565 MHz, $CDCl_3$) δ/ppm = -59.74. **MS** (EI) *m/z* (%): 197 (12), 196 (100) $[M]^+$, 195 (27), 177 (16), 146 (33). These data are in agreement with those reported previously in the literature.[243]

3-(Trifluoromethyl)fluoranthene (2)

[vi]The procedure of quantification with capillary was developed in collaboration with Filip Opincal.

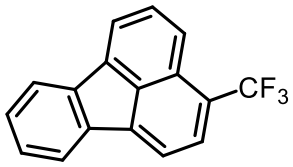

The trifluoromethylation was performed according to GFP by using 3-iodofluoranthene (131.3 mg, 0.40 mmol, 1.0 equiv.). The crude mixture was dissolved in DCM/CF_3CH_2OH=1:1 (20 ml) and *p*-TsOH•H_2O (760.8 mg, 4.0 mmol, 10.0 equiv.), mCPBA (896.3 mg, 4.00 mmol, 10.0 equiv.) were added subsequently. The obtained solution was stirred for 1 h and then evaporated under reduced pressure. The title product was obtained after purification of the residue by silica gel column chromatography (*n*-pentane) as a colorless solid (80.0 mg, 0.296 mmol, 74%).

R_f = 0.37 (*n*-pentane). **^{1}H NMR** (600 MHz, $CDCl_3$) δ/ppm = 8.10-8.03 (m, 1H), 7.96-7.93 (m, 2H), 7.93-7.87 (m, 3H), 7.73-7.69 (m, 1H), 7.45-7.38 (m, 2H). **^{13}C NMR** (151 MHz, $CDCl_3$) δ/ppm = 141.3, 140.2, 138.4, 137.6, 133.0, 129.7, 129.0, 128.2, 126.6 (q, *J* = 5.5 Hz), 126.2, 126.0, 125.8, 124.4-124.3 (m), 122.4, 121.9, 121.0, 118.4. **^{19}F NMR** (565 MHz, $CDCl_3$) δ/ppm = -57.51 (s, 3F). **HRMS** (APCI) calculated for $C_{17}H_{10}F_3$: 271.0729 $[M+H]^+$, found: 271.0733.

9-(Trifluoromethyl)anthracene (3)

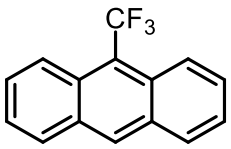

The trifluoromethylation was performed according to GFP by using 9-iodoanthracene (121.7 mg, 0.40 mmol, 1.0 equiv.). The crude mixture was dissolved in DCM/CF_3CH_2OH=1:1 (20 ml) and *p*-TsOH•H_2O (760.8 mg, 4.0 mmol, 10.0 equiv.), mCPBA (896.3 mg, 4.0 mmol, 10.0 equiv.) were added subsequently. The obtained solution was stirred for 1 h and then evaporated under reduced pressure. The title product was obtained after purification of the residue by silica gel column chromatography (*n*-pentane) as a yellow solid (30.5 mg, 0.12 mmol, 31%). The ^{19}F NMR yield was 40%.

R_f = 0.47 (*n*-pentane). **^{1}H NMR** (600 MHz, $CDCl_3$) δ/ppm = 8.64-8.50 (m, 3H), 8.05 (d, *J* = 8.4 Hz, 2H), 7.64-7.58 (m, 2H), 7.56-7.47 (m, 2H). **^{13}C NMR** (151 MHz, $CDCl_3$) δ/ppm = 133.5, 131.3, 129.8-129.7 (m), 129.4, 128.0 (m), 126.9 (q, *J* = 277.3 Hz) 125.3, 124.7 (q, *J* = 6.2 Hz), 120.4 (q, *J* = 28.0 Hz). **^{19}F NMR** (565 MHz, $CDCl_3$) δ/ppm = -48.46 (s, 3F). **MS** (EI) *m/z* (%): 247 (16), 246 (100) $[M]^+$, 245 (19), 196 (28), 98 (15). These data are in agreement with those previously reported in literature.[182]

1-Methyl-4-(trifluoromethyl)naphthalene (4)

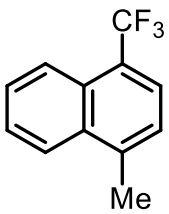

The trifluoromethylation was performed according to GFP by using 1-iodo-4-methylnaphthalene (107.2 mg, 0.40 mmol, 1.0 equiv.). The title product was obtained after purification by silica gel column chromatography (*n*-pentane) as a colorless oil (56.3 mg, 0.27 mmol, 67%).

R_f = 0.50 (*n*-pentane). **^{1}H NMR** (600 MHz, $CDCl_3$) δ/ppm = 8.24-8.19 (m, 1H), 8.11-8.07 (m, 1H), 7.76 (d, *J* = 7.4 Hz, 1H), 7.65-7.60 (m, 2H), 7.36 (d, *J* = 7.4 Hz, 1H), 2.75 (s, 3H). **^{13}C NMR** (151 MHz, $CDCl_3$) δ/ppm = 139.7, 133.2, 129.2, 127.3, 126.6, 125.1, 125.08 (q, *J* = 273.0 Hz), 125.0 (q, *J* = 2.5 Hz), 124.9, 124.6 (q, *J* = 6.4 Hz), 124.5, 20.1. **^{19}F NMR** (565 MHz, $CDCl_3$) δ/ppm = -59.34 (m, 3F). **MS** (EI) *m/z* (%): 211 (13), 210 (100) $[M]^+$, 209 (11), 141 (59). These data are in agreement with those reported previously in the literature.[244]

1-(*p*-Tolyl)-4-(trifluoromethyl)naphthalene (5)

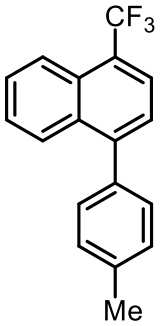

The trifluoromethylation was performed according to GFP by using 1-iodo-4-(*p*-tolyl)naphthalene (137.7 mg, 0.40 mmol, 1.0 equiv.). The crude mixture was dissolved in DCM/CF_3CH_2OH=1:1 (20 ml) and *p*-TsOH•H_2O (760.8 mg, 4.0 mmol, 10.0 equiv.), mCPBA (896.3 mg, 4.0 mmol, 10.0 equiv.) were added subsequently. The obtained solution was stirred for 1 h and then evaporated under reduced pressure. The title product was obtained after purification of the residue by silica gel column chromatography (*n*-pentane) as a colorless solid (63.0 mg, 0.22 mmol, 55%). The ^{19}F NMR yield was 78%.

R_f = 0.59 (*n*-pentane). **^{1}H NMR** (600 MHz, $CDCl_3$) δ/ppm = 8.30-8.21 (m, 1H), 8.01-7.95 (m, 1H), 7.90 (d, *J* = 7.5 Hz, 1H), 7.67-7.58 (m, 1H), 7.52-7.49 (m, 1H), 7.44 (d, *J* = 7.4 Hz, 1H), 7.36 (d, *J* = 8.0 Hz, 2H), 7.33 (d, *J* = 8.0 Hz, 2H), 2.47 (s, 3H). **^{13}C NMR** (151 MHz, $CDCl_3$) δ/ppm = 145.2, 137.9, 137.0, 132.5, 129.9, 129.6, 129.3, 127.5, 127.3, 126.7, 125.3, 125.0 (q, *J* = 273.4 Hz), 124.7-124.5 (m), 124.4 (q, *J* = 5.9 Hz), 21.4 (the resolution of the ^{13}C NMR does not allow for accurate assignment of all signals). **^{19}F NMR** (565 MHz, $CDCl_3$) δ/ppm = -59.54 (s, 3F). **HRMS** (APCI) calculated for $C_{18}H_{14}F_3$: 287.1042 $[M+H]^+$, found: 287.1040.

1-*n*-Butyl-4-(trifluoromethyl)naphthalene (6)

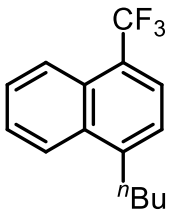

The trifluoromethylation was performed according to GFP by using 1-*n*-butyl-4-iodonaphthalene (129.7 mg, 0.40 mmol, 1.0 equiv.). The title product was obtained after purification by silica gel column chromatography (*n*-pentane) and preparative HPLC (*n*-hexane) as a colorless oil (68.5 mg, 0.27 mmol, 68%).

R_f = 0.59 (*n*-pentane). **^{1}H NMR** (600 MHz, $CDCl_3$) δ/ppm = 8.25-8.20 (m, 1H), 8.16-8.12 (m, 1H), 7.78 (d, *J* = 7.4 Hz, 1H), 7.64-7.59 (m, 2H), 7.36 (d, *J* = 7.4 Hz, 1H), 3.15-3.08 (m, 2H), 1.79-1.71 (m, 2H), 1.48 (sext, *J* = 7.4 Hz, 2H), 0.99 (t, *J* = 7.4 Hz, 3H). **^{13}C NMR** (151 MHz, $CDCl_3$) δ/ppm = 144.4, 132.5, 129.5, 127.2, 126.5, 125.09 (q, *J* = 2.4 Hz), 125.08 (q, *J* = 273.1 Hz), 124.7, 124.6 (q, *J* = 5.9 Hz), 124.4, 33.3, 32.9, 23.0, 14.1 (the resolution of the ^{13}C NMR does not allow for accurate assignment of all signals). **^{19}F NMR** (565 MHz, $CDCl_3$) δ/ppm = -59.35 (m, 3F). **MS** (EI) *m/z* (%): 252 (52) $[M]^+$, 210 (51), 209 (100), 159 (12), 141 (26) (attempts to measure HRMS (APCI, ESI) resulted in no detection of the molecule).

1-((4-(*t*-Butyl)phenyl)ethynyl)-4-(trifluoromethyl)naphthalene (7)

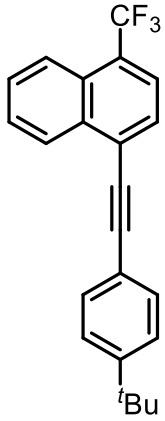

The trifluoromethylation was performed according to GFP by using 1-((4-(*t*-butyl)phenyl)ethynyl)-4-iodonaphthalene (164.1 mg, 0.40 mmol, 1.0 equiv.). The title product was obtained after purification by silica gel column chromatography (*n*-pentane) as a colorless solid (116.7 mg, 0.33 mmol, 83%).

R_f = 0.45 (*n*-pentane). **^{1}H NMR** (600 MHz, $CDCl_3$) δ/ppm = 8.58-8.53 (m, 1H), 8.24-8.17 (m, 1H), 7.84 (d, *J* = 7.6 Hz, 1H), 7.76 (d, *J* = 7.6 Hz, 1H), 7.70-7.65 (m, 2H), 7.60 (d, *J* = 8.4 Hz, 2H), 7.44 (d, *J* = 8.4 Hz, 2H), 1.36 (s, 9H). **^{13}C NMR** (151 MHz, $CDCl_3$) δ/ppm = 152.6, 133.8, 131.7, 129.0, 128.5, 128.2, 127.4, 127.3, 126.3, 126.0 (q, *J* = 30.2 Hz), 125.7, 124.72 (q, *J* = 3.0 Hz), 124.68 (q, *J* = 273.4 Hz), 124.3 (q, *J* = 6.2 Hz), 119.8, 97.1, 86.1,

35.1, 31.3. **^{19}F NMR** (565 MHz, $CDCl_3$) δ/ppm = -59.55 (m, 3F). **HRMS** (APCI) calculated for $C_{23}H_{19}F_3$: 352.1433 $[M]^+$, found: 352.1425.

1-(Benzyloxy)-3-(trifluoromethyl)benzene (8)

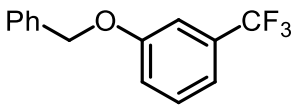

The trifluoromethylation was performed according to GFP by using 1-(benzyloxy)-3-iodobenzene (124.1 mg, 0.40 mmol, 1.0 equiv.). The title product was obtained after purification of the crude mixture by silica gel column chromatography (*n*-pentane to 20:1 *n*-pentane/PhMe) as a colorless solid (24.2 mg, 0.096 mmol, 24%).

R_f = 0.33 (*n*-pentane). **^{1}H NMR** (600 MHz, $CDCl_3$) δ/ppm = 7.47-7.31 (m, 6H), 7.24-7.20 (m, 2H), 7.16-7.12 (m, 1H), 5.10 (s, 2H). **^{13}C NMR** (151 MHz, $CDCl_3$) δ/ppm = 159.0, 136.4, 132.0 (q, *J* = 32.2 Hz), 130.2, 128.8, 128.4, 127.7, 124.1 (q, *J* = 272.4 Hz), 118.4, 117.8 (q, *J* = 4.1 Hz), 111.9 (q, *J* = 4.1 Hz), 70.4. **^{19}F NMR** (565 MHz, $CDCl_3$) δ/ppm = -62.72 (s, 3F). **HRMS** (EI) calculated for $C_{14}H_{11}F_3O$: 252.0762 $[M]^+$, found: 252.0756. These data are in agreement with those previously reported in literature.[182]

6-(Trifluoromethyl)-1*H*,3*H*-benzo[*de*]isochromane (9)

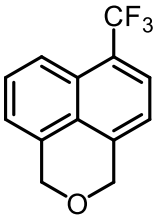

The trifluoromethylation was performed according to GFP by using 6-iodo-1*H*,3*H*-benzo[*de*]isochromane (118.4 mg, 0.40 mmol, 1.0 equiv.). The title product was obtained after purification of the crude mixture by silica gel column chromatography (20:1 *n*-pentane/EtOAc) as a colorless solid (78.1 mg, 0.328 mmol, 82%).

R_f = 0.51 (20:1 *n*-pentane/EtOAc). **^{1}H NMR** (600 MHz, $CDCl_3$) δ/ppm = 8.11-8.06 (m, 1H), 7.82 (d, *J* = 7.3 Hz, 1H), 7.61-7.56 (m, 1H), 7.29 (d, *J* = 7.0 Hz, 1H), 7.22 (d, *J* = 7.4 Hz, 1H), 5.09 (s, 4H). **^{13}C NMR** (151 MHz, $CDCl_3$) δ/ppm = 137.5, 133.3, 128.9, 127.52, 127.51, 125.1 (d, *J* = 30.3 Hz), 124.8 (q, *J* = 273.4 Hz), 124.5 (q, *J* = 6.0 Hz), 123.3 (q, *J* = 2.5 Hz), 121.2, 118.8, 69.5. **^{19}F NMR** (565 MHz, $CDCl_3$) δ/ppm = -59.87 (s, 3F). **HRMS** (EI) calculated for $C_{13}H_9F_3O$: 238.0600 $[M]^+$, found: 238.0602.

***N*,*N*-Dimethyl-4-(trifluoromethyl)naphthalen-1-amine (10)**

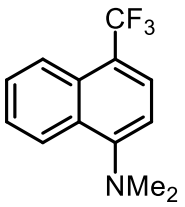

The trifluoromethylation was performed according to GFP by using 4-iodo-*N*,*N*-dimethylnaphthalen-1-amine (118.9 mg, 0.40 mmol, 1.0 equiv.). The title product was obtained after purification by silica gel column chromatography (30:1 *n*-pentane/EtOAc) and preparative HPLC (85:15 *n*-hexane/EtOAc) as a yellow oil (42.1 mg, 0.176 mmol, 44%). The ^{19}F NMR yield was 64%.

R_f = 0.55 (20:1 *n*-pentane/EtOAc). **^{1}H NMR** (600 MHz, $CDCl_3$) δ/ppm = 8.31-8.27 (m, 1H), 8.19-8.14 (m, 1H), 7.77 (d, *J* = 7.9 Hz, 1H), 7.62-7.53 (m, 2H), 7.00 (d, *J* = 7.9 Hz, 1H), 2.95 (s, 6H). **^{13}C NMR** (151 MHz, $CDCl_3$) δ/ppm = 154.9, 130.7, 128.9, 127.4, 125.6, 125.4 (q, *J* = 5.9 Hz), 125.3 (q, *J* = 272.4 Hz), 125.2, 124.8 (q, *J* = 2.5 Hz), 120.1 (q, *J* = 30.2 Hz), 111.7 (the resolution of the ^{13}C NMR does not allow for accurate assignment of all signals). **^{19}F NMR** (565 MHz, $CDCl_3$) δ/ppm = -58.94 – -59.02 (m, 3F). **HRMS** (ESI) calculated for $C_{13}H_{13}F_3N$: 240.0995 $[M+H]^+$, found: 240.0992.

1-Nitro-4-(trifluoromethyl)naphthalene (11)

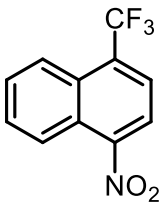

The trifluoromethylation was performed according to GFP by using 1-iodo-4-nitronaphthalene (119.6 mg, 0.40 mmol, 1.0 equiv.). The title product was obtained after purification of the crude mixture by silica gel column chromatography (22:1 *n*-pentane/EtOAc) as a yellow solid (86.6 mg, 0.359 mmol, 90%).

R_f = 0.49 (22:1 *n*-pentane/EtOAc). **^{1}H NMR** (600 MHz, $CDCl_3$) δ/ppm = 8.51-8.39 (m, 1H), 8.33-8.25 (m, 1H), 8.09 (d, *J* = 7.9 Hz, 1H), 7.97 (d, *J* = 7.9 Hz, 1H), 7.86-7.72 (m, 2H). **^{13}C NMR** (151 MHz, $CDCl_3$) δ/ppm = 150.2, 131.1 (q, *J* = 31.0 Hz), 130.4, 129.8, 129.3, 125.5, 124.9 (q, *J* = 2.9 Hz), 123.7 (q, *J* = 274.5 Hz), 123.62 (q, *J* = 5.9 Hz), 123.61, 121.2. **^{19}F NMR** (565 MHz, $CDCl_3$) δ/ppm = -59.83 – -59.87 (m, 3F). **HRMS** (EI) calculated for $C_{11}H_6F_3NO_2$: 241.0345 $[M]^+$, found: 241.0346.

6-(Trifluoromethyl)naphtho[1,8-*cd*][1,2]oxathiole 2,2-dioxide (12)

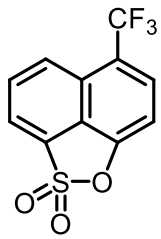

The trifluoromethylation was performed according to GFP by using 6-iodonaphtho[1,8-*cd*][1,2]oxathiole 2,2-dioxide (132.8 mg, 0.40 mmol, 1.0 equiv.). The title product was obtained after purification by preparative TLC (2:1 *n*-pentane/DCM) as a colorless solid (27.1 mg, 0.099 mmol, 25%). The ^{19}F NMR yield was 40%.

R_f = 0.30 (2:1 *n*-pentane/DCM). **^{1}H NMR** (600 MHz, $CDCl_3$) δ/ppm = 8.47-8.43 (m, 1H), 8.13 (d, *J* = 7.2 Hz, 1H), 8.04 (d, *J* = 7.9 Hz, 1H), 8.01-7.97 (m, 1H), 7.21 (d, *J* = 7.9 Hz, 1H). **^{13}C NMR** (151 MHz, $CDCl_3$) δ/ppm = 149.8, 130.6, 129.5-129.4 (m), 129.4, 128.8 (q, *J* = 5.5 Hz), 127.5, 123.8 (q, *J* = 272.6 Hz), 122.1, 122.0, 121.3 (q, *J* = 32.4 Hz), 105.2. **^{19}F NMR** (565 MHz, $CDCl_3$) δ/ppm = -59.54 (m, 3F). **HRMS** (APCI) calculated for $C_{11}H_5F_3O_3S$: 273.9906 $[M]^+$, found: 273.9913.

4-(Trifluoromethyl)-1-naphthonitrile (13)

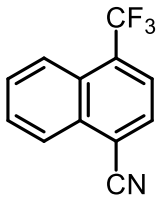

The trifluoromethylation was performed according to GFP by using 4-iodo-1-naphthonitrile (111.6 mg, 0.40 mmol, 1.0 equiv.). The title product was obtained after purification by silica gel column chromatography (25:1 *n*-pentane/Et_2O) and preparative HPLC (9:1 *n*-hexane/EtOAc) as a colorless solid (32.7 mg, 0.148 mmol, 37%). The ^{19}F NMR yield was 50%.

R_f = 0.20 (25:1 *n*-pentane/Et_2O). **^{1}H NMR** (600 MHz, $CDCl_3$) δ/ppm = 8.40-8.34 (m, 1H), 8.31-8.25 (m, 1H), 7.97 (d, *J* = 7.6 Hz, 1H), 7.93 (d, *J* = 7.6 Hz, 1H), 7.85-7.75 (m, 2H). **^{13}C NMR** (151 MHz, $CDCl_3$) δ/ppm = 132.9, 131.1, 130.9 (q, *J* = 30.9 Hz), 129.5, 129.4, 128.9, 126.2, 125.2 (q, *J* = 2.6 Hz), 123.8 (q, *J* = 274.4 Hz), 123.7 (d, *J* = 6.1 Hz), 116.9, 115.2. **^{19}F NMR** (565 MHz, $CDCl_3$) δ/ppm = -60.10 – -60.23 (m, 3F). **HRMS** (APCI) calculated for $C_{12}H_7F_3N$: 222.0525 $[M+H]^+$, found: 222.0534.

1-Chloro-4-(trifluoromethyl)naphthalene (14)

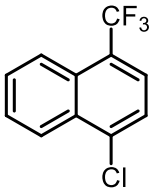

The trifluoromethylation was performed according to GFP by using 1-chloro-4-iodonaphthalene (115.4 mg, 0.40 mmol, 1.0 equiv.). The title product was obtained after purification of the crude mixture by silica gel column chromatography (*n*-pentane) as a colorless oil (77.5 mg, 0.336 mmol, 84%).

R_f = 0.81 (*n*-pentane). **^{1}H NMR** (600 MHz, $CDCl_3$) δ/ppm = 8.45-8.33 (m, 1H), 8.25-8.14 (m, 1H), 7.79 (d, *J* = 7.9 Hz, 1H), 7.73-7.67 (m, 2H), 7.63 (d, *J* = 7.9 Hz, 1H). **^{13}C NMR** (151 MHz, $CDCl_3$) δ/ppm = 137.1, 131.4, 130.3, 128.6, 127.9, 125.5 (q, *J* = 30.4 Hz), 125.4, 124.9-124.6 (m), 124.5 (q, *J* = 273.3 Hz). **^{19}F NMR** (565 MHz, $CDCl_3$) δ/ppm = -59.50 (s, 3F). **HRMS** (EI) calculated for $C_{11}H_6{}^{35}ClF_3$: 230.0105 $[M]^+$, found: 230.0105.

1-Bromo-4-(trifluoromethyl)naphthalene (15)

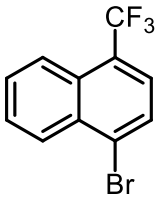

The trifluoromethylation was performed by using 1-bromo-4-iodonaphthalene (133.2 mg, 0.40 mmol, 1.0 equiv.). The crude mixture was dissolved in DCM/CF_3CH_2OH=1:1 (20 ml) and *p*-TsOH•H_2O (760.8 mg, 4.0 mmol, 10.0 equiv.), mCPBA (896.3 mg, 4.0 mmol, 10.0 equiv.) were added subsequently. The obtained solution was stirred for 1 h and then evaporated under reduced pressure. The title product was obtained after purification of the residue by silica gel column chromatography (*n*-pentane) as a colorless oil (72.0 mg, 0.267 mmol, 64%). ^{19}F NMR yield is 64%.

R_f = 0.64 (*n*-pentane). **^{1}H NMR** (600 MHz, $CDCl_3$) δ/ppm = 8.42-8.34 (m, 1H), 8.24-8.16 (m, 1H), 7.87-7.82 (m, 1), 7.73-7.67 (m, 3H). **^{13}C NMR** (151 MHz, $CDCl_3$) δ/ppm = 132.5, 130.2, 128.6, 128.3, 128.3, 128.2, 127.9, 126.2 (q, *J* = 30.8 Hz), 125.0 (q, *J* = 6.0 Hz), 124.9 (q, *J* = 2.7 Hz), 124.5 (q, *J* = 273.5 Hz). **^{19}F NMR** (565 MHz, $CDCl_3$) δ/ppm = -59.55 (s, 3F). **HRMS** (EI) calculated for $C_{11}H_6{}^{79}BrF_3$: 273.9599 $[M]^+$, found: 273.9592. These data are in agreement with those reported previously in the literature.[245]

5

Literature

5 Literature

[1] G. J. Sherborne, A. G. Gevondian, I. Funes-Ardoiz, A. Dahiya, C. Fricke, F. Schoenebeck, 'Modular and Selective Arylation of Aryl Germanes (C–$GeEt_3$) over C–Bpin, C–SiR_3 and Halogens Enabled by Light-Activated Gold Catalysis', *Angew. Chem. Int. Ed.* **2020**, *59*, 15543-15548.

[2] P. J. Hajduk, M. Bures, J. Praestgaard, S. W. Fesik, 'Privileged molecules for protein binding identified from NMR-based screening', *J Med Chem* **2000**, *43*, 3443-3447.

[3] D. A. Horton, G. T. Bourne, M. L. Smythe, 'The combinatorial synthesis of bicyclic privileged structures or privileged substructures', *Chem Rev* **2003**, *103*, 893-930.

[4] J. Klekota, F. P. Roth, 'Chemical substructures that enrich for biological activity', *Bioinformatics* **2008**, *24*, 2518-2525.

[5] D. S. Surry, S. L. Buchwald, 'Biaryl phosphane ligands in palladium-catalyzed amination', *Angew Chem Int Edit* **2008**, *47*, 6338-6361.

[6] T. Yamamoto, 'Synthesis of π-Conjugated Polymers Bearing Electronic and Optical Functionalities by Organometallic Polycondensations. Chemical Properties and Applications of the π-Conjugated Polymers', *Synlett* **2003**, *2003*, 0425-0450.

[7] M. Gomberg, W. E. Bachmann, 'THE SYNTHESIS OF BIARYL COMPOUNDS BY MEANS OF THE DIAZO REACTION', *J. Am. Chem. Soc.* **1924**, *46*, 2339-2343.

[8] F. Ullmann, J. Bielecki, 'Ueber Synthesen in der Biphenylreihe', *Berichte der deutschen chemischen Gesellschaft* **1901**, *34*, 2174-2185.

[9] P. E. Fanta, 'The Ullmann Synthesis of Biaryls', *Synthesis* **1974**, *1974*, 9-21.

[10] C. Sambiagio, S. P. Marsden, A. J. Blacker, P. C. McGowan, 'Copper catalysed Ullmann type chemistry: from mechanistic aspects to modern development', *Chem. Soc. Rev.* **2014**, *43*, 3525-3550.

[11] T. Amaya, Y. Jin, M. Tobisu, 'Recent advances in Gomberg-Backmann biaryl synthesis', *Tetrahedron Lett.* **2019**, *60*, 151062.

[12] F.-X. Felpin, S. Sengupta, 'Biaryl synthesis with arenediazonium salts: cross-coupling, CH-arylation and annulation reactions', *Chem. Soc. Rev.* **2019**, *48*, 1150-1193.

[13] D. Astruc, 'The 2010 Chemistry Nobel Prize to R.F. Heck, E. Negishi, and A. Suzuki for palladium-catalyzed cross-coupling reactions', *Analytical and Bioanalytical Chemistry* **2011**, *399*, 1811-1814.

[14] C. C. C. Johansson Seechurn, M. O. Kitching, T. J. Colacot, V. Snieckus, 'Palladium-Catalyzed Cross-Coupling: A Historical Contextual Perspective to the 2010 Nobel Prize', *Angew. Chem. Int. Ed.* **2012**, *51*, 5062-5085.

[15] M. Kumada, 'Nickel and palladium complex catalyzed cross-coupling reactions of organometallic reagents with organic halides', *Pure Appl. Chem.* **1980**, *52*, 669-679.

[16] E.-i. Negishi, 'Magical Power of Transition Metals: Past, Present, and Future (Nobel Lecture)', *Angew. Chem. Int. Ed.* **2011**, *50*, 6738-6764.

[17] A. Suzuki, 'Cross-Coupling Reactions Of Organoboranes: An Easy Way To Construct C-C Bonds (Nobel Lecture)', *Angew. Chem. Int. Ed.* **2011**, *50*, 6722-6737.

[18] T. Hiyama, 'How I came across the silicon-based cross-coupling reaction', *J. Organomet. Chem.* **2002**, *653*, 58-61.

[19] S. E. Denmark, A. Ambrosi, 'Why You Really Should Consider Using Palladium-Catalyzed Cross-Coupling of Silanols and Silanolates', *Org. Process Res. Dev.* **2015**, *19*, 982-994.

[20] J. K. Stille, 'The Palladium-Catalyzed Cross-Coupling Reactions of Organotin Reagents with Organic Electrophiles [New Synthetic Methods (58)]', *Angew. Chem. Int. Ed. Engl.* **1986**, *25*, 508-524.

[21] J. W. Faller, R. G. Kultyshev, 'Palladium-Catalyzed Cross-Coupling Reactions of Allyl, Phenyl, Alkenyl, and Alkynyl Germatranes with Aryl Iodides', *Organometallics* **2002**, *21*, 5911-5918.

[22] C. Fricke, G. J. Sherborne, I. Funes-Ardoiz, E. Senol, S. Guven, F. Schoenebeck, 'Orthogonal Nanoparticle Catalysis with Organogermanes', *Angew. Chem. Int. Ed.* **2019**, *58*, 17788-17795.

[23] G. Dyker, 'An Eldorado for Homogeneous Catalysis?', *Angew. Chem. Int. Ed.* **2000**, *39*, 4237-4239.

[24] C. Fricke, W. B. Reid, F. Schoenebeck, 'A Review on Oxidative Gold-Catalyzed C-H Arylation of Arenes – Challenges and Opportunities', *Eur. J. Org. Chem.* **2020**, *2020*, 7119-7130.

[25] A. Nijamudheen, A. Datta, 'Gold-Catalyzed Cross-Coupling Reactions: An Overview of Design Strategies, Mechanistic Studies, and Applications', *Chem. Eur. J.* **2020**, *26*, 1442-1487.

[26] S. Kramer, 'Homogeneous Gold-Catalyzed Aryl–Aryl Coupling Reactions', *Synthesis* **2020**, *52*, 2017-2030.

[27] L. T. Ball, G. C. Lloyd-Jones, C. A. Russell, 'Gold-Catalyzed Direct Arylation', *Science* **2012**, *337*, 1644-1648.

[28] X. C. Cambeiro, N. Ahlsten, I. Larrosa, 'Au-Catalyzed Cross-Coupling of Arenes via Double C–H Activation', *J Am Chem Soc* **2015**, *137*, 15636-15639.

[29] W. Li, D. Yuan, G. Wang, Y. Zhao, J. Xie, S. Li, C. Zhu, 'Cooperative Au/Ag Dual-Catalyzed Cross-Dehydrogenative Biaryl Coupling: Reaction Development and Mechanistic Insight', *J Am Chem Soc* **2019**, *141*, 3187-3197.

[30] S. Witzel, A. S. K. Hashmi, J. Xie, 'Light in Gold Catalysis', *Chem. Rev.* **2021**, *121*, 8868-8925.

[31] V. Gauchot, A.-L. Lee, 'Dual gold photoredox C(sp^2)–C(sp^2) cross couplings – development and mechanistic studies', *Chem. Commun.* **2016**, *52*, 10163-10166.

[32] T. Cornilleau, P. Hermange, E. Fouquet, 'Gold-catalysed cross-coupling between aryldiazonium salts and arylboronic acids: probing the usefulness of photoredox conditions', *Chem. Commun.* **2016**, *52*, 10040-10043.

[33] S. Witzel, J. Xie, M. Rudolph, A. S. K. Hashmi, 'Photosensitizer-Free, Gold-Catalyzed C–C Cross-Coupling of Boronic Acids and Diazonium Salts Enabled by Visible Light', *Adv. Synth. Catal.* **2017**, *359*, 1522-1528.

[34] I. Chakrabarty, M. O. Akram, S. Biswas, N. T. Patil, 'Visible light mediated desilylative C(sp^2)–C(sp^2) cross-coupling reactions of arylsilanes with aryldiazonium salts under Au(I)/Au(III) catalysis', *Chem. Commun.* **2018**, *54*, 7223-7226.

[35] M. O. Akram, P. S. Shinde, C. C. Chintawar, N. T. Patil, 'Gold(I)-catalyzed cross-coupling reactions of aryldiazonium salts with organostannanes', *Org. Biomol. Chem.* **2018**, *16*, 2865-2869.

[36] J. Xie, K. Sekine, S. Witzel, P. Krämer, M. Rudolph, F. Rominger, A. S. K. Hashmi, 'Light-Induced Gold-Catalyzed Hiyama Arylation: A Coupling Access to Biarylboronates', *Angew. Chem. Int. Ed.* **2018**, *57*, 16648-16653.

[37] C. Fricke, A. Dahiya, W. B. Reid, F. Schoenebeck, 'Gold-Catalyzed C–H Functionalization with Aryl Germanes', *ACS Catal.* **2019**, *9*, 9231-9236.

[38] A. Dahiya, C. Fricke, F. Schoenebeck, 'Gold-Catalyzed Chemoselective Couplings of Polyfluoroarenes with Aryl Germanes and Downstream Diversification', *J. Am. Chem. Soc.* **2020**, *142*, 7754-7759.

[39] P. A. Cox, M. Reid, A. G. Leach, A. D. Campbell, E. J. King, G. C. Lloyd-Jones, 'Base-Catalyzed Aryl-$B(OH)_2$ Protodeboronation Revisited: From Concerted Proton Transfer to Liberation of a Transient Aryl Anion', *J. Am. Chem. Soc.* **2017**, *139*, 13156-13165.

[40] M. P. Robinson, G. C. Lloyd-Jones, 'Au-Catalyzed Oxidative Arylation: Chelation-Induced Turnover of ortho-Substituted Arylsilanes', *ACS Catal.* **2018**, *8*, 7484-7488.

[41] C. M. Marian, 'Spin–orbit coupling and intersystem crossing in molecules', *WIREs Computational Molecular Science* **2012**, *2*, 187-203.

[42] R. Cai, M. Lu, E. Y. Aguilera, Y. Xi, N. G. Akhmedov, J. L. Petersen, H. Chen, X. Shi, 'Ligand-Assisted Gold-Catalyzed Cross-Coupling with Aryldiazonium Salts: Redox Gold Catalysis without an External Oxidant', *Angew. Chem. Int. Ed.* **2015**, *54*, 8772-8776.

[43] L. Huang, M. Rudolph, F. Rominger, A. S. K. Hashmi, 'Photosensitizer-Free Visible-Light-Mediated Gold-Catalyzed 1,2-Difunctionalization of Alkynes', *Angew. Chem. Int. Ed.* **2016**, *55*, 4808-4813.

[44] A. Dahiya, A. G. Gevondian, F. Schoenebeck, 'Orthogonal C–O Bond Construction with Organogermanes', *J. Am. Chem. Soc.* **2023**, *145*, 7729-7735.

[45] A. Dahiya, A. G. Gevondian, A. Selmani, F. Schoenebeck, 'Site-Selective Nitration of Aryl Germanes at Room Temperature', *Org. Lett.* **2023**, *25*, 7209-7213.

[46] G. Evano, J. Wang, A. Nitelet, 'Metal-mediated C–O bond forming reactions in natural product synthesis', *Org. Chem. Front.* **2017**, *4*, 2480-2499.

[47] S. D. Roughley, A. M. Jordan, 'The Medicinal Chemist's Toolbox: An Analysis of Reactions Used in the Pursuit of Drug Candidates', *J. Med. Chem.* **2011**, *54*, 3451-3479.

[48] N. Schneider, D. M. Lowe, R. A. Sayle, M. A. Tarselli, G. A. Landrum, 'Big Data from Pharmaceutical Patents: A Computational Analysis of Medicinal Chemists' Bread and Butter', *J. Med. Chem.* **2016**, *59*, 4385-4402.

[49] K. A. Scott, P. B. Cox, J. T. Njardarson, 'Phenols in Pharmaceuticals: Analysis of a Recurring Motif', *J. Med. Chem.* **2022**, *65*, 7044-7072.

[50] A. Williamson, 'XLV. Theory of ætherification', *The London, Edinburgh, and Dublin Philosophical Magazine and Journal of Science* **1850**, *37*, 350-356.

[51] A. Weissberg, A. Dahan, M. Portnoy, 'Williamson Ether Synthesis on Solid Support: Substitution versus Elimination', *J. Comb. Chem.* **2001**, *3*, 154-156.

[52] S. A. Ahmed, M. Tanaka, 'Synthesis of Oligo(ethylene glycol) toward 44-mer', *J. Org. Chem.* **2006**, *71*, 9884-9886.

[53] F. Ullmann, P. Sponagel, 'Ueber die Phenylirung von Phenolen', *Berichte der deutschen chemischen Gesellschaft* **1905**, *38*, 2211-2212.

[54] H. Weingarten, 'Ullmann Condensation', *J. Org. Chem.* **1964**, *29*, 977-978.

[55] R. Giri, A. Brusoe, K. Troshin, J. Y. Wang, M. Font, J. F. Hartwig, 'Mechanism of the Ullmann Biaryl Ether Synthesis Catalyzed by Complexes of Anionic Ligands: Evidence for the Reaction of Iodoarenes with Ligated Anionic CuI Intermediates', *J. Am. Chem. Soc.* **2018**, *140*, 793-806.

[56] T. G. R. Q. Brewster, 'p-NITRODIPHENYL ETHER', *Org. Synth.* **1934**, *14*, 66.

[57] R. G. R. Bacon, O. J. Stewart, '912. Metal ions and complexes in organic reactions. Part IV. Copper-promoted preparations of diaryl ethers and completing hydrogen-transfer processes', *J. Chem. Soc.* **1965**, DOI 10.1039/JR9650004953, 4953-4961.

[58] R. A. Altman, A. Shafir, A. Choi, P. A. Lichtor, S. L. Buchwald, 'An Improved Cu-Based Catalyst System for the Reactions of Alcohols with Aryl Halides', *J. Org. Chem.* **2008**, *73*, 284-286.

[59] D. Maiti, S. L. Buchwald, 'Cu-Catalyzed Arylation of Phenols: Synthesis of Sterically Hindered and Heteroaryl Diaryl Ethers', *J. Org. Chem.* **2010**, *75*, 1791-1794.

[60] M. Palucki, J. P. Wolfe, S. L. Buchwald, 'Synthesis of Oxygen Heterocycles via a Palladium-Catalyzed C–O Bond-Forming Reaction', *J. Am. Chem. Soc.* **1996**, *118*, 10333-10334.

[61] M. Palucki, J. P. Wolfe, S. L. Buchwald, 'Palladium-Catalyzed Intermolecular Carbon–Oxygen Bond Formation: A New Synthesis of Aryl Ethers', *J. Am. Chem. Soc.* **1997**, *119*, 3395-3396.

[62] R. A. Widenhoefer, H. A. Zhong, S. L. Buchwald, 'Direct Observation of C–O Reductive Elimination from Palladium Aryl Alkoxide Complexes To Form Aryl Ethers', *J. Am. Chem. Soc.* **1997**, *119*, 6787-6795.

[63] R. A. Widenhoefer, S. L. Buchwald, 'Electronic Dependence of C–O Reductive Elimination from Palladium (Aryl)neopentoxide Complexes', *J. Am. Chem. Soc.* **1998**, *120*, 6504-6511.

[64] G. Mann, J. F. Hartwig, 'Palladium-Catalyzed Formation of Diaryl Ethers from Aryl Bromides. Electron Poor Phosphines enhance Reaction Yields', *Tetrahedron Lett.* **1997**, *38*, 8005-8008.

[65] G. Mann, C. Incarvito, A. L. Rheingold, J. F. Hartwig, 'Palladium-Catalyzed C−O Coupling Involving Unactivated Aryl Halides. Sterically Induced Reductive Elimination To Form the C−O Bond in Diaryl Ethers', *J. Am. Chem. Soc.* **1999**, *121*, 3224-3225.

[66] G. Mann, Q. Shelby, A. H. Roy, J. F. Hartwig, 'Electronic and Steric Effects on the Reductive Elimination of Diaryl Ethers from Palladium(II)', *Organometallics* **2003**, *22*, 2775-2789.

[67] S. Harkal, K. Kumar, D. Michalik, A. Zapf, R. Jackstell, F. Rataboul, T. Riermeier, A. Monsees, M. Beller, 'An efficient catalyst system for diaryl ether synthesis from aryl chlorides', *Tetrahedron Lett.* **2005**, *46*, 3237-3240.

[68] S. Gowrisankar, A. G. Sergeev, P. Anbarasan, A. Spannenberg, H. Neumann, M. Beller, 'A General and Efficient Catalyst for Palladium-Catalyzed C−O Coupling Reactions of Aryl Halides with Primary Alcohols', *J. Am. Chem. Soc.* **2010**, *132*, 11592-11598.

[69] K. E. Torraca, X. Huang, C. A. Parrish, S. L. Buchwald, 'An Efficient Intermolecular Palladium-Catalyzed Synthesis of Aryl Ethers', *J. Am. Chem. Soc.* **2001**, *123*, 10770-10771.

[70] X. L. Han, G. X. Liu, X. Y. Lu, 'β-hydride elimination in palladium-catalyzed reactions', *Chinese Journal of Organic Chemistry* **2005**, *25*, 1182-1197.

[71] A. V. Vorogushin, X. Huang, S. L. Buchwald, 'Use of Tunable Ligands Allows for Intermolecular Pd-Catalyzed C−O Bond Formation', *J. Am. Chem. Soc.* **2005**, *127*, 8146-8149.

[72] X. Wu, B. P. Fors, S. L. Buchwald, 'A Single Phosphine Ligand Allows Palladium-Catalyzed Intermolecular C□O Bond Formation with Secondary and Primary Alcohols', *Angew. Chem. Int. Ed.* **2011**, *50*, 9943-9947.

[73] H. Zhang, P. Ruiz-Castillo, A. W. Schuppe, S. L. Buchwald, 'Improved Process for the Palladium-Catalyzed C−O Cross-Coupling of Secondary Alcohols', *Org. Lett.* **2020**, *22*, 5369-5374.

[74] P. M. MacQueen, J. P. Tassone, C. Diaz, M. Stradiotto, 'Exploiting Ancillary Ligation To Enable Nickel-Catalyzed C−O Cross-Couplings of Aryl Electrophiles with Aliphatic Alcohols', *J. Am. Chem. Soc.* **2018**, *140*, 5023-5027.

[75] J. A. Terrett, J. D. Cuthbertson, V. W. Shurtleff, D. W. C. MacMillan, 'Switching on elusive organometallic mechanisms with photoredox catalysis', *Nature* **2015**, *524*, 330-334.

[76] E. R. Welin, C. Le, D. M. Arias-Rotondo, J. K. McCusker, D. W. C. MacMillan, 'Photosensitized, energy transfer-mediated organometallic catalysis through electronically excited nickel(II)', *Science* **2017**, *355*, 380-385.

[77] D. M. T. Chan, K. L. Monaco, R.-P. Wang, M. P. Winters, 'New N- and O-arylations with phenylboronic acids and cupric acetate', *Tetrahedron Lett.* **1998**, *39*, 2933-2936.

[78] D. A. Evans, J. L. Katz, T. R. West, 'Synthesis of diaryl ethers through the copper-promoted arylation of phenols with arylboronic acids. An expedient synthesis of thyroxine', *Tetrahedron Lett.* **1998**, *39*, 2937-2940.

[79] P. Y. S. Lam, C. G. Clark, S. Saubern, J. Adams, M. P. Winters, D. M. T. Chan, A. Combs, 'New aryl/heteroaryl C-N bond cross-coupling reactions via arylboronic acid/cupric acetate arylation', *Tetrahedron Lett.* **1998**, *39*, 2941-2944.

[80] D. M. T. Chan, K. L. Monaco, R. Li, D. Bonne, C. G. Clark, P. Y. S. Lam, 'Copper promoted C-N and C-O bond cross-coupling with phenyl and pyridylboronates', *Tetrahedron Lett.* **2003**, *44*, 3863-3865.

[81] D. Zarzeczańska, A. Adamczyk-Woźniak, A. Kulpa, T. Ossowski, A. Sporzyński, 'Fluorinated Boronic Acids: Acidity and Hydrolytic Stability of Fluorinated Phenylboronic Acids', *Eur. J. Inorg. Chem.* **2017**, *2017*, 4493-4498.

[82] L. Chen, H. Francis, B. P. Carrow, 'An "On-Cycle" Precatalyst Enables Room-Temperature Polyfluoroarylation Using Sensitive Boronic Acids', *ACS Catal.* **2018**, *8*, 2989-2994.

[83] K. Gondo, J. Oyamada, T. Kitamura, 'Palladium-Catalyzed Desilylative Acyloxylation of Silicon−Carbon Bonds on (Trimethylsilyl)arenes: Synthesis of Phenol Derivatives from Trimethylsilylarenes', *Org. Lett.* **2015**, *17*, 4778-4781.

[84] C. Fricke, F. Schoenebeck, 'Organogermanes as Orthogonal Coupling Partners in Synthesis and Catalysis', *Acc. Chem. Res.* **2020**, *53*, 2715-2725.

[85] T. Yoneyama, R. H. Crabtree, 'Pd(II) catalyzed acetoxylation of arenes with iodosyl acetate', *J. Mol. Catal. A: Chem.* **1996**, *108*, 35-40.

[86] A. R. Dick, K. L. Hull, M. S. Sanford, 'A Highly Selective Catalytic Method for the Oxidative Functionalization of C−H Bonds', *J. Am. Chem. Soc.* **2004**, *126*, 2300-2301.

[87] D. Kalyani, M. S. Sanford, 'Regioselectivity in Palladium-Catalyzed C−H Activation/Oxygenation Reactions', *Org. Lett.* **2005**, *7*, 4149-4152.

[88] M. H. Emmert, A. K. Cook, Y. J. Xie, M. S. Sanford, 'Remarkably High Reactivity of $Pd(OAc)_2$/Pyridine Catalysts: Nondirected C-H Oxygenation of Arenes', *Angew. Chem. Int. Ed.* **2011**, *50*, 9409-9412.

[89] C. Huang, N. Ghavtadze, B. Godoi, V. Gevorgyan, 'Pd-Catalyzed Modifiable Silanol-Directed Aromatic C-H Oxygenation', *Chem. Eur. J.* **2012**, *18*, 9789-9792.

[90] N. Ono, 'The Nitro Group in Organic Synthesis', Wiley-VCH, Weinheim, **2001**.

[91] H. Fiedler, W. Mücke, 'Nitro Derivatives of Polycyclic Aromatic Hydrocarbons (NO_2-PAH)' in '*The Handbook of Environmental Chemistry*', Ed. O. Hutzinger, Springer, Berlin, **1991**, pp. 97-137.

[92] H. Zollinger, 'Color chemistry: syntheses, properties, and applications of organic dyes and pigments', Wiley-VCH, New York, **2003**.

[93] F.-R. F. Fan, Y. Yao, L. Cai, L. Cheng, J. M. Tour, A. J. Bard, 'Structure-Dependent Charge Transport and Storage in Self-Assembled Monolayers of Compounds of Interest in Molecular Electronics: Effects of Tip Material, Headgroup, and Surface Concentration', *J. Am. Chem. Soc.* **2004**, *126*, 4035-4042.

[94] H. Mustroph, 'Dyes, General Survey' in '*Ullmann's Encyclopedia of Industrial Chemistry*', Wiley-VCH Verlag GmbH & Co. KGaA, Weinheim, **2014**, pp. 1-38.

[95] A. A. Kulkarni, 'Continuous flow nitration in miniaturized devices', *Beilstein J. Org. Chem.* **2014**, *10*, 405-424.

[96] K. Muto, T. Okita, J. Yamaguchi, 'Transition-Metal-Catalyzed Denitrative Coupling of Nitroarenes', *ACS Catal.* **2020**, *10*, 9856-9871.
[97] H.-U. Blaser, H. Steiner, M. Studer, 'Selective Catalytic Hydrogenation of Functionalized Nitroarenes: An Update', *ChemCatChem* **2009**, *1*, 210-221.
[98] R. V. Jagadeesh, T. Stemmler, A.-E. Surkus, M. Bauer, M.-M. Pohl, J. Radnik, K. Junge, H. Junge, A. Brückner, M. Beller, 'Cobalt-based nanocatalysts for green oxidation and hydrogenation processes', *Nat. Protoc.* **2015**, *10*, 916-926.
[99] D. Formenti, F. Ferretti, F. K. Scharnagl, M. Beller, 'Reduction of Nitro Compounds Using 3d-Non-Noble Metal Catalysts', *Chem. Rev.* **2019**, *119*, 2611-2680.
[100] D. Zou, W. Wang, Y. Hu, T. Jia, 'Nitroarenes and nitroalkenes as potential amino sources for the synthesis of N-heterocycles', *Org. Biomol. Chem.* **2023**, *21*, 2254-2271.
[101] K. Nepali, H.-Y. Lee, J.-P. Liou, 'Nitro-Group-Containing Drugs', *J. Med. Chem.* **2019**, *62*, 2851-2893.
[102] O. Pongs, 'Chloramphenicol' in '*Mechanism of Action of Antibacterial Agents*', Ed. F. E. Hahn, Springer Berlin Heidelberg, Berlin, Heidelberg, **1979**, pp. 26-42.
[103] G. A. Olah, H. C. Lin, 'Synthetic Methods and Reactions; VI.1 Boron Trifluoride Catalyzed Mononitration of Tetramethylbenzenes and Pentamethylbenzene with Methyl Nitrate in Nitromethane Solution. A New Selective Nitration Method', *Synthesis* **1973**, *1973*, 488-490.
[104] G. A. Olah, S. C. Narang, A. P. Fung, 'Aromatic substitution. 47. Acid-catalyzed transfer nitration of aromatics with N-nitropyrazole, a convenient new nitrating agent', *J. Org. Chem.* **1981**, *46*, 2706-2709.
[105] S. A. Shackelford, M. B. Anderson, L. C. Christie, T. Goetzen, M. C. Guzman, M. A. Hananel, W. D. Kornreich, H. Li, V. P. Pathak, A. K. Rabinovich, R. J. Rajapakse, L. K. Truesdale, S. M. Tsank, H. N. Vazir, 'Electrophilic Tetraalkylammonium Nitrate Nitration. II. Improved Anhydrous Aromatic and Heteroaromatic Mononitration with Tetramethylammonium Nitrate and Triflic Anhydride, Including Selected Microwave Examples', *J. Org. Chem.* **2003**, *68*, 267-275.
[106] R. Calvo, K. Zhang, A. Passera, D. Katayev, 'Facile access to nitroarenes and nitroheteroarenes using N-nitrosaccharin', *Nat. Commun.* **2019**, *10*, 3410.
[107] S. Muppidi, C. R. Kamatala, S. C. Voruvala, S. K. Mukka, 'Hydro peroxides /$NaNO_2$/$KHSO_4$ mediated synthesis, kinetics and mechanistic study of nitration of aromatic compounds in aqueous acetonitrile', *Chemical Data Collections* **2019**, *21*, 100222.
[108] Y. Wang, F. Yu, X. Han, M. Li, Y. Tong, J. Ding, H. Hou, 'From Surprising Solvothermal Reaction to Uncommon Zinc(II)-Catalyzed Aromatic C–H Activation Reaction for Direct Nitroquinoline Synthesis', *Inorg. Chem.* **2017**, *56*, 5953-5958.
[109] S. Mondal, S. Samanta, A. Hajra, 'Regioselective C-7 Nitration of 8-Aminoquinoline Amides Using *tert*-Butyl Nitrite', *Adv. Synth. Catal.* **2018**, *360*, 1026-1031.
[110] S. P. Blum, C. Nickel, L. Schäffer, T. Karakaya, S. R. Waldvogel, 'Electrochemical Nitration with Nitrite', *ChemSusChem* **2021**, *14*, 4936-4940.
[111] Y.-K. Liu, S.-J. Lou, D.-Q. Xu, Z.-Y. Xu, 'Regiospecific Synthesis of Nitroarenes by Palladium-Catalyzed Nitrogen-Donor-Directed Aromatic C–H Nitration', *Chem. Eur. J.* **2010**, *16*, 13590-13593.
[112] L. Zhang, Z. Liu, H. Li, G. Fang, B.-D. Barry, T. A. Belay, X. Bi, Q. Liu, 'Copper-Mediated Chelation-Assisted Ortho Nitration of (Hetero)arenes', *Org. Lett.* **2011**, *13*, 6536-6539.
[113] W. Zhang, S. Lou, Y. Liu, Z. Xu, 'Palladium-Catalyzed Chelation-Assisted Aromatic C–H Nitration: Regiospecific Synthesis of Nitroarenes Free from the Effect of the Orientation Rules', *J. Org. Chem.* **2013**, *78*, 5932-5948.
[114] F. Xie, Z. Qi, X. Li, 'Rhodium(III)-Catalyzed Azidation and Nitration of Arenes by C–H Activation', *Angew. Chem. Int. Ed.* **2013**, *52*, 11862-11866.
[115] W. Zhang, J. Zhang, S. Ren, Y. Liu, 'Palladium-Catalyzed Aromatic C–H Bond Nitration Using Removable Directing Groups: Regiospecific Synthesis of Substituted o-Nitrophenols from Related Phenols', *J. Org. Chem.* **2014**, *79*, 11508-11516.
[116] W. Zhang, D. Wu, J. Zhang, Y. Liu, 'Regiospecific Synthesis of Substituted 2-Nitrobenzaldehydes from Benzaldehydes through Palladium-Catalyzed Chelation-Assisted C–H Nitration', *Eur. J. Org. Chem.* **2014**, *2014*, 5827-5835.
[117] D. Katayev, K. F. Pfister, T. Wendling, L. J. Gooßen, 'Copper-Mediated *ortho*-Nitration of (Hetero)Arenecarboxylates', *Chem. Eur. J.* **2014**, *20*, 9902-9905.
[118] C. J. Whiteoak, O. Planas, A. Company, X. Ribas, 'A First Example of Cobalt-Catalyzed Remote C–H Functionalization of 8-Aminoquinolines Operating through a Single Electron Transfer Mechanism', *Adv. Synth. Catal.* **2016**, *358*, 1679-1688.
[119] S. Saito, Y. Koizumi, 'Copper-catalyzed coupling of aryl halides and nitrite salts: a mild Ullmann-type synthesis of aromatic nitro compounds', *Tetrahedron Lett.* **2005**, *46*, 4715-4717.
[120] B. P. Fors, S. L. Buchwald, 'Pd-Catalyzed Conversion of Aryl Chlorides, Triflates, and Nonaflates to Nitroaromatics', *J. Am. Chem. Soc.* **2009**, *131*, 12898-12899.
[121] G. K. S. Prakash, T. Mathew, '*ipso*-Nitration of Arenes', *Angew. Chem. Int. Ed.* **2010**, *49*, 1726-1728.
[122] J. P. Das, P. Sinha, S. Roy, 'A Nitro-Hunsdiecker Reaction: From Unsaturated Carboxylic Acids to Nitrostyrenes and Nitroarenes', *Org. Lett.* **2002**, *4*, 3055-3058.
[123] P. Natarajan, R. Chaudhary, P. Venugopalan, '*Ipso*-nitration of carboxylic acids using a mixture of nitronium tetrafluoroborate, base and 1-hexyl-3,4,5-trimethyl-1H-imidazolium tetrafluoroborate', *Tetrahedron Lett.* **2019**, *60*, 1720-1723.
[124] S. Salzbrunn, J. Simon, G. K. Surya Prakash, N. A. Petasis, G. A. Olah, 'Regioselective Nitration of Arylboronic Acids', *Synlett* **2000**, *2000*, 1485-1487.

[125] G. K. S. Prakash, C. Panja, T. Mathew, V. Surampudi, N. A. Petasis, G. A. Olah, '*ipso*-Nitration of Arylboronic Acids with Chlorotrimethylsilane−Nitrate Salts', *Org. Lett.* **2004**, *6*, 2205-2207.
[126] X.-F. Wu, J. Schranck, H. Neumann, M. Beller, 'Convenient and mild synthesis of nitroarenes by metal-free nitration of arylboronic acids', *Chem. Commun.* **2011**, *47*, 12462-12463.
[127] S. Manna, S. Maity, S. Rana, S. Agasti, D. Maiti, '*ipso*-Nitration of Arylboronic Acids with Bismuth Nitrate and Perdisulfate', *Org. Lett.* **2012**, *14*, 1736-1739.
[128] M. Jiang, H. Yang, Y. Li, Z. Jia, H. Fu, 'Efficient *ipso*-nitration of arylboronic acids with iron nitrate as the nitro source', *RSC Adv.* **2013**, *3*, 25602-25604.
[129] N. Chatterjee, D. Bhatt, A. Goswami, 'A novel transition metal free [bis-(trifluoroacetoxy)iodo]benzene (PIFA) mediated oxidative *ipso* nitration of organoboronic acids', *Org. Biomol. Chem.* **2015**, *13*, 4828-4832.
[130] K. Zhang, A. Budinská, A. Passera, D. Katayev, '*N*-Nitroheterocycles: Bench-Stable Organic Reagents for Catalytic *Ipso*-Nitration of Aryl- and Heteroarylboronic Acids', *Org. Lett.* **2020**, *22*, 2714-2719.
[131] R. W. Murray, R. Jeyaraman, L. Mohan, 'A new synthesis of nitro compounds using dimethyldioxirane', *Tetrahedron Lett.* **1986**, *27*, 2335-2336.
[132] K. R. Reddy, C. U. Maheswari, M. Venkateshwar, M. L. Kantam, 'Selective Oxidation of Aromatic Amines to Nitro Derivatives using Potassium Iodide-tert-Butyl Hydroperoxide Catalytic System', *Adv. Synth. Catal.* **2009**, *351*, 93-96.
[133] V. V. Patil, G. S. Shankarling, 'Steric-Hindrance-Induced Regio- and Chemoselective Oxidation of Aromatic Amines', *J. Org. Chem.* **2015**, *80*, 7876-7883.
[134] V. Fargeas, F. Favresse, D. Mathieu, I. Beaudet, P. Charrue, B. Lebret, M. Piteau, J.-P. Quintard, 'Nitration of Heteroaryltrimethyltins by Tetranitromethane and Dinitrogen Tetroxide: Mechanistic Aspects, Scope and Limitations', *Eur. J. Org. Chem.* **2003**, *2003*, 1711-1721.
[135] K. Tani, K. Lukin, P. E. Eaton, 'Nitration of Organolithiums and Grignards with Dinitrogen Tetroxide: Success at Melting Interfaces', *J. Am. Chem. Soc.* **1997**, *119*, 1476-1477.
[136] P. Natarajan, R. Chaudhary, P. Venugopalan, 'Silver(I)-Promoted *ipso*-Nitration of Carboxylic Acids by Nitronium Tetrafluoroborate', *J. Org. Chem.* **2015**, *80*, 10498-10504.
[137] M. Zarei, E. Noroozizadeh, A. R. Moosavi-Zare, M. A. Zolfigol, 'Synthesis of Nitroolefins and Nitroarenes under Mild Conditions', *J. Org. Chem.* **2018**, *83*, 3645-3650.
[138] K. Zhang, B. Jelier, A. Passera, G. Jeschke, D. Katayev, 'Synthetic Diversity from a Versatile and Radical Nitrating Reagent', *Chem. Eur. J.* **2019**, *25*, 12929-12939.
[139] C. R. Bock, J. A. Connor, A. R. Gutierrez, T. J. Meyer, D. G. Whitten, B. P. Sullivan, J. K. Nagle, 'Estimation of excited-state redox potentials by electron-transfer quenching. Application of electron-transfer theory to excited-state redox processes', *J. Am. Chem. Soc.* **1979**, *101*, 4815-4824.
[140] S. Bouayad-Gervais, C. D. T. Nielsen, A. Turksoy, T. Sperger, K. Deckers, F. Schoenebeck, 'Access to Cyclic N-Trifluoromethyl Ureas through Photocatalytic Activation of Carbamoyl Azides', *J. Am. Chem. Soc.* **2022**, *144*, 6100-6106.
[141] T. Fujiwara, D. O'Hagan, 'Successful fluorine-containing herbicide agrochemicals', *J. Fluorine Chem.* **2014**, *167*, 16-29.
[142] Y. Ogawa, E. Tokunaga, O. Kobayashi, K. Hirai, N. Shibata, 'Current Contributions of Organofluorine Compounds to the Agrochemical Industry', *iScience* **2020**, *23*, 101467.
[143] K. Müller, C. Faeh, F. Diederich, 'Fluorine in Pharmaceuticals: Looking Beyond Intuition', *Science* **2007**, *317*, 1881-1886.
[144] J. Wang, M. Sánchez-Roselló, J. L. Aceña, C. del Pozo, A. E. Sorochinsky, S. Fustero, V. A. Soloshonok, H. Liu, 'Fluorine in Pharmaceutical Industry: Fluorine-Containing Drugs Introduced to the Market in the Last Decade (2001–2011)', *Chem. Rev.* **2014**, *114*, 2432-2506.
[145] M. Inoue, Y. Sumii, N. Shibata, 'Contribution of Organofluorine Compounds to Pharmaceuticals', *ACS Omega* **2020**, *5*, 10633-10640.
[146] S. Preshlock, M. Tredwell, V. Gouverneur, '^{18}F-Labeling of Arenes and Heteroarenes for Applications in Positron Emission Tomography', *Chem. Rev.* **2016**, *116*, 719-766.
[147] R. Ragni, A. Punzi, F. Babudri, G. M. Farinola, 'Organic and Organometallic Fluorinated Materials for Electronics and Optoelectronics: A Survey on Recent Research', *Eur. J. Org. Chem.* **2018**, *2018*, 3500-3519.
[148] P. Kirsch, A. Hahn, 'Liquid Crystals Based on Hypervalent Sulfur Fluorides: Exploring the Steric Effects of ortho-Fluorine Substituents', *Eur. J. Org. Chem.* **2005**, *2005*, 3095-3100.
[149] L. Xia, S. Lee, Y. Jiang, Y. Xia, G. Z. Chen, Z. Liu, 'Fluorinated Electrolytes for Li-Ion Batteries: The Lithium Difluoro(oxalato)borate Additive for Stabilizing the Solid Electrolyte Interphase', *ACS Omega* **2017**, *2*, 8741-8750.
[150] S. Purser, P. R. Moore, S. Swallow, V. Gouverneur, 'Fluorine in medicinal chemistry', *Chem. Soc. Rev.* **2008**, *37*, 320-330.
[151] E. P. Gillis, K. J. Eastman, M. D. Hill, D. J. Donnelly, N. A. Meanwell, 'Applications of Fluorine in Medicinal Chemistry', *J. Med. Chem.* **2015**, *58*, 8315-8359.
[152] C. J. Wenthur, M. R. Bennett, C. W. Lindsley, 'Classics in Chemical Neuroscience: Fluoxetine (Prozac)', *ACS Chemical Neuroscience* **2014**, *5*, 14-23.
[153] H. L. Yale, 'The Trifluoromethyl Group in Medical Chemistry', *Journal of Medicinal and Pharmaceutical Chemistry* **1959**, *1*, 121-133.
[154] P. Jeschke, 'The unique role of halogen substituents in the design of modern agrochemicals', *Pest Management Science* **2010**, *66*, 10-27.
[155] F. Swarts, 'Sur quelques dérivés fluorés du toluol', *Bull. Akad. R. Belg.* **1898**, *35*, 375-420.

[156] M. A. McClinton, D. A. McClinton, 'Trifluoromethylations and related reactions in organic chemistry', *Tetrahedron* **1992**, *48*, 6555-6666.

[157] T. Umemoto, A. Ando, 'Synthesis and Reactivity of *N*-Trifluoromethyl-*N*-nitrosotrifluoromethanesulfonamide as a New Type of Trifluoromethylating Agent', *Bull. Chem. Soc. Jpn.* **1986**, *59*, 447-452.

[158] Y. Tanabe, N. Matsuo, N. Ohno, 'Direct perfluoroalkylation including trifluoromethylation of aromatics with perfluoro carboxylic acids mediated by xenon difluoride', *J. Org. Chem.* **1988**, *53*, 4582-4585.

[159] A. Gregorcic, M. Zupan, 'Fluorination with xenon difluoride. 21. Evidence for free-radical intermediates in trifluoroacetic acid catalyzed fluorinations', *J. Org. Chem.* **1979**, *44*, 4120-4122.

[160] J. M. Birchall, G. P. Irvin, R. A. Boyson, 'Reactions of trifluoromethyl radicals. Part I. The photochemical reactions of trifluoroiodomethane with benzene and some halogenobenzenes', *J. Chem. Soc., Perkin Trans. 2* **1975**, DOI 10.1039/P29750000435, 435-439.

[161] M. Tordeux, B. Langlois, C. Wakselman, 'Reactions of bromotrifluoromethane and related halides. 8. Condensations with dithionite and hydroxymethanesulfinate salts', *J. Org. Chem.* **1989**, *54*, 2452-2453.

[162] J. Charpentier, N. Früh, A. Togni, 'Electrophilic Trifluoromethylation by Use of Hypervalent Iodine Reagents', *Chem. Rev.* **2015**, *115*, 650-682.

[163] U. Teruo, I. Sumi, 'Power-variable trifluoromethylating agents, (trifluoromethyl)dibenzothio- and -selenophenium salt system', *Tetrahedron Lett.* **1990**, *31*, 3579-3582.

[164] C. Zhang, 'Recent advances in trifluoromethylation of organic compounds using Umemoto's reagents', *Org. Biomol. Chem.* **2014**, *12*, 6580-6589.

[165] X. Liu, C. Xu, M. Wang, Q. Liu, 'Trifluoromethyltrimethylsilane: Nucleophilic Trifluoromethylation and Beyond', *Chem. Rev.* **2015**, *115*, 683-730.

[166] V. C. R. McLoughlin, J. Thrower, 'A route to fluoroalkyl-substituted aromatic compounds involving fluoroalkylcopper intermediates', *Tetrahedron* **1969**, *25*, 5921-5940.

[167] Y. Kobayashi, I. Kumadaki, 'Trifluoromethylation of aromatic compounds', *Tetrahedron Lett.* **1969**, *10*, 4095-4096.

[168] D. J. Burton, Z.-Y. Yang, 'Fluorinated organometallics: Perfluoroalkyl and functionalized perfluoroalkyl organometallic reagents in organic synthesis', *Tetrahedron* **1992**, *48*, 189-275.

[169] M. Oishi, H. Kondo, H. Amii, 'Aromatic trifluoromethylation catalytic in copper', *Chem. Commun.* **2009**, 1909-1911.

[170] T. Knauber, F. Arikan, G.-V. Röschenthaler, L. J. Gooßen, 'Copper-Catalyzed Trifluoromethylation of Aryl Iodides with Potassium (Trifluoromethyl)trimethoxyborate', *Chem. Eur. J.* **2011**, *17*, 2689-2697.

[171] C. F. Harris, C. S. Kuehner, J. Bacsa, J. D. Soper, 'Photoinduced Cobalt(III)−Trifluoromethyl Bond Activation Enables Arene C−H Trifluoromethylation', *Angew. Chem. Int. Ed.* **2018**, *57*, 1311-1315.

[172] K. Monir, A. K. Bagdi, M. Ghosh, A. Hajra, 'Regioselective Oxidative Trifluoromethylation of Imidazoheterocycles via C(sp^2)−H Bond Functionalization', *J. Org. Chem.* **2015**, *80*, 1332-1337.

[173] G. Shi, C. Shao, S. Pan, J. Yu, Y. Zhang, 'Silver-Catalyzed C–H Trifluoromethylation of Arenes Using Trifluoroacetic Acid as the Trifluoromethylating Reagent', *Org. Lett.* **2015**, *17*, 38-41.

[174] H. Egami, T. Ide, Y. Kawato, Y. Hamashima, 'Benzylic C–H trifluoromethylation of phenol derivatives', *Chem. Commun.* **2015**, *51*, 16675-16678.

[175] Y. Li, Y. Liu, D. Hao, C. Li, Y. Liu, Y. Gu, L. Vaccaro, P. Liu, 'Cu-catalyzed direct C1–H trifluoromethylation of pyrrolo[1,2-a]quinoxalines', *Tetrahedron* **2022**, *105*, 132610.

[176] J. Pletz, C. Koeberl, M. Fuchs, O. Steiner, W. Goessler, W. Kroutil, 'Cu and Hydroquinone for the Trifluoromethylation of Unprotected Phenols', *Eur. J. Org. Chem.* **2019**, *2019*, 682-690.

[177] J. Xu, L. Qiao, J. Shen, K. Chai, C. Shen, P. Zhang, 'Nickel(II)-Catalyzed Site-Selective C–H Bond Trifluoromethylation of Arylamine in Water through a Coordinating Activation Strategy', *Org. Lett.* **2017**, *19*, 5661-5664.

[178] E. A. Meucci, S. N. Nguyen, N. M. Camasso, E. Chong, A. Ariafard, A. J. Canty, M. S. Sanford, 'Nickel(IV)-Catalyzed C–H Trifluoromethylation of (Hetero)arenes', *J. Am. Chem. Soc.* **2019**, *141*, 12872-12879.

[179] X. Wang, L. Truesdale, J.-Q. Yu, 'Pd(II)-Catalyzed *ortho*-Trifluoromethylation of Arenes Using TFA as a Promoter', *J. Am. Chem. Soc.* **2010**, *132*, 3648-3649.

[180] R. P. Hughes, 'Organo-Transition Metal Compounds Containing Perfluorinated Ligands' in '*Adv. Organomet. Chem.',* F. G. A. Stone, R. West, Academic Press, **1990**, pp. 183-267.

[181] J. A. Morrison, 'Trifluoromethyl-Containing Transition Metal Complexes' in '*Adv. Organomet. Chem.',* F. G. A. Stone, R. West, Academic Press, **1993**, pp. 211-239.

[182] J. Cho Eun, D. Senecal Todd, T. Kinzel, Y. Zhang, A. Watson Donald, L. Buchwald Stephen, 'The Palladium-Catalyzed Trifluoromethylation of Aryl Chlorides', *Science* **2010**, *328*, 1679-1681.

[183] M. C. Nielsen, K. J. Bonney, F. Schoenebeck, 'Computational Ligand Design for the Reductive Elimination of $ArCF_3$ from a Small Bite Angle Pd^{II} Complex: Remarkable Effect of a Perfluoroalkyl Phosphine', *Angew. Chem. Int. Ed.* **2014**, *53*, 5903-5906.

[184] D. M. Ferguson, J. R. Bour, A. J. Canty, J. W. Kampf, M. S. Sanford, 'Stoichiometric and Catalytic Aryl–Perfluoroalkyl Coupling at Tri-tert-butylphosphine Palladium(II) Complexes', *J. Am. Chem. Soc.* **2017**, *139*, 11662-11665.

[185] D. M. Ferguson, J. R. Bour, A. J. Canty, J. W. Kampf, M. S. Sanford, 'Aryl–CF_3 Coupling from Phosphinoferrocene-Ligated Palladium(II) Complexes', *Organometallics* **2019**, *38*, 519-526.

[186] V. V. Grushin, W. J. Marshall, 'Facile Ar−CF_3 Bond Formation at Pd. Strikingly Different Outcomes of Reductive Elimination from [$(Ph_3P)_2Pd(CF_3)Ph$] and [(Xantphos)$Pd(CF_3)Ph$]', *J. Am. Chem. Soc.* **2006**, *128*, 12644-12645.

[187] V. I. Bakhmutov, F. Bozoglian, K. Gómez, G. González, V. V. Grushin, S. A. Macgregor, E. Martin, F. M. Miloserdov, M. A. Novikov, J. A. Panetier, L. V. Romashov, 'CF_3–Ph Reductive Elimination from [(Xantphos)Pd(CF_3)(Ph)]', *Organometallics* **2012**, *31*, 1315-1328.

[188] J. M. Brown, P. J. Guiry, 'Bite angle dependence of the rate of reductive elimination from diphosphine palladium complexes', *Inorg. Chim. Acta* **1994**, *220*, 249-259.

[189] P. C. J. Kamer, P. W. N. M. van Leeuwen, J. N. H. Reek, 'Wide Bite Angle Diphosphines: Xantphos Ligands in Transition Metal Complexes and Catalysis', *Acc. Chem. Res.* **2001**, *34*, 895-904.

[190] V. P. Ananikov, D. G. Musaev, K. Morokuma, 'Critical Effect of Phosphane Ligands on the Mechanism of Carbon–Carbon Bond Formation Involving Palladium(II) Complexes: A Theoretical Investigation of Reductive Elimination from Square-Planar and T-Shaped Species', *Eur. J. Inorg. Chem.* **2007**, *2007*, 5390-5399.

[191] V. P. Ananikov, D. G. Musaev, K. Morokuma, 'Real size of ligands, reactants and catalysts: Studies of structure, reactivity and selectivity by ONIOM and other hybrid computational approaches', *J. Mol. Catal. A: Chem.* **2010**, *324*, 104-119.

[192] P. Anstaett, F. Schoenebeck, 'Reductive Elimination of $ArCF_3$ from Bidentate Pd^{II} Complexes: A Computational Study', *Chem. Eur. J.* **2011**, *17*, 12340-12346.

[193] D. Naumann, N. V. Kirij, N. Maggiarosa, W. Tyrra, Y. L. Yagupolskii, M. S. Wickleder, 'Synthesen und Charakterisierungen der ersten Tris- und Tetrakis(trifluormethyl)palladate(II) und -platinate(II), $[M(CF_3)_3(PPh_3)]$— und $[M(CF_3)_4]_2$— (M = Pd, Pt)', *Z. Anorg. Allg. Chem.* **2004**, *630*, 746-751.

[194] S. T. Keaveney, F. Schoenebeck, 'Palladium-Catalyzed Decarbonylative Trifluoromethylation of Acid Fluorides', *Angew. Chem. Int. Ed.* **2018**, *57*, 4073-4077.

[195] S. Martinez de Salinas, A. L. Mudarra, J. Benet-Buchholz, T. Parella, F. Maseras, M. H. Perez-Temprano, 'New Vistas in Transmetalation with Discrete "$AgCF_3$" Species: Implications in Pd-Mediated Trifluoromethylation Reactions', *Chem. Eur. J.* **2018**, *24*, 11895-11898.

[196] S. Martinez de Salinas, A. L. Mudarra, C. Odena, M. Martinez Belmonte, J. Benet-Buchholz, F. Maseras, M. H. Perez-Temprano, 'Exploring the Role of Coinage Metalates in Trifluoromethylation: A Combined Experimental and Theoretical Study', *Chem. Eur. J.* **2019**, *25*, 9390-9394.

[197] Á. L. Mudarra, S. Martínez de Salinas, M. H. Pérez-Temprano, 'Beyond the traditional roles of Ag in catalysis: the transmetalating ability of organosilver(I) species in Pd-catalysed reactions', *Org. Biomol. Chem.* **2019**, *17*, 1655-1667.

[198] V. V. Grushin, W. J. Marshall, 'Unexpected H_2O-Induced Ar–X Activation with Trifluoromethylpalladium(II) Aryls', *J. Am. Chem. Soc.* **2006**, *128*, 4632-4641.

[199] J. W. Dolan, 'Mobile-Phase Degassing: What, Why, and How', *LC-GC North America* **2014**, *32*, 482-487.

[200] E. A. Merritt, V. M. T. Carneiro, L. F. Silva, Jr., B. Olofsson, 'Facile Synthesis of Koser's Reagent and Derivatives from Iodine or Aryl Iodides', *J. Org. Chem.* **2010**, *75*, 7416-7419.

[201] B. Wrackmeyer, 'Organoboron Chemistry' in '*Modern Magnetic Resonance*', Ed. G. A. Webb, Springer, Dordrecht, **2006**, pp. 455-457.

[202] B. Xing, C. Ni, J. Hu, 'Hypervalent Iodine(III)-Catalyzed Balz–Schiemann Fluorination under Mild Conditions', *Angew. Chem. Int. Ed.* **2018**, *57*, 9896-9900.

[203] X. Ma, S. B. Herzon, 'Cobalt bis(acetylacetonate)–*tert*-butyl hydroperoxide–triethylsilane: a general reagent combination for the Markovnikov-selective hydrofunctionalization of alkenes by hydrogen atom transfer', *Beilstein J. Org. Chem.* **2018**, *14*, 2259-2265.

[204] P. Nikolaienko, M. Rueping, 'Trifluoromethylselenolation of Aryldiazonium Salts: A Mild and Convenient Copper-Catalyzed Procedure for the Introduction of the $SeCF_3$ Group', *Chem. Eur. J.* **2016**, *22*, 2620-2623.

[205] W. Erb, A. Hellal, M. Albini, J. Rouden, J. Blanchet, 'An Easy Route to (Hetero)arylboronic Acids', *Chem. Eur. J.* **2014**, *20*, 6608-6612.

[206] W.-J. Zhou, K.-H. Wang, J.-X. Wang, D.-F. Huang, 'Reusable, Polystyrene-Resin-Supported, Palladium-Catalyzed, Atom-Efficient Cross-Coupling Reaction of Aryl Halides with Triarylbismuths', *Eur. J. Org. Chem.* **2010**, *2010*, 416-419.

[207] X. Chen, L. Zhou, Y. Li, T. Xie, S. Zhou, 'Synthesis of Heteroaryl Compounds through Cross-Coupling Reaction of Aryl Bromides or Benzyl Halides with Thienyl and Pyridyl Aluminum Reagents', *J. Org. Chem.* **2014**, *79*, 230-239.

[208] S. Chakraborty, J. Ahmed, B. K. Shaw, A. Jose, S. K. Mandal, 'An Iron-Based Long-Lived Catalyst for Direct C–H Arylation of Arenes and Heteroarenes', *Chem. Eur. J.* **2018**, *24*, 17651-17655.

[209] W.-L. Chen, C.-Y. Chen, Y.-F. Chen, J.-C. Hsieh, 'Hydride-Induced Anionic Cyclization: An Efficient Method for the Synthesis of 6-H-Phenanthridines via a Transition-Metal-Free Process', *Org. Lett.* **2015**, *17*, 1613-1616.

[210] S. Bernhardt, G. Manolikakes, T. Kunz, P. Knochel, 'Preparation of Solid Salt-Stabilized Functionalized Organozinc Compounds and their Application to Cross-Coupling and Carbonyl Addition Reactions', *Angew. Chem. Int. Ed.* **2011**, *50*, 9205-9209.

[211] J. M. Hammann, F. H. Lutter, D. Haas, P. Knochel, 'A Robust and Broadly Applicable Cobalt-Catalyzed Cross-Coupling of Functionalized Bench-Stable Organozinc Pivalates with Unsaturated Halides', *Angew. Chem. Int. Ed.* **2017**, *56*, 1082-1086.

[212] D.-Y. Wang, C. Wang, M. Uchiyama, 'Stannyl-Lithium: A Facile and Efficient Synthesis Facilitating Further Applications', *J. Am. Chem. Soc.* **2015**, *137*, 10488-10491.

[213] J.-H. Ho, Y.-C. Lin, L.-T. Chou, Y.-Z. Chen, W.-Q. Liu, C.-L. Chuang, 'Syntheses of p-terphenyls and 11,12-dihydroindeno[2,1-a]fluorene by one-pot benzannulation of Diels–Alder reactions of trans-1,2-dichloroethene and dienes', *Tetrahedron Lett.* **2013**, *54*, 1991-1993.

[214] M. R. Yadav, M. Nagaoka, M. Kashihara, R.-L. Zhong, T. Miyazaki, S. Sakaki, Y. Nakao, 'The Suzuki–Miyaura Coupling of Nitroarenes', *J. Am. Chem. Soc.* **2017**, *139*, 9423-9426.

[215] I. Kalvet, T. Sperger, T. Scattolin, G. Magnin, F. Schoenebeck, 'Palladium(I) Dimer Enabled Extremely Rapid and Chemoselective Alkylation of Aryl Bromides over Triflates and Chlorides in Air', *Angew. Chem. Int. Ed.* **2017**, *56*, 7078-7082.

[216] S. S. Muddana, A. M. Price, M. M. MacBride, B. R. Peterson, '11β-Alkyl-Δ9-19-Nortestosterone Derivatives: High-Affinity Ligands and Potent Partial Agonists of the Androgen Receptor', *J. Med. Chem.* **2004**, *47*, 4985-4988.

[217] S. P, P. Sarkar, S. Dutta, A. Das, S. K. Pati, S. K. Mandal, 'Regioselective ring-opening of epoxides towards Markovnikov alcohols: a metal-free catalytic approach using abnormal N-heterocyclic carbene', *Chem. Commun.* **2022**, *58*, 9540-9543.

[218] J. Wu, P. S. Grant, X. Li, A. Noble, V. K. Aggarwal, 'Catalyst-Free Deaminative Functionalizations of Primary Amines by Photoinduced Single-Electron Transfer', *Angew. Chem. Int. Ed.* **2019**, *58*, 5697-5701.

[219] C.-L. Sun, Y.-F. Gu, W.-P. Huang, Z.-J. Shi, 'Neocuproine–KOtBu promoted intramolecular cross coupling to approach fused rings', *Chem. Commun.* **2011**, *47*, 9813-9815.

[220] Z. Shen, S. Zhang, H. Geng, J. Wang, X. Zhang, A. Zhou, C. Yao, X. Chen, W. Wang, 'Trideuteromethylation Enabled by a Sulfoxonium Metathesis Reaction', *Org. Lett.* **2019**, *21*, 448-452.

[221] S. Geng, J. Zhang, S. Chen, Z. Liu, X. Zeng, Y. He, Z. Feng, 'Development and Mechanistic Studies of Iron-Catalyzed Construction of Csp^2–B Bonds via C–O Bond Activation', *Org. Lett.* **2020**, *22*, 5582-5588.

[222] R. Narobe, S. J. S. Düsel, J. Iskra, B. König, 'Photocatalytic Oxidative Iodination of Electron-Rich Arenes', *Adv. Synth. Catal.* **2019**, *361*, 3998-4004.

[223] H.-X. Zheng, X.-H. Shan, J.-P. Qu, Y.-B. Kang, 'Strategy for Overcoming Full Reversibility of Intermolecular Radical Addition to Aldehydes: Tandem C–H and C–O Bonds Cleaving Cyclization of (Phenoxymethyl)arenes with Carbonyls to Benzofurans', *Org. Lett.* **2018**, *20*, 3310-3313.

[224] M. Tobisu, Y. Kita, Y. Ano, N. Chatani, 'Rhodium-Catalyzed Silylation and Intramolecular Arylation of Nitriles via the Silicon-Assisted Cleavage of Carbon–Cyano Bonds', *J. Am. Chem. Soc.* **2008**, *130*, 15982-15989.

[225] P. Chen, H. Yang, H. Zhang, W. Chen, Z. Zhang, J. Zhang, H. Li, X. Wang, X. Xie, X. She, 'Total Synthesis of (−)-Gardmultimine A', *Org. Lett.* **2020**, *22*, 2022-2025.

[226] M. J. Frisch, G. W. Trucks, H. B. Schlegel, G. E. Scuseria, M. A. Robb, J. R. Cheeseman, G. Scalmani, V. Barone, G. A. Petersson, H. Nakatsuji, X. Li, M. Caricato, A. V. Marenich, J. Bloino, B. G. Janesko, R. Gomperts, B. Mennucci, H. P. Hratchian, J. V. Ortiz, A. F. Izmaylov, J. L. Sonnenberg, Williams, F. Ding, F. Lipparini, F. Egidi, J. Goings, B. Peng, A. Petrone, T. Henderson, D. Ranasinghe, V. G. Zakrzewski, J. Gao, N. Rega, G. Zheng, W. Liang, M. Hada, M. Ehara, K. Toyota, R. Fukuda, J. Hasegawa, M. Ishida, T. Nakajima, Y. Honda, O. Kitao, H. Nakai, T. Vreven, K. Throssell, J. A. Montgomery Jr., J. E. Peralta, F. Ogliaro, M. J. Bearpark, J. J. Heyd, E. N. Brothers, K. N. Kudin, V. N. Staroverov, T. A. Keith, R. Kobayashi, J. Normand, K. Raghavachari, A. P. Rendell, J. C. Burant, S. S. Iyengar, J. Tomasi, M. Cossi, J. M. Millam, M. Klene, C. Adamo, R. Cammi, J. W. Ochterski, R. L. Martin, K. Morokuma, O. Farkas, J. B. Foresman, D. J. Fox, *Gaussian 16, Revision A.03*, **2016**, Gaussian, Inc., Wallingford, CT.

[227] T. Yang, X. Li, S. Deng, X. Qi, H. Cong, H.-G. Cheng, L. Shi, Q. Zhou, L. Zhuang, 'From N–H Nitration to Controllable Aromatic Mononitration and Dinitration–The Discovery of a Versatile and Powerful *N*-Nitropyrazole Nitrating Reagent', *JACS Au* **2022**, *2*, 2152-2161.

[228] R. D. Faulkner, J. P. Lambooy, 'Synthesis and Biological Activity of 7-Bromo-8-methyl-10-(1-D-ribityl)isoalloxazine, an Analog of Riboflavin[1,2]', *J. Med. Chem.* **1966**, *9*, 495-497.

[229] D. A. Patrick, M. A. Ismail, R. K. Arafa, T. Wenzler, X. Zhu, T. Pandharkar, S. K. Jones, K. A. Werbovetz, R. Brun, D. W. Boykin, R. R. Tidwell, 'Synthesis and Antiprotozoal Activity of Dicationic m-Terphenyl and 1,3-Dipyridylbenzene Derivatives', *J. Med. Chem.* **2013**, *56*, 5473-5494.

[230] M. C. Mahawaththa, H. W. Orton, I. Adekoya, T. Huber, G. Otting, C. Nitsche, 'Organoarsenic probes to study proteins by NMR spectroscopy', *Chem. Commun.* **2022**, *58*, 701-704.

[231] H. Bloux, A. Dahiya, A. Hébert, F. Fabis, F. Schoenebeck, T. Cailly, 'Base-Mediated Radio-Iodination of Arenes by Using Organosilane and Organogermane as Radiolabelling Precursors', *Chem. Eur. J.* **2023**, *29*, e202203366.

[232] F. Neese, 'Software update: The ORCA program system—Version 5.0', *WIREs Computational Molecular Science* **2022**, *12*, e1606.

[233] T. B. Demissie, K. Ruud, J. H. Hansen, 'DFT as a Powerful Predictive Tool in Photoredox Catalysis: Redox Potentials and Mechanistic Analysis', *Organometallics* **2015**, *34*, 4218-4228.

[234] H. G. Roth, N. A. Romero, D. A. Nicewicz, 'Experimental and Calculated Electrochemical Potentials of Common Organic Molecules for Applications to Single-Electron Redox Chemistry', *Synlett* **2016**, *27*, 714-723.

[235] L. F. Tietze, C. Eichhorst, T. Hungerland, M. Steinert, 'A Fast Way to Fluorescence: A Fourfold Domino Reaction to Condensed Polycyclic Compounds', *Chem. Eur. J.* **2014**, *20*, 12553-12558.

[236] L. Tanwar, J. Börgel, J. Lehmann, T. Ritter, 'Selective C–H Iodination of (Hetero)arenes', *Org. Lett.* **2021**, *23*, 5024-5027.

[237] A. J. McGrath, G. E. Garrett, L. Valgimigli, D. A. Pratt, 'The Redox Chemistry of Sulfenic Acids', *J. Am. Chem. Soc.* **2010**, *132*, 16759-16761.

[238] T. Miura, N. Iwasawa, 'Reactions of Iodinated Vinylidene Complexes Generated from 1-Iodo-1-alkynes and $W(CO)_5$(thf)', *J. Am. Chem. Soc.* **2002**, *124*, 518-519.

[239] Y. Uozumi, M. Kikuchi, 'Controlled Monoarylation of Dibromoarenes in Water with a Polymeric Palladium Catalyst', *Synlett* **2005**, *2005*, 1775-1778.

[240] X. Luo, H. Zhang, H. Duan, Q. Liu, L. Zhu, T. Zhang, A. Lei, 'Superior Effect of a π-Acceptor Ligand (Phosphine−Electron-Deficient Olefin Ligand) in the Negishi Coupling Involving Alkylzinc Reagents', *Org. Lett.* **2007**, *9*, 4571-4574.

[241] A. Suda, K.-i. Kawasaki, S. Komiyama, Y. Isshiki, D.-O. Yoon, S.-J. Kim, Y.-J. Na, K. Hasegawa, T. A. Fukami, S. Sato, T. Miura, N. Ono, T. Yamazaki, R. Saitoh, N. Shimma, Y. Shiratori, T. Tsukuda, 'Design and synthesis of 2-amino-6-(1H,3H-benzo[de]isochromen-6-yl)-1,3,5-triazines as novel Hsp90 inhibitors', *Bioorganic & Medicinal Chemistry* **2014**, *22*, 892-905.

[242] C. Monnereau, E. Blart, F. Odobel, 'A cheap and efficient method for selective para-iodination of aniline derivatives', *Tetrahedron Lett.* **2005**, *46*, 5421-5423.

[243] X. Wang, Y. Xu, F. Mo, G. Ji, D. Qiu, J. Feng, Y. Ye, S. Zhang, Y. Zhang, J. Wang, 'Silver-Mediated Trifluoromethylation of Aryldiazonium Salts: Conversion of Amino Group into Trifluoromethyl Group', *J. Am. Chem. Soc.* **2013**, *135*, 10330-10333.

[244] J.-Y. Yang, X.-H. Xu, F.-L. Qing, 'Copper-mediated trifluoromethylation of diaryliodonium salts with difluoromethyltriflate', *J. Fluorine Chem.* **2016**, *186*, 45-51.

[245] T. D. Senecal, A. T. Parsons, S. L. Buchwald, 'Room Temperature Aryl Trifluoromethylation via Copper-Mediated Oxidative Cross-Coupling', *J. Org. Chem.* **2011**, *76*, 1174-1176.